Dreiundfünfzigster Band

Volume 53

Ambiguity Resolution Techniques in Geodetic and Geodynamic Applications of the Global Positioning System

Leos Mervart

1995

Geodätisch-geophysikalische Arbeiten in der Schweiz

Dreiundfünfzigster Band
Volume 53

Ambiguity Resolution Techniques in Geodetic and Geodynamic Applications of the Global Positioning System

Leos Mervart

1995

VORWORT

Geodätische und geophysikalische Anwendungen des amerikanischen Globalen Positionierungs-Systems (GPS) beinhalten meist globale Phänomene wie Polschwankung, Nutation, Plattentektonik oder regionale Effekte wie den Post Glacial Rebound. Werden Aufgaben dieser Art mit GPS untersucht, sind sie nicht zu trennen von der Bahnbestimmung im weitesten Sinn und gehören damit zu den anspruchsvollsten Fragestellungen der Satellitengeodäsie.

Die vorliegende Arbeit gliedert sich in einen ersten eher theoretischen Teil (Kapitel 1-6) und einen angewandten Teil (Kapitel 7-8). Die Modellierung von Satellitenbahnen und GPS Observablen, sowie die Definition und die GPS-technische Realisierung des Referenzsystems sind zentral für Herrn Mervart. Diese Aspekte sind in den Kapiteln 2 bis 5 kompetent abgehandelt: Man findet dort eine prägnante Diskussion der neuesten Satellitenbahnmodelle, der relativistischen Effekte, der atmosphärischen Refraktion, aber auch die Definition des Phasenzentrums von Satelliten- und Empfängerantennen.

Kapitel 6 gibt einen Überblick über die verschiedenen Methoden zur Bestimmung der Phasenmehrdeutigkeiten (Ambiguities). Der GPS Empfänger misst ja zum Zeitpunkt der Beobachtung die Trägerphase, welche interpretiert werden kann als Summe der Distanz zwischen Empfänger und Satellit, und einer unbekannten, aber ganzen Zahl von Wellenlängen der Trägerwelle des GPS-Signals. Kann diese ganze Zahl für jedes Paar (Station, Satellit) bestimmt werden, ist die Observable äquivalent der Distanz zwischen Satellit und Empfänger zum Zeitpunkt der Messung. Bei geodynamischen Fragestellungen ist eine operationelle, das eigentliche Parameterbestimmungsverfahren nicht belastende Bestimmung der Phasenmehrdeutigkeiten schon deshalb von Bedeutung, weil sich dadurch die Zahl der Unbekannten um etwa 90 % reduziert (von etwa 6000 auf 500 Parameter im Falle einer Dreitageslösung, so wie sie vom CODE-Rechenzentrum von IGS jeden Tag produziert wird). Die eingehend erläuterte QIF-Strategie (QIF = Quasi Ionosphere Free) zur Bestimmung der erwähnten Mehrdeutigkeiten unterscheidet sich von den meisten andern Methoden dadurch, dass sie die von den Satelliten ausgesandte Code-Information nicht verwendet. Sie ist somit auch unter AS (Anti-Spoofing) voll einsetzbar.

Im zweiten Teil der Arbeit erprobt Herr Mervart die vorgestellten Algorithmen in regionalen und globalen Netzen. Vier Datensätze von je etwa zwei Wochen Länge werden analysiert. Wichtig ist, dass der Autor konsequent die Errungenschaften des International GPS Service for Geodynamics (IGS) zurückgreift. So gelingt es ihm, die unbekannten Phasenmehrdeutigkeiten für jede Basislinie einzeln, und nicht erst im globalen Netz, zu bestimmen. Dieses Vorgehen birgt den Schlüssel zu einem operationellen Verfahren.

Die erste Kampagne (ein europaweites Netz unter Einbezug eines Teils des schweizerischen Landesnetzes, vermessen im Jahre 1992) zeigte schon, dass die Verfahren im Prinzip funktionieren, und dass generell eine Verbesserung der Genauigkeit der geodynamisch relevanten Parameter resultierte.

Die Auswertung eines europäischen Datensatzes von zwei Wochen zu Beginn des Jahres 1993 zeigte, dass die gegenüber 1992 gesteigerte Qualität der IGS-Satellitenbahnen (mehr Beobachtungen, bessere Auswerteverfahren) eine wesentliche Rolle spielte. Im Vergleich mit unseren damaligen operationellen Lösungen konnte die Konsistenz der Lagekoordinaten wesentlich (etwa um einen Faktor 2) gesteigert werden.

Zwei zweiwöchige Datensätze wurden im Jahr 1994 ausgewertet. Der erste stammt vom Januar, der zweite vom Mai 1994. Die beiden Sätze unterscheiden sich dadurch, dass -wegen des geänderten Übertragungsmodus' unter AS- im Mai die meisten Empfänger des IGS-Netzes nicht mehr in der Lage waren, genaue Code-Messungen durchzuführen. Dass die Phasenmehrdeutigkeiten im Mai trotzdem bestimmt werden konnten, ist der oben erwähnten QIF-Strategie zu verdanken. Beide Datensätze lieferten etwa gleich gute (im Vergleich zu 1993 nochmals deutlich bessere) Resultate. Neue Aspekte wurden behandelt: Der Einfluss der Ambiguity-Lösung auf einzelne Bahnparameter wurde untersucht, und es konnte gezeigt werden, dass bei gelösten Phasenmehrdeutigkeiten die direkte Bestimmung der täglichen Stationsbewegungen (z.B. infolge der Kontinentalgezeiten) in den Bereich des Möglichen rückt.

Es verdient festgehalten zu werden, dass Herr Mervart seine Verfahren so weit optimieren konnte, dass sie seit Herbst 1994 routinemässig, zusätzlich zu den offiziellen Lösungen des Schweizer IGS Rechenzentrums, eingesetzt werden konnten. Seit Juni 1995 liefern Herrn Mervart's Algorithmen sogar die offiziellen Resultate des CODE-Rechenzentrums.

Die Schweizerische Geodätische Kommission (SGK) dankt Herrn Mervart für diesen wesentlichen Beitrag im Rahmen der Internationalen Assoziation für Geodäsie. Die Schweizerische Akademie der Naturwissenschaften (SANW) hat die Druckkosten übernommen, wofür die SGK ihren Dank ausspricht.

Prof. Dr. G. Beutler
Direktor des Astronomischen
Instituts der Universität Bern

Direktor F. Jeanrichard
Bundesamt für Landestopographie
Vizepräsident der SGK

Prof. Dr. H.-G. Kahle
ETH Zürich
Präsident der SGK

PREFACE

Des phénomènes globaux tels que mouvements du pôle, nutation, tectonique des plaques ou des effets régionaux tels que le „Post Glacial Rebound" influencent les applications géodésiques et géophysiques basées sur le système américain GPS (Global Positioning System). L'étude de tels phénomènes ne peut pas être séparée de la détermination des orbites au sens large et fait ainsi partie des problèmes de la géodésie par satellites les plus difficiles à résoudre.

Le travail présenté ici se divise en une partie théorique (chapitres 1-6) et en une partie pratique (chapitres 7-8). Les préoccupations principales de M. Mervart sont d'une part la modélisation des orbites des satellites et des observations GPS et d'autre part la définition et la réalisation technique du système de référence du point de vue GPS. Ces aspects sont traités de façon compétente dans les chapitres 2 à 5: on y trouve une discussion pertinente de nouveaux modèles d'orbites des satellites, des effets relativistes et de la réfraction atmosphérique. Une définition du centre de phase aussi bien des antennes sur le satellite que celles des récepteurs complète cette discussion.

Le chapitre 6 donne une vue d'ensemble des différentes méthodes de la résolution des ambiguïtés de phase. Au moment de l'observation, le récepteur GPS mesure la phase de l'onde porteuse qui peut être interprétée en tant que somme de la distance entre le récepteur et le satellite et d'un nombre entier, mais inconnu, de longueurs d'onde de la porteuse du signal GPS. Si ce nombre entier peut être déterminé pour chaque couple station - satellite, l'observation correspond alors à la distance entre la station et le satellite. Lors du traitement de problèmes géodynamiques, il est important d'avoir à sa disposition un procédé permettant de résoudre préalablement les ambiguïtés. Ainsi le nombre des paramètres inconnus peut être réduit d'environ 90%. Le centre de calcul CODE de l'IGS produit quotidiennement des solutions comprenant 3 jours d'observations (three-day solution). Dans ce cas, le nombre de paramètres inconnus peut être réduit de 6000 à 500 environ. La stratégie QIF (QIF = Quasi Ionosphere Free) décrite abondamment et utilisée pour la résolution des ambiguïtés se différencie de la plupart des autres méthodes en ce sens qu'elle est indépendante du code émis par les satellites. Elle est donc pleinement applicable également lorsque le signal GPS est brouillé par AS (Anti-Spoofing).

Dans la deuxième partie de son mémoire, M. Mervart teste les algorithmes présentés dans des réseaux régionaux et globaux. Quatre séries de données, correspondant chacune à environ deux semaines d'observations, sont analysées. Il est important de remarquer que le travail de l'auteur s'intègre pleinement dans les nouvelles techniques mises au point par l'IGS (International GPS Service for Geodynamics). Ainsi, il lui est possible de déterminer les ambiguïtés de phase pour chaque base indépendament et non plus seulement de façon globale. Cette approche constitue la clef de voûte d'un procédé rationnel.

La première campagne (un réseau européen, comprenant une partie du réseau suisse mesuré en 1992) démontra déjà que la méthode fonctionne et qu'une amélioration de la précision des paramètres déterminants pour la géodynamique en résulte.

L'analyse d'une série de mesures effectuées à l'échelon européen durant deux semaines au début de 1993, montra l'importance de la qualité des orbites des satellites calculées par l'IGS. Celle-ci s'est nettement améliorée par rapport à 1992 suite à l'augmentation du nombre des observations et à une meilleure méthode de calcul. En comparaison avec les méthodes appliquées autrefois, la cohérence des coordonnées planimétriques a augmenté de façon sensible (d'un facteur 2 environ).

Deux séries d'observations de deux semaines chacune furent analysées en 1994. La première série date de janvier, la seconde de mai 1994. La série de mai fut observée alors que le signal GPS était brouillé par AS, ce qui n'était pas le cas en janvier. Il est à remarquer que la plupart des récepteurs du réseau IGS n'étaient alors plus en mesure d'effectuer des observations précises de code. Cette perturbation put être contrée grâce à la stratégie QIF, qui permit de résoudre les ambiguïtés également lors de la campagne de mai. Les deux séries d'observations fournirent des résultats de qualité équivalente et bien meilleure encore qu'en 1993. De nouveaux aspects furent étudiés, entre autre l'influence de la résolution des ambiguïtés sur différents paramètres d'orbite. On a pu aussi démontrer que la détection de mouvements journaliers dus par exemple aux marées continentales devenait envisageable.

Il est important de souligner que les méthodes de M. Mervart ont pu être optimalisées de telle façon que, depuis l'automne 1994, elles sont utilisées régulièrement par le centre suisse de calcul IGS. Depuis juin 1995, les algorithmes développés par M. Mervart sont utilisés par le centre de calcul CODE pour la production de résultats officiels.

Prof. Dr. G. Beutler
Directeur de l' Institut d'astronomie
de l' Université de Berne

F. Jeanrichard, Directeur
de l' Office fédéral de topographie
Vice-président de la CGS

Prof. Dr. H.-G. Kahle
ETH Zurich
Président de la CGS

FOREWORD

In geodesy and geophysics, the American Global Positioning System (GPS) is usually applied to the investigation of global phenomena, such as polar motion, nutation, plate tectonics, or regional effects such as post glacial rebound. When investigating such occurrences with GPS, they cannot be separated from orbit determination in the widest sense, and are therefore considered to be some of the most demanding questions in satellite geodesy.

This publication is divided into two parts; the first part (chapters 1-6) covers the more theoretical aspects while the second part (chapters 7-8) refers to the application. Modeling satellite orbit and GPS observables, as well as defining and realizing a reference system with the aid of GPS technology, are an important topic in this publication. These aspects are covered in a competent manner in chapters 2 to 5 and a concise discussion is presented regarding the most up-to-date satellite orbit models, the relativity effect, atmospheric refraction, as well as a definition of the phase center of satellite and receiver antennas.

Chapter 6 gives an overview of the various methods for determining the ambiguities. At the epoch of observation the GPS receiver measures the carrier phase, which can be interpreted as the sum of the distance between the receiver and the satellite plus a unknown, but integer number, of wavelengths of the carrier wave of the GPS signal. If this unknown integer can be determined for every pair (station/satellite), the observable is equivalent to the distance between the satellite and the receiver at the epoch of measurement. For geodynamic investigations, it is important to have an operational approach for determining the ambiguities, which does not burden the actual parameter computation. Thus the amount of unknowns can be reduced by about 90 % (from about 6000 to 500 parameters in the case of a three-day solution, such as the one produced on a daily basis by IGS' CODE-analysis center). The QIF-strategy (QIF = Quasi Ionosphere Free) which is explained in detail and which is used to determine the above mentioned ambiguities, differs from most other methods in that it does not use the code information sent out by the satellite. It is therefore also fully applicable under AS (Anti-Spoofing).

In the second part of this volume Mr. Mervart tests the algorithms presented in regional and global networks. Four data sets, each covering two weeks, are analyzed. An important factor is the consistency and integration of this strategy within the framework of the International GPS Service for Geodynamics (IGS). The author was able to determine the ambiguities for each base line individually, as opposed to using the global network. This method is the key to an operational procedure.

The first campaign (a Europe-wide network, which included part of the Swiss network measured in 1992) already showed, that the procedure worked in principle, and that it resulted in a general improvement of the accuracy of the geodynamically relevant parameters.

The evaluation of a European data set covering a two-week period at the beginning of 1993, showed that the quality increase of the IGS-satellite orbits due to a permanent increase of the amount of observations and improved evaluation procedures since 1992, played a fundamental role. Compared to our earlier operational results, the consistency of the horizontal coordinates could be increased considerably (by about factor 2).

Two two-week data sets were evaluated in 1994. The first was from January, the second from May 1994. Both sets differ from one another in that -due to the changed modus of transmission under AS- most receivers of the IGS-network were no longer able to carry out accurate code measurements in May. The fact that the ambiguities could still be determined in May, was due to the above mentioned QIF-strategy. Both data sets delivered about equally good results (even clearly better than those of 1993). New aspects were addressed: The influence of the ambiguity solution on individual orbit parameters was investigated and it was possible to show that the direct determination of the daily movements of the stations (e.g. due to continental tides) would soon be realizable.

It must be said that Mr. Mervart was able to perfect his procedure to such an extent, that since the autumn of 1994 it is routinely used in addition to the official results of the Swiss IGS analysis center. Since June 1995, Mr. Mervart's algorithms are also included in the processing of the official results of the CODE analysis center.

The Swiss Geodetic Commission (SGC) would like to thank Mr. Mervart for his fundamental contribution within the framework of the International Association for Geodesy. The SGC is most grateful to The Swiss Academy of Sciences (SANW) who kindly offered to carry the printing costs.

Prof. Dr. G. Beutler
Director of the Astronomical
Institute, University of Berne

F. Jeanrichard
Federal Office of Topography
Vice President

Prof. Dr. H.-G. Kahle
ETH Zurich
President

Contents

Part I

Theory

1. NAVSTAR GPS

The abbreviations in the title of this chapter stand for NAVigation Satellite Timing And Ranging Global Positioning System [Rothacher, 1991]. It should be said that other authors interpret the abbreviation "NAVSTAR" as NAVigation System with Time And Ranging [Wübbena, 1991] or NAVigation System using Time And Ranging [Landau, 1988] or NAVigation System using Timing And Ranging [Hofmann-Wellenhof, 1992]. Apart from this small terminological problem the name of the system expresses its basic features. There are several other Global Positioning Systems either operational or under development. Let us mention the TRANSIT, DORIS, PRARE or GLONASS systems. Each system uses its own measurement types (doppler, ranges, phases, one-way or two-way observation etc.) depending on the application type, the accuracies to be obtained, and the potential users. Undoubtedly the system NAVSTAR has the greatest impact on the scientific community at present. It is fully operational and yields highest accuracy. Therefore this thesis deals only with NAVSTAR GPS and from now on we will use the term GPS as a synonymous to NAVSTAR GPS. However many methods and processing techniques are similar for the other systems too. In 1973 the U.S. Department of Defence decided to establish, develop, test, acquire, and deploy a spaceborne positioning system. The result of this decision is the present NAVSTAR GPS. According to [Wooden, 1985]

"The NAVSTAR Global Positioning System (GPS) is an all-weather, space-based navigation system under development by the U.S. Department of Defence to satisfy the requirements for the military forces to accurately determine their position, velocity, and time in a common reference system, anywhere on or near the Earth on a continuous basis."

From this definition it is clear that the primary goals for developing GPS were of a military nature. But the U.S. Congress has allowed the civilians to use this system with some restrictions. The first geodetic instruments, the Macrometer Interferometric Surveyor^{TM} and the Texas Instruments TI-4100 were in commercial use at the time the military was still testing navigation receivers. The first civilian applications of the GPS were attempts to establish high-accuracy geodetic networks.

1.1 The Principle of Operation

The principle of satellite positioning is quite simple: the geocentric satellite position vector $\underline{r}^i$ is assumed to be known and the position vector of the receiver $\underline{\varrho}_k$ is to be estimated using the measurements which contain information about the topocentric satellite position vector $\underline{\varrho}$. The GPS measurements are based on receiving and processing of electromagnetic waves transmitted by the satellite (see Section 1.3). It is obvious that the accuracy of the position is affected by the following factors:

- accuracy of the satellite's position,
- accuracy of the measurements, and
- geometry.

It is worth noting that the main error source – the accuracy of satellite orbits – may be considerably reduced if so-called relative positioning is used. Let us assume two sites which receive simultaneously the signal from the same satellites. In that case the relative position of these two sites is much more accurate than the position of each of these sites in a global coordinate system. According to Baueršíma's rule

$$\frac{|\Delta \underline{b}|}{|\underline{b}|} \doteq \frac{|\Delta \underline{\varrho}|}{|\underline{\varrho}|} \; ; \tag{1.1}$$

$\underline{b}$ is the baseline vector (pointing from one site to the other), $\Delta\underline{b}$ is the error of this vector, $\underline{\varrho}$ is the topocentric satellite position vector and $\Delta\underline{\varrho}$ the corresponding orbit error. The orbit accuracy will be discussed in Chapter 2. GPS consists of three integral design parts: *the space segment*, *the control segment*, and *the user segment* which will be briefly described. Then the structure of the satellite signal and the measurement types will be introduced.

1.2 The Segments of the NAVSTAR GPS

The Space Segment

The proposed constellation of the GPS has been subject to several changes due to budgetary problems. The present full constellation should provide global coverage with four to eight simultaneously observable satellites above 15° elevation. This is accomplished by 24 satellites (21 production satellites and 3 active spares). The satellites are located in six planes in almost circular orbits with an altitude of about 20 200 km above the earth, an inclination of 55° and with an orbital period of approximately 11 hours 58 minutes or half a sidereal day. Thus almost the same earth–satellite configuration will repeat itself 4 minutes earlier every day. There is no essential difference between the production satellites and the active spares. The spare satellites are used to replace a malfunctioning production satellite to maintain the required coverage. Three replacements are possible before a new satellite has to be launched.

The GPS satellites provide a platform for radio transceivers, atomic clocks, computers, and various equipment used for positioning requirements and for a series of other military

projects (e.g. atomic flash detection). The electronic equipment of the satellites allows the user to operate a receiver to measure quasi-simultaneously topocentric distances to more than three satellites. Each satellite broadcasts a message which allows the user to recognize the satellite and to determine its spatial position $\underline{r}^i$ for arbitrary time instants. The satellites are equipped with solar panels for power supply, the reaction wheels for attitude control and a propulsion system for orbit adjustments. The first satellites launched (1978 – 1985) were Block I satellites for the test phase of the project. Three of these satellites were still operational in 1992, one was still operational in 1994. They differed from the newer satellites by their orbit characteristics. According to proposed constellation of that time, their orbits were inclined 63° to the equator. For the first operational constellation the Block II satellites (see Figure 1.1) are designed.
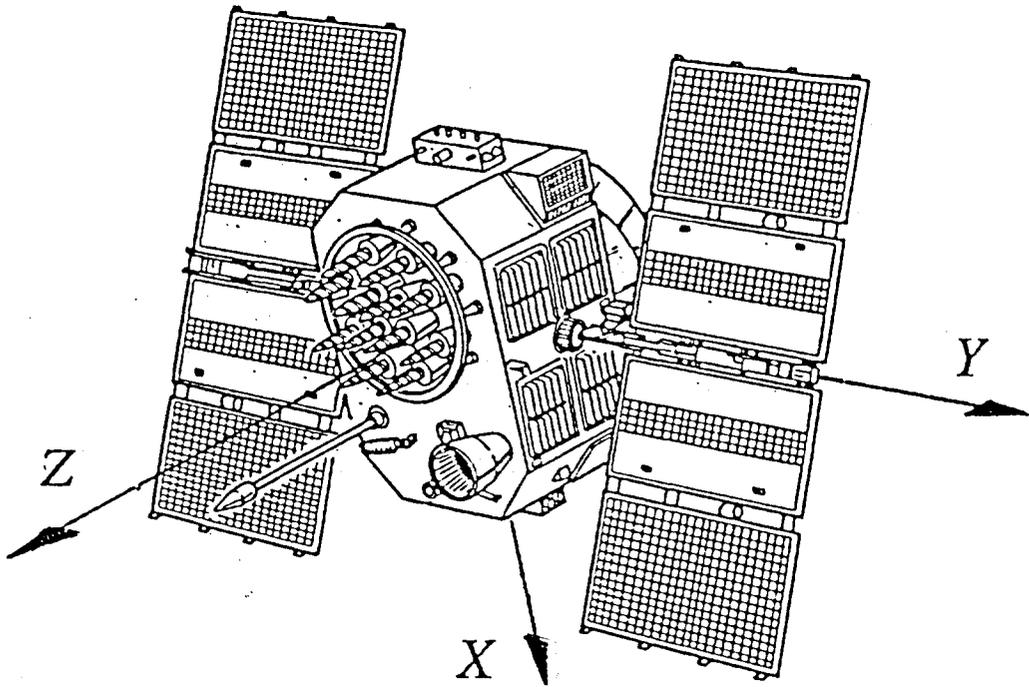
Figure 1.1: NAVSTAR Block II spacecraft [Fliegel et al., 1992]

The first Block II satellite was launched in February 1989. The satellites currently being launched are Block IIa satellites. Altogether 28 Block II and Block IIa satellites are designated for the first operational constellation. An important difference between Block I and Block II satellites is related to U.S. national security. Block I satellites signals were fully available to civilian users while some Block II signals are restricted. There are already plans for satellites which will replace the Block II's. These satellites are called Block IIR (the "R" denotes replacement). They will introduce some new design features (e.g. inter-satellite communications and ranging) and they are expected to have on-board hydrogen masers, which are at least one order of magnitude more precise than the atomic clocks in the Block II satellites. Block IIR satellites should be available by 1995.

The Control Segment

The control segment monitors the functioning of the satellites and uploads orbital, clock-correction, and auxiliary data into the satellite memories. The so-called Operational Control System (OCS) consists of a *master control station*, worldwide *monitor stations*, and *ground control stations*. This system became operational in September 1985. The *master control station* is located in Colorado Springs. It collects the tracking data from the monitor stations and calculates the satellite orbit and clock parameters to be broadcast by the satellites in real time. The results are passed to the ground control stations for upload to the satellite.

Colorado Springs is a *monitor station* as well. Four additional monitor stations are located at Hawaii (Pacific Ocean), Ascension Island (South Atlantic), Diego Garcia (Indian Ocean) and Kwajalein (Pacific Ocean). These five stations are equipped with precise cesium time standards and P-code receivers. The measurements are transmitted to the master control station. The monitor stations form the official network for determining the *broadcast ephemerides* and for modeling the satellite clocks. This orbit information is modulated onto the satellite signal and thus available for real-time navigation. For a posteriori geodetic and geophysical analysis more precise orbits are required. Since 1992 such high precision orbits are determined by the *International GPS Service for Geodynamics (IGS)* – see Section 2.2.

The stations at Ascension Island, Diego Garcia, and Kwajalein, are at the same time so-called *ground control stations*. They are equipped with communication links to the satellites. The satellite ephemerides and the clock information, calculated at the master control station, are uploaded to each GPS satellite. At present the uploading is performed once per day.

The User Segment

The user segment consists of all the GPS receivers. There are different receiver types commercially available by now. A simple classification based on the availability of the codes is presented in the next section. All national and international groups and organizations established for distributing GPS information might be considered as a part of the user segment, too. Chapter 2 deals with one of the most important of such organizations – the International GPS Service for Geodynamics (IGS).

1.3 The Satellite Signal

All signals transmitted by the satellite (see Table 1.1) are derived from the fundamental frequency f_0 of the satellite oscillator. Its stability is in the range of 10^{-13} over one day for Block II satellites [McCaskill et al., 1985].

Table 1.1: Components of the satellite signal [Hofmann-Wellenhof et al., 1992]

Component	Frequency [MHz]		
Fundamental frequency	f_0	=	10.23
Carrier L_1	$f_1 = 154\ f_0$	=	1575.42 ($\lambda_1 \doteq 19.0$ cm)
Carrier L_2	$f_2 = 120\ f_0$	=	1227.60 ($\lambda_2 \doteq 24.4$ cm)
P-code $P(t)$	f_0	=	10.23
C/A-code $C(t)$	$f_0/10$	=	1.023
Navigation message $D(t)$	$f_0/204600$	=	$50 \cdot 10^{-6}$

The two sinusoidal carrier signals with frequencies f_1 and f_2 (corresponding wavelengths $\lambda_1 \approx 19$ cm and $\lambda_2 \approx 24$ cm) are modulated with the codes and the navigation message to transmit information such as the readings of the satellite clocks, the orbital parameters etc. The so-called biphase modulation is used. The two codes $P(t)$, $C(t)$ and the navigation message $D(t)$ consist of a sequences with two states $+1$, -1, where according to [Baueršíma, 1982] the resulting signals may be described as

$$
\begin{aligned}
L_1(t) &= a_p\ P(t)\ D(t)\ \cos 2\pi(f_1 t) + a_c\ C(t)\ D(t)\ \sin 2\pi(f_1 t) \\
L_2(t) &= b_p\ P(t)\ D(t)\ \cos 2\pi(f_2 t)
\end{aligned}
\tag{1.2}
$$

where a_p, a_c and b_p are the amplitudes of the signals which are not of interest in our context.

1.3.1 Pseudorandom Codes

The reading of the satellite clocks at the transmission time t^i is coded into the signal. The receiver decoding this signal at time t_k may compute the so-called pseudorange to the satellite from the relation:

$$
\varrho_k^i = c \cdot (t_k - t^i)
\tag{1.3}
$$

where c is the velocity of light. The term ϱ_k^i is called *pseudorange* because it is a biased distance. The largest bias is due to the receiver clock error. For real-time navigation the receiver clock error δ_k must be introduced as the fourth unknown parameter (three parameters describe the position of the receiver). Thus at least four satellites have to be observed simultaneously to estimate these four unknowns. For geodetic positioning different methods and different observables may be used. Both codes consist of so-called pseudorandom noise (PRN) sequences. The generation of these sequences is based on hardware devices called tapped feedback shift registers [Wells et al., 1986]. The C/A-code (Coarse-Acquisition or Clear-Access) is generated by the combination of two 10-bit tapped feedback shift registers where the output of both registers are added again by binary operation to produce the code sequence. A unique code is assigned to each satellite, the sequence has a length of 1023 bits and because of the basic frequency of 1.023 MHz it repeats itself every millisecond. The time interval between two subsequent bits ($\approx 10^{-6}$ s)

approximately corresponds to 300 meters. The achievable code accuracy of about 3 m is a function of this 300 m C/A-code wavelength.

The generation of the P-code (Precise or Protected) is similar but the length of the resulting sequence is approximately $2.3547 \cdot 10^{14}$ bits corresponding to a time span of approximately 266 days. The total code is partitioned into 37 one-week segments. To each satellite one segment is assigned which defines the *PRN number* of the satellite. The P-code repeats itself every week. The time interval between subsequent bits is 10 times smaller than in the case of the C/A-code. Therefore the accuracy is approximately 10 times higher than for the C/A-code. The P-code may be encrypted. This procedure is called *Anti-Spoofing* (AS) and converts the P-code to the Y-code which is only useable when a secret conversion algorithm is accessible to the receiver.

1.3.2 The Navigation Message

The navigation message is 1500 bits long and contains information concerning the satellite clock, the satellite orbit, the satellite health status, and various other data. The message is subdivided into five *subframes*. Each subframe contains 10 words. The first word is the so-called *telemetry word* (TLM) containing a synchronization pattern and some diagnostic messages. The second word of each subframe is the *hand-over word* (HOW). This word contains also the so-called *Z-count* which gives the number of 1.5 s intervals since the beginning of the current GPS week. This number and the P-code give the reading of the satellite clock at signal transmission time. The first subframe contains various flags and the polynomial coefficients which define the satellite clock correction (see Table 1.2).

Table 1.2: Broadcast clock parameters [Wübbena, 1991]

Parameter	Explanation
Code-Flag L_2	Indicator for C/A or P-code on L_2
Week No.	GPS week
L_2-P-Data-Flag	Indicator for data on L_2-P-code
SV-Accuracy (URA)	Measure for distance accuracy
SV-Health	Satellite health indicator
T_{GD}	Group delay difference L_1-L_2-P-Code
AODC	Age of clock data
t_{0c}	Reference epoch
a_0, a_1, a_2	Clock correction polynomial coefficients

The second and the third subframe contain the broadcast ephemerides of the satellite (see Table 1.3).

Table 1.3: Broadcast ephemerides [Hofmann-Wellenhof et al., 1992]

Parameter	Explanation
AODE	Age of ephemerides data
t_e	Ephemerides reference epoch
$\sqrt{a}$, e, M_0, ω_0, i_0, ℓ_0	Keplerian parameters at t_e
$d\,n$	Mean motion difference
$d\,i$	Rate of inclination angle
$d\,\Omega$	Rate of node's right ascension
C_{uc}, C_{us}	Correction coeff. (argument of perigee)
C_{rc}, C_{rs}	Correction coeff. (geocentric distance)
C_{ic}, C_{is}	Correction coeff. (inclination)

Using the broadcast ephemerides the following set of elements (compare also Appendix A) for epoch t may be computed:

$$
\begin{aligned}
M &= M_0 + \left[\sqrt{\tfrac{\mu}{a^3}} + d\,n\right] (t - t_e) \,, \\
\ell &= \ell_0 + d\,\Omega\,(t - t_e) - \omega_E\,(t - t_0) \,, \\
\omega &= \omega_0 + C_{uc}\,\cos(2u) + C_{us}\,\sin(2u) \,, \\
r &= r_0 + C_{rc}\,\cos(2u) + C_{rs}\,\sin(2u) \,, \\
i &= i_0 + C_{ic}\,\cos(2u) + C_{is}\,\sin(2u) + d\,i\,(t - t_e) \,.
\end{aligned}
\tag{1.4}
$$

M is the mean anomaly, ℓ is the longitude of the ascending node, r is the length of the geocentric radius vector, i is the inclination of the orbital plane with respect to the equatorial plane, ω_E is the earth rotation rate, and t_0 is time at the beginning of the current GPS week. The equations for the computation of the Cartesian coordinates in the earth-fixed system (WGS-84 – see [Decker, 1986]) are listed in Appendix A.

The fourth and the fifth subframe contain data for military use, information on the ionosphere and so-called almanac data (low-accuracy orbits of all the GPS satellites).

1.3.3 Signal Processing

The receiver contains elements for signal reception and signal processing (antenna, pre-amplifier, radio frequency section, microprocessor, storage device, control device and power supply). The main part of the receiver is the radio frequency (RF) section. The receivers may be divided into three groups:

1. Codeless receivers.
2. C/A-code receivers.
3. P-code receivers (which may use the C/A-code in adition).

According to the number of frequencies there are two groups of receivers:

1. Single-band receivers (only L_1 may be processed).

2. Dual-band receivers (both frequencies may be processed).

Another classification may be introduced according to the number of satellites which may be simultaneously tracked. Essentially there are

1. Single-channel receivers.
2. Multi-channel receivers.

Multi-channel receivers assign a physical channel to each satellite, where the satellite is continuously tracked. The receivers with a limited number of physical channels have to alternate satellite tracking by rapid sequencing (20 milliseconds). The modern receivers for precise geodetical measurements are usually dual-band P-code multi-channel receivers.

After signal input from the antenna, the signals are discriminated. Usually this is achieved through the C/A-codes which are unique for each satellite. The basic elements of the RF section are oscillators to generate a reference frequency, filters to eliminate undesired frequencies, and mixers. The *pseudorange measurements* are done as follows: A reference carrier is generated in the receiver and then modulated with a copy of the known PRN code. This modulated reference signal is then correlated with the received satellite signal. This correlation gives the time difference $t_k - t^i$ – see Equation (1.3). From the received satellite signal the PRN code is removed, the navigation message is decoded and eliminated by high-pass filtering. The result of this technique consists of:

the pseudorange $\varrho_k^i = c \cdot (t_k - t^i)$.

the navigation message, and

the unmodulated Doppler-shifted satellite signal, the so-called reconstructed carrier.

The *phase measurements* are based on processing the reconstructed signal carrier. This signal is usually obtained by the code demodulation technique using the correlation between the received signal and the signal copy generated by the receiver. Other techniques must be used for the L_2 phase in C/A-code receivers or for both phases in the case of the code-less receiver. One technique is the so-called squaring technique, where the received signal is multiplied with itself and hence all "$\pm\pi$ modulations" are removed. The result is the unmodulated squared carrier with half the period. From this squared carrier a sine-wave is derived the wavelength of which is only half the wavelength of the original signal.

The receiver receives the signal at time t_k (reading of the receiver clock). This signal was transmitted by the satellite at time t^i (reading of the satellite clock). At time t^i the phase of the satellite oscillator equals $\phi^i(t^i)$ and at time t_k the phase of the receiver oscillator equals $\phi_k(t_k)$. The receiver thus compares the following two signals:

$$y^i = a^i \cos 2\pi\phi^i(t^i) \quad \text{and} \quad y_k = a_k \cos 2\pi\phi_k(t_k) , \tag{1.5}$$

where a^i and a_k are the amplitudes of the signals. Multiplying these two signals we obtain:

$$y = y^i y_k = \frac{a^i a_k}{2} \left\{ \cos 2\pi \left[\phi^i(t^i) - \phi_k(t_k) \right] + \cos 2\pi \left[\phi^i(t^i) + \phi_k(t_k) \right] \right\} . \tag{1.6}$$

After applying a low-pass filter, the high frequency part $\phi^i(t^i) + \phi_k(t_k)$ is eliminated and

$$\psi_k^i = \phi^i(t^i) - \phi_k(t_k) + n_k^i \tag{1.7}$$

may be measured. The accuracy of the phase measurements is about 1-3 mm, but the exact number of integer wavelength between the satellite and the receiver n_k^i is not known at the time of the first measurement. The unknown integer number of cycles n_k^i to be added to the phase measurement to get a range is called the *initial phase ambiguity* (see Section 5.1). This phase ambiguity remains the same as long as the receiver keeps lock on the phase transmitted by the satellite.

2. The International GPS Service
for Geodynamics (IGS)

The International Association of Geodesy (IAG), member of the International Union of Geodesy and Geophysics (IUGG), recognized that the GPS is becoming one of the most important geodetic measurement systems. The GPS offers new possibilities in different fields of science such as monitoring of the pole motion and the crustal deformation, precise positioning of mobile platforms, monitoring of ionospheric conditions and the time transfer. The primary motivation in planning the *International GPS Service for Geodynamics (IGS)* was the recognition by 1989 that the most demanding civilian users of the GPS satellites, the geophysical community, were purchasing receivers in exceedingly large numbers, but the observations as well as the subsequent data analyses were not based on common standards and thus the geodynamical interpretation of the results generally based on repeated observations performed sometimes by diverse groups could not be trusted [Mueller and Beutler, 1992]. Standards for equipment, site selection and preparation, data handling, data analysis, etc. were needed. The other motivation was the generation of precise ephemerides for the satellites together with by-products such as earth orientation parameters and the monitoring of ionospheric conditions. At its XX-th General Assembly in Vienna in August 1991 the IUGG adopted the following resolution:

> **RESOLUTION No. 5. The IUGG**
>
> *recognizing* that the use of the Global Positioning System (GPS) for Geodesy and Geophysics is rapidly increasing and that this system will play a major role over the next decades in global and regional studies of the Earth and its evolution, and
>
> *noting* that is fully scientific potential can only be realized with international cooperation and coordination to deploy and operate a global tracking network with data analysis and effective dissemination of data,
>
> *recommends* that the concept of an International GPS Service for Geodynamics (IGS) be explored over the next four years, that as a first step one or more campaigns be conducted to test and evaluate the concept, that all Member Countries participate to the best of their ability, and that this activity be coordinated as closely as possible with comparable global deployments by other member associations, as well as those by other organization, and
>
> *requests* that existing global geodetic systems such as Very Long Baseline Interferometry (VLBI) and Satellite Laser Ranging (SLR) be used to carry out intensive observing campaigns in conjunction with the proposed IGS work.

Based on this resolution the IGS was planned and established. The primary goal of the IGS is to provide the scientific community with the following products:

- high precision orbits, including force model parameters,
- earth orientation parameters (EOPs),
- ionosphere information,
- GPS clock estimates, and
- ties to the terrestrial frame through co-location with other techniques.

2.1 Structure of the IGS

To fulfill the tasks mentioned above the following structure of the IGS has been established:

A **core network**, comprising approximately 40 globally distributed, very high quality GPS receiver-sites, with continuous, reliable operation, near-real-time data acquisition and transmission to data/processing centers (see Figure 2.1).

GPS TRACKING NETWORK OF THE INTERNATIONAL GPS SERVICE FOR GEODYNAMICS OPERATIONAL AND PLANNED STATIONS
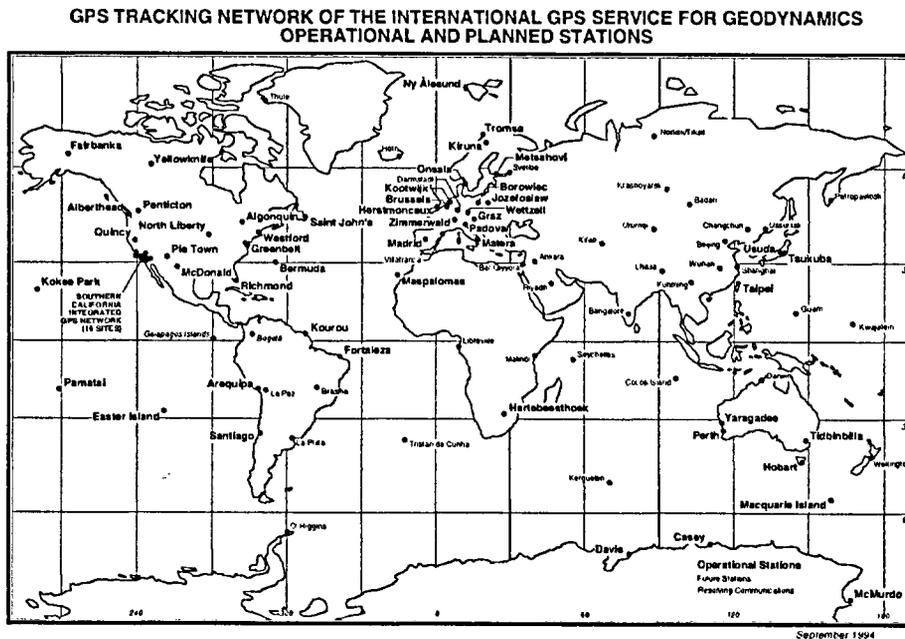
Figure 2.1: IGS 1994 Core Network

A much larger set of **fiducial stations** (between 100 and 200) providing denser coverage of tectonic deformation zones, regions of post-glacial rebound etc. Such sites might be occupied at regular intervals to determine secular geodetic signals. These stations will also provide direct access to the terrestrial reference frame through their ties to the core network.

Local sites which meet local needs and programs. There are no IGS constraints on these sites as they are clearly of local importance. However it is recommended that, on

the local level, they are treated in the same manner as higher level IGS sites.

Data Centers receive the data from the stations and facilitate transfer of the data to the analysis centers [Morgan and Gurtner, 1992]. The data centers structure is hierarchical: *Operational Centers* are responsible for the operation of a number of instruments (the data flow between the instruments and the center being a local matter). The center is responsible for transforming the data into the Receiver INdependent EXchange [Gurtner and Mader, 1990] format and performing on-site archiving of the raw instrument and RINEX format. *Regional Data Centers* are responsible for the collection, distribution and archiving of regional core and fiducial data (and not local data any more). Three *Global Data Centers* or *Network Centers* (see Table 2.1) are linked in a triangle with each other. Each center has a complete copy of core station data, all status reports and campaign output products.

Table 2.1: Global Data Centers of IGS

Abbreviation	Institution	Location	Country
CDDIS	Crustal Dynamics Data Information System	Greenbelt	USA
IGN	Intitute Géographique National	Paris	France
SIO	Scripps Institution of Oceanography	San Diego	USA

Analysis Centers provide analyses of the core and fiducial station data and derive the desired products. Analysis centers fall into the following categories: *Processing Centers* focus on the global analysis of data collected by the core and fiducial stations. The list of processing centers active end of 1993 is given in Table 2.2.

Table 2.2: Processing Centers of IGS

Abbreviation	Institution	Location	Country
CODE*	Center for Orbit Determination in Europe	Berne	Switzerland
EMR	Energy, Mines and Resources	Ottawa	Canada
ESOC	European Space Operations Center	Darmstadt	Germany
GFZ	German Geod. Research Institute	Potsdam	Germany
JPL	Jet Propulsion Laboratory, USA	Pasadena	USA
NOAA	National Oceanic and Atmospheric Administration	Silver Spring	USA
SIO	Scripps Inst. of Oceanography	San Diego	USA

*) Joint project of the Astronomical Institute University of Berne (AIUB), the Federal Institute of Topography, Berne, the Institut Géographique National (IGN), Paris, and the Institute of Applied Geodesy (IfAG), Frankfurt

The processing centers provide the products on a regular basis with a delay of a few days only. *Associate Processing Centers* will also provide global analysis, but will focus

on specific time periods or data sets. *Evaluation Centers* will evaluate the products of the Processing Centers and the Associate Processing Centers.

The organization responsible for the general management of the service and for providing internal coordination of IGS activities is the **Central Bureau** located at the Jet Propulsion Laboratory (JPL) in Pasadena.

The controlling institution of the IGS is the **Governing Board**. It consists of 15 members.

The 1992 and 1993 IGS Activities

In May 1992 the IGS organized the communications test which showed, that the capacity of the international scientific data network was sufficient to handle data from the core network. Then a 3-month test campaign, the 1992 IGS Test Campaign (June 21 – September 23, 1992) took place. During this campaign the data from the global core network were processed with a delay of several days only. To densify the core network the two-weeks intensive observation campaign Epoch'92 (July 27 – August 9) was organized and the data from the fiducial sites were collected. On 23 September 1992 the 1992 IGS Campaign officially ended. The participating organizations decided to establish the IGS Pilot Service starting November 1, 1992 to bridge the gap between the 1992 IGS Campaign and the start of the official IGS on January 1, 1994.

2.2   IGS Data Processing at the CODE

In this section the IGS Data Processing at the Center for Orbit Determination in Europe (CODE) will be briefly described. The CODE is one of the processing centers of the IGS (see Table 2.2) which produce the IGS products (orbits, earth rotation parameters etc.). The processing centers use different processing strategies and different software packages and their results are regularly compared (see e.g. [Goad, 1993]). The CODE was planned in 1991, the contributors to the CODE are

- the Astronomical Institute, University of Berne (AIUB), Berne
- the Federal Office of Topography (L+T), Berne
- the Institut Géographique National, (IGN), Paris
- the Institut für Angewandte Geodäsie (IfAG), Frankfurt

The computing center is located at the AIUB and the data processing is done with the Bernese GPS Software [Rothacher et al., 1993a]. The data have been processed (including days with Anti-Spoofing) since the beginning of the 1992 Campaign (June 21, 1992) and the results (satellite ephemerides, earth rotation parameters and station coordinates) are available at CODE directly and/or through the network centers (Table 2.1).

Processing Strategy

The input data are sent to the CODE automatically through Internet from the IGN and from the IfAG. The data are decompressed and pre-processed. The broadcast orbits are used as a priori orbit information. Than one-day solution is performed for check purposes. The final products stem from overlapping 3-days solutions (see Figure 2.2).

Day 1   Day 2   Day 3

first 3-days solution

second 3-days solution

third 3-days solution

resulting orbit
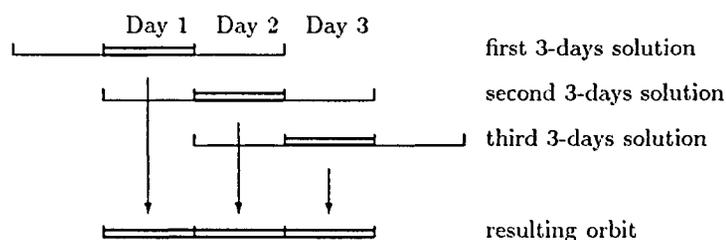
Figure 2.2: Overlapping 3-days solutions [Brockmann et al., 1993]

All solutions are based on the ionosphere-free linear combination, the modeling follows the IGS standards [Goad, 1992], and the following types of parameters are estimated:

- coordinates of the non-VLBI/SLR sites,

- 6 orbital elements plus radiation pressure parameters per satellite (see Chapter 4),

- 4 troposphere zenith delays per day and site,

- daily values of the x- and y-pole coordinates and the derivative $\frac{d}{dt}(UT1 - UTC)$, and

- initial carrier phase ambiguities.

The approximate size of one 3-days solution may be characterized by 35 sites, more than 3000 unknown parameters and more than 80000 double difference observations when working with a sampling of 1 observation per 2 minutes.

Orbit Consistency

It is difficult to estimate the orbit quality. We use the overlapping solutions to check the consistency. We take the resulting ephemerides from consecutive middle days (of 3-days solutions), and we fit a new arc through these days. The rms of this fit is a measure for the consistency of the orbits [Rothacher et al., 1993b]. Figure 2.3 shows the results for PRN 2.

Residuals for PRN 2
PRN = 2
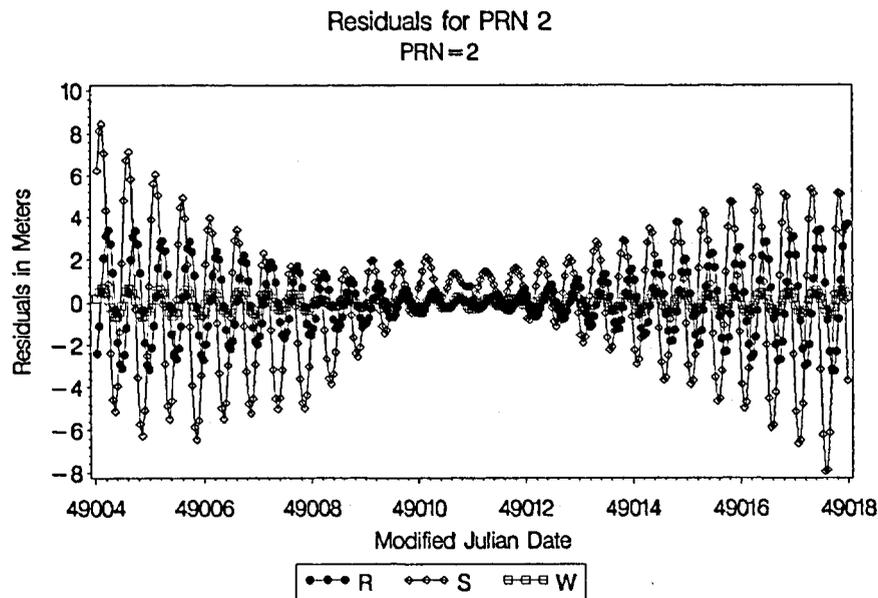
Figure 2.3: Orbit consistency [Beutler et al., 1994a]

Another possibility to estimate the accuracy of the orbits is to compare the results of various processing centers. The centers use different models and different software packages however they use almost the same data. IGS orbit comparisons were one of responsibilities of the IGS Analysis Center Coordinator (Prof. Clyde Goad from the Ohio State University). The rms of the Helmert transformation between the orbits of two processing centers reaches the value of about 20–30 cm at present [Goad, 1993].

Earth Rotation Parameters

The results of the earth rotation parameters estimation from June 21, 1992 to November 19, 1994 are shown in Figure 2.4. The quality of the pole coordinates was about 1 mas initially, and is now of the order of 0.4 mas for the x- and y- coordinate compared to the IERS solution C04 [Feissel, 1993]. The estimates of UT1 – UTC drift agree with the IERS values on the level of 0.05 ms per day [Rothacher et al., 1993b]. This high accuracy is achieved thanks to the use of longer arcs (the main reason for using 3-days arcs). The UT1 – UTC values (see Figure 2.4) may not be directly estimated using GPS (this value is strongly correlated to the right ascensions of the ascending nodes of the GPS orbits) but it is integrated from the UT1 – UTC drift (or length of day) estimations. The stability of the UT1 – UTC obtained from GPS is remarkable. Since the beginning of 1994 UT1 – UTC estimations of the CODE processing center are used for the UT1 prediction by the IERS Rapid Service.
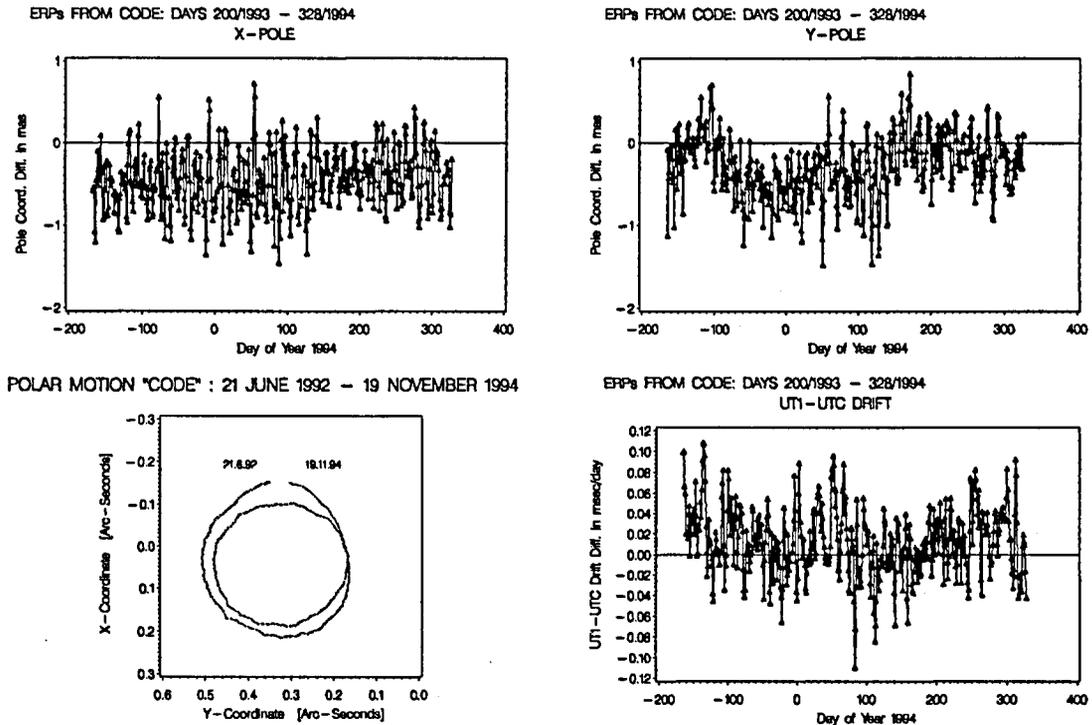
Figure 2.4: Earth rotation parameters

The long-term stability of the GPS solution might be guaranteed through monthly VLBI contributions. The advantage of GPS is its high data rate (diurnal or even sub-diurnal) and its low production price [Gambis et al., 1993], [Brockmann et al., 1993].

Table 2.3: Residuals of a 7-parameter Helmert transformation between the mean GPS coordinates (days 171-285, only European stations) and the ITRF91 [Rothacher, 1993c]

Station name	VLBI / SLR	Residuals in Meter		
		North	East	Up
Graz Lustbühl	SLR	0.0047	-0.0192	0.0041
Herstmonceux	SLR	-0.0013	-0.0097	0.0039
Kootwijk	SLR	0.0057	-0.0019	-0.0249
Madrid	VLBI	0.0007	0.0174	0.0105
Matera	SLR	-0.0096	-0.0031	0.0092
Tromsoe	VLBI	-0.0009	0.0077	0.0070
Wettzell	VLBI	0.0153	0.0076	-0.0065
Onsala	VLBI	0.0062	-0.0007	0.0068
Metsahovi	VLBI	-0.0167	0.0053	0.0030
Zimmerwald	SLR	-0.0039	-0.0032	-0.0130
rms of transformation		0.0111		

Site Coordinates

The stations of the core network with well-established VLBI/SLR coordinates are kept fixed, the coordinates of other stations are estimated. The quality of the results may be estimated from Table 2.3 where the residuals of a Helmert transformation are shown. The first set of coordinates is the ITRF91 set derived from VLBI and SLR solutions [Boucher et al., 1992], the second set is the mean set of 115 3-days solutions [Brockmann et al., 1993], all stations estimated (with loose a priori constraints). From Table 2.3 we conclude, that the GPS solutions agree with the ITRF91 coordinates (established through VLBI and SLR) on the 1 cm level.

3. Reference Systems in Space Geodesy

3.1 Coordinate Systems

The geometric distance ϱ_k^i between the receiver k and satellite i is the most important constituent of the range measured by GPS receivers (see Section 5.1). This distance is a (very simple) function of the receiver position vector $\underline{\varrho}_k$ and the satellite position vector $\underline{r}^i$.

The components of the receiver position vector $\underline{\varrho}_k$ are considered in the *International Terrestrial Reference Frame (ITRF)*. The origin, the reference directions, and the scale of the ITRF are implicitly defined by the cartesian coordinates and velocities adopted for various "primary" observing stations of the IERS [Seidelmann, 1992]. The origin of the ITRF is located at the center of mass of the Earth with an uncertainty of less than ± 10 cm. The standard unit of length is SI meter. The ITRF shows no global net rotation or translation with time due to the motions of the stations or the tectonic plates they lie on, and therefore the coordinates of the receiver in this frame are (nearly) time-independent.

ITRF is not suitable for orbit determination purposes because the satellite motion is (almost) independent on the earth rotation. The equations of motion of the satellite have the most convenient form if a celestial reference frame is used. *International Celestial Reference Frame (ICRF)* is defined using the coordinates of "primary" radio sources [Seidelmann, 1992]. The origin is at the barycenter of the solar system. The so-called ephemeris pole is given for epoch J2000.0 by the IAU 1976 Precession and the IAU 1980 Nutation Theory. The parameters that describe the rotation of the ITRF relative to the ICRF (in conjunction with the given precession and nutation model) are the *Earth rotation parameters (ERP)*.

The two reference frames mentioned above are supplemented by the *IERS Standards*. The IERS Standards (parameters and methods of data reduction) describe how observation will be used in order to determine the dynamic connection between terrestrial system and a celestial one. The IERS Reference Frames and the IERS Standards represent the *IERS Reference System*.

24

3.1.1 Transformation Between the ITRF and the ICRF

The celestial and the terrestrial coordinate systems are connected at any given instant using a rotation matrix $\mathfrak{R}$. One could express this matrix as a function of three Eulerian angles. However, for historical reasons, and in order to associate the motions of the Earth with physical processes and to allow for successive approximation of the motion, this matrix is expressed in terms of *precession*, *nutation*, *polar motion*, and *rotation* about the Earth's axis:

$$\underline{r}_k = \mathfrak{R} \cdot \underline{\varrho}_k \ , \qquad \mathfrak{R} = P^T \cdot N^T \cdot R^T \cdot Y \cdot X \ , \tag{3.1}$$

with

$\underline{r}_k$ ... coordinates of the receiver position vector in the space-fixed reference frame,

$\underline{\varrho}_k$ ... coordinates of the receiver position vector in the earth-fixed reference frame,

P ... Precession Matrix[1],

N ... Nutation Matrix[1],

R ... Apparent Sidereal Time Matrix[1] (contains UT1–UTC),

X, Y ... Polar Coordinate Matrices.

Rotation and Polar Motion

The polar coordinate matrices are

$$X = R_2(x_p) \ , \qquad Y = R_1(y_p) \ , \tag{3.2}$$

where $R_i(\alpha)$ denotes a particular rotation matrix about axis i and angle α, and x_p, y_p are the pole coordinates evaluated from VLBI, SLR and GPS observations and published in IERS Bulletins. *IERS Bulletin A* is published by the National Earth Orientation Service (NEOS). It is issued each week and contains Earth rotation parameters determined from the combination of other recently determined ERP series, predictions of Earth rotation parameters daily for up to 90 days in the future and other miscellaneous data. *IERS Bulletin B* is published by the Central Bureau of the IERS. It is issued each month and contains final ERP values. It should be mentioned that up to parts in 10^{12}

$$X \cdot Y = Y \cdot X \tag{3.3}$$

Earth rotation matrix R has the form

$$R = R_3(\text{GAST}) \tag{3.4}$$

where GAST is the Greenwich Apparent Sidereal Time, which is given by the *equation of equinoxes*:

$$\text{GAST} = \text{GMST} + \Delta\psi \cos(\epsilon_0 + \Delta\epsilon) \ , \tag{3.5}$$

where GMST is the Greenwich Mean Sidereal Time (see (3.16) to (3.19)), ϵ_0 is the mean obliquity of date and $\Delta\psi$, $\Delta\epsilon$ are nutations in longitude and obliquity, which are given by IAU 1980 nutation series. For numerical computation of these terms see [Seidelmann, 1992].

---

[1]The denotation in (3.1) corresponds to [Seidelmann, 1992]. In "IERS Standards (1992)" the matrices P^T, N^T, R^T are denoted P, N, R.

Nutation

The *nutation* is the sum of periodic motions of the ephemeris pole around the mean ephemeris pole with the greatest amplitude of about 9" and a variety of periods of up to 18.6 years. The nutation matrix is given by [Seidelmann, 1992]

$$N = R_1(-\epsilon) \cdot R_3(-\Delta\psi) \cdot R_1(\epsilon_0) , \quad \epsilon = \epsilon_0 + \Delta\epsilon , \tag{3.6}$$

where ϵ it the true obliquity of date.

Precession

The *lunisolar precession* is the smooth, long-period motion of the mean pole of the equator about the pole of the ecliptic, with a period of about 26,000 years. Both, the precession and the nutation are due to the torque of the Sun and Moon. *Planetary precession* is the motion of the ecliptic pole due to the gravitational action of the planets on the Earth's orbit. The precession matrix P may be expressed as

$$P = R_3(-z_A) \cdot R_2(\theta_A) \cdot R_3(-\zeta_A) . \tag{3.7}$$

The series for the precession angles z_A, θ_A, and ζ_A (IAU 1976 precession parameters) may be found e.g. in [Seidelmann, 1992].

3.1.2 Crustal Motion

Solid Earth Tides

The solid earth tides is the response of the solid earth to lunar and solar attraction (the effect of other bodies is negligible). This effect is rather complicated due to the coupling with the ocean tides and the effects of local geology. The vector displacement of the station due to the tidal deformation may be computed from [Seidelmann, 1992]

$$\Delta\underline{\varrho} = \sum_j \left[\frac{GM_j \varrho^4}{GM R_j^3} \right] \left\{ [3l_2(\underline{R}_{0j} \cdot \underline{\varrho}_0)]\underline{R}_{0j} + \left[3\left(\frac{h_2}{2} - l_2\right)(\underline{R}_{0j} \cdot \underline{\varrho}_0)^2 - \frac{h_2}{2}\right]\underline{\varrho}_0 \right\} , \tag{3.8}$$

where

GM_j	is the gravitational parameter for the attracting body j (Moon or Sun),
GM	is the gravitational parameter for the Earth,
$\underline{R}_{0j}$, R_j	is the unit vector from the geocenter to the tide-producing body and the magnitude of that vector,
$\underline{\varrho}_0$, ϱ	is the unit vector from the geocenter to the station and the magnitude of that vector,
h_2	is the nominal second-degree Love number, and
l_2	is the nominal Shida number.

Apart from the expression above [Seidelmann, 1992] introduces a small correction for frequency-dependent Love number h. This correction represents a periodic change in station height with maximum amplitude of about 1 cm.

Ocean Loading

Ocean loading is the elastic response of the earth's crust to ocean tides. Modeling of this effect is rather difficult, several similar models have been proposed in the past decade (see e.g. [Pagiatakis et al., 1982]). The receiver motions caused by ocean loading appear to be limited to approximately 3 cm for sites well removed from the coast. The radial, N–S and E–W components of the displacement vector $\underline{E}(t)$ are given by [Seidelmann, 1992]

$$\underline{E}(t) = \sum_{i=1}^{N} \left\{ \begin{array}{l} A_i^r \cos(\omega_i t + \phi_i - \delta_i^r) \\ A_i^{NS} \cos(\omega_i t + \phi_i - \delta_i^{NS}) \\ A_i^{EW} \cos(\omega_i t + \phi_i - \delta_i^{EW}) \end{array} \right. , \tag{3.9}$$

where ω_i is the frequency of the tidal constituents and ϕ_i the corresponding astronomical argument. The amplitudes A_i^r, A_i^{NS}, A_i^{EW}, and the Greenwich phase lags δ_i^r, δ_i^{NS}, δ_i^{EW} of each tidal component are determined by the particular model assumed for the deformation of the Earth.

Polar Tides

Another secondary tidal effect are the polar tides. It is the elastic response of the earth's crust to displacements of the spin relativ to the principal axis or earth inertia. This effect should be taken into account if centimeter accuracy is desired, especially for measurements spanning an appreciable fraction of a year. According to [Seidelmann, 1992] the radial displacement S_r, and the horizontal displacements S_Θ and S_λ, positive upward, south, and east, respectively, may be computed as

$$S_r = -32 \sin 2\Theta (x_p \cos \lambda - y_p \sin \lambda) \text{ mm} , \tag{3.10}$$

$$S_\Theta = -9 \cos 2\Theta (x_p \cos \lambda - y_p \sin \lambda) \text{ mm} , \tag{3.11}$$

$$S_\lambda = 9 \cos \Theta (x_p \sin \lambda + y_p \cos \lambda) \text{ mm} , \tag{3.12}$$

where Θ is the colatitude, λ is the eastward longitude, and x_p, y_p are expressed in seconds of arc. Taking into account that x_p and y_p vary, at most, 0.3 arcsec, the maximum radial displacement is approximately 10 mm, and the maximum horizontal displacement is about 3 mm.

Plate Motions

The results of investigations in the field of plate motions show that for global high precision networks the following model for the coordinates of stations should be introduced:

$$\underline{r} = \underline{r}_0 + \underline{\dot{r}}_0 (t - t_0) , \tag{3.13}$$

where t is the epoch of measurement, t_0 is a reference epoch, to which the receiver coordinates $\underline{r}_0$ and velocities $\underline{\dot{r}}_0$ refer. Precise reference frames (e.g. the ITRF) contain the velocity vectors $\underline{\dot{r}}_0$ based on geodynamical models in addition to the station coordinates. The time derivations of the coordinates may reach a few centimeters per year.

3.2 Time Scale

In the international system of physical units SI the time unit 1 SI second is defined as fixed multiple of oscillation periods of the resonance frequency which belongs to the transition between two energy levels of the cesium 133. The energy levels and the state of cesium atom are exactly specified. It is important that this definition uses the proper time. Such approach is suitable for most of physical measurements when the experiment and the clock are close together. For the astronomical measurement the difference between the proper time and the coordinate time due to relativistic effects should be taken into account. The following time scales are important for GPS processing:

International Atomic Time (TAI)

International Atomic Time (*Temps Atomique International,* or TAI) is a coordinate timescale defined on the geoid of a "nonrotating Earth". The unit of TAI is the *atomic second.* On the geoid 1 atomic second is equal to 1 SI second. Practically TAI is made available by the dissemination of corrections to be added to the readings of national time scales and clocks.

Universal Coordinated Time UTC

This time is based on TAI but it is keeping close to Universal Time UT1 (see below) by inserting integer leap second at distinct epochs:

$$\text{UTC} = \text{TAI} + n \cdot 1^s \ , \qquad |\text{UT1} - \text{UTC}| < 0.9^s \tag{3.14}$$

UTC is used as civil time due to small difference from UT1.

Time GPS

GPS system time is defined by

$$\text{GPS} = \text{TAI} - 19^s \tag{3.15}$$

This time was selected so that the difference between GPS and UTC was zero at so-called standard GPS epoch on January 6th, 1980.

Universal Time UT1

The Universal Time UT1 is defined by the equation [Seidelmann, 1992]

$$\text{GMST} = \text{GMST of } 0^h \text{UT1} + r \cdot \text{UT1} \ , \tag{3.16}$$

where

$$r = 1.002737909350795 + 5.9006 \cdot 10^{-11} \cdot T_u - 5.9 \cdot 10^{-15} \cdot T_u^2 \ , \tag{3.17}$$

$$T_u = \frac{(\text{Julian UT1 date}) - 2451545.0}{36525} \ , \tag{3.18}$$

and GMST of 0^hUT1 (Greenwich Mean Sidereal Time at 0^h UT1, the Greenwich hour angle of the mean (FK5) equinox of date) may be expressed as

$$\text{GMST of } 0^h\text{UT1} = \tag{3.19}$$
$$6^h41^m50.54841^s + 8640184.812866^s\ T_u + 0.093104^s\ T_u^2 - 6.2^s \cdot 10^{-6} \cdot T_u^3 \ .$$

These expressions produce UT1 which tracks the Greenwich hour angle of the real sun to within 16^m. However, it really is sidereal time, modified to fit our intuitive desire to have the sun directly overhead at noon on the Greenwich meridian. The differences of UT1 from an independent measure of time e.g. the difference

$$\text{UT1} - \text{UTC} \tag{3.20}$$

is used to specify the orientation of the earth.

Julian Date

The Julian Date (JD) defines the number of days elapsed since the epoch 4713 B.C., January 1.5^d. The Modified Julian Date (MJD) is obtained by subtracting 2,400,000.5 days from JD.

Table 3.1: Standard epochs

Civilian Date	Julian Date	Explanation
1980 January 6.0^d	2444244.5	GPS standard epoch
2000 January 1.5^h	2451545.0	Current standard epoch (J2000.0)

In Table 3.1 the standard epochs used at present and the corresponding Julian Dates are shown.

4. Modeling the Satellite Motion

The equation of motion for an artificial earth satellite may be written as

$$\ddot{\underline{r}} = -\frac{GM}{r^3} \cdot \underline{r} + \underline{a}\left(t, \underline{r}, \dot{\underline{r}}, p_1, \ldots, p_n\right) , \tag{4.1}$$

where

$\underline{r}$ or $\underline{r}(t, p_1, \ldots, p_n)$ is the geocentric position vector of the satellite at time t. At the same time $\underline{r}$ represents the coordinate column matrix of this vector in an inertial coordinate system $\underline{r} = (x_1, x_2, x_3)^T$, $r = |\underline{r}|$.

$\dot{\underline{r}}$ and $\ddot{\underline{r}}$ are the first and the second time derivatives of $\underline{r}(t)$.

$GM = \mu$ is the product gravitational constant times mass of the earth.

$\underline{a}$ is the acceleration caused by perturbing forces (see Table 4.1)

p_k, $k = 1, 2, \ldots, n$ are the parameters of the force field to be solved for.

A particular (unique) solution of the differential equation (4.1) may e.g. be defined by

1. supplying initial values (position and velocity) at epoch t_0

$$\begin{aligned}
\underline{r}(t_0) &= \underline{r}_0\,(q_1, q_2, \ldots, q_6) \\
\dot{\underline{r}}(t_0) &= \dot{\underline{r}}_0\,(q_1, q_2, \ldots, q_6)
\end{aligned} \tag{4.2}$$

2. supplying boundary values at epochs t_1 and t_2.

$$\begin{aligned}
\underline{r}(t_1) &= \underline{r}_1\,(q_1, q_2, \ldots, q_6) \\
\underline{r}(t_2) &= \underline{r}_2\,(q_1, q_2, \ldots, q_6)
\end{aligned} \tag{4.3}$$

where the q_i, $i = 1, \ldots, 6$ are six parameters uniquely defining the vectors $\underline{r}_0$ and $\dot{\underline{r}}_0$ or $\underline{r}_1$ and $\underline{r}_2$ respectively. If we know the parameters q_i, $i = 1, \ldots, 6$ and all force model parameters p_j, $j = 1, \ldots, n$ the satellite orbit is uniquely defined and may be computed using numerical integration techniques. The techniques used in the Bernese GPS Software are described in [Beutler, 1990].

The perturbing acceleration $\underline{a}$ consists of a big variety of components, a selection based on [Landau, 1988] is given in Table 4.1.

30

Table 4.1: Effect of perturbing forces on GPS satellites

Perturbing Force	Acceleration [m/s^2]	Orbit Effect [m]	
		After 1 Day	After 7 Days
Earth's oblatness (C_{20})	$5 \cdot 10^{-5}$	10 000	100 000
Non-sphericity of the earth (C_{nm}, S_{nm}, $n, m \leq 8$)	$3 \cdot 10^{-7}$	200	3 400
Non-sphericity of the earth (C_{nm}, S_{nm}, $n, m > 8$)		0.03	0.1
Attraction by the moon	$5 \cdot 10^{-6}$	3 000	8 000
Attraction by the sun	$2 \cdot 10^{-6}$	800	3 500
Earth's tidal potential	$1 \cdot 10^{-9}$	0.3	1.2
Ocean tides	$5 \cdot 10^{-10}$	0.04	0.2
Direct solar rad. pressure	$6 \cdot 10^{-8}$	200	1 000
y-bias effect	$5 \cdot 10^{-10}$	1.4	51
Albedo	$4 \cdot 10^{-10}$	0.03	
Relativistic effects	$3 \cdot 10^{-10}$		

In the Bernese GPS Software Version 3.4 [Rothacher et al., 1993a] the force model consists of

- The earth's gravity potential (complete up to degree and order 8 or higher).
- The gravitational attraction from sun and moon.
- Earth's tidal potential.
- Solar radiation pressure.

4.1 Estimation of Satellite Orbits

For the estimation of the satellite orbits we need observations. Two types of observations may be used used in the Bernese GPS software:

1. Double difference GPS carrier phases and, optionally, code observations.
2. Geocentric satellite positions as fictitious observations. These positions are computed either from broadcast elements or they are given in so-called precise ephemerides files.

In our case orbit determination is always an orbit improvement process. Initially even a Keplerian orbit might be used as a first approximation. In any case, it is necessary to linearize the observation equation. In the linearization scheme below the observation site parameters (coordinates, tropospheric corrections etc.) are disregarded. Be $O(t, \underline{r}(t))$ a GPS observable, then

$$O(t, \underline{r}(t)) = O(t, \underline{r}^a(t)) + \frac{\partial O}{\partial \underline{r}} \cdot (\underline{r}(t) - \underline{r}^a(t)) , \qquad (4.4)$$

where the partial derivation has to be taken at the point $\underline{r}^a(t)$. The improved orbit $\underline{r}(t)$ is defined by equation (4.1) and by the initial conditions (4.2). The approximated orbit $\underline{r}^a(t)$ is defined by the following initial value problem:

$$\underline{\ddot{r}}^a = -\frac{GM}{r^{a3}} \cdot \underline{r}^a + \underline{a}\left(t, \underline{r}^a, \underline{\dot{r}}^a, p_1^a, \ldots, p_n^a\right) \tag{4.5}$$

or, in abbreviated notation:

$$\underline{\ddot{r}}^a = \underline{f} + \underline{a}\ , \tag{4.6}$$

where:

$\underline{f} = (f_1, f_2, f_3)^T$ is the column matrix with the Keplerian term of the force field in the inertial coordinate system,

$\underline{a} = (a_1, a_2, a_3)^T$ is the column matrix with the perturbation terms in the inertial co-ordinate system.

The corresponding initial conditions are

$$\underline{r}^a(t_0) = \underline{r}_0^a\ (q_1^a, q_2^a, \ldots, q_6^a)\ , \quad \underline{\dot{r}}^a(t_0) = \underline{\dot{r}}_0^a\ (q_1^a, q_2^a, \ldots, q_6^a)\ . \tag{4.7}$$

All the approximate values q_i^a, $i = 1, \ldots, 6$ and p_j^a, $j = 1, \ldots, n$ are assumed to be known. The initial value problem (4.5) is solved by numerical integration techniques, where highest accuracy is required [Beutler, 1990]. The integration technique used in Bernese software [Rothacher et al., 1993a] is the following: the arc is divided into subintervals of the same length (1 hour for GPS satellites). Within each subinterval the solution is approximated by a polynomial function of order q (usually $q = 10$ or $q = 12$ is used):

$$\underline{r}(t) = \sum_{i=0}^{q} \underline{c}_i \cdot (t - t_0)^i\ . \tag{4.8}$$

In the *first* subinterval the coefficients $\underline{c}_i$ of the polynomial are defined by asking that

1. the approximating function fulfils the same initial (or boundary) conditions (4.7) as the true solution,

2. the approximating function fulfils the differential equation system (4.5) for $q - 1$ different time arguments t_j, $j = 1, 2, \ldots, q - 1$ in the partial interval.

The solution of a system of differential equations has thus been reduced to the solution of a system of nonlinear algebraic equations. This system is solved iteratively, starting with approximate values for the coefficients $\underline{c}_i$ which are then successively improved. This procedure may be applied in the first subinterval containing the initial epoch resp. the two boundary epochs. In the other partial intervals the polynomial from the preceeding interval has to be used to define new initial conditions at the common interval boundary. The numerical approximation of the orbit is thus defined by several sets of polynomial coefficients. Neglecting rounding errors the approximation errors may be kept below any

given limit and therefore the resulting approximation may be considered as a true solution of the equations of motion. Using the notation

$$\Delta q_i = q_i - q_i^a \ , \quad \Delta p_j = p_j - p_j^a \tag{4.9}$$

the improved orbit $\underline{r}(t)$ may be expressed as

$$\underline{r}(t) = \underline{r}^a(t) + \sum_{i=1}^{6} \underline{z}_{q_i}(t)\Delta q_i + \sum_{j=1}^{n} \underline{z}_{p_j}(t)\Delta p_j \ , \tag{4.10}$$

where

$$\underline{z}_{q_i}(t) = \left(\frac{\partial \underline{r}}{\partial q_i}\right)_{\substack{q=q^a \\ p=p^a}} \ , \quad \underline{z}_{p_j}(t) = \left(\frac{\partial \underline{r}}{\partial p_j}\right)_{\substack{q=q^a \\ p=p^a}} \ . \tag{4.11}$$

The functions $\underline{z}_{q_i}(t)$ and $\underline{z}_{p_j}(t)$ are solutions of the initial value problems we obtain from the primary problem (4.5) and (4.7) by taking the derivative of the equations (4.5) and (4.7) with respect to the parameters q_i, $i = 1,\ldots,6$ and p_j, $j = 1,\ldots,n$ respectively and changing the sequence of derivating with respect to these parameters and with respect to time. Using the abbreviated notation (4.6) we get the so-called *variational equations*

$$\ddot{\underline{z}}_{q_i} = \left(\frac{\partial(\underline{f}+\underline{a})}{\partial \underline{r}}\right)_{\substack{q=q^a \\ p=p^a}} \underline{z}_{q_i} + \left(\frac{\partial(\underline{f}+\underline{a})}{\partial \dot{\underline{r}}}\right)_{\substack{q=q^a \\ p=p^a}} \dot{\underline{z}}_{q_i} \tag{4.12}$$

with the initial conditions

$$\underline{z}_{q_i}(t_0) = \frac{\partial \underline{r}_0^a}{\partial q_i} \ , \quad \dot{\underline{z}}_{q_i}(t_0) = \frac{\partial \dot{\underline{r}}_0^a}{\partial q_i} \tag{4.13}$$

and

$$\ddot{\underline{z}}_{p_j} = \left(\frac{\partial(\underline{f}+\underline{a})}{\partial \underline{r}}\right)_{\substack{q=q^a \\ p=p^a}} \underline{z}_{p_j} + \left(\frac{\partial(\underline{f}+\underline{a})}{\partial \dot{\underline{r}}}\right)_{\substack{q=q^a \\ p=p^a}} \dot{\underline{z}}_{p_j} + \frac{\partial \underline{a}}{\partial p_j} \tag{4.14}$$

with initial conditions

$$\underline{z}_{p_j}(t_0) = \underline{0} \ , \quad \dot{\underline{z}}_{p_j}(t_0) = \underline{0} \ . \tag{4.15}$$

This means that in each iteration step of the orbit improvement process we have to solve one system of differential equations (4.5), six systems of type (4.12), and n systems of type (4.14). The orbit improvement process may then be seen as a standard least-squares adjustment.

4.2 Modeling the Perturbing Forces

4.2.1 Gravitational Effects

Non-Central Part of the Earth Gravitational Potential

The non-spherical part V' of the earth's gravity potential may be represented by a spherical harmonic expansion. In the earth-fixed geocentric system (e.g. the International Terrestrial Reference Frame, ITRF) we may write:

$$V' = \frac{GM}{r} \sum_{n=2}^{\infty} \left(\frac{a_e}{r}\right)^n \cdot \sum_{m=0}^{n} P_{nm}(\sin\beta) \cdot (C_{nm} \cdot \cos m\lambda + S_{nm} \cdot \sin m\lambda) \ . \tag{4.16}$$

where:

a_e is the mean equatorial radius of the earth,

r is the geocentric satellite distance,

λ is the geocentric longitude of the satellite,

β is the geocentric latitude of the satellite,

P_{nm} is the associated Legendre function of degree n and order m,

C_{nm}, S_{nm} are the coefficients of the development (the terms with $m = 0$ are the zonal, those with $m = n$ the sectorial, and those with $m \neq 0$, $m \neq n$ are the tesseral coefficients).

The perturbing acceleration $\underline{a}_v(t)$ due to the non-sphericity of the earth's potential is then given by:

$$\underline{a}_v(t) = \boldsymbol{P}^T(t) \cdot \boldsymbol{N}^T(t) \cdot \boldsymbol{R}_3(-GAST) \cdot \boldsymbol{R}_1(y_p) \cdot \boldsymbol{R}_2(x_p) \cdot \vec{\nabla}V' \qquad (4.17)$$

where

the matrices $\boldsymbol{P}^T(t)$, $\boldsymbol{N}^T(t)$, $R_3(-\Theta)$, $R_1(y_p)$ and $R_2(x_p)$ are used for the transformation from the earth-fixed into the inertial coordinate system – see 3.1),

$\vec{\nabla}V'$ is the gradient of the non-spherical geopotential.

Supposing that $\underline{r} = (x_1, x_2, x_3)^T$ are the cartesian coordinates of the satellite in the earth-fixed system, the gradient $\vec{\nabla}V'$ may be computed as

$$\vec{\nabla}V' = \underbrace{\begin{pmatrix} \partial r/\partial x_1 & \partial\beta/\partial x_1 & \partial\lambda/\partial x_1 \\ \partial r/\partial x_2 & \partial\beta/\partial x_2 & \partial\lambda/\partial x_2 \\ \partial r/\partial x_3 & \partial\beta/\partial x_3 & \partial\lambda/\partial x_3 \end{pmatrix}}_{\boldsymbol{D}} \cdot \begin{pmatrix} \partial V'/\partial r \\ \partial V'/\partial\beta \\ \partial V'/\partial\lambda \end{pmatrix} \qquad (4.18)$$

where

$$\frac{\partial V'}{\partial r} = -\frac{GM}{r^2} \sum_{n=2}^{\infty} \left(\frac{a_e}{r}\right)^n \cdot (n+1) \cdot \sum_{m=0}^{n} P_{nm}(\sin\beta) \cdot$$
$$\cdot (C_{nm} \cdot \cos m\lambda + S_{nm} \cdot \sin m\lambda) \qquad (4.19)$$

$$\frac{\partial V'}{\partial\beta} = \frac{GM}{r} \sum_{n=2}^{\infty} \left(\frac{a_e}{r}\right)^n \cdot \sum_{m=0}^{n} [P_{nm+1}(\sin\beta) - m \cdot \tan\beta \cdot P_{nm}(\sin\beta)] \cdot$$
$$\cdot (C_{nm} \cdot \cos m\lambda + S_{nm} \cdot \sin m\lambda) \qquad (4.20)$$

$$\frac{\partial V'}{\partial\lambda} = \frac{GM}{r} \sum_{n=2}^{\infty} \left(\frac{a_e}{r}\right)^n \cdot \sum_{m=0}^{n} m \cdot P_{nm}(\sin\beta) \cdot$$
$$\cdot (-C_{nm} \cdot \sin m\lambda + S_{nm} \cdot \cos m\lambda) \qquad (4.21)$$

and the elements of the matrix $\boldsymbol{D}$ are given by

$$\frac{\partial r}{\partial x_1} = \frac{x_1}{r} \ , \quad \frac{\partial r}{\partial x_2} = \frac{x_2}{r} \ , \quad \frac{\partial r}{\partial x_3} = \frac{x_3}{r} \qquad (4.22)$$

$$\frac{\partial \beta}{\partial x_1} = \frac{-x_1 x_3}{r^2 \sqrt{x_1^2 + x_2^2}} \,, \quad \frac{\partial \beta}{\partial x_2} = \frac{-x_2 x_3}{r^2 \sqrt{x_1^2 + x_2^2}} \,, \quad \frac{\partial \beta}{\partial x_3} = \frac{\sqrt{x_1^2 + x_2^2}}{r^2} \tag{4.23}$$

$$\frac{\partial \lambda}{\partial x_1} = \frac{-x_2}{x_1^2 + x_2^2} \,, \quad \frac{\partial \lambda}{\partial x_2} = \frac{x_1}{x_1^2 + x_2^2} \,, \quad \frac{\partial \lambda}{\partial x_3} = 0 \tag{4.24}$$

Because the GPS satellites are in high altitude orbits, they are much less affected by the short wavelength terms of the geopotential than low orbiting satellites. Therefore it is usually sufficient to use an earth potential model up to degree and order 8 [Beutler et al., 1985] and to assume that the potential coefficients C_{nm}, S_{nm} are known. Nevertheless it it possible to estimate some coefficients too. In that case the partial derivative $\underline{a}_p(t)$ of the gravitational acceleration $\underline{a}(t)$ has to be computed as

$$\underline{a}_p(t) = \boldsymbol{P}^T(t) \cdot \boldsymbol{N}^T(t) \cdot \boldsymbol{R}_3(-GAST) \cdot \boldsymbol{R}_1(y_p) \cdot \boldsymbol{R}_2(x_p) \cdot$$

$$\tag{4.25}$$

$$\vec{\nabla} \left[\frac{GM}{r} \left(\frac{a_e}{r} \right)^n \cdot P_{nm}(\sin \beta) \cdot \left\{ \begin{array}{l} \cos m\lambda \\ \sin m\lambda \end{array} \right] \begin{array}{l} \text{if} \quad p = C_{nm} \\ \text{if} \quad p = S_{nm} \end{array} \right.$$

Direct Gravitational Effects of Moon, Sun and Planets

The gravitational perturbations due to third bodies are caused only by the difference between the force on the satellite and that on the earth. The perturbing acceleration is given by

$$\underline{a}(t) = -G \sum_i M_i \left(\frac{\underline{r} - \underline{r}_i}{|\underline{r} - \underline{r}_i|^3} + \frac{\underline{r}_i}{|\underline{r}_i|^3} \right) \tag{4.26}$$

where

$\underline{r}$ is the geocentric position vector of the satellite,

$\underline{r}_i$ is the geocentric position vector of the third body (moon, sun etc.) and

M_i is the mass of the corresponding third body.

In the Bernese software only the perturbations due to the moon and the sun are considered. According to [Landau and Hagmaier, 1986] the total effect on the GPS orbit due to all planets is only about 30 cm for an arc of one week.

Solid Earth Tides and Ocean Loading

The gravitational attraction of third bodies also has an indirect effect on the satellite orbit due to the tidal deformations of the earth's gravity potential. The perturbing acceleration due to the potential caused by the solid earth tides may be found in [Melchior, 1983]:

$$\underline{a}(t) = k_2 \frac{G a_e^5}{|\underline{r}|^4} \sum_i \frac{M_i}{|\underline{r}_i|^3} \left(P_2'(\cos z_i) \frac{\underline{r}}{|\underline{r}|} - P_3'(\cos z_i) \frac{\underline{r}_i}{|\underline{r}_i|} \right) \tag{4.27}$$

where the same notation as in equation (4.26) is used. k_2 is Love number of degree 2, the angle z_i is defined by

$$\cos z_i = \frac{\underline{r} \cdot \underline{r}_i}{|\underline{r}| \, |\underline{r}_i|} \tag{4.28}$$

35

and

$$P_2'(\cos z_i) = 3 \cdot \cos z_i \ , \quad P_3'(\cos z_i) = \frac{3}{2} \cdot (5 \cdot \cos^2 z_i - 1) \tag{4.29}$$

In the Bernese software only the contributions due to moon and sun are considered.

Ocean loading is the elastic response of the earth's crust to ocean tides. The most complete model for ocean loading appears to be that described by [Pagiatakis et al., 1982]. It should be noted that this effect is difficult to model because the ocean waves caused by the moon and the sun cannot propagate without friction and interact with the sea floor too (shallow waters). Therefore the acceleration of the order $5 \cdot 10^{-10}$ m.s^{-2} [Landau, 1988] due to ocean loading is neglected in our model.

4.2.2 Solar Radiation Pressure

The modeling of the solar radiation pressure seems to be the most difficult part in the force model due to the complicated shape and changes of the orientation of the satellites. Resulting perturbing acceleration is quite large. The neglection of this effect will result in orbit errors of the order of 200 m for one day arc. Since the orientation of the orbits with respect to the sun changes slowly, solar radiation also causes considerable resonance effects [Rothacher, 1991]. The effect of the solar radiation pressure may be divided into two parts:

1. direct radiation pressure (drp) and

2. earth albedo radiation pressure (arp).

Direct Radiation Pressure

As a priori models for the direct radiation pressure we use the ROCK 4 model (for Block I satellites) and the ROCK 42 model (for Block II satellites). [Fliegel et al., 1992]. Fliegel makes the distinction between the S- and T-models (T-models include thermal re-radiation). Both are implemented in the Bernese software, at present we are using the T10-model for the Block I satellites and the T20-model for Block II satellites. In principle the models are based on the equation [Cappellari et al., 1976]

$$\underline{a} = \nu \cdot \left[P_s \cdot a_s^2 \cdot \frac{(1+\eta) \, A}{m} \cdot \frac{\underline{r} - \underline{r}_\odot}{|\underline{r} - \underline{r}_\odot|^3} + \underline{a}_y \right] \tag{4.30}$$

where

ν is the eclipse factor

$\nu = 0$ if the satellite is in the shadow
$\nu = 1$ if the satellite is in the sunlight
$0 < \nu < 1$ if the satellite is in the penumbra

P_s is the radiation pressure of the sun acting on an ideal absorbing body in a distance of 1 Astronomical Unit. According to [Willson, 1978] $P_s = 4.5605 \cdot 10^{-6}$ N.m^{-2},

a_s is the Astronomical Unit (semi-major axis of the earth's orbit around the sun),

$(1 + \eta)$ is reflection coefficient depending on the reflective properties of the material,

A is effective cross-section area of the satellite,

m is mass of the satellite,

$\underline{r}$ is geocentric position of the satellite,

$\underline{r}_\odot$ is geocentric position of the sun and

$\underline{a}_y$ is acceleration perpendicular to the incident radiation, this acceleration has the direction of the y-axis in a satellite fixed coordinate system (see Figure 1.1) and is therefore called y-bias. The y-bias is caused probably by a misalignment of the solar panels and the asymmetric thermal radiation (preferably in the direction of the y-axis).

The ROCK 4 and ROCK 42 models depict the satellite as a number of flat or cylindrical surfaces. For each surface element the reflexion coefficient η and the coefficient μ for the so-called diffusion reflexion are assumed to be known. The resulting acceleration caused by each surface element depends on these two coefficients, on the shape of the surface (flat or cylindrical) and on the angle θ between the normal of the surface and the direction to the sun. The y-bias is considered to be constant. The details may be found in [Fliegel et al., 1992]. However the modeling is extremely difficult because the factor P_s may vary in an unpredictable way over the year, the values of the coefficients η and μ are not exactly known (and might not be constant in time), because the shadowing effect due to the antennas and the satellite body is not considered, and because the orientation of the satellite with respect to inertial system is not perfect as it should. For all these reasons we use the following model [Beutler et al., 1994a]

$$\underline{a}_{\mathrm{drp}} = \underline{a}_{\mathrm{Rock}} + X_1(t) \cdot \underline{e}_1 + X_2(t) \cdot \underline{e}_2 + X_3(t) \cdot \underline{e}_3 \qquad (4.31)$$

where the unit vectors $\underline{e}_i$, $i = 1, 2, 3$ are defined by

$$\underline{e}_1 = \frac{\underline{r} - \underline{r}_\odot}{|\underline{r} - \underline{r}_\odot|}, \qquad \underline{e}_2 = \underline{e}_y, \qquad \underline{e}_3 = \underline{e}_1 \times \underline{e}_2 \qquad (4.32)$$

The vector $\underline{e}_y$ is one of the unit vectors of the satellite fixed coordinate system. The vectors $\underline{e}_x$, $\underline{e}_y$ and $\underline{e}_z$ ($\underline{e}_z$ has the direction from the satellite to the center of the earth) and hence the orientation of the satellite are defined by the following equations:

$$\underline{e}_z = -\frac{\underline{r}}{|\underline{r}|}, \qquad \underline{e}_y = \frac{\underline{e}_z \times (\underline{r} - \underline{r}_\odot)}{|\underline{e}_z \times (\underline{r} - \underline{r}_\odot)|}, \qquad \underline{e}_x = \underline{e}_y \times \underline{e}_z \qquad (4.33)$$

It is easy to verify that the vectors $\underline{e}_i$, $i = 1, 2, 3$ are orthogonal and form a right-handed system. The coefficients $X_i(t)$, $i = 1, 2, 3$ are modeled with *three* parameters each:

$$X_i(t) = X_{0i} + A_i \cdot \cos(u + \phi_i), \qquad i = 1, 2, 3 \qquad (4.34)$$

where $u = v(t) + \omega \approx M(t) + \omega$ is the argument of latitude. In the actual parameter estimation it is not possible to solve directly for the phase angles ϕ_i, but we have to introduce auxiliary unknowns $X_{Ci} = A_i \cdot \cos\phi_i$, $X_{Si} = -A_i \cdot \sin\phi_i$ and our model is

$$X_i(t) = X_{0i} + X_{Ci} \cdot \cos(M + \omega) + X_{Si} \cdot \sin(M + \omega) , \quad i = 1, 2, 3 \qquad (4.35)$$

The test results with this new radiation pressure model were of the same quality whether or not the Rock 4, Rock 42 term $\underline{a}_{Rock}$ was used in the equation (4.31) [Beutler et al., 1994a]. This is due to the fact that the major part of the term $\underline{a}_{Rock}$ may be absorbed by the terms (4.35).

Albedo Radiation Pressure

The earth and its atmosphere reflect some of the received solar radiation back into space. The albedo radiation pressure is caused by this reflected radiation. The modeling of the resulting acceleration is more complicated than that of the direct radiation pressure because of the necessity to integrate over all surface elements of the earth illuminated by the sun. On the other hand this acceleration is small (see Table 4.1) and therefore we adopt the following simplifications:

1. all surface elements $d\sigma$ have the same diffusion properties (we do not distinguish between land, sea, clouds etc.) and

2. the total power (energy per time unit) received by the element $d\sigma$ is proportional to $\cos z_\odot \cdot d\sigma$ according to Lambert's law ($z_\odot$ is the angle between the normal of the surface element and the direction to the source of the radiation – in our case $z_\odot$ is the zenith angle of the sun). The energy reradiated into a direction with the zenith distance z is proportional to $\cos z \cdot \cos z_\odot \cdot d\sigma$.

The radiation received at the satellite position on a unit surface normal to the direction surface element $\rightarrow$ satellite is then proportional to $\cos z_\odot \cdot \cos z \cdot d\sigma / \varrho^2$. For a spherical satellite the resulting acceleration may be modeled by

$$\underline{a} = \int_\Omega p \cdot \frac{A\,(1+\eta)}{m} \cdot \frac{\cos z_\odot \cdot \cos z}{\varrho^2}\,d\sigma \qquad (4.36)$$

where ϱ and z are the topocentric distance and zenith angle of the satellite seen from the earth's surface element $d\sigma$, A is the cross-section of the satellite, $(1 + \eta)$ is the reflection coefficient, m is the mass of the satellite, and p is unknown parameter of the model. The integration must be performed over all the illuminated surface elements of the earth. [Beutler et al., 1994a] introduces such a model for GPS satellites and depict the GPS satellite into two parts – the spherically symmetrical central body and the solar panels. The sunlit semi-sphere of the earth is divided into $n \cdot m$ surface elements with the same surface area (n is the number of zones, m the number of sectors) and the integration is approximated by a summation over these elements.

Eclipses

The radiation pressure (direct and albedo) vanishes if the satellite enters into the earth's shadow. Each GPS satellite has two eclipse seasons per year, each lasting for about seven weeks. In the Bernese software a simple cylinder model for the shadow of the earth is used. The shadow coefficient ν in equation (4.30) is given by

$$\nu = \begin{cases} 0 & \text{if} \quad \cos\gamma = \frac{\underline{r} \cdot \underline{r}_\odot}{|\underline{r} \cdot \underline{r}_\odot|} < 0 \quad \text{and} \quad |\underline{r}| \sqrt{1 - \cos^2\gamma} < a_e \\ 1 & \text{else} \end{cases} \tag{4.37}$$

The orbit quality during eclipse seasons may be considerably degraded for a number of reasons (e.g. penumbra problem, but also attitude control problems).

Further Perturbations and Empirical Modeling

There are further small perturbing accelerations which are not considered in our force model. The first one is a part of the *general relativistic effect* due to the gravity field of the earth. This effect is described in [Zhu et al., 1987]. The second effect – atmospheric drag – due to the interaction with the particles of the atmosphere is very small for GPS satellites which are very far from the earth's surface. It should be mentioned that the parameters of the radiation pressure model (4.35) may also absorb unmodeled perturbations. In this sense our force model is close to the model proposed by [Colombo, 1989]. Colombo's empirical model is based on the assumption that many of the small unmodeled forces acting on GPS satellites are either constant or periodic with the satellites' revolution times as basic periods. The perturbing accelerations may be developed into a Fourier series. Using the (R,S,W) components (R=radial, S=perpendicular to R in the orbital plane and W=out of plane) the acceleration may be expressed as

$$\underline{a} = \sum_{i=0}^{\infty} \begin{pmatrix} R_{Ci} \cdot \cos iM + R_{Si} \cdot \sin iM \\ S_{Ci} \cdot \cos iM + S_{Si} \cdot \sin iM \\ W_{Ci} \cdot \cos iM + W_{Si} \cdot \sin iM \end{pmatrix} \tag{4.38}$$

[Colombo, 1989] suggests to consider only the terms $i = 0$ and $i = 1$. The resulting model

$$\underline{a} = \begin{pmatrix} R_0 + R_{C1} \cdot \cos M + R_{S1} \cdot \sin M \\ S_0 + S_{C1} \cdot \cos M + S_{S1} \cdot \sin M \\ W_0 + W_{C1} \cdot \cos M + W_{S1} \cdot \sin M \end{pmatrix} \tag{4.39}$$

is similar to the model (4.35) proposed by [Beutler et al., 1994a]. The difference is subtle, but important. In both cases we have a set of three orthogonal forces which are rotating once per satellite revolution in the inertial space. But the rotation axes and the angular velocities of the rotation of the two systems are different: in Colombo's model the rotation axis is normal to the orbital plane and the angular velocity is uniform, in Beutler's model the rotation axis is the direction satellite ↔ sun and the angular velocity depends on the inclination of the orbit with respect to the terminator plane. [Beutler et al., 1994a] claim that with the same number of parameters (9 parameters) the model (4.35) gives significantly better results than the model (4.39).

5. Modeling the GPS Observables

5.1 Phase Pseudoranges

In the Section 1.3.3 we described the principle of the signal processing. In this section we want to introduce the observation equations. We assume that the both oscillators (satellite and receiver) are biased and their frequencies f_F^i and f_{Fk} are generally not identical and equal to the nominal frequency f_F. It should be mentioned that we simplify our notation and we do not distinguish explicitly between different reference frames. More exactly we should say that e.g. f_F^i is not equal to the nominal frequency in satellite-fixed reference frame. We use the fact that the receiver compares the phases of two signals and that the phases are *invariant with respect to the Lorentz transformation*. Let us introduce the following notation:

t_p is the epoch of the measurement (GPS system time), to this time all the quantities should be referred,

$\psi_{Fk}^i(t_p)$ is the phase measurement (in cycles) for the epoch t_p, i is a satellite index, k is the receiver index and F is the frequency index,

$\phi_F^i(t^i)$ is the phase of the carrier at the emission time t^i (reading of the satellite clock),

$\phi_{Fk}(t_k)$ is the phase generated by receiver at signal reception time t_k (reading of the receiver clock),

n_{Fk}^i is the unknown integer number of cycles (so-called ambiguity), and

$\epsilon_{Fk}^i(t_p)$ is the measurement noise.

Using this notation we can write the initial form of the observation equation [Remondi, 1985b] :

$$\psi_{Fk}^i(t_p) = \phi_F^i(t^i) - \phi_{Fk}(t_k) - n_{Fk}^i + \epsilon_{Fk}^i(t_p) \ . \tag{5.1}$$

The signal reception time t_k may be written as:

$$t_k = t_p + \delta_k(t_p) \ , \tag{5.2}$$

where $\delta_k(t_p)$ is the error of the receiver clock at time t_p with respect to GPS system time. Similarly, the emission time t^i may be written as:

$$t^i = t_p + \delta_k(t_p) - \tau(t_k, t^i) \ , \tag{5.3}$$

where $\tau(t_k, t^i)$ is the signal travel time (about 0.07 seconds). According to [McCaskill et al., 1985] the stability of the satellite oscillator $\Delta f^i / f^i$ is about 10^{-13} within one second. The stability of the receiver clocks is only of the order of 10^{-11} [Remondi, 1985a]. Thanks to such a high stability of the oscillators the following approximations may be used:

$$\phi_F^i(t^i) = \phi_F^i(t_p) + (\delta_k(t_p) - \tau(t_k, t^i))\, f_F^i \, , \tag{5.4}$$

$$\phi_{Fk}(t_k) = \phi_{Fk}(t_p) + \delta_k(t_p)\, f_{Fk} \, , \tag{5.5}$$

where f_{Fk} is the frequency of the receiver oscillator and f_F^i is the frequency of the satellite oscillator. Substituting last two equations into the equation (5.1) yields:

$$\psi_{Fk}^i(t_p) = \phi_F^i(t_p) + \delta_k(t_p)\,(f_F^i - f_{Fk}) - f_F^i\,\tau(t_k, t^i) - \phi_{Fk}(t_p) - n_{Fk}^i + \epsilon_{Fk}^i(t_p) \, , \tag{5.6}$$

Let us assume that the phase of an ideal oscillator is exactly zero at time t_0. Then the phases of the satellite and receiver oscillators at time t_0 are

$$\phi_F^i(t_0) = f_F\,(-\delta^i(t_0)) \, , \quad \phi_{Fk}(t_0) = f_F\,(-\delta_k(t_0)) \, . \tag{5.7}$$

The last two equations define the satellite clock error $\delta^i(t_0)$ at time t_0 and the receiver clock error $\delta_k(t_0)$ at time t_0. The phases of both signals at time t_p are then expressed as

$$\phi_F^i(t_p) = \int_{t_0}^{t_p} f_F^i(t)\, \mathrm{d}t + \phi_F^i(t_0) \, , \tag{5.8}$$

$$\phi_{Fk}(t_p) = \int_{t_0}^{t_p} f_{Fk}(t)\, \mathrm{d}t + \phi_{Fk}(t_0) \, . \tag{5.9}$$

The integrals on the right hand side are (according to definition of δ^i and δ_k)

$$\int_{t_0}^{t_p} f_F^i(t)\, \mathrm{d}t = f_F \cdot \left(t_p - \delta^i(t_p) - (t_0 - \delta^i(t_0))\right) \, , \tag{5.10}$$

$$\int_{t_0}^{t_p} f_{Fk}(t)\, \mathrm{d}t = f_F \cdot \left(t_p - \delta_k(t_p) - (t_0 - \delta_k(t_0))\right) \, , \tag{5.11}$$

which finally yields

$$\phi_F^i(t_p) - \phi_{Fk}(t_p) = f_F \cdot \left(\delta_k(t_p) - \delta^i(t_p)\right) \, . \tag{5.12}$$

Substituting this expression into the equation (5.6) the observation equation takes on the form

$$\psi_{Fk}^i(t_p) = \delta_k(t_p)\,(f_F^i - f_{Fk}) - f_F^i\,\tau(t_k, t^i) + f_F\left(\delta_k(t_p) - \delta^i(t_p)\right) - n_{Fk}^i + \epsilon_{Fk}^i(t_p) \, . \tag{5.13}$$

In equation (5.13) all the terms are referred to the time t_p. The only exception is the signal travel time $\tau(t_k, t^i)$. We may assume this time interval to be a function of reception time t_k and expand it into a Taylor series with the time t_p as an origin. Because the second time derivative is negligible (at maximum $8.7 \cdot 10^{-10}$ s^{-1} according to [Landau, 1988]) we have:

$$t_k - t^i = \tau(t_k) = \tau(t_p) + \frac{\mathrm{d}}{\mathrm{d}t}\tau(t_p)\, \delta_k(t_p) \, . \tag{5.14}$$

Substituting this expression into equation (5.13) the observation equation is given by

$$\psi_{Fk}^i(t_p) = \delta_k(t_p)\left(f_F^i - f_{Fk} - f_F^i\,\frac{\mathrm{d}}{\mathrm{d}\,t}\tau(t_p)\right) - f_F^i\,\tau(t_p) + f_F\left(\delta_k(t_p) - \delta^i(t_p)\right) - n_{Fk}^i + \epsilon_{Fk}^i(t_p)\;.$$

(5.15)

Because of the high stability of the satellite oscillator $(\Delta f_F^i/f_F^i \approx 10^{-13})$ it is possible to neglect the difference between the nominal frequency f_F and the frequency of the satellite oscillator f_F^i:

$$\psi_{Fk}^i(t_p) = \delta_k(t_p)\left(2f_F - f_{Fk} - f_F\,\frac{\mathrm{d}}{\mathrm{d}\,t}\tau(t_p)\right) - f_F\,\tau(t_p) - f_F\,\delta^i(t_p) - n_{Fk}^i + \epsilon_{Fk}^i(t_p)\;.\quad(5.16)$$

The terms $2\delta_k(t_p)\,f_F$ and $\delta_k(t_p)\,f_{Fk}$ only depend on the receiver and are the same for all satellites. On the contrary the term $f_F\,\delta^i(t_p)$ depends on the satellite only and remains the same for all receivers which receive the signal from one satellite. These terms may be eliminated using the double difference techniques like e.g. in the Bernese GPS software [Rothacher et al., 1993a]. Let us denote the geometrical distance between the satellite (at the emission time) and the receiver (at the reception time) $\varrho_k^i(t_p) = \tau(t_p)\,c$, where c is the velocity of light (this distance is biased by tropospheric and ionospheric delays). Then

$$f_F\,\frac{\mathrm{d}}{\mathrm{d}\,t}\tau(t_p) = \frac{1}{\lambda_F}\frac{\mathrm{d}}{\mathrm{d}\,t}\varrho_k^i(t_p)\;,$$

(5.17)

where $\lambda_F = c/f_F$ is the carrier wavelength. Multiplying equation (5.16) by $-\lambda_F$ and using the notation

$$L_{Fk}^i = -\lambda_F\,\psi_{Fk}^i\;,\quad \Delta^i = c\,\delta^i(t_p)\;,\quad \Delta_k = 2\,c\,\delta_k(t_p) - c\,\delta_k(t_p)\frac{f_{Fk}}{f_F}\;,\quad w_{Fk}^i = \lambda_F\,\epsilon_{Fk}^i\quad(5.18)$$

we get the observation equation in the "final" form:

$$L_{Fk}^i = \varrho_k^i + \delta_k\,\dot{\varrho}_k^i + \lambda_F\,n_{Fk}^i + \Delta^i - \Delta_k - w_{Fk}^i\;.$$

(5.19)

5.2 Code Pseudoranges

Using the known codes modulated on the GPS carriers, the GPS receivers are able to measure directly the biased travel time τ of the signal. Because the bias is caused by satellite and receiver clock errors the distance $c \cdot \tau$ is called the *pseudorange* between the satellite and the receiver. Using the same notation as in the previous section we may write

$$P_{Fk}^i = c\left[t_k - \delta_k(t_p) - (t^i - \delta^i(t^i))\right] + K_{Fk} + w_{Fk}^i\;,$$

(5.20)

where K_{Fk} is the difference between the reference time for the detection of the signal and the reference time for the generation of the signal in receiver [Landau, 1988]. K_{Fk} remains constant for each receiver channel. Due to the high stability of the satellite oscillator we may exchange $\delta^i(t^i)$ and $\delta^i(t_p)$. Thus the last equation gets the form

$$P_{Fk}^i = c\left[(t_k - \delta_k(t_p) - (t^i - \delta^i(t_p))\right] + K_{Fk} + w_{Fk}^i\;.$$

(5.21)

Using equations (5.14) and (5.17) we get:

$$P_{Fk}^i = \varrho_k^i + \delta_k(t_p)\,\frac{\mathrm{d}}{\mathrm{d}\,t}\varrho_k^i - c\,\delta_k(t_p) + c\,\delta^i(t_p) + K_{Fk} + w_{Fk}^i\;.$$

(5.22)

5.3 Biases

The phase measurements (equation (5.19)), and the code pseudoranges (equation (5.22)) are affected by both, systematic errors and random noise. The errors sources may be classified according to [Hoffman-Wellenhof et al., 1992] into three groups, namely *satellite related errors*, *propagation medium related errors*, and *receiver related errors*. Some of these biases are listed in Table 5.1.

Table 5.1: Range biases

Source	Effect
Satellite	Orbital errors (if not estimated)
	Clock biases
	Antenna offsets
	Antenna phase center variations
Signal propagation	Tropospheric refraction
	Ionospheric refraction
Receiver	Antenna phase center variations
	Clock biases

5.3.1 Forming Differences

Using the differencing techniques as e.g. described by [King et al., 1985] or [Wells et al., 1986] allows us to eliminate or reduce some of the mentioned biases. Let us define the *single difference operator* (between a pair of receivers) by

$$d(X_k^i, X_l^i) = X_k^i - X_l^i = X_{kl}^i , \tag{5.23}$$

and the *double difference operator* (between a pair of receivers and between a pair of satellites) by

$$dd(X_k^i, X_l^i, X_k^j, X_l^j) = X_{kl}^i - X_{kl}^j = X_{kl}^{ij} . \tag{5.24}$$

Applying the double difference operator in equation (5.19) we get:

$$L_{Fkl}^{ij} = \varrho_{kl}^{ij} + \delta_k \cdot (\dot{\varrho}_k^i - \dot{\varrho}_k^j) - \delta_l \cdot (\dot{\varrho}_l^i - \dot{\varrho}_l^j) + \lambda_F \, n_{Fkl}^{ij} - w_{Fkl}^{ij} , \tag{5.25}$$

where F denotes the frequency, k, l are the receiver indices and i, j are the satellite indices. The maximum radial velocity $\dot{\varrho}_k^i$ in the case of a stationary receiver is about 900 m.s^{-1} and therefore the clock bias δ_k should be known with an accuracy of about 10^{-6} s if the millimeter accuracy is required. The receiver clock biases are estimated with an accuracy better than 10^{-6} s using the code pseudoranges [Schildknecht, 1986] which allows to correct the phase measurements. By transfering these corrections into the absolute term L_{Fkl}^{ij} the (double difference) observation equation may be written in the very simple form:

$$L_{Fkl}^{ij} = \varrho_{kl}^{ij} + \lambda_F \, n_{Fkl}^{ij} - w_{Fkl}^{ij} , \tag{5.26}$$

Double differences are the basic observables in the Bernese GPS software [Rothacher et al., 1993a] and the mathematical correlations of the observations are taken into account [Beutler et al., 1986] .

Using double difference observations $L_{Fkl}^{ij}(t)$ from two different epochs t_1 and t_2 the triple difference may be formed (the noise is neglected):

$$L_{Fkl}^{ij}(t_2) - L_{Fkl}^{ij}(t_1) = \varrho_{kl}^{ij}(t_2) - \varrho_{kl}^{ij}(t_1) \ . \tag{5.27}$$

In the above equation we assumed that the unknown ambiguity parameter n_{Fkl}^{ij} remained unchanged within the time interval $< t_1, t_2 >$ and therefore the phase ambiguity bias was eliminated. This is indeed true if the receiver did not loose lock within this time interval and no cycle slip (see Section 6.2) occurred.

5.3.2 Atmospheric Effects

In equation (5.26) the ionospheric delay, the tropospheric delay, and the relativistic effects are not given explicitly. After separating these terms from the geometric double difference distance ϱ_{kl}^{ij} the observation equation reads as

$$L_{Fkl}^{ij} = \varrho_{kl}^{ij} - \Delta_{ion} + \Delta_{trop} - \Delta_{rel} + \lambda_F \, n_{Fkl}^{ij} - w_{Fkl}^{ij} \ , \tag{5.28}$$

where

ϱ_{kl}^{ij} is now the unbiased double difference distance,

Δ_{ion} is the ionospheric refraction correction,

Δ_{trop} is the tropospheric refraction correction, and

Δ_{rel} is the correction due to the theory of relativity.

Phase and Group Velocity

Let us assume that a single electromagnetic wave with wavelength λ and frequency f propagates through the atmosphere. The velocity of its phase

$$v_{ph} = f \, \lambda \tag{5.29}$$

is called *phase velocity*. The carrier waves L_1 and L_2 are propagating with this velocity. Actually every radio signal is composed of many electromagnetic waves with slightly different frequencies. The signal width is the difference between the highest and the lowest frequency. The energy propagates with the so-called group velocity. Let us assume two different frequencies f and f'. Their elongations are given by

$$y = A \, \sin \left[2\pi \cdot \left(f \, t - \frac{x}{\lambda} \right) \right] \ , \quad y' = A \, \sin \left[2\pi \cdot \left(f' \, t - \frac{x}{\lambda'} \right) \right] \ , \tag{5.30}$$

where x is the distance from the transmitter. The summation of both waves $y + y'$ results in signal with periodical changes of the amplitude with the frequency

$$f_{gr} = \frac{f - f'}{2} \tag{5.31}$$

and with the width of the group of waves

$$\frac{1}{\lambda_{gr}} = \frac{1}{2} \cdot \left(\frac{1}{\lambda} - \frac{1}{\lambda'} \right) \tag{5.32}$$

The propagation velocity of the group of waves (and of the energy) is given by

$$v_{gr} = \lambda_{gr} \; f_{gr} = -\frac{f - f'}{\lambda - \lambda'} \cdot \lambda\lambda' \; . \tag{5.33}$$

For slightly different frequencies the group velocity may be expressed as

$$v_{gr} = -\frac{\mathrm{d}f}{\mathrm{d}\lambda} \; \lambda^2 \; . \tag{5.34}$$

Forming the total differential of equation (5.29) and using equation (5.34) we obtain the *Rayleigh's equation*:

$$v_{gr} = v_{ph} - \lambda \, \frac{\mathrm{d}\, v_{ph}}{\mathrm{d}\,\lambda} \; . \tag{5.35}$$

The refractive indices n_{ph} and n_{gr} are defined

$$n_{ph} = \frac{c}{v_{ph}} \; , \qquad n_{gr} = \frac{c}{v_{gr}} \; . \tag{5.36}$$

Differentiation of the phase velocity with respect to λ yields

$$\frac{1}{n_{gr}} = \frac{1}{n_{ph}} \left(1 + \lambda \, \frac{1}{n_{ph}} \frac{\mathrm{d}\, n_{ph}}{\mathrm{d}\,\lambda} \right) \; . \tag{5.37}$$

Using approximation $(1 + \varepsilon)^{-1} = 1 - \varepsilon$ yields so called *modified Rayleigh's equation*

$$n_{gr} = n_{ph} - \lambda \, \frac{\mathrm{d}\, n_{ph}}{\mathrm{d}\,\lambda} \; . \tag{5.38}$$

Ionospheric Refraction

The ionosphere (the part of the earth's atmosphere containing free electrons) extends from about 50 km to 1 000 km above the earth's surface. The ionosphere is a *dispersive medium* for the GPS radio signals, which means that the refractive index is frequency-dependent. The influence of the ionosphere on the propagation of the electromagnetic waves is called *ionospheric refraction*. According to [Stein, 1982] or [Seeber, 1989] we may write

$$n_{ph} = 1 - \frac{k}{f^2} \; , \qquad k = 40.3 \; N_e \; [\mathrm{Hz^2m^3}] \; , \tag{5.39}$$

where N_e is the electron density (i.e. number of free electrons per m³). The modified Rayleigh's equation yields

$$n_{gr} = 1 + \frac{k}{f^2} \; . \tag{5.40}$$

A consequence of the last two equations is the delay of GPS code measurements and the advance of carrier phases. The effect has the same absolute value for code and phase

measurements, but the signs are opposite. As a consequence of the Fermat's principle, the measured range s is

$$s = \int n \, \mathrm{d}s \, , \tag{5.41}$$

where the integral is extended along the path of the signal. The unbiased distance results for $n \equiv 1$:

$$s_0 = \int \mathrm{d}s \, . \tag{5.42}$$

Thus the ionospheric refraction $s - s_0$ may be written as

$$\Delta_{ion,ph} = - \int \frac{k}{f^2} \, \mathrm{d}s = -\Delta_{ion} \, , \quad \Delta_{ion,gr} = \int \frac{k}{f^2} \, \mathrm{d}s = \Delta_{ion} \, . \tag{5.43}$$

Let us assume that we observe a satellite at zenith. Then the total electron content N_c is given by

$$N_c = \int N_e \, \mathrm{d}s \tag{5.44}$$

and the ionospheric refraction correction by

$$\Delta_{ion} = \frac{40.3}{f^2} \, N_c \, [\mathrm{Hz}^2\mathrm{m}^3] \, . \tag{5.45}$$

In the general case the zenith distance of the satellite must be taken into account. Using a single layer model according to [Wild et al., 1989] the ionospheric refraction correction may be written as

$$\Delta_{ion} = \frac{1}{\cos z'} \frac{40.3}{f^2} \, N_c \, [\mathrm{Hz}^2\mathrm{m}^3] \, , \tag{5.46}$$

where the reduced zenith distance z' is given by

$$\sin z' = \frac{R}{R + h_{ion}} \, \sin z \, , \tag{5.47}$$

where R is the mean radius of the earth, z is the zenith distance of the satellite and the height of the layer h_{ion} is according to [Wild et al., 1989] about 350 km.

Tropospheric Refraction

Tropospheric refraction is the effect of the neutral (i.e. the non-ionized) part of the earth's atmosphere. The troposphere is a nondispersive medium with respect to radio waves up to frequencies of about 15 GHz (see e.g. [Baueršíma, 1983]). The tropospheric refraction is thus the same for both carriers L_1 and L_2. The tropospheric path delay is defined by

$$\Delta_{trop} = \int (n - 1) \, \mathrm{d}s = 10^{-6} \int N^{trop} \, \mathrm{d}s \, , \tag{5.48}$$

where n is the refractive index and N^{trop} the so-called refractivity. According to [Hopfield, 1969] it is possible to separate N^{trop} into a dry and a wet component

$$N^{trop} = N_d^{trop} + N_w^{trop} \, , \tag{5.49}$$

where the dry part is due to the dry atmosphere and the wet part due to the water vapor in the atmosphere. About 90 % of the tropospheric refraction stems from the dry component [Janes et al., 1989]. Using the last equation we may write

$$\Delta_{trop} = \Delta_{trop,d} + \Delta_{trop,w} = 10^{-6} \int N_d^{trop} \, ds + 10^{-6} \int N_w^{trop} \, ds \ . \qquad (5.50)$$

According to [Essen and Froome, 1951] we have

$$N_{d,0}^{trop} = 77.64 \, \frac{p}{T} \left[\frac{K}{mb} \right] \quad \text{and} \quad N_{w,0}^{trop} = -12.96 \, \frac{e}{T} \left[\frac{K}{mb} \right] + 3.718 \cdot 10^5 \frac{e}{T^2} \left[\frac{K^2}{mb} \right] \ , \qquad (5.51)$$

where p is the atmospheric pressure in millibars, T the temperature in degrees Kelvin and e is the partial pressure of water vapor in millibars. The coefficients have been determined empirically.

The tropospheric delay depends on the distance travelled by the radio wave through the neutral atmosphere and is therefore also a function of the satellite's elevation angle. To show this elevation-dependence the tropospheric delay is often written as the product of the delay at zenith Δ_{trop}^0 and the so-called *mapping function* $f(z)$:

$$\Delta_{trop} = f(z) \, \Delta_{trop}^0 \ . \qquad (5.52)$$

According to [Rothacher, 1991] it is better to use different mapping functions for the dry and wet part of the tropospheric delay:

$$\Delta_{trop} = f_d(z) \, \Delta_{trop,d}^0 + f_w(z) \, \Delta_{trop,w}^0 \ . \qquad (5.53)$$

The same author states, however, that for elevations above about 20° the approximation

$$f_d(z) = f_w(z) = f(z) = \frac{1}{\cos z} \qquad (5.54)$$

is sufficient if some a priori model for the tropospheric refraction is used and only the correction with respect to this model is estimated.

Several models for the tropospheric refraction are implemented in the Bernese GPS software:

- the Saastamoinen model [Saastamoinen, 1973],

- the modified Hopfield model [Goad and Goodman, 1974],

- the simplified Hopfield model [Wells, 1974], and

- the differential refraction model based on formulae by Essen and Froome [Rothacher et al., 1986].

Usually the Saastamoinen model is used as a priori model for the tropospheric refraction. This model is based on the gas laws, when some approximations are made. [Saastamoinen, 1973] gives the equation

$$\Delta_{trop} = \frac{0.002277}{\cos z} \left[p + \left(\frac{1255}{T} + 0.05 \right) e - \tan^2 z \right] \ , \qquad (5.55)$$

where the atmospheric pressure p and the partial water vapor pressure e are in millibars, and the temperature T in degrees Kelvin. The result is in meters. [Baueršíma, 1983] uses the special correction terms B and δR:

$$\Delta_{trop} = \frac{0.002277}{\cos z} \left[p + \left(\frac{1255}{T} + 0.05 \right) e - B \ \tan^2 z \right] + \delta R \ . \qquad (5.56)$$

The correction term B is a function of the height of the observing site, the second term δR depends on the height and on the elevation of the satellite.

In the model either measured data (pressure, temperature, humidity) or the values derived from a standard atmosphere model may be used. Experience shows that the estimation of troposphere parameters is necessary if highest accuracy is required. In the Bernese GPS software usually the deterministic estimation of several zenith delays per session is used (only the corrections with respect to a priori model are estimated). A priori constraints for these parameters may be introduced.

5.3.3 Relativistic Effects

The fundamental frequency $f = 10.23$ MHz of the GPS signal is biased by the effects of special and general relativity. Because these effects are small only the linear terms are usually taken into account:

$$\delta_{rel,1} = \frac{f' - f}{f} = \frac{1}{2} \left(\frac{v}{c} \right)^2 + \frac{\Delta U}{c^2} \ . \qquad (5.57)$$

v is the velocity of the satellite and ΔU is the difference of the gravitational potential between the position of the satellite and the position of the receiver. Assuming a circular orbit and a spherical earth gives the numerical value

$$\frac{f' - f}{f} = 4.464 \cdot 10^{-10} \ . \qquad (5.58)$$

[Ashby, 1987] shows that taking into account the J_2-term for the potential yields the slightly different result $4.465 \cdot 10^{-10}$. According to [Spilker, 1980] this effect is eliminated by emitting the frequency 10.22999999545 MHz instead of 10.23 MHz.

Another small periodic effect due to the non-circular orbit is given by [Gibson, 1983]

$$\delta_{rel,2} = \frac{2}{c} \sqrt{GM \cdot a} \ e \ \sin E \ , \qquad (5.59)$$

where e denotes the eccentricity, a the semimajor axis, and E the eccentric anomaly. This effect cancels out in the case of relative positioning.

The receiver oscillator located at the earth's surface is biased by a relativistic effect due to the rotation of the earth. This effect is usually corrected by the receiver firmware.

5.3.4 Effects of Antenna Orientation

The phase measurements depend on the orientation of the antennas of transmitter and receiver, and the direction of the line of sight. With increasing accuracy in the GPS this effect becomes important. It should be mentioned that this effect is not eliminated completely using the differenced observables and that it may reach a maximum value of half a cycle.

The formulas expressing this effect were derived by [Wu et al., 1992] where it was assumed that the GPS signal is a right-handed circularly polarized (RCP) wave. An *effective dipole* $\vec{D}$ of a crossed dipole receiver antenna is defined by

$$\vec{D} = \hat{x} - \hat{k}(\hat{k} \cdot \hat{x}) + \hat{k} \times \hat{y} , \tag{5.60}$$

where $\hat{x}$ and $\hat{y}$ are the unit vectors in the directions of the two dipole elements in the receiving antenna and $\hat{k}$ is a unit vector pointing from the transmitter to the receiver. The difference of the first two terms on the right hand side is the projection of $\hat{x}$ onto a plane normal to $\hat{k}$, and the last term is the projection of $\hat{y}$ onto the same plane rotated by 90°. Introducing the third unit vector $\hat{z}$ which is orthogonal to $\hat{x}$ and $\hat{y}$ we may express the vector multiplication as

$$\hat{k} \times \hat{y} = \hat{k} \times (\hat{z} \times \hat{x}) = \hat{z}(\hat{k} \cdot \hat{x}) - \hat{x}(\hat{k} \cdot \hat{z}) . \tag{5.61}$$

Thus

$$\vec{D} = \hat{x}(1 - \hat{k} \cdot \hat{z}) - \hat{k}(\hat{k} \cdot \hat{x}) + \hat{z}(\hat{k} \cdot \hat{x}) . \tag{5.62}$$

Similarly we define an effective dipole for the transmitter by

$$\vec{D}' = \hat{x}' + \hat{k}(\hat{k} \cdot \hat{x}') - \hat{k} \times \hat{y}' . \tag{5.63}$$

The phase correction Δ_Φ is determined by the angle between the two effective dipoles and its past history:

$$\Delta_\Phi = 2 \, N \, \pi + \delta\phi , \tag{5.64}$$

where $\delta\phi$ is a fractional part of a cycle given by

$$\delta\phi = \text{sign}(\zeta) \, \arccos\left(\frac{\vec{D}' \cdot \vec{D}}{|\vec{D}'||\vec{D}|}\right) \tag{5.65}$$

$$\zeta = \hat{k} \cdot (\vec{D}' \times \vec{D}) \tag{5.66}$$

and N is an integer given by

$$N = \text{nint} \left[(\Delta_{\Phi,prev} - \delta\phi)/2\pi \right] , \tag{5.67}$$

where $\Delta_{\Phi,prev}$ is the previous value of phase correction and "nint" is the nearest integer. This equation assumes that the computation is done at a sampling rate which is high enough so that the change in the correction is always less than 180° between successive epochs. The value N could be chosen arbitrarily at the beginning of a phase tracking session, usually it is set to zero. The sign convention is such that a positive value of Δ_Φ has the same effect on the computed value of the carrier phase as an increased geometric range.

5.3.5 Antenna Phase Center Variations

The GPS measurements are referred to the so-called antenna phase center. The phase centers are *not* identical for the L_1 and L_2 measurements. Choosing the L_1 phase center as a reference and assuming that the phase centers are both on the vertical axis of the antenna, the observation equations for the two frequencies are

$$
\begin{aligned}
L_{1k}^i &= \varrho_k^i + \delta_k \ \dot{\varrho}_k^i + \lambda_1 \ n_{1k}^i + \Delta^i - \Delta_k \\
L_{2k}^i &= \varrho_k^i + \delta_k \ \dot{\varrho}_k^i + \lambda_2 \ n_{1k}^i + \Delta^i - \Delta_k - \Delta_\varrho \cos z_k^i \ ,
\end{aligned}
\tag{5.68}
$$

where z_k^i is the zenith distance of the satellite . The distance between the two phase centers Δ_ϱ (usually several millimeters) should be known for all antenna types.

Experience shows that the position of the antenna phase center is not constant but it depends on the direction the radio signal is comming from. The azimuth dependence is not highly significant but the correction due to the *zenith distance* should be applied for precise positioning. Using the same antenna types greatly reduced this effect at least for short baselines, but not necessarily for long baselines because the zenith distances z_k^i, z_l^i are not equal. The antenna phase center variations must be carefully modeled if different antenna types are used.

5.3.6 Multipath

Multipath implies that the signal arrives at the receiver's antenna via more than one path. It is mainly caused by reflecting surfaces near by the receiver, but according to [Young et al., 1985] reflections near the satellite may show up too. It is almost impossible to model multipath because it depends on the very variable geometrical situation. However using a special combination of L_1 and L_2 code and carrier phase measurements, multipath effects may be estimated because all biases mentioned in previous sections (with exception of ionospheric refraction and multipath) influence code and carrier phases by the same amount. The difference between the ionosphere-free combination of phase measurements L_3 and the same combination of code measurements P_3 is biased by multipath only. The only problem is the low accuracy of the code measurements, which means that small multipath effects remain undetected. The best way to reduce multipath is using the signal polarization method. GPS signals are right-handed circularly polarized, whereas the reflected signals are left-handed polarized. Modern antenna types reduce the effect of multipath considerably.

5.4 Linear Combinations of Observables

A dual-band P-code receiver allows us to form more linear combinations of the original carrier phase measurements L_1, L_2 and/or code measurements P_1, P_2:

$$
\begin{aligned}
L_m &= \alpha_{m,1} \cdot L_1 + \alpha_{m,2} \cdot L_2 \\
P_m &= \beta_{m,1} \cdot P_1 + \beta_{m,2} \cdot P_2 \\
W_m &= L_m - P_m
\end{aligned}
\tag{5.69}
$$

Different linear combinations allows us to eliminate or reduce different biases. Only the linear combinations available in the Bernese GPS software are discussed below.

The Original Carrier Observations L_1 and L_2

The original carriers L_1 and L_2 are biased by all effects mentioned in the previous sections. Their measurement noise is very small. According to [Rothacher, 1991] the noise of the L_3, resp. L_4, resp. L_5 linear combinations (see below) are roughly 3 times, resp. 1.4 times, resp. 5 times larger than the noise of a L_1 or L_2 observation. Using the original carriers is recommended in small networks only, where the biases are reduced enough by differencing.

The Ionosphere-free Linear Combination L_3

The linear combination

$$
L_3 = \frac{1}{f_1^2 - f_2^2}(f_1^2\ L_1 - f_2^2\ L_2)
\tag{5.70}
$$

is often called "ionosphere-free" because the ionospheric path delay is practicaly eliminated (the formal "wavelength" of this linear combination is discussed in Section 6.3.1). The same is true for the combination of code measurements

$$
P_3 = \frac{1}{f_1^2 - f_2^2}(f_1^2\ P_1 - f_2^2\ P_2) \ .
\tag{5.71}
$$

The difference $W_3 = L_3 - P_3$ may be used for multipath detection (see section 5.3.6).

The Geometry-free Linear Combination L_4

The linear combination

$$
L_4 = L_1 - L_2
\tag{5.72}
$$

is independent of receiver clocks and of the geometry (orbits, station coordinates). It contains the ionospheric delays and the initial phase ambiguities and may be used for the estimation of ionosphere. The same linear combination may be formed using the code observations too.

Wide-lane Linear Combination L_5

If we neglect all biases with the exception of the initial phase ambiguities the basic equations for L_1 and L_2 measurements may be written as

$$
\begin{aligned}
L_1 &= \varrho + \lambda_1 n_1 \\
L_2 &= \varrho + \lambda_2 n_2 \ .
\end{aligned}
\tag{5.73}
$$

Using equation (5.69) the general linear combination of phase observations is

$$
L_m = (\alpha_{m,1} + \alpha_{m,2})\varrho + \alpha_{m,1}\lambda_1 n_1 + \alpha_{m,2}\lambda_2 n_2 \quad .
\tag{5.74}
$$

The wide-lane combination has to meet the following condition:

$$
L_m = \varrho + \lambda_m n_m \ ,
\tag{5.75}
$$

where n_m should be an integer again. Comparing to (5.74) leads the following two equations:

$$
\alpha_{m,1} + \alpha_{m,2} = 1
\tag{5.76}
$$

$$
\alpha_{m,1}\lambda_1 n_1 + \alpha_{m,2}\lambda_2 n_2 = \lambda_m n_m \ .
\tag{5.77}
$$

[Cocard and Geiger, 1992] look for the coefficients $\alpha_{m,1}$ and $\alpha_{m,2}$ leading the maximum wavelength λ_m. They introduce two integers $i_{m,1}$ and $i_{m,2}$ with

$$
i_{m,1} = \frac{\alpha_{m,1}\ \lambda_1}{\lambda_m} \ , \quad i_{m,2} = \frac{\alpha_{m,2}\ \lambda_2}{\lambda_m} \ .
\tag{5.78}
$$

Thus

$$
n_m = i_{m,1}\ n_1 + i_{m,2}\ n_2
\tag{5.79}
$$

and n_m is an integer by design. The corresponding wavelength λ_m is given by

$$
\lambda_m = \frac{\lambda_1\ \lambda_2}{i_{m,1}\ \lambda_2 + i_{m,2}\ \lambda_1} = \frac{\lambda_2}{q \cdot i_{m,1} + i_{m,2}} \ , \quad q = \frac{\lambda_2}{\lambda_1} = \frac{77}{60} \ .
\tag{5.80}
$$

[Cocard and Geiger, 1992] show e.g. that the wavelength of a combination of L_1 and L_2 reaches 14.653 m for $i_{m,1} = -7$ and $i_{m,2} = 9$. The problem is the propagation of stochastic and systematic errors. Expressing the first equation (5.69) in cycles

$$
\phi_m = i_{m,1}\ \phi_1 + i_{m,2}\ \phi_2 \ ,
\tag{5.81}
$$

and assuming the mean square error σ_1 in cycles of L_1 being equal to the mean square error σ_2 in cycles of L_2

$$
\frac{\sigma_1}{\lambda_1} \doteq \frac{\sigma_2}{\lambda_2} \doteq \sigma_\phi
\tag{5.82}
$$

the mean square error of our combination is (in cycles of L_m)

$$
\sigma_m = \sqrt{i_{m,1}^2 + i_{m,2}^2}\ \sigma_\phi \ .
\tag{5.83}
$$

This formula shows that the noise expressed in cycles of the corresponding wavelength is always greater than the noise of L_1 or L_2 separately.

We have to assume that the influence of the tropospheric refraction Δ_{trop} is identical on both frequencies (in meters). Thus (using (5.76))

$$\Delta_{m,trop} = (\alpha_{m,1} + \alpha_{m,2}) \Delta_{trop} = \Delta_{trop} \ . \tag{5.84}$$

Assuming that the influence of the ionospheric refraction equals Δ_{ion} for the observations on L_1 we have (notice (5.45), (5.80))

$$\Delta_{m,ion} = (\alpha_{m,1} + q^2 \cdot \alpha_{m,2}) \ \Delta_{ion} \ , \tag{5.85}$$

or using (5.78)

$$\frac{\Delta_{m,ion}}{\lambda_m} = \frac{\Delta_{ion}}{\lambda_1} \ (i_{m,1} + q \cdot i_{m,2}) \ . \tag{5.86}$$

To minimize the fraction on the left-hand side of the equation (5.86) (if the ionosphere refraction is small comparing to the formal wavelength, the ionosphere refraction is not dangerous for ambiguity resolution) we should require

$$c_2 = |\ i_{m,1} + q \cdot i_{m,2}\ | \ \rightarrow \ \min. \tag{5.87}$$

On the other hand according to (5.84) and (5.80)

$$\frac{\Delta_{m,trop}}{\lambda_m} = \frac{\Delta_{trop}}{\lambda_m} = \frac{\Delta_{trop}}{\lambda_2} \ (q \cdot i_{m,1} + i_{m,2}) \tag{5.88}$$

and we should ask

$$c_1 = |\ q \cdot i_{m,1} + i_{m,2}\ | \ \rightarrow \ \min. \tag{5.89}$$

Obviously it is not possible to meet both requirements (5.87) and (5.89) for $i_{m,1} \cdot i_{m,2} \neq 0$. A good idea seems to be to minimize the sum $c_1 + c_2$. Using the unequality

$$|\ q \cdot i_{m,1} + i_{m,2}\ | + |\ i_{m,1} + q \cdot i_{m,2}\ | \geq |\ q \cdot i_{m,1} + i_{m,2} + i_{m,1} + q \cdot i_{m,2}\ | \tag{5.90}$$

we can conclude that it is necessary to require

$$q \cdot i_{m,1} + i_{m,2} + i_{m,1} + q \cdot i_{m,2} = (1+q) \cdot (i_{m,1} + i_{m,2}) = 0 \Longrightarrow i_{m,1} = -i_{m,2} \tag{5.91}$$

According to (5.83) the choice

$$i_{m,1} = 1 \ , \quad i_{m,2} = -1 \tag{5.92}$$

seems to be optimal. This combination called L_5 is used in the Bernese GPS software. In length units it may be written as

$$L_5 = \frac{1}{f_1 - f_2}(f_1 \ L_1 - f_2 \ L_2) \ . \tag{5.93}$$

The wavelength of this combination (about 0.86 m) is roughly 4 times longer than λ_1 or λ_2. It means that ambiguity resolution is usually much simpler in L_5 than in L_1 or L_2. According to (5.79) the L_5 initial phase ambiguity is

$$n_5 = n_1 - n_2 \ , \tag{5.94}$$

where n_1 and n_2 are the initial phase ambiguities for the original carriers. The corresponding linear combination P_5, using code observations is not of importance in processing.

53

The Melbourne-Wübbena Linear Combination

The Melbourne-Wübbena combination is a linear combination of both, carrier phase (L_1 and L_2) and P-code (P_1 and P_2) observables described by [Wübbena, 1985] and [Melbourne, 1985]. This combination eliminates the effect of the ionosphere, of the geometry, of the clocks, and of the troposphere. It may therefore even be used in the kinematic case. Three conditions have to be met (notice (5.69)), the "geometry-, clock- and troposphere-free" condition

$$\beta_{m,1} + \beta_{m,2} = \alpha_{m,1} + \alpha_{m,2} \ , \tag{5.95}$$

the "ionosphere-free" condition

$$\alpha_{m,1} + q^2 \ \alpha_{m,2} = -\beta_{m,1} - q^2 \ \beta_{m,2} \tag{5.96}$$

and the third condition which is the same as for the wide-lane combination and makes sure that the resulting ambiguity is an integer. Therefore the coefficients $\alpha_{m,1}$, $\alpha_{m,2}$ may be expressed using the integers $i_{m,1}$, $i_{m,2}$ - see equation (5.78).

Neglecting the phase noise the rms of such a combination (expressed in meters) is given by

$$\sigma_W = \sqrt{\beta_{m,1}^2 + \beta_{m,2}^2} \ \sigma_P \ , \tag{5.97}$$

where σ_P is the rms of the code measurements. Using $i_{m,1} = 1$, $i_{m,2} = -1$ we get the following set of coefficients:

$$\alpha_{m,1} = \frac{f_1}{f_1 - f_2} \ , \quad \alpha_{m,2} = -\frac{f_2}{f_1 - f_2} \ , \quad \beta_{m,1} = \frac{f_1}{f_1 + f_2} \ , \quad \beta_{m,2} = \frac{f_2}{f_1 + f_2} \ . \tag{5.98}$$

The combination may be written as

$$W_5 = L_5 - \tilde{P}_5 \ , \tag{5.99}$$

where L_5 is given by equation (5.93) and $\tilde{P}_5$ by equation

$$\tilde{P}_5 = \frac{1}{f_1 + f_2}(f_1 \ P_1 + f_2 \ P_2) \ . \tag{5.100}$$

The corresponding observation equation reads as

$$W_5 = \lambda_5 n_5 = \lambda_5(n_1 - n_2) \ . \tag{5.101}$$

The only problem may be the multipath. With good P-code data this linear combination may be used for the resolution of the wide-lane ambiguities n_5.

Table 5.2: Values of the factor $Q = \sigma_W/(\lambda_m \cdot \sigma_P)$ [m^{-1}]

$i_{m,1}$	$i_{m,2}$						
	-3	-2	-1	0	1	2	3
-3	-160.95	-134.23	-107.51	-	-54.08	-27.40	-2.48
-2	-134.03	-107.30	-80.58	-	-27.16	-1.65	26.40
-1	-107.10	-80.38	-53.65	-	-0.83	26.55	53.27
0	-	-	-	-	-	-	-
1	-53.27	-26.55	0.83	-	53.65	80.38	107.10
2	-26.40	1.65	27.16	-	80.58	107.30	134.03
3	2.48	27.40	54.08	-	107.51	134.23	160.95

Theoretically it would be possible to use other combinations of $i_{m,1}$, $i_{m,2}$. But the factor $Q = \sigma_W/(\lambda_m \cdot \sigma_P)$ (see equation (5.97)) is too high in those cases (see Table 5.2).

6. Ambiguity Resolution Strategies

6.1 Optimization of the Differencing

[Goad and Mueller, 1988] propose an algorithm for generating an optimum set of independent single and double difference observables for a network with an arbitrary number of receivers. In the case of single (between receivers) differences the basic idea is to order the baselines according to some criterion (e.g. the baseline length) and to form step by step the best independent baselines. The Cholesky decomposition method is proposed to decide whether a particular set of baselines is independent.

In the Bernese GPS software a different, more efficient algorithm to check the independence is used. First, like in the above method, the baselines are ordered according to a criterion (we use either the baseline length or the number of available single difference observables as our criterion). Then all the stations receive the initial flag 0. We take the best baseline into the optimal set, the two corresponding stations receive the flags 1. The "maximum flag" is set to 1. Now we proceed to the second baseline. If the corresponding stations have the flag 0 we change them to 2, and 2 is the value of the "maximum flag", too. In the opposite case (one station has the flag 0 and the other 1), both flags will be 1 and the "maximum flag" remains 1. From now on we proceed as follows: we choose the next baseline according to our criterion and have to distinguish the following four cases:

- Both stations of the new baseline have the flags 0 – in this case these two stations receive flags equal to "maximum flag +1", and we have to increment the "maximum flag" accordingly.

- One station has the flag 0 but the flag of the other station is not equal to 0 – in this case the station with flag 0 receives the (non zero) flag of the other station. The "maximum flag" is not changed.

- The two flags are not equal and both flags are not equal to 0 – let us assume that the first station has a lower flag than the second one. We have to change the flags of all stations which have the same flag as the first station. They obtain flags equal to the flag of the second station.

- The two flags have the same values but are different from 0 – this means that this baseline is dependent and cannot be added to the optimal set.

This procedure is repeated until all independent baselines have been formed.

6.2 Pre-Processing

It was shown in the previous sections that the receiver can measure the difference between the phase of the satellite transmitted carrier and the phase of the receiver generated replica of the signal. This measurement yields a value between 0 and 1 cycle (0 and 2π). After turning on the receiver an integer counter is initialized. During tracking the counter is incremented by one whenever the fractional phase changes from 2π to 0. Thus for every epoch the accumulated phase is the sum of the direct measured fractional phase and the integer count. The initial integer number n^i_{Fk} of cycles between the satellite i and receiver k is unknown and has to be estimated (see equation (5.19)). This phase ambiguity remains unchanged as long as no loss of the signal lock occurs. A loss of lock causes a jump in the instantaneous accumulated phase by an integer number of cycles. The difference

$$n^i_{Fk}(t_{i+1}) - n^i_{Fk}(t_i) \neq 0 \tag{6.1}$$

is called cycle slip. According to [Hofmann-Wellenhof et al., 1992] the following sources for cycle slips have to be distinguished:

- obstructions of the satellite signal due to trees, buildings, etc.,
- low signal-to-noise ratio due to bad ionospheric conditions, multipath, high receiver dynamics, or low satellite elevation,
- failure in the receiver software, and
- malfunctioning of the satellite oscillator.

A crucial of the processing of GPS measurements is the so-called pre-processing. The following tasks have to be accomplished:

1. Check all the observations and find the time intervals $< t_i, t_{i+1} >$ which are corrupted by cycle slips.

2. Repair the cycle slips. It means to estimate the difference $n^i_{Fk}(t_{i+1}) - n^i_{Fk}(t_i)$ and to correct all observations following the epoch t_i by this difference. If it is not possible to estimate this difference with a sufficient confidential level, a new unknown ambiguity parameter $n^i_{Fk}(t_{i+1})$ must be introduced.

In the Bernese GPS software [Rothacher et al., 1993a] two pre-processing programs may be used. The first program checks the *undifferenced observations* using the Melbourne-Wübbena linear combination. This program may therefore only be used if P-code measurements are available on both frequencies. It should be mentioned that this method cannot detect cycle slips if the equation

$$n^i_{1k}(t_{i+1}) - n^i_{1k}(t_i) = n^i_{2k}(t_{i+1}) - n^i_{2k}(t_i) \tag{6.2}$$

holds. Therefore, using the second pre-processing program is mandatory even if the check with the Melbourne-Wübbena combination was performed before.

The principal pre-processing program in the Bernese GPS software is called MAUPRP (Manual and AUtomatic PRe-Processing). It screens *single difference observation* files forming and analyzing all useful linear combinations of phase observations. The program either assumes that the wide-lane combination is not corrupted by cycle slips (this is true if the previous pre-processing program was used) or it looks for the wide-lane cycle slips too. The quality of results is the same in both cases, the difference is the required CPU time. MAUPRP does not use code measurements, the pre-processing is thus code-independent. This aspect is e.g. important when processing A/S data. The preprocessing program consists of the following parts:

- **Checking by smoothing:** The goal is to identify time intervals within which with utmost certainty there are no cycle slips. Usually a fair amount of data not corrupted by cycle slips may be found. The program checks whether the observations are values of a smooth function of time and whether they may be represented within an interval of a few minutes by a polynomial of low degree, say q, by computing the $(q + 1)^{st}$ derivative and by checking whether or not this quantity is zero within its expected bias. If this is true the current time interval considered is shifted by one epoch, if it is false, the last observation of the current interval is marked and replaced by the following one.

- **Triple difference solution:** With those data identified as clean in the first step a triple difference (see 5.27)) solution is performed (the overview of the adjustment methods used is given in Appendix C). This solution is not as accurate as the result of the least-squares adjustment using double differences, but it is a fair approximation of the final solution. The main advantage is that an undetected cycle slip corrupts one triple difference only.

- **The automatic cycle slip detection** is the nucleus of the program. First the program eliminates big jumps on the single difference level. Such jumps usually originate from the receiver clock and are common to all satellites. Therefore these clock jumps are irrelevant for double difference processing algorithms. Then the results of the previous two parts (coordinates of the receiver) are used to detect the cycle slips in the following way:

Let us assume that the positions of the satellites are known for every epoch t_i in the same coordinate system in which the coordinates of the receivers were computed within first two parts of the program MAUPRP. We may thus compute for every epoch t_i the distances between the satellites and the receivers. Let us denote ϱ the corresponding triple difference of these distances. Using the measurements from the epochs t_{i-1} and t_i, this triple difference distance may be computed again using the phase measurement differences between the two epochs either on the first or on the second frequency. In the ideal case the both corresponding triple differences ϱ_1 and ϱ_2 are identical and equal to ϱ. The terms

$\varrho - \varrho_i$ are called residuals:

$$\varrho - \varrho_1 = r_1 \quad , \qquad \varrho - \varrho_2 = r_2 \tag{6.3}$$

The program MAUPRP interprets the residuals as follows:

$$r_1 = b_1 \lambda_1 + ddd\,(\Delta_{ion}) \quad , \qquad r_2 = b_2 \lambda_2 + ddd\left(\frac{f_1^2}{f_2^2}\Delta_{ion}\right) \quad , \tag{6.4}$$

where $ddd(\Delta_{ion})$ is the change of the ionospheric refraction in the triple difference as "seen" by the L_1 carrier. Now, the *no-cycle-slip hypothesis* ($b_1 = 0$ and $b_2 = 0$) is checked. The ionosphere-free residual is computed as

$$r_3 = \alpha_1 \cdot r_1 + \alpha_2 \cdot r_2 \quad , \quad \text{where} \quad \alpha_1 = \frac{f_1^2}{f_1^2 - f_2^2} \quad \text{and} \quad \alpha_2 = -\frac{f_2^2}{f_1^2 - f_2^2} \quad , \tag{6.5}$$

where the following condition should be met:

$$|r_3| \leq 3\sqrt{8}\sqrt{(\alpha_1\sigma_1)^2 + (\alpha_2\sigma_1)^2} \tag{6.6}$$

($\sqrt{8} = \sqrt{2^3}$ due to triple differences). Equations (6.4) allow us to compute $ddd(\Delta_{ion})$ independently from both carriers (we assume $b_1 = b_2 = 0$ at present). The mean value m is computed as

$$m = \frac{1}{2}\left(r_1 + \frac{f_2^2}{f_1^2}r_2\right) \tag{6.7}$$

and we now check whether the condition

$$m \leq M_{ion} \tag{6.8}$$

is met. The value of M_{ion} and a priori rms of the zero difference observables σ_1 and σ_2 are input variables. If conditions (6.6) and (6.8) hold, *the no-cycle-slip hypothesis is accepted.* In the opposite case a search over the values b_1 and b_2 is performed. All combinations

$$\begin{aligned} b_{1i} &= \text{nint}\left(\tfrac{r_1}{\lambda_1}\right) + i \quad , & i &= -J_1, \ldots, -1, 0, 1, \ldots, J_1 \\ b_{2j} &= \text{nint}\left(\tfrac{r_2}{\lambda_2}\right) + i + j \quad , & j &= -J_5, \ldots, -1, 0, 1, \ldots, J_5 \end{aligned} \tag{6.9}$$

(nint = nearest integer) are formed and the "corrected" residuals

$$r_{1i} = r_1 - b_{1i}\lambda_1 \quad , \quad r_{2j} = r_2 - b_{2j}\lambda_2 \tag{6.10}$$

are tested in the same way as the original residuals r_1 and r_2. The program user has to specify the search ranges J_1 and J_5. If one combination of r_{1i}, r_{2j} meet the no-cycle-slip hypothesis, the observation are corrected by $b_{1i}\lambda_1$, $b_{2j}\lambda_2$. If no "good" combination is found, a new ambiguity parameter is introduced.

6.3 Ambiguity Resolution

The unknown integer number of cycles in the observation equations has to be estimated in a first step as a real valued parameter. Under certain conditions some or all of the real valued estimates for the ambiguities can be related unmistakably to the true integer values. By introducing these true ambiguities into a subsequent least-squares adjustment (see Appendix C) as known values, the solution will get much more stable. The accuracy of the results may improve by a factor of up to 4 [Gurtner et al., 1985]. Numerous methods have been proposed dealing with the resolution of initial phase ambiguity parameters. We distinguish two cases:

Classic Static Positioning: The site occupation time is long (hours to days), the number of measurements is big. This implies that on short baselines the rms of the estimated ambiguities is much smaller than 1 cycle.

Rapid Static Positioning: The site occupation time is small (several minutes), the rms of the real valued ambiguity estimates is of the order of 1 cycle or even greater. Ambiguity resolution still may be possible on short baselines using the FARA (Fast Ambiguity Resolution Approach). For more information see [Frei and Beutler, 1990], [Frei, 1991].

In the present investigation we are only considering the case of classic static positioning.

6.3.1 Review of Existing Techniques

The Observation Equations

We consider dual-band P-code receiver. Four double difference observation equations are available at epoch t for a set of two receivers k, l and two satellites i, j. According to equations (5.28) and (5.45) we may write these equations as follows:

$$L_{1kl}^{ij} = \varrho_{kl}^{ij} - dd(\Delta_{ion}) + \lambda_1\, n_{1kl}^{ij} \tag{6.11}$$

$$L_{2kl}^{ij} = \varrho_{kl}^{ij} - \frac{f_1^2}{f_2^2} \cdot dd(\Delta_{ion}) + \lambda_2\, n_{2kl}^{ij} \tag{6.12}$$

$$P_{1kl}^{ij} = \varrho_{kl}^{ij} + dd(\Delta_{ion}) \tag{6.13}$$

$$P_{2kl}^{ij} = \varrho_{kl}^{ij} + \frac{f_1^2}{f_2^2} \cdot dd(\Delta_{ion}) \tag{6.14}$$

All observables have the dimension of length, terms due to noise, tropospheric refraction and multipath are not explicitly shown, and higher-order ionospheric terms are ignored. The main differences between the phase- and the code- observation equations are: (1) the presence of the ambiguity term in the phase equations, (2) the opposite sign of the ionospheric range corrections, and (3) the measurement noise, where we may assume that the rms errors of the code is much larger than the rms error of the phase.

Wide-Lane and Narrow-Lane Ambiguity Resolution

In equations (6.11) – (6.14) four unknowns, namely ϱ_{kl}^{ij}, $dd(\Delta_{ion})$, n_{1kl}^{ij} and n_{2kl}^{ij} are present on the right hand side. We can obtain the following relations for n_{1kl}^{ij} and n_{2kl}^{ij} by eliminating the other unknowns:

$$L_{1kl}^{ij} - \frac{f_1^2 + f_2^2}{f_1^2 - f_2^2} \cdot P_{1kl}^{ij} + \frac{2 \cdot f_2^2}{f_1^2 - f_2^2} \cdot P_{2kl}^{ij} = \lambda_1 \cdot n_{1kl}^{ij} , \qquad (6.15)$$

$$L_{2kl}^{ij} - \frac{f_1^2 + f_2^2}{f_1^2 - f_2^2} \cdot P_{2kl}^{ij} + \frac{2 \cdot f_1^2}{f_1^2 - f_2^2} \cdot P_{1kl}^{ij} = \lambda_2 \cdot n_{2kl}^{ij} . \qquad (6.16)$$

It would be possible to use these relations for resolution of the n_1 and n_2 ambiguities, but the accuracy analysis (see e.g. [Beutler et al., 1994b]) show that the minimum number of observation epochs which are necessary for a safe resolution of the n_1 or n_2 ambiguities is too high. Much easier is to resolve the wide-lane ambiguity $n_5 = n_1 - n_2$ using the linear combination

$$\frac{1}{f_1 - f_2}(f_1 \, L_1 - f_2 \, L_2) - \frac{1}{f_1 + f_2}(f_1 \, P_1 + f_2 \, P_2) = \lambda_5 \cdot n_5 , \quad \text{where} \quad \lambda_5 = \frac{c}{f_1 - f_2} . \qquad (6.17)$$

Therefore many ambiguity resolution strategies resolve first the wide-lane ambiguity parameter $n_5 = n_1 - n_2$ (see (5.94)). The idea to resolve the wide-lane ambiguities using the linear combination (6.17) was proposed independently by [Melbourne, 1985] and [Wübbena, 1985]. Using the observations of precise dual-band P-code receivers it is possible to resolve the wide-lane ambiguities without any assumptions concerning the ionosphere, the troposphere, the orbits, and the clocks (receivers and satellites).

After wide-lane ambiguity resolution the ionosphere-free combination (5.70)

$$L_{3kl}^{ij} = \varrho_{kl}^{ij} + B_{3kl}^{ij} \qquad (6.18)$$

may be used to resolve the ambiguity n_1. The ionosphere-free linear combination could not be used for ambiguity resolution directly because the ionosphere-free bias

$$B_{3kl}^{ij} = \frac{1}{f_1^2 - f_2^2} \left(f_1^2 \lambda_1 n_{1kl}^{ij} - f_2^2 \lambda_2 n_{2kl}^{ij} \right) \qquad (6.19)$$

could not be expressed in form $\lambda_3 \cdot n_3$, where n_3 is an integer ambiguity. Introducing the known wide-lane ambiguity $n_5 = n_1 - n_2$, the ionosphere-free bias (6.19) may be written as

$$B_{3kl}^{ij} = c \, \frac{f_2}{f_1^2 - f_2^2} \, n_{5kl}^{ij} + \underbrace{\frac{c}{f_1 + f_2}}_{\lambda_3} \, n_{1kl}^{ij} , \qquad (6.20)$$

where the first term on the right hand side is known. The main advantage is the fact that the ionosphere refraction has been eliminated. But the formal wavelength λ_3 is about 11 cm only. Therefore the remaining unknown bias $\lambda_3 \cdot n_1$ is called narrow-lane ambiguity. Due to the small wavelength λ_3 all other biases (e.g. orbits or troposphere) have to be modeled very carefully.

If Anti-Spoofing (AS) is turned on, the precise code observations will no longer be available. [Bock et al., 1986] proposes a different approach. Let us extend the equations equations (6.11) and (6.12) by a pseudoobservation equation for the ionospheric effect $dd(\Delta_{ion})$:

$$L_{1kl}^{ij} = \varrho_{kl}^{ij} - dd(\Delta_{ion}) + \lambda_1\, n_{1kl}^{ij} \qquad (6.21)$$

$$L_{2kl}^{ij} = \varrho_{kl}^{ij} - \frac{f_1^2}{f_2^2}dd(\Delta_{ion}) + \lambda_2\, n_{2kl}^{ij} \qquad (6.22)$$

$$L_{Ikl}^{ij} = dd(\Delta_{ion})\,. \qquad (6.23)$$

The third equation incorporates a priori information concerning the ionosphere in the form of weighted constraints. Introducing such a pseudoobservation may be used for various unknown parameters. No doubt, it is now possible to use the least-squares adjustment. The most important question is, which a priori variance σ_I^2 for the parameters Δ_{ion} is to be used. It may be assumed, that $\sigma_1^2 = \sigma_2^2 = \sigma_0^2$ (i.e. the measurement noise is the same for L_1 and L_2. Two extremes may be considered for the a priori weights of Δ_{ion}. Assuming $\sigma_I^2 = 0$ implies that we ignore the contribution of the ionosphere completely. The other extreme, $\sigma_I^2 \to \infty$, is equivalent to the ionosphere-free combination (5.70). The advantage of this approach is that it is possible to assign σ_I^2 "appropriately" according to the baseline length.

Another method proposes [Blewitt, 1989]. The geometry-free linear combination (5.72) may be written as

$$L_{4kl}^{ij} = I_{kl}^{ij} + \frac{f_1^2 - f_2^2}{f_1 f_2}\left(\lambda_5 n_{5kl}^{ij} - B_{3kl}^{ij}\right)\,, \qquad I_{kl}^{ij} = dd\left(\frac{f_2^2 - f_1^2}{f_2^2}\Delta_{ion}\right)\,, \qquad (6.24)$$

where B_{3kl}^{ij} is given by equation (6.19). From the equation (6.24) the wide-lane ambiguity may be expressed:

$$n_{5kl}^{ij} = \frac{1}{\lambda_5}\left[\frac{f_1 f_2}{f_1^2 - f_2^2}\left(L_{4kl}^{ij} - I_{kl}^{ij}\right) + B_{3kl}^{ij}\right]\,. \qquad (6.25)$$

The ionosphere-free bias B_{3kl}^{ij} may be estimated using ionosphere-free linear combination. The precision of this estimation is typically much better than 10 cm and its contribution to the error in the wide-lane bias is usually insignificant. The problem is the unknown value of the differential ionospheric delay I_{kl}^{ij} which is nominally assumed to be zero. [Blewitt, 1989] proposes to estimate (6.25) when the $|I_{kl}^{ij}|$ is expected to be at a minimum. This time is approximately when the undifferenced ionospheric delay I_k^i and L_{4k}^i are at a minimum. Thus the single difference $L_{4kl}^i \equiv (L_{4k}^i - L_{4l}^i)$ is evaluated when $(L_{4k}^i + L_{4l}^i)$ is at a minimum, and similarly for L_{4kl}^j. The principle is that instead of approximation

$$L_{4kl}^{ij} - I_{kl}^{ij} \doteq L_{4kl}^{ij} \qquad (6.26)$$

the more optimal differencing (at different times)

$$L_{4kl}^{ij} - I_{kl}^{ij} \doteq \left(L_{4kl}^i\right)_{min|L_{4k}^i + L_{4l}^i|} - \left(L_{4kl}^j\right)_{min|L_{4k}^j + L_{4l}^j|} \qquad (6.27)$$

must be met if, and only if the ambiguities for the same pair of satellites and for the same pair of receivers but for different carriers are tested. The geometry free linear combination (5.72) yields:

$$L_{4kl}^{ij} = I_{kl}^{ij} + \lambda_1 n_{1kl}^{ij} - \lambda_2 n_{2kl}^{ij} , \qquad I_{kl}^{ij} = dd \left(\frac{f_2^2 - f_1^2}{f_2^2} \Delta_{ion} \right) . \tag{6.31}$$

Using this combination the difference between two geometry-free biases

$$x_{4kl}^{ij} - x_{A4kl}^{ij} , \tag{6.32}$$

where

$$x_{4kl}^{ij} = \lambda_1 x_{1kl}^{ij} - \lambda_2 x_{2kl}^{ij} , \qquad x_{A4kl}^{ij} = \lambda_1 x_{A1kl}^{ij} - \lambda_2 x_{A2kl}^{ij} \tag{6.33}$$

is computed. x_{1kl}^{ij}, x_{2kl}^{ij} are the real valued ambiguities and x_{A1kl}^{ij}, x_{A2kl}^{ij} are the alternative integer values. The value (6.32) is the difference between the ionosphere bias which was estimated during the initial ambiguity-free solution and the ionosphere bias which would be the result of the alternative ambiguity-fixed solution. The difference should be very small in any case. This test represents graphically a narrow confidence band if the alternative ambiguities x_{A1kl}^{ij}, x_{A1kl}^{ij} are plotted [Frei and Beutler, 1990].

The Ambiguity Function Method

This method was first proposed by [Counselman and Gourewitch, 1981], it was further developed by [Remondi, 1984]. Due to problems with systematic errors this method is applicable for small networks only. The method is summarized here for the sake of completeness.

Let us assume that a single baseline is processed. The position of the first receiver is fixed, the coordinates of the second receiver were estimated (using e.g. a triple difference solution). We now introduce a cube with this approximate position as a center and the dimensions $2\xi\sigma \times 2\xi\sigma \times 2\xi\sigma$ (σ is the standard deviation of the estimated coordinates, ξ is the confidence factor) and we partition the cube into a regular grid. Each of the grid points is considered as a candidate for the true solution. The coordinates are known for each grid point as well as the corresponding single differences ϱ_{kl}^j (the satellite positions are known). The single difference observation equation may be written in the form (aplying the single difference operator on the equation (5.19))

$$\frac{2\pi}{\lambda} (L_{kl}^j - \varrho_{kl}^j) = 2\pi \, n_{kl}^j - 2\pi \, f\Delta_{kl} . \tag{6.34}$$

The key is to circumvent the ambiguities n_{kl}^j by defining the following complex-valued function:

$$e^{i \left[\frac{2\pi}{\lambda} (L_{kl}^j - \varrho_{kl}^j) \right]} = e^{i \left[2\pi \, n_{kl}^j - 2\pi \, f\Delta_{kl} \right]} = e^{i \, 2\pi \, n_{kl}^j} \cdot e^{-i \, 2\pi \, f\Delta_{kl}} . \tag{6.35}$$

If the ambiguity n_{kl}^j is an integer number

$$e^{i \, 2\pi \, n_{kl}^j} = \cos(2\pi \, n_{kl}^j) + i \, \sin(2\pi \, n_{kl}^j) = 1 + i \cdot 0 \tag{6.36}$$

is used. However the effectiveness of this method depends on ionospheric conditions. Under worse ionospheric conditions this method could not be used for baselines longer than about 100 km. The other problem is that the differencing between different times introduces the clock errors.

The "Search" Strategy

This strategy implemented as FARA (Fast Ambiguity Resolution Approach) in the Bernese GPS software [Frei and Beutler, 1990] uses the following information from the initial adjustment:

$\underline{x} = (x_1, \ldots, x_u)^T$, the part of the solution vector consisting of all real-valued (double difference) ambiguities,

Q, the corresponding cofactor matrix, and

σ_0^2, the a posteriori variance factor,

where u is the number of double difference ambiguities. From the a posteriori variance factor and the cofactor matrix the standard deviation m_i for the ambiguity parameter x_i or the standard deviation m_{ij} for the difference x_{ij} between any two parameters x_i, x_j may be computed:

$$m_i = \sigma_0 \sqrt{Q_{ii}} \,, \qquad m_{ij} = \sigma_0 \sqrt{Q_{ii} - 2 \cdot Q_{ij} + Q_{jj}} \,. \tag{6.28}$$

Choosing a confidence level α and using the Student's distribution we compute the upper and lower range-width ξ for the integer valued alternative parameter x_{Ai} or for the difference x_{Aij} between two such parameters. Thus

$$x_i - \xi \cdot m_i \leq \quad x_{Ai} \quad \leq x_i + \xi \cdot m_i \,, \quad i = 1, 2, \ldots, u \tag{6.29}$$

$$x_{ij} - \xi \cdot m_{ij} \leq \quad x_{Aij} \quad \leq x_{ij} + \xi \cdot m_{ij} \,, \quad i, j = 1, 2, \ldots, u \,, \quad i \neq j \,. \tag{6.30}$$

All possible combinations of integer values which meet the conditions (6.29) and (6.30) are used to form alternative ambiguity vectors $\underline{x}_{Ah}$, $h = 1, \ldots, N$ to the initial ambiguity estimate $\underline{x}$. These alternatives are generated in forming all possible combinations of vector components using the integer values within corresponding confidence ranges. Each of these alternative vectors should be introduced into a subsequent adjustment run. The integer ambiguities are treated in these adjustments as known quantities. The resulting standard deviations σ_h are indicators for the success of the process: the integer vector $\underline{x}_h$ yielding the smallest standard deviation is selected as the final solution unless either its standard deviation is not compatible with σ_0 (the fraction σ_h/σ_0 is too high), or there is another vector $\underline{x}_q$ yielding almost identical standard deviation (the fraction $\sigma_q/\sigma_h \approx 1$). The problem is computation time: in general it is difficult to compute the least-squares adjustments for all alternative vectors because this number may be rather large.

The FARA [Frei and Beutler, 1990] improves the situation considerably if only short baselines are involved and both frequencies (L_1 and L_2) are processed. A new condition

and the equation (6.35) may be simply written as

$$e^{i\left[\frac{2\pi}{\lambda}\left(L^j_{kl}-\varrho^j_{kl}\right)\right]} = e^{-i\ 2\pi\ f\Delta_{kl}} \ . \tag{6.37}$$

Now, we can form the sum over all satellites observed in one epoch:

$$\sum_{j=1}^{N_s} e^{i\left[\frac{2\pi}{\lambda}\left(L^j_{kl}-\varrho^j_{kl}\right)\right]} = N_s\ e^{-i\ 2\pi\ f\Delta_{kl}} \ , \tag{6.38}$$

where N_s is number of satellites observed. The right-hand side of the last equation does not depend on the satellite. Its absolute value is N_s. The left-hand side is a sum of unit vectors in the complex plane. The absolute value of this sum is lower than or equal to N_s. Thus

$$A(t_i) = \left|\sum_{j=1}^{N_s} e^{i\left[\frac{2\pi}{\lambda}\left(L^j_{kl}-\varrho^j_{kl}\right)\right]}\right| \le N_s \ . \tag{6.39}$$

Both sides of the inequality (6.39) are equal if, and only if single differences

$$L^j_{kl} - \varrho^j_{kl} \tag{6.40}$$

are the same for all satellites j. This is true if the coordinates of the receivers are correct and there are no systematic and random errors. Now, we may sum the $A(t_i)$ from the equation (6.39) over all epochs t_i , $i = 1, 2, \ldots$:

$$\sum_i A(t_i) \ . \tag{6.41}$$

This sum considered as a function of the grid point is called *ambiguity function*. According to (6.39) this function is bounded and therefore it has a supremum. [Remondi, 1984] proposes to accept as a solution the grid point from the grided cube which coordinates yield the maximum of the ambiguity function (6.41).

The Search using Kalman Filtering

This method was proposed by [Magill, 1965] for kinematic applications and by [Brown and Hwang, 1983] for geodetical applications. The method was also described by [Landau, 1988]. We assume that we know some alternative ambiguity vectors $\underline{x}_i$, $i = 1, \ldots, N$ (compare the section about the search strategy) and we want to select one of these vectors as a true solution. The method is based on Kalman filter processes (see Appendix C).

We estimate unknown parameters (coordinates, troposphere etc.) using Kalman filter estimator. The ambiguities are fixed (they have integer values $\underline{x}_i$). Each alternative vector $\underline{x}_i$, $i = 1, \ldots, N$ define one filter process (the only difference between various filter processes are the initial conditions – the initial phase ambiguities). Denoting by $\underline{\ell}^*_{k_i}$ the observations predicted by the filter process i for the epochs t_k , $k = 1, \ldots, n$ and by $\underline{\ell}_k$ the actual observations for the same epochs, the filter process with minimum mean square

difference $\tilde{\ell}_{k_i}^{2} = (\ell_k - \ell_{k_i}^*)^2$ is accepted as a true solution. The probability $p(\ldots)$ of the observations $\underline{\ell} = (\ell_1, \ldots, \ell_n)^T$ under the assumption that the ambiguities have values $\underline{x}_i$ may be for the filter express by the product of n probability density functions [Magill, 1965]

$$p(\underline{\ell}|\underline{x}_i) = \prod_{k=1}^{n} \frac{1}{\sqrt{2\,\pi}\,\sqrt{|Q_k|}} \cdot e^{-\frac{1}{2}\,\tilde{\ell}_{k_i}^T Q_k^{-1} \tilde{\ell}_{k_i}} \,, \quad \tilde{\ell}_k = \ell_k - A\underline{x}_k^* \,, \tag{6.42}$$

where the covariance matrix Q_k is given by (equation C.50)

$$Q_k = \left(Q_l + AQ_x A^T\right) \,. \tag{6.43}$$

The Bayes' law yields the a posteriori probability density

$$p(\underline{x}_i|\underline{\ell}) = \frac{p(\underline{\ell}|\underline{x}_i)\,p(\underline{x}_i)}{\sum_{j=1}^{N} p(\underline{\ell}|\underline{x}_j)\,p(\underline{x}_j)} \,, \tag{6.44}$$

where the sum is done over all N filters (over all N various initial ambiguity parameter sets). Assuming $p(\underline{x}_j) = 1/N = \text{konst.}$ the equation (6.44) may be simply written as

$$p(\underline{x}_i|\underline{\ell}) = \frac{p(\underline{\ell}|\underline{x}_i)}{\sum_{j=1}^{N} p(\underline{\ell}|\underline{x}_j)} \,. \tag{6.45}$$

Assuming that the matrices Q_k are the same for all filters and using the equation (6.42) yields

$$p(\underline{x}_i|\underline{\ell}) = \frac{e^{-\frac{1}{2}\sum_{k=1}^{n} \tilde{\ell}_{k_i}^T Q_k^{-1} \tilde{\ell}_{k_i}}}{\sum_{j=1}^{N} e^{-\frac{1}{2}\sum_{k=1}^{n} \tilde{\ell}_{k_j}^T Q_k^{-1} \tilde{\ell}_{k_j}}} \,. \tag{6.46}$$

The denominator on the right hand side remains the same for all filters. Therefore the maximum probability $p(\underline{x}_i|\underline{\ell})$ may be found as maximum of the function

$$L_n(x_i) = -\sum_{k=1}^{n} \tilde{\ell}_{k_i}^T Q_k^{-1} \tilde{\ell}_{k_i} \,. \tag{6.47}$$

It means that the filter which has the maximum probability $p(\underline{x}_i|\underline{\ell})$ has at the same time the minimum mean square residuum $\tilde{\ell}^{2}$ if the weight matrix Q_k^{-1} is used. The problem is that if many filters were tested the computational burden could become overwhelming.

6.3.2 Our Approach

We have to distinguish between the strategy used for ambiguity resolution and the algorithm implemented to reach that goal.

Strategy

Since 21 June 1992 the data from the IGS Core Network (see Section 2.1) are processed on a daily basis at the Astronomical Institute of the University of Berne. We assume that the International GPS Service for Geodynamics (IGS) will provide us with:

1. high accuracy orbits (better than 0.5 m), and

2. regional ionosphere models.

The first IGS product should allow us to resolve the narrow-lane ambiguities *not* in a network-mode *but* in a baseline-oriented mode. This strategy promises to be much more efficient than usual network-oriented processing schemes, because the computing time grows not linearly but with a much higher power with the number of ambiguities involved (depending somewhat on the algorithm chosen). It also promises to be more reliable, because in our case the search ranges can be opened up in a "generous" way, and more runs can be made.

The second product should allow us to resolve the wide-lane ambiguities without having access to the P-code. This aspect is most important because soon the P-code will no longer be available to the scientific community. Again, the wide-lane ambiguity resolution is done in the baseline-mode and the idea was (and is) to take out the principal ionosphere-induced biases by a ionosphere model and to hope that the "irregular" part of the ionosphere will be averaged out by using long observation sessions. The ionosphere model produced by Bernese software [Wild et al., 1989] is a *single layer model computed from zero difference phase observations of one or more reference stations.* The reference stations have to be equipped with dual-band receivers. The model is based on the following assumptions (see also section 5.3.2):

- All free electrons are concentrated in a spherical layer of infinitesimal thickness at height h_{ion} above earth surface. The height h_{ion} is an input parameter. Usually the value 350 km is used.

- The total electron content N_c is an analytical function of two spherical coordinates. The geocentric latitude β and the hour angle of the sun $t_\odot$ are used as the coordinates. layer.

- The ionospheric refraction correction for phase observations is given by the equation (5.45), β and $t_\odot$ are computed for the intersection point of the spherical layer with the line connecting the receiver and the satellite.

In the model the total electron content N_c is represented as a Taylor series development:

$$N_c(t_\odot, \beta) = \sum_{i=0}^{\infty} N_{c,kl} \, (t_\odot - t_{0,\odot})^k \, (\beta - \beta_0)^l \, , \quad k + l = i \, . \tag{6.48}$$

The degrees of Taylor series development, separated for latitude, hour angle and for mixed terms, may be defined by the user. The origin for the Taylor development is automatically computed. The origin β_0 in latitude is the mean value of the latitudes of all stations, the time origin t_0 is computed as the mean value of the lowest start time and of the highest ending time of all observation files of one session. $t_{0,\odot}$ is then computed as the hour angle of the sun at time t_0 refered to the meridian of the mean station of the session considered. This model is used when processing the wide-lane linear combination of baselines up to

300 km in the "vicinity" of the reference receiver the data of which were used to define the local ionosphere model. Such data are e.g. available from the IGS permanent stations.

As mentioned above we are going to use the IGS products for the ambiguity resolution. On the other hand fixing the ambiguity biases provide a better type of observables which improve the estimations of other parameters (in Chapter 7 we will e.g. demonstrate a very close relation between the ambiguities and the orbit parameters) and using ambiguity fixing techniques for routine IGS processing is very attractive. Therefore we tested our ambiguity resolution strategy with data from the IGS Core Network. These data have the following features:

- The session lengths are 24 hours generally.

- Many long baselines (the distances between the receivers) are involved.

- A big variety of parameters (coordinates, orbits, earth rotation, atmosphere) has to be estimated.

These facts imply the algorithm.

The Algorithm

The Bernese GPS software uses double difference observations and therefore the double difference ambiguities are estimated. Single difference (between receivers) ambiguities are then saved. For each session and each baseline we have to select one single difference bias n^j_{Fkl} as reference and actually our unknown ambiguity parameters are the differences

$$n^{ij}_{Fkl} = n^i_{Fkl} - n^j_{Fkl} \ . \tag{6.49}$$

The choice of the reference ambiguity is in principle arbitrary. In practice usually the ambiguity associated with the biggest number of observations is selected as reference. If there are N single difference ambiguities for one session and one baseline, there are $N - 1$ linearly independent unknown ambiguity parameters. (If there is an epoch when all the single difference phase measurements were initialized again, the session breaks up into two parts and for each part one reference ambiguity must be selected. In that case only $N - 2$ ambiguity parameters have to be estimated.)

Figure 6.1 shows the satellite visibility for a short (several minutes) session. For short session there is usually one (or more) satellite(s) which was observed all the time. One of these satellites may be selected as the reference satellite (the corresponding ambiguity as reference ambiguity).
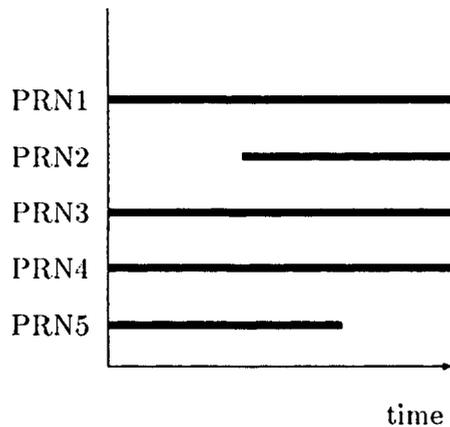
Figure 6.1: Satellite visibility plot for a short session and a short baseline

For longer sessions the situation is different:

- No satellite is observed during the entire session.

- There are periods during which only few satellites were observed. For very long baselines there are even periods during which only one or two satellites were observed.

The typical situation shows Figure (6.2):
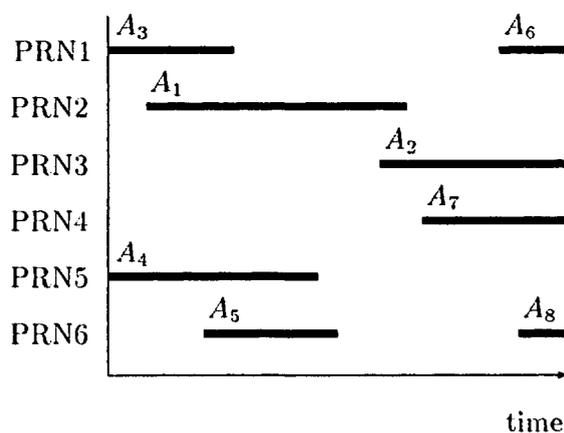
Figure 6.2: Satellite visibility plot for a long session and a long baseline

In this case our algorithm selects (single difference) ambiguity A_1 as a reference. Typically general search finds several alternative ambiguity vectors which lead almost to the same a posteriori rms. A detailed inspection shows that the (double difference) ambiguities $A_2 - A_1, A_6 - A_1, A_7 - A_1, A_8 - A_1$ have large a posteriori rms errors. On the other hand

69

the parameters $A_3 - A_1, A_4 - A_1, A_5 - A_1$ are well estimated. We suspect that this result is a consequence of the selection of the reference ambiguity. This actually is the case: if we select A_2 as our reference the parameters $A_6 - A_2, A_7 - A_2, A_8 - A_2$ have small a posteriori rms errors and the parameters $A_1 - A_2, A_3 - A_2, A_4 - A_2, A_5 - A_2$ large ones. The following conclusions may be drawn:

- The differences between certain single difference ambiguities and the reference ambiguity are well estimated the other differences have large a posteriori rms errors. Which parameters are well estimated depends on the selection of the reference ambiguity.

- It is difficult to resolve *all* the ambiguities if the long sessions are processed because each selection of the reference ambiguity lead to some ambiguity parameters with large a posteriori rms errors. This is a problem if the search strategy is used (this strategy could resolve either all the ambiguities or none).

These considerations show that it is necessary to *optimize* the (double) differencing. Such optimization was proposed by [Blewitt, 1989], who processes undifferenced data and forms an optimal set of statistically independent linear combinations. Our approach is in principle equivalent to that proposed by [Blewitt, 1989] with the following differences:

- We process double differenced data. The single (between receivers) differences are created explicitly and stored in files (about the optimization of this differencing see Section 6.1), the double differences are created during the initial least-squares adjustment.

- We are not actually forming statistically independent linear combinations of ambiguities. We replace this procedure by an iterative scheme, where in each iteration step we are only resolving "the best" ambiguity. Assuming that n^j_{Fkl} denotes our reference ambiguity, we are resolving either the double difference ambiguity parameter

$$n^{ij}_{Fkl} = n^i_{Fkl} - n^j_{Fkl} \tag{6.50}$$

directly or the difference between two of these terms

$$n^{i_1 i_2}_{Fkl} = n^{i_1 j}_{Fkl} - n^{i_2 j}_{Fkl} \,, \tag{6.51}$$

which, as a matter of fact, is a double difference ambiguity again.

In more detail our algorithm works as follows: we adopt a similar notation as in the section "The Search Strategy": let x_i, x_j be (double difference) ambiguity parameters. For the each parameter x_i we compute the a posteriori rms error in the initial least-squares adjustment:

$$\sigma_i = \sigma_0 \sqrt{Q_{ii}} \tag{6.52}$$

and for each difference $x_i - x_j$ the error is

$$\sigma_{ij} = \sigma_0 \sqrt{Q_{ii} - 2 \cdot Q_{ij} + Q_{jj}} \,. \tag{6.53}$$

σ_i and σ_{ij} are sorted according to their value. Within one iteration step the N_{max} best determined ambiguities (or differences between ambiguities) are resolved (rounded to nearest integers) provided:

- The corresponding sigma is compatible with σ_0 ($\sigma_i \leq \sigma_{max}$ or $\sigma_{ij} \leq \sigma_{max}$), and
- within the confidence interval $(x_i - \xi\sigma_i, x_i + \xi\sigma_i)$ or $(x_{ij} - \xi\sigma_{ij}, x_{ij} + \xi\sigma_{ij})$ is exactly one integer number.

N_{max}, σ_{max} and ξ are the input parameters of the program. In the next iteration step the integer values are introduced for the resolved ambiguities and for the resolved differences between ambiguities. The iteration process terminates if:

1. All the ambiguities have been resolved, or

2. in the last step no ambiguity could be resolved based on the above criteria.

The iteration process described above may be applied for every linear combination. It may be used in the baseline mode, in session mode or even if several sessions are treated in the same program run.

6.4 Quasi-Ionosphere-Free (QIF) Ambiguity Resolution Strategy

6.4.1 Principles

1994 Anti-spoofing (AS) was turned on for all Block II satellites and the quality of code measurements of the Rogue receivers dramatically decreased. We wanted to find a new approach how to resolve the ambiguities for long baselines (up to about 1000 km) without using code measurements. The result is the Quasi-Ionosphere-Free (QIF) ambiguity resolution strategy.

The simplified form of the observation equations reads as (see (5.28))

$$L_1 = \varrho - \Delta + \lambda_1 \, n_1 \,, \tag{6.54}$$

$$L_2 = \varrho - \frac{f_1^2}{f_2^2} \cdot \Delta + \lambda_2 \, n_2 \,. \tag{6.55}$$

The corresponding equation for the ionosphere-free linear combination thus may be written as

$$L_3 = \varrho + B_3 = \varrho + \frac{c}{f_1^2 - f_2^2} \, (f_1 \, n_1 - f_2 \, n_2) \,. \tag{6.56}$$

The initial least-squares adjustment using both frequencies L_1 and L_2 adjustment give real-valued ambiguity estimates b_1 and b_2 and we may compute the corresponding ionosphere-free bias $\tilde{B}_3$ as

$$\tilde{B}_3 = \frac{c}{f_1^2 - f_2^2} \, (f_1 \, b_1 - f_2 \, b_2) \,. \tag{6.57}$$

This bias may be expressed in narrow-lane cycles (one cycle corresponding to a wavelength of $\lambda_3 = c/(f_1 + f_2) \approx 11$ cm):

$$\tilde{b}_3 = \frac{\tilde{B}_3}{\lambda_3} = \tilde{B}_3 \cdot \frac{f_1 + f_2}{c} = \frac{f_1}{f_1 - f_2} \, b_1 - \frac{f_2}{f_1 - f_2} \, b_2$$

$$= \beta_1 \, b_1 + \beta_2 \, b_2 \; . \tag{6.58}$$

Denoting the correct integer (resolved) ambiguity values n_{1i} and n_{2j} and introducing the associated L_3-bias

$$b_{3ij} = \beta_1 \, n_{i1} + \beta_2 \, n_{2j} \tag{6.59}$$

we may use the difference

$$d_{3ij} = |\tilde{b}_3 - b_{3ij}| \tag{6.60}$$

as a criterion for the selection of the "best" pair of integers n_{1i}, n_{2j}. However, many pairs n_{1i}, n_{2j} give differences d_{ij} of the same (small) order of magnitude. These pairs lie on a narrow band in the (n_1, n_2) space. The equation of the center line of this band is

$$\beta_1 \, n_{i1} + \beta_2 \, n_{2j} = \tilde{b}_3 \; . \tag{6.61}$$

The band-width is essentially given by the rms of the bias $\tilde{b}_3$. A unique solution only results if it is possible to limit the search range. This principle is shown in Figure 6.3.
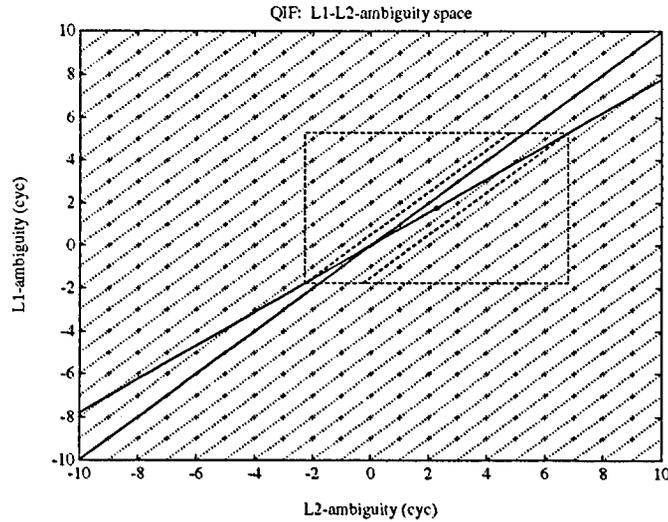
Figure 6.3: Search ranges in (n_1, n_2) space

One solid line is described by the equation (6.61). It goes through the real valued estimate (b_1, b_2) as well as through the point $(n_{1,i}, n_{2,j})$ which is accepted as "true" solution. This line represents an ionosphere–free combination (constant ionosphere-free bias). The second solid line represents the constant wide-lane ambiguity (accepted as "true" value) and goes through the point $(n_{1,i}, n_{2,j})$ too. The dashed rectangle represents a search range in (n_1, n_2) space and the dashed trapezoid represents the search range in (n_1, n_5) space – equation (6.67).

6.4.2 The Estimation of the Ionosphere

For baselines longer than about 10 km the processing of the two frequencies L_1 and L_2 separately does not give sufficiently good initial real valued estimates b_1 and b_2 due to the influence of the ionospheric refraction. Two types of models to reduce the ionospheric biases were considered.

Satellite and Epoch Specific Ionosphere Estimation

[Schaer, 1994] proposes to estimate one ionospheric correction $\Delta_{kl}^i(t_j)$ for each satellite i, each receiver pair kl and each epoch (t_j). The method is similar to that described by [Bock et al., 1986]. Estimating these parameters without any a priori constraints would be equivalent to processing the ionosphere-free linear combination. If we want to resolve the integer ambiguities it is necessary to constrain these parameters to within a few decimeters. This constraining may be achieved by introducing an artificial observation

$$\Delta_{kl}^i(t_j) - \Delta_{kl,apr}^i(t_j) = 0 \tag{6.62}$$

each epoch with the a priori weight. The actual a priori values $\Delta_{kl,apr}^i(t_j)$ may stem from an ionosphere model. In many cases (relatively short baselines) $\Delta_{kl,apr}^i(t_j) = 0$ may be sufficient. It is of course necessary to pre-eliminate all epoch specific ionosphere parameters $\Delta_{kl,apr}^i(t_j)$, $i = 1, 2, \ldots, n_s$ (n_s is the number of satellites per epoch) after having processed epoch t_j because a "terrible" number of parameters would have to be handled in the normal equation system after n_e epochs.

Deterministic Model

For longer baselines it seems to be necessary to introduce an a priori ionospheric model or to estimate such a model during the initial solution. As a priori models the single-layer models described by [Wild et al. 1989] may be used. These models develop the electron content in the layer into a Taylor series in the latitude and the hour angle of Sun. These models reduce the ionosphere biases considerably for baselines up to about 200 km as shown in [Mervart et al., 1994] and they enable to resolve wide-lane ambiguities using wide-lane linear combination. However using the QIF strategy no a priori model is necessary up to baseline length about 400 km. For the baselines up to 1000 km we used the model based on the following assumptions:

- All the free electrons are considered to be concentrated in a spherical layer of infinitesimal thickness at height h_{ion} above earth surface. The height h_{ion} is an input parameter. Usually the value $h_{ion} = 350$ km is used.

- The total electron content N_c is given by the equation

$$N_c = \sum_{n=0}^{\infty} \sum_{m=0}^{n} P_n^m(\cos(\phi_\otimes - \phi_\odot)) \cdot$$

$$(a_{n,m} \cdot \cos m \cdot (\lambda_\odot - \lambda_\odot) + b_{n,m} \cdot \sin m \cdot (\lambda_\otimes - \lambda_\odot)) , \tag{6.63}$$

where

P_n^m : associated Legendre function of the degree n and order m,

$\phi_\otimes$: latitude of the intersection point of the spherical layer with the line connecting the receiver and the satellite,

$\lambda_\otimes$: longitude of the intersection point of the spherical layer with the line connecting the receiver and the satellite,

$\phi_\odot$: latitude of Sun,

$\lambda_\odot$: longitude of Sun.

It is possible to estimate several sets of model parameters $a_{n,m}$, $b_{n,m}$ per observation session. An example of the result is given in Section 7.

6.4.3 Implementation of the QIF Strategy

The QIF approach is implemented in our "Sigma" strategy [Mervart et al., 1994]. Let us denote by b_{1i}, b_{1i_1}, b_{1i_2} the (real valued) double difference L_1-ambiguities. Similarly b_{2j}, b_{2j_1} and b_{2j_2} are the L_2-ambiguities. Now we check whether the pair

$$b_{1i} \,, \quad b_{2j}$$

or the pair

$$b_{1i_1} - b_{1i_2} \,, \quad b_{2j_1} - b_{2j_2} \,,$$

which, as a matter of fact, is a pair of double difference ambiguities again, meets the requirements to be round to integers and accepted as the pair of correct integer valued ambiguities. In particular we proceed as follows. We compute the rms error for each L_3 ambiguity bias $\bar{b}_3$ associated with a pair b_{1i}, b_{2j} or with a pair of differences $b_{1i_1} - b_{1i_2}$, $b_{2j_1} - b_{2j_2}$:

$$\sigma = \sigma_0 \cdot \sqrt{\beta_1^2 \, Q_{11} + 2 \, \beta_1 \, \beta_2 \, Q_{12} + \beta_2^2 \, Q_{22}} \,, \tag{6.64}$$

where

$$Q_{11} = Q(b_{1i}, b_{1i}) \,, \quad Q_{12} = Q(b_{1i}, b_{2j}) \,, \quad Q_{22} = Q(b_{2j}, b_{2j}) \tag{6.65}$$

in the case of pair b_{1i}, b_{2j} ($Q(\ldots)$ is an element of the variance-covariance matrix) or

$$
\begin{aligned}
Q_{11} &= Q(b_{1i_1}, b_{1i_1}) - 2\, Q(b_{1i_1}, b_{1i_2}) + Q(b_{1i_1}, b_{1i_2}) \\
Q_{12} &= Q(b_{1i_1}, b_{2j_1}) - Q(b_{1i_1}, b_{2j_2}) - Q(b_{1i_2}, b_{2j_1}) + Q(b_{1i_2}, b_{2j_2}) \\
Q_{22} &= Q(b_{2j_1}, b_{2j_1}) - 2\, Q(b_{2j_1}, b_{2j_2}) + Q(b_{2j_2}, b_{2j_2})
\end{aligned}
\tag{6.66}
$$

in the case of pair of differences $b_{1i_1} - b_{1i_2}$, $b_{2j_1} - b_{2j_2}$. Now, we sort the ambiguity pairs according to values σ. For the ambiguity pair (or pair of the differences) with the smallest σ

(if this σ is lower than adopted $\sigma_{\max}$) we define the search ranges (omitting the "solution indices" i, j)

$$\tilde{n}_1 = \mathrm{nint}(b_1) \pm i , \quad i = 0; 1; \ldots; i_{max}$$
$$\tilde{n}_5 = \mathrm{nint}(b_1 - b_2) \pm k , \quad k = 0; 1; \ldots; k_{max} \tag{6.67}$$
$$\tilde{n}_2 = \tilde{n}_1 - \tilde{n}_5$$

and for each pair $\tilde{n}_1, \tilde{n}_2$ of integers within the search range we compute the test value (6.60)

$$d_3 = |\beta_1 \ (b_1 - \tilde{n}_1) + \beta_2 \ (b_2 - \tilde{n}_2)| . \tag{6.68}$$

The pair associated with the smallest value d_3 is accepted as a solution unless

$$d_3 \geq d_{\max} , \tag{6.69}$$

where $d_{\max}$ is a user defined maximum value. If no ambiguity set passed the test we proceed to the next pair of ambiguities associated with the second smallest σ. After accepting one pair the entire least-squares adjustment and the procedure described above are repeated. The ambiguities are thus resolved iteratively. All or only a subset of ambiguity pairs may be resolved in the iteration process.

Part II

Test Campaigns and Results

7. Test Campaigns and Results

7.1 Epoch'92 and EUREF–CH

The International GPS Service for Geodynamics (IGS) [Mueller and Beutler, 1992], [Beutler et al., 1994c] organized two campaigns in 1992:

- The IGS test campaign (21 June 1992 – 23 September 1992). This campaign was followed by the so-called Pilot Service to bridge the gap between the 1992 IGS Test Campaign and the start of the official IGS service on January 1, 1994.

- Epoch'92 – a two weeks campaign centered around August 1, 1992.

The main purpose of the 3 months campaign was to prove that the scientific community is able to produce high-accuracy orbits on an operational basis. Data (code and phase on both carrier frequencies) were gathered by a core network of about 30 globally distributed stations (equipped with high precision dual-band P-Code receivers and near-real time data links to the network centers) – see [Beutler, 1993b].

Table 7.1: Stations and baselines used from the IGS Core Network

Station	Abbreviations		Baseline	Length (km)
Graz	GRAZ	GZ	GZ–WZ	300
Kootwijk	KOSG	KO	WZ–ZA	480
Mas Palomas	MASP	MP	KO–ZA	600
Madrid	MADR	MD	KO–ON	700
Matera	MATE	MT	GZ–MT	720
Metsahovi	METS	MS	MS–ON	780
Onsala	ONSA	ON	MS–TR	1080
Tromso	TROM	TR	MD–ZA	1180
Wettzell	WETT	WZ	MD–MP	1740
Zimmerwald	ZIMA	ZA		

The main purpose of Epoch'92 is a first densification of the core network: in addition to the 30 core stations about 100 so-called fiducial stations were collecting data during

Epoch'92. From this campaign we selected 10 stations listed in Table 7.1 and formed the linear independent set of shortest baselines. All the stations were (and still are) equipped with dual band P-code receivers. Because for test purposes we wanted to use the P-code measurements we have chosen four sessions without anti-spoofing (AS). The sessions are given in Table 7.2 (where the session number is identical with the day number of the year 1992). The session lengths are 24 hours in each case.

Table 7.2: List of sessions used from Epoch'92

Session	Date	Time
217	4th AUG 1992	0 - 24
218	5th AUG 1992	0 - 24
219	6th AUG 1992	0 - 24
220	7th AUG 1992	0 - 24

At the same time the EUREF-CH campaign was organized by the Swiss Federal Office of Topography. The 5 EUREF stations in Switzerland were occupied from 3 to 8 August 1992. Two different receiver types were used (see Table 7.3). The campaign took place during Epoch'92 in order to take advantage of the highest possible orbit accuracy. The main goal of the campaign was to improve the coordinates of the Swiss EUREF stations in the ITRF. These EUREF stations will provide the reference frame for the new first order GPS survey in Switzerland.

4 Trimble 4000 SLD and 2 Trimble 4000 SST receivers were used. At the Satellite Laser Ranging (SLR) site in Zimmerwald (which is at the same time also an IGS station) both receiver types were used simultaneously in order to allow baseline formation with the same receiver type. It should be mentioned that the Trimble 4000 SLD are non-P-code receivers. They reconstruct the L_2 carrier using a squaring technique which leads to half-cycle ambiguities for the L_2 phase. The Trimble SST uses a different (cross correlation) technique allowing to work with full-cycle ambiguities on L_2. Both receivers have full-cycle ambiguities on the L_1 carrier, which implies that for the resolution of the narrow-lane ambiguities we may work with full-cycle ambiguities.

Table 7.3: Stations and baselines of the EUREF-CH campaign

Station	Abbreviations		Receiver	Baseline	Length (km)
Zimmerwald 1	ZIM1	Z1	Trimble 4000 SLD	Z1–CH	78
Zimmerwald 2	ZIM2	Z2	Trimble 4000 SST	Z1–LG	114
Chrischona	CHRI	CH	Trimble 4000 SLD	Z2–MG	159
La Givrine	LAGI	LG	Trimble 4000 SLD	Z1–PF	190
Mt. Generoso	MTGE	MG	Trimble 4000 SST		
Pfänder	PFAN	PF	Trimble 4000 SLD		

We processed the 7 sessions of Table 7.4. Due to technical reasons it was not possible to generate 1 day sessions.

Table 7.4: List of sessions used from EUREF-CH campaign

Session	Date					
2171	4th AUG 1992	6:00	–	4th AUG 1992	18:00
2172	4th AUG 1992	18:00	–	5th AUG 1992	6:00
2181	5th AUG 1992	6:00	–	5th AUG 1992	18:00
2182	5th AUG 1992	18:00	–	6th AUG 1992	6:00
2191	6th AUG 1992	6:00	–	6th AUG 1992	18:00
2192	6th AUG 1992	18:00	–	7th AUG 1992	6:00
2201	7th AUG 1992	6:00	–	7th AUG 1992	18:00

For both campaigns we have used the orbits computed by the Center for Orbit Determination in Europe (CODE) using the measurements of the IGS stations.

Ambiguity Resolution Strategy

For the resolution of the initial phase ambiguities we used the following two products of the International GPS Service for Geodynamics (IGS):

1. High accuracy orbits (better than 0.5 m).

2. Regional ionosphere models.

The first IGS product should allow us to resolve the narrow-lane ambiguities *not* in a network-mode *but* in a baseline-oriented mode. This strategy promises to be much more efficient than the usual network-oriented processing schemes, because the computing time grows not linearly but with a much higher power with the number of ambiguities involved (depending somewhat on the algorithm chosen). It also promises to be more reliable, because in our case the search ranges can be opened up in a "generous" way, and more test runs can be made.

WIDE-LANE AMBIGUITIES
(all ambiguities, the EUREF-CH campaign)
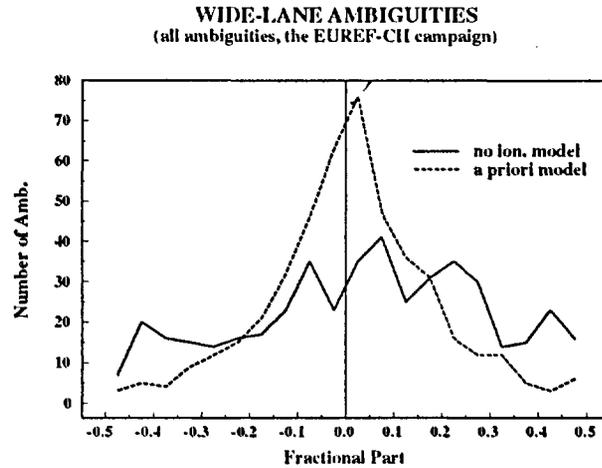
Figure 7.1: Distribution of the fractional parts

The second product should allow us to resolve the wide-lane ambiguities without having access to the P-code. This aspect is most important because today the P-code is no longer available to the scientific community. Below we will use local single-layer models for the total electron content based on the phase measurements of one dual-band receiver in the IGS network. These models are used when processing the wide-lane linear combination of baselines up to 300 km in the "vicinity" of the reference receiver. Again, the wide-lane ambiguity resolution is done in the baseline-mode. The idea was (and is) to take out the principal ionosphere-induced biases by a model and to hope that the "irregular" part of the ionosphere will be averaged out by using long observation sessions.

Wide-Lane Ambiguity Resolution

For the Epoch'92 data set we used the Melbourne-Wübbena linear combination of the two phase and the two code observations (see Section 5.4) for ambiguity resolution. This approach is very reliable. In Table 7.6 (column L_5) the number of resolved wide-lane ambiguities is shown. For the EUREF-CH data we did not have this possibility because P-code measurements were not available. The most serious problem – ionospheric refraction – was addressed by using the ionosphere models produced by program IONEST of the Bernese GPS Software *(Wild,1989)* using the L_1 and L_2 observations of the Trimble SST receiver located at Zimmerwald. In Figure 7.1 the distribution of the fractional parts of the wide-lane ambiguities before the first iteration step of our ambiguity resolution scheme (see Section 6.3.2) is shown for all baselines and session (458 ambiguities). The mean square fractional parts of wide-lane ambiguities for all EUREF-CH baselines are listed in Table 7.5.

Table 7.5: The results of the wide-lane ambiguity resolution

Baseline	Length (km)	sess.	amb.	Mean square fract. part		amb. resolved
				no ion. model	ion. model	
Z1–CH	78	7	125	0.253	0.164	116
Z1–LG	114	7	122	0.274	0.172	110
Z2–MG	159	7	92	0.197	0.117	89
Z1–PF	190	7	119	0.277	0.230	97

Without using the ionosphere model it was not possible to resolve the ambiguities. With the ionosphere model we resolved about 90 % of all ambiguities. The coordinates were fixed on the values obtained using the ionosphere free linear combination without resolving the ambiguities (compare also [Wild, 1993]).

Narrow-Lane Ambiguity Resolution

As mentioned this step was performed baseline by baseline. The iterative approach is very important because it is necessary to estimate not only the ambiguities, but coordinates and troposphere parameters too. For each baseline we held one station fixed and we estimated the coordinates of the second one. For each station we estimated one troposphere parameter per 6 hours. The results from both campaigns (Epoch'92 and EUREF-CH) are presented together. In Figure 7.2 a typical example is shown for the development of the fractional part of the narrow-lane ambiguities during the iteration process (three double difference ambiguities stemming from satellites 13, 14, 23 and 25).
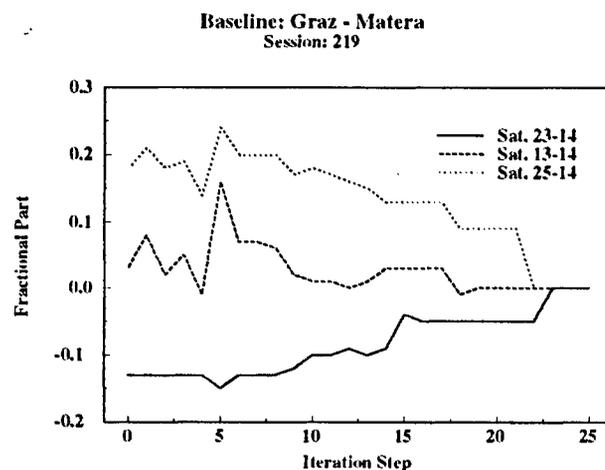
Figure 7.2: Development of the fractional part of the narrow-lane ambiguities (double differences 25–14, 13–14 and 23–14) during the iteration process

In Table 7.6 the number of resolved ambiguities is shown. The number of resolved ambiguities depends on the confidence level in our statistical tests. We used a very conservative confidence level (about 99 %) and therefore we could only resolve about 85 % of the ambiguities. In the same table the results using the broadcast orbits instead of IGS orbits are shown.

Table 7.6: The results of the narrow-lane ambiguity resolution

					Broadcast orbits		CODE orbits	
Baseline	Length (km)	sess.	amb. total	L_5 amb. resolved	mean sq. frac. part	amb. res.	mean sq. frac. part	amb. res.
Z1–CH	78	7	125	116*	0.252	105	0.160	103
Z1–LG	114	7	122	110*	0.287	80	0.238	107
Z2–MG	159	7	92	89*	0.294	65	0.119	87
Z1–PF	190	7	119	97*	0.281	82	0.302	69
GZ–WZ	300	4	103	103**	0.276	54	0.201	93
WZ–ZA	480	4	101	94**	0.278	53	0.258	72
KO–ZA	600	4	104	95**	0.311	57	0.217	66
KO–ON	700	4	109	104**	0.288	60	0.233	97
GZ–MT	720	4	100	100**	0.292	63	0.214	94
MS–ON	780	4	126	126**	0.285	80	0.217	119
MS–TR	1080	4	130	127**	0.280	89	0.226	106
MD–ZA	1180	4	106	95**	0.277	70	0.222	67
MD–MP	1740	4	113	96**	0.277	39	0.236	64

* ionosphere models used

** Melbourne-Wübbena approach used

It is very interesting to inspect the distribution of the fractional part of narrow-lane ambiguities before resolution (Figure 7.3). In essence we conclude that narrow-lane ambiguity resolution is most successful using the IGS orbits and almost impossible using the broadcast orbits for baselines longer than about 100 km.

NARROW-LANE AMBIGUITIES
(all ambiguities, EUREF-CH and Epoch'92)
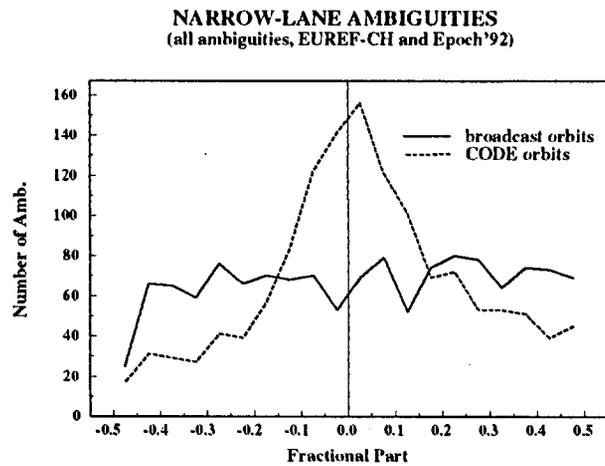
Figure 7.3: Distribution of the fractional parts

Quality of Results

Below, the day to day repeatabilities of our baseline estimations are used as a measure for the success of ambiguity resolution. All the ambiguities previously resolved were fixed and we produced a solution based on the ionosphere-free linear combination. We estimated the troposphere parameters (one parameter per station and 6 hours interval) and the coordinates of all the stations (Epoch'92 and EUREF-CH) with respect to Zimmerwald. We used various observation windows i.e. we used the data from the entire sessions and then from 8, 4, 2 and 1 hours only. The results may be found in Figures 7.4 and 7.5.
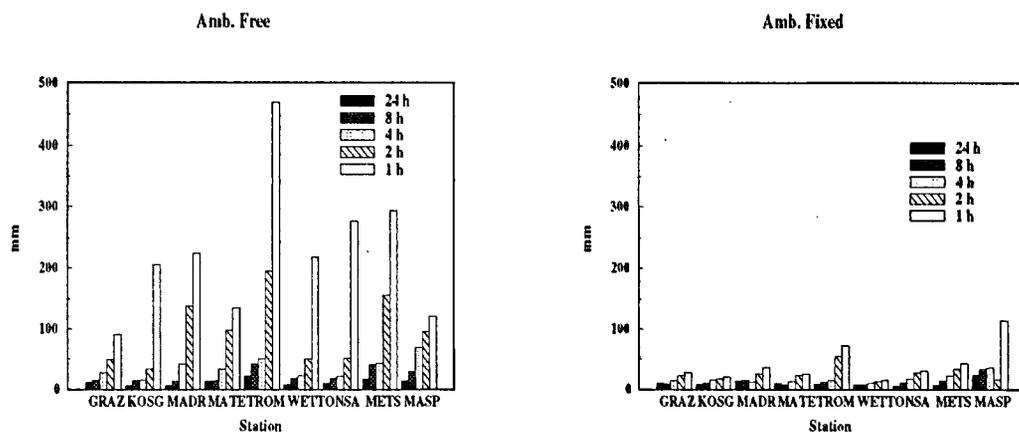
Figure 7.4: Day to day repeatability of the horizontal position (ϕ, λ) for different session lengths; stations of the Europen Core Network

85
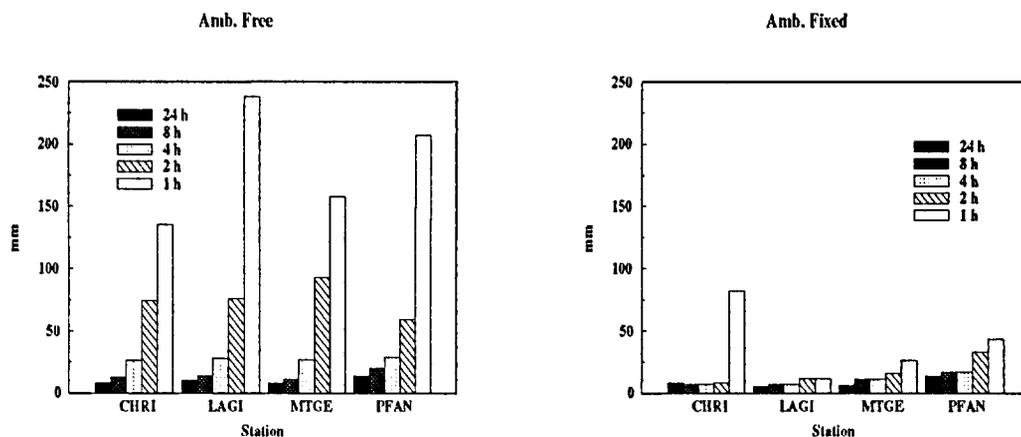
Figure 7.5: Day to day repeatability of the horizontal position (ϕ, λ) for different session lengths; Swiss EUREF stations

The repeatability of the coordinates is a good indicator for the stability of the solutions. To show the quality of various types of solutions (ambiguities fixed or free and various data intervals) we computed a set of mean coordinates for each type of solution from all sessions. We used the full-session ambiguity fixed solution as a reference and computed the Helmert transformation between this reference solution and all others. The results (horizontal positions) are given in Figure 7.6. The residuals in height component were about 2 times larger and we did not detected any significant difference between ambiguity fixed and ambiguity free solutions.
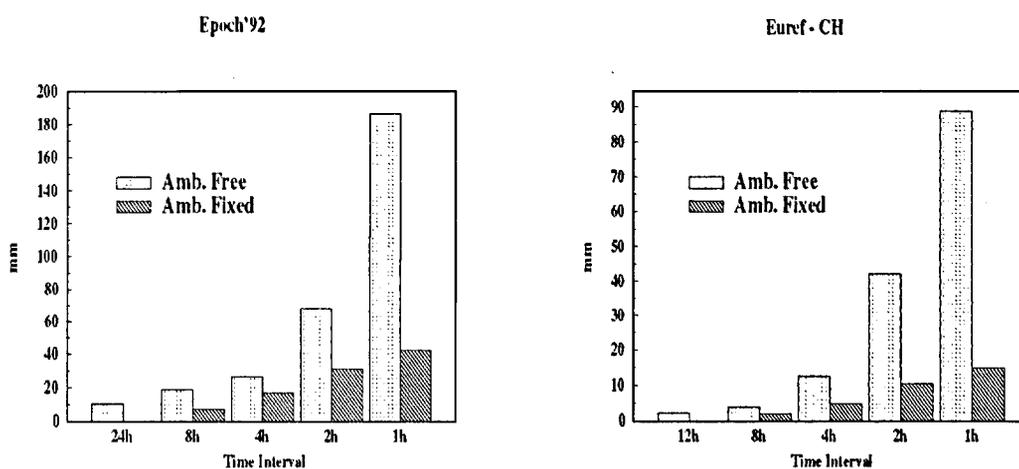
Figure 7.6: Rms of residuals in the horizontal position (ϕ, λ) after Helmert transformation

7.2 January'93

In January'93 seven IGS Analysis Centers (see Table 2.2) were producing GPS orbits, earth rotation parameters, station coordinates, and other relevant parameters using the data from the IGS Core Network (see Section 2.1). The results of the IGS processing centers were regularly compared by [Goad, 1993]. These comparisons showed that the consistency of the daily orbit systems from different centers approached the 25 cm level, after a 7-parameter Helmert transformation. In order to improve the consistency between the different processing centers even more and to detect the reason for some small systematic differences between the results of different IGS Analysis Centers the Analysis Center Coordinator during the IGS Pilot Service, Prof. C.C. Goad, selected two weeks (17 – 30 January 1993, GPS weeks 680 and 681) to be reprocessed by all IGS processing centers, using the same coordinates (and local ties, antenna heights) for the stations held fixed. We used this data set to test our ambiguity resolution strategies, where we focused our attention on the data from 10 European IGS Core Stations. Our test network is given in Figure 7.7. It covers an area of roughly 5000 km (N-S) × 2000 km (E-W).
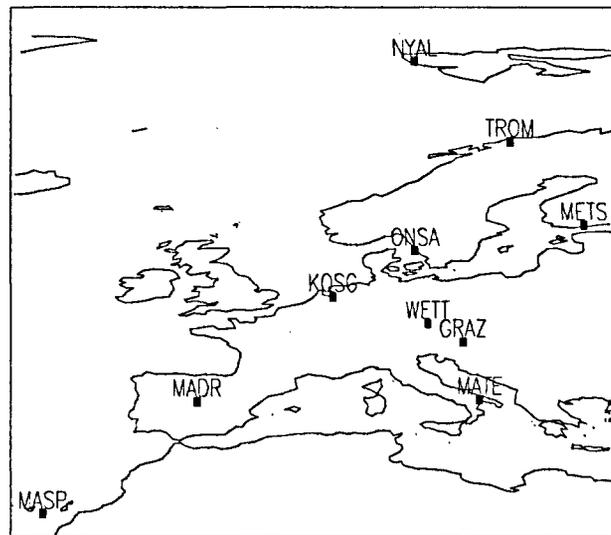
Figure 7.7: Test network

Because the CODE Analysis Center works with overlapping 3-days solutions, where the result for the middle day of every 3-days solution is extracted and delivered to the IGS data centers [Rothacher, 1993b], we had to use the data from 16 days (16 – 31 January 1993). The station names, abbreviations and the availability of data are listed in Table 7.7.

Table 7.7: List of stations

STATION	ABBREV.		Date															
			1	1	1	1	2	2	2	2	2	2	2	2	2	2	3	3
			6	7	8	9	0	1	2	3	4	5	6	7	8	9	0	1
Graz	GRAZ	GZ	X	X	X	X	X	X	X	X	X	X	X	X	X	X	X	X
Kootwijk	KOSG	KO	X	X	X	X	X	X	X	X	X	X	X	X	X	X	X	X
Madrid	MADR	MD	X	X	+	X	X	X	X	X	X	X	X	X	X	X	X	+
Matera	MATE	MT	X	X	X	X	X	X	X	X	X	X	X	X	X	+	X	X
Tromso	TROM	TR	X	X	X	X	X	X	X	X	X	X	X	X	X	X	X	X
Wettzell	WETT	WZ	X	X	X	X	X	X	X	X	X	X	X	X	X	X	X	X
Onsala	ONSA	ON	X	X	X	X	X	X	X	X	X	X	X	X	X	X	X	X
Metsahovi	METS	MS	X	X	X	X	X	X	X	X	X	X	X	X	X	X	X	X
Ny Allesund	NYAL	NA	X	X	X	X	X	X	X	o	o	+	X	X	o	X	o	o
Mas Palomas	MASP	MP	X	+	+	X	X	X	X	X	X	X	X	X	X	X	X	X

X ...data available   + ...few hours of data only   o ...data not available

The Bernese GPS Software explicitly creates the so-called single difference files (differences of quasi-simultaneous observations to the same satellite as seen from different stations). For ambiguity resolution purposes we used the set of the shortest linearly independent baselines. The distances between all stations may be extracted from Table 7.8. The baselines selected according to the above mentioned criterion are underlined. The distance lengths vary between 700 km and 1700 km.

Table 7.8: Distances between stations (km) for the January'93 campaign

	NYAL	GRAZ	KOSG	MADR	MATE	TROM	ONSA	METS	WETT
MASP	5646	3409	3209	1745	3244	5019	3874	4590	3361
	NYAL	3508	2964	4264	4190	1053	2387	2119	3283
		GRAZ	899	1741	719	2507	1172	1572	302
			KOSG	1512	1523	2054	700	1449	602
				MADR	1765	3480	2205	2930	1655
					MATE	3198	1886	2231	990
						TROM	1406	1079	2296
							ONSA	784	919
								METS	1433

All the stations were occupied with dual band P-code receivers (Rogues). Because anti-spoofing (AS) was not switched on during that time we could use all four types of observables (L_1 and L_2 phases and both P-codes).

Wide–Lane Ambiguity Resolution

In a first step we resolved the wide-lane ambiguities using the Melbourne-Wübbena linear combination. Figure 7.8 shows the distribution of the fractional parts of wide-lane ambiguities after the initial solution. It should be mentioned that during the initial least-squares adjustment all the unknown ambiguity parameters from one session are refered to one (single difference) reference ambiguity (see Section 6.3.2).

WIDE-LANE AMBIGUITIES (EUROPE)
Fractional Parts after Initial Solution
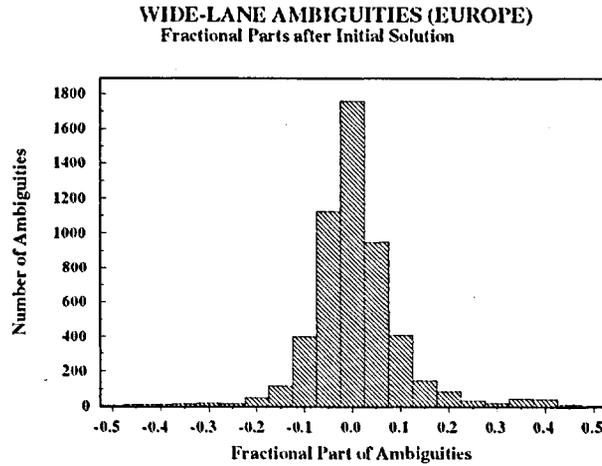
Figure 7.8: Distribution of the fractional parts for the January'93 campaign

The main advantage of our new ambiguity resolution strategy [Mervart et al., 1994] is the optimization of the double differencing. Actually we resolve the differences (see Section 6.3.2)

$$n_{kl}^{i_1 i_2} = n_{kl}^{i_1 j} - n_{kl}^{i_2 j} = b_{kl}^{i_1} - b_{kl}^{i_2} , \qquad (7.1)$$

where the satellite pairs i_1, i_2 are selected in order to minimize the a posteriori rms of the ambiguity parameters. The power of this approach is demonstrated in Figure 7.9 which shows the distribution of the fractional parts of the wide-lane ambiguities actually resolved. From the Figures 7.8 and 7.9 we conclude that the wide-lane ambiguity resolution using the Melbourne-Wübbena linear combination is highly successful and very reliable. In this case we were able to resolve 97 % of 5234 unknown ambiguity parameters. It should be mentioned that this number depends on the confidential level ξ and maximal a posteriori rms σ_{max} (Section 6.3.2). In this case we used $\xi = 3$ and $\sigma_{max} = 0.1$.

Narrow–Lane Ambiguity Resolution

Narrow-lane ambiguity resolution was attempted up to baseline-lengths of about 2000 km. Previous experiences (Epoch'92 campaign) told us that narrow-lane ambiguity resolution would be possible only with orbits of excellent quality. The same tests indicated that ambiguity resolution considerably improves the accuracy of results (repeatability of coordinates etc.) for sessions shorter than 24 hours. During the Epoch'92 campaign we resolved the ambiguities on the simple baseline level, then we processed the entire network keeping the orbits fixed. Our January'93 test should answer the following questions:

1. Is it possible to resolve the narrow-lane ambiguities on the baseline level using IGS orbits?

WIDE-LANE AMBIGUITIES (EUROPE)
Fractional Parts in the Moment of Fixing
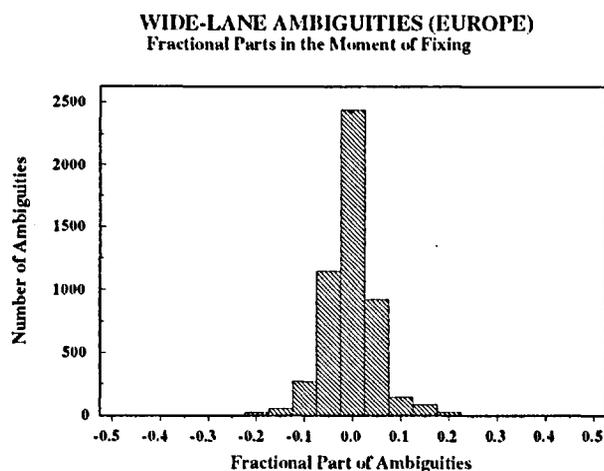
Figure 7.9: Distribution of the fractional parts

2. Which criterion should be applied to check the quality of results?

3. Does ambiguity resolution improve the accuracy of results of 3-days solutions too?

4. Is it necessary to improve the orbits during the final network adjustment?

To answer the first question we used the following two strategies:

Strategy A: The entire network was processed 'en bloc' for each session (24 hours). We estimated the ambiguities, the coordinates of all the stations with the exception of Wettzell, troposphere parameters (one parameter per station and per 6 hours observation time interval), and 7 orbit parameters for each satellite (6 initial conditions plus the direct solar radiation pressure parameter p_0 [Beutler et al., 1994a]). The y-biases were kept fixed on the values obtained in the standard 3-days solution.

Strategy B: Each baseline was processed separately. We constrained the coordinates to 1 cm to the mean coordinates obtained from the 14 standard IGS 3-days solutions. For this mean set of coordinates an accuracy of about 1 cm could be expected. In addition to station coordinates and ambiguities we solved for the troposphere parameters (one parameter per station and per 6 hours observation time interval) too. We used the IGS orbits from the Center for Orbit Determination in Europe (CODE) and made no further orbits improvement. The essential difference between the two strategies thus besides in the fact that in strategy A we make an attempt for a regional orbit improvement, in strategy B the orbits are kept fixed.

The iterative approach to resolve ambiguities described in [Mervart et al., 1994] is an essential element because of the correlations between various parameter types. Within one

iteration step only the limited (selected) number of the best-determined ambiguities are fixed and the following least-squares adjustment serves as an initial solution for the next iteration step. The first impression concerning the reliability of the ambiguity resolution stemms from the distribution of the fractional parts of the ambiguities when they are actually fixed (i.e. in the iteration step when the ambiguities were actually fixed). This distribution of the fractional parts of ambiguities in the moment of fixing for both strategies is given in Figure 7.10.

NARROW-LANE AMBIGUITIES (EUROPE)
Session Level Adjustment

NARROW-LANE AMBIGUITIES (EUROPE)
Baseline Level Adjustment
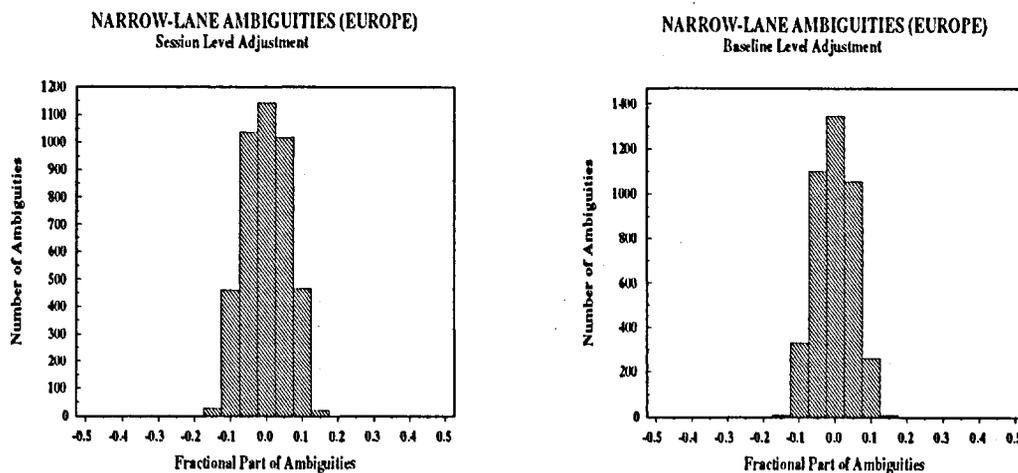
Figure 7.10: Distribution of the fractional parts of the ambiguities when accepted to be fixed

We used a very conservative confidence level in our statistical tests ($\xi = 3$ and $\sigma_{max} = 0.07$ and nevertheless we were able to resolve in both cases 82 % of the narrow-lane ambiguities (about 18 % of fractional parts outside the $3 \cdot 0.07 = 0.21$ limit should be added in Figure 7.10). We may conclude that ambiguity resolution was highly successful.

According to the distribution of the fractional parts the resolution of the narrow-lane ambiguities on the baseline level seems to be slightly better than the strategy A. This result is important because it demonstrates the possibility to resolve the narrow-lane ambiguities using IGS orbits without further orbit improvement. We want to study this aspect in more detail by taking into account the quality of the solutions (using strategies A and B) too. The following aspects are considered:

- We expect sub-centimeter accuracy for our results. Therefore only the "free network" approach (only one station kept fixed) is valid because the a priori coordinates (ITRF) of the fiducial stations have rms errors of the order of 1 cm.

- It is not sufficient to simply study the coordinates' repeatability because the resulting network of stations may be corrupted by small rotations if only one station is kept fixed. This argument is certainly relevant in the case of Strategy A. Therefore a

Helmert transformation must be used to compare the daily solutions.

- Orbit quality and orbit parametrization are crucial. It should be kept in mind that the observations used for ambiguity resolution were also used (together with data from stations outside Europe) for orbit détermination. Therefore it would not be correct to use the same fixed orbits to test the quality of results. The only possibility is to estimate the orbit parameters again, but this time with fixed ambiguities. The fixing of ambiguities potentially provides a better type of (unbiased) observable and promises higher orbit accuracy.

Taking into account these considerations the following approach was chosen: fourteen 3-days solutions were performed, where the coordinates of all stations (with the exception of Wettzell) were computed. For the tropospheric delay we used the Saastamoinen model (see Section 5.3.2) as an a priori model and we estimated one zenith correction per station and per each 6 hours time interval. The following sets of solutions were inspected.

Solution Type 1: float solution. All the ambiguities were estimated as real numbers. As an orbit model we used our stochastic model [Beutler et al., 1994a] where apart from the standard 8 orbit parameters (6 initial conditions, direct solar pressure parameter p_0 and y–bias parameter p_2) we solved for three stochastic force parameters (in radial, along track and out of plane directions) per satellite and per satellite revolution (12 hours).

Solution Type 2: ambiguities fixed solution. 82 % of the narrow-lane ambiguities were kept fixed on the values obtained from the previous ambiguity resolution step using the strategy A (session level ambiguity resolution). The same (stochastic) orbit model was used as in the solution of Type 1.

Solution Type 3: ambiguities fixed solution but this time the integer values of the ambiguities stem from the ambiguity resolution performed using strategy B (baseline level ambiguity resolution). The stochastic orbit model described above was used again.

Solution Type 4: an ambiguities fixed solution differing from the solution type 3 by the orbit model – the standard model (8 parameters per arc and per satellite) were estimated.

We chose the set of a priori ITRF coordinates as a reference system and for each 3-days solution we computed the residuals after the 7 parameters Helmert transformation into the reference system. Thus for each type of solution and for each individual coordinate (three components for each station) we obtained 14 sets of residuals. The residuals depend on the (arbitrary) choice of the reference system and can not be used as a good criterion for the solutions quality. But the repeatability, in particular the standard deviation of these 14 values may serve as the criterion to judge our solution types.

STANDARD DEVIATION OF THE RESIDUALS
COMP=NORTH

STANDARD DEVIATION OF THE RESIDUALS
COMP=EAST
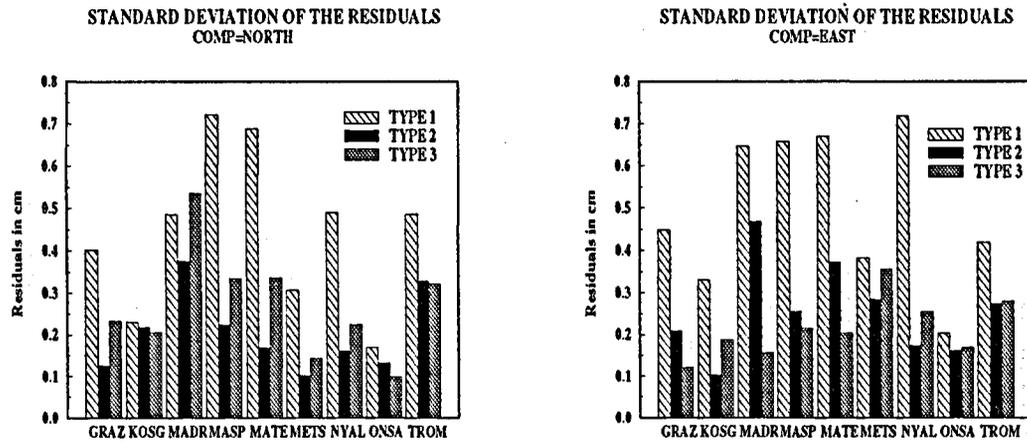
Figure 7.11: Standard deviations of the residuals after the Helmert transformation into the reference system

Figure 7.11 shows the results of the solutions 1, 2 and 3. The ambiguities fixed solutions (2 and 3) show smaller deviations of the residuals, which means that these types of solutions provide better consistency of results and better coordinates repeatability.

Figure 7.11 shows almost the same quality for the solution types 2 and 3. It is interesting to compare solutions 3 and 4 in Figure 7.12. We conclude that the orbit parametrization actually is relevant and that the standard orbit model (solution type 4) is not sufficient for hightest accuracy applications.

STANDARD DEVIATION OF THE RESIDUALS
COMP=NORTH

STANDARD DEVIATION OF THE RESIDUALS
COMP=EAST
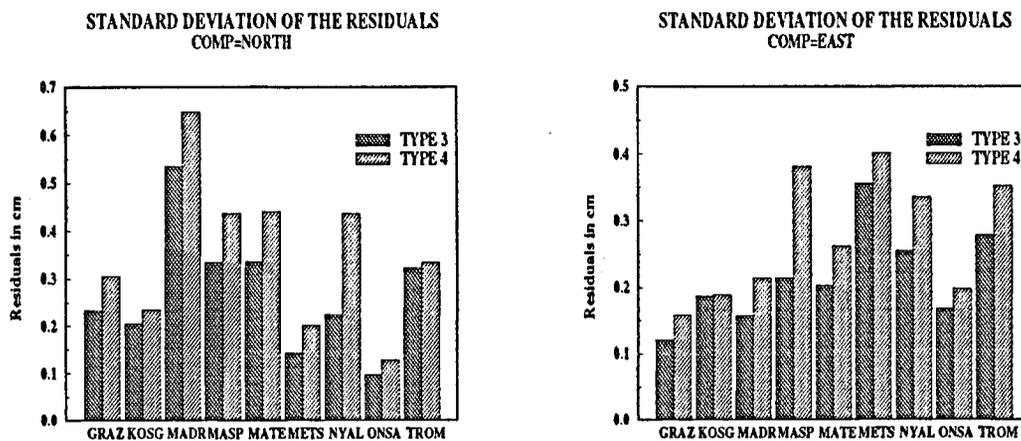
Figure 7.12: Standard deviations of the residuals after the Helmert transformation into the reference system

The ambiguity parameters are identical for both solutions, the only difference is the orbit model. The solution 4 is still better than the float solution but the superiority of solution 3 over solution 4 is obvious. It proves the importance of the orbit model.

Conclusions

Let us summarize the findings of this section: Observations from 16 days in January 1993 stemming from the European part of the IGS netork were used to test our ambiguity resolution methods. We used the Melbourne-Wübbena approach to fix the wide lane ambiguities. This step could be performed without any problems (Figures 7.8, 7.9). We used two strategies to fix the narrow lane ambiguities: Strategy A was a network approach (the entire 10 stations network was analysed for each day), strategy B was a baseline approach (the ambiguities were resolved baseline by baseline, separately on each day). The success and the results were very similar in both cases. This aspect is important becuase strategy B is much more flexible and much less CPU demanding. From Figures 7.11a,b we conclude that ambiguity resolution actually improves the results: The coordinate consistency in the network improved by a factor of up to 2 for strategy A as well as for strategy B. A similar effect could not be seen for the station heights. The results from January 1993 campaign we used to prepare more detailed tests which are described in the following chapter.

8. Test Campaigns in 1994

8.1 January 1994

The IGS went through a remarkable development in 1993 [Beutler et al., 1994c]. The global coverage of tracking sites could be improved considerably, the analysis was refined, the terrestrial reference frame was improved dramatically (transit from the ITRF 91 to the ITRF 92), and, last but not least there is a combined IGS orbit available since November 1993. The theory behind this combined orbit may be found in [Springer and Beutler, 1993], it is produced by the analysis center coordinator Dr. Jan Kouba from National Resources, Canada. His weekly analyses (IGS report series, e.g. reports No. 1079, 1099, 1109) clearly demonstrate that the consistency of the orbit series from individual IGS processing centers approach the 10 cm level in 1994. For the CODE processing center the rms uncertainty per satellite coordinate is of the order of 12 cm, an estimated improvement of about a factor of 2 since January 1993. The estimated accuracy of the combined IGS orbit for the time period of January 1994 is of the same order of magnitude.

January 1994 was the last AS-free month: AS is turned on permanently since GPS week 734. It seemed therefore worthwhile to go through essentially the same analysis as in section 7.2, but using the state-of-the-art IGS orbit quality.

We selected 14 days in January 1994 (2nd January - 15th January) and we wanted to use all 15 European Core stations which were at our disposal at that time (see Figure 2.1). Unfortunately the data stemming from the stations Kiruna and Herstmonceux could no be used due to their bad quality. Therefore only 13 stations were processed. The station names and abbreviations are given in Table 8.1.

Table 8.1: List of stations

STATION	Abbreviation	Receiver
Brussels	BRUS	Rogue SNR-8000
Graz	GRAZ	Rogue SNR-8C
Jozefoslaw	JOZE	Trimble 4000SSE
Kootwijk	KOSG	Rogue SNR-8
Madrid	MADR	Rogue SNR-8
Mas Palomas	MASP	Rogue SNR-8C
Matera	MATE	Rogue SNR-8
Metsahovi	METS	Rogue SNR-8C
Ny Allesund	NYAL	Rogue SNR-8
Onsala	ONSA	Rogue SNR-8000
Tromso	TROM	Rogue SNR-8
Wettzell	WETT	Rogue SNR-800
Zimmerwald	ZIMM	Trimble 4000SSE

Using the data from this network we wanted to answer the same questions as in Section 7.2. In addition we are considering the following aspects:

- Is there a substantial difference (repeatability of coordinates, ambiguity resolution capability) if CODE orbits instead of IGS orbits are used? A positive answer would not be surprising because the CODE orbits are based on a network including many European stations.

- We will refine the discussion by taking into account the formal errors, too. This is a delicate issue because formal errors tend to be too optimistic. This argument is not valid, however, if we look e.g. at the fraction rms(ambiguity fixed solution)/rms(ambiguity float solution) for the parameters of interest (coordinates, orbit parameters).

- We will further refine the discussion by looking into the dependence on the baseline length (fractional parts of wide lane (no effect expected) and narrow lane ambiguities, repeatability of coordinates).

- We will carefully analyse the height components. It was puzzling in the previous analyses that there was no obvious difference between the fixed and the free solutions regarding the heights. This effect has to be understood.

- We will look in more detail into the problem of the session length. We will try to define the optimum session length taking into account economical considerations. We will also more carefully analyse the repeatability of short sessions (daily variations) by producing time series of one hour solutions.

- We will produce purely regional orbits using floating resp. fixed ambiguities and compare the quality of these regional orbits with the quality of the global orbit. This problem area is of interest even independently of the ambiguity resolution aspect: what orbit quality can be achieved from a regional tracking network?

- Last but not least the analysis in this section will serve as a valid reference for the analysis in the next section, where we will look into the effect of AS (by analysing data from May 1994).

Wide–Lane Ambiguity Resolution

For the wide-lane ambiguity resolution we wanted to use the Melbourne-Wübbena approach. This method should be independent of the geometry (and therefore of the baseline length). An important question is whether the combination of different receiver types has any influence on the quality of results (on the fractional parts of wide-lane ambiguities). Considering this aspect we tried to form the baselines between receivers of the same type. The baselines we selected are given in Table 8.2.

Table 8.2: List of baselines

Station 1	Station 2	Receiver Types*	Length (km)
BRUS	KOSG	Turbo – Rogue	184
BRUS	MADR	Turbo – Rogue	1329
BRUS	ONSA	Turbo – Turbo	884
BRUS	WETT	Turbo – Rogue	638
GRAZ	WETT	Rogue – Rogue	302
JOZE	ZIMM	Trimb – Trimb	1138
MADR	MASP	Rogue – Rogue	1745
MATE	WETT	Rogue – Rogue	990
METS	TROM	Rogue – Rogue	1082
NYAL	TROM	Rogue – Rogue	1053
ONSA	METS	Turbo – Rogue	784
WETT	ZIMM	Rogue – Trimb	476

*) Receivers Rogue SNR-8, 8C and 800 are denoted as Rogue,
Rogue SNR-8000 as Turbo and Trimble 4000SSE as Trimb

For the wide-lane ambiguity resolution we used the same method and program options as described in Section 7.2. The distribution of the fractional parts of the ambiguities after the initial least-squares adjustment and in the moment of fixing are given in Figures 8.1 and 8.2:

FRACTIONAL PARTS OF WIDE-LANE AMBIGUITIES
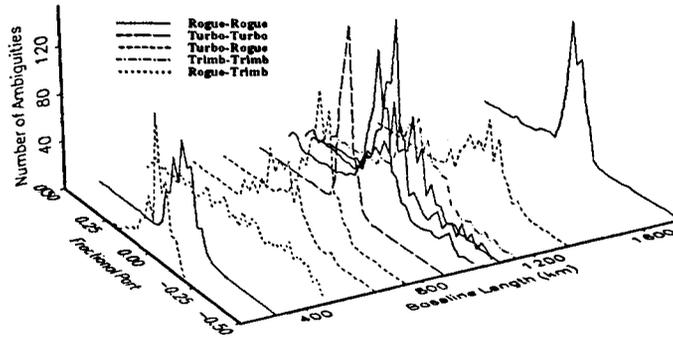
Figure 8.1: Fractional parts of wide-lane ambiguities for various baselines after the initial adjustment

FRACTIONAL PARTS OF WIDE-LANE AMBIGUITIES
In the Moment of Fixing
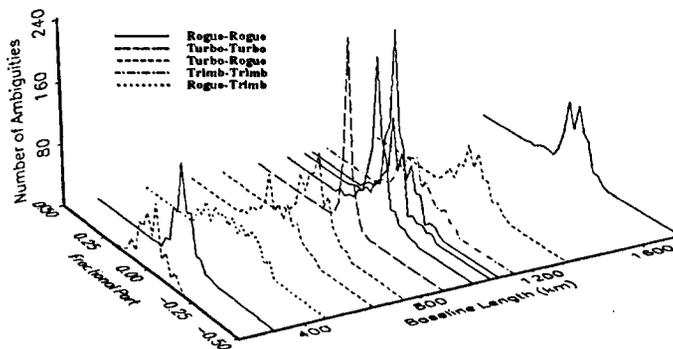
Figure 8.2: Fractional parts of wide-lane ambiguities for various baselines in the moment of fixing

According to Figures 8.1 and 8.2 we may conclude that the distribution of the fractional parts of the wide-lane ambiguities does not depend on the baseline length but on the receiver types. Especially the combination of different receivers seems to be critical. To see this effect in more detail we produced histograms for the different receiver combinations:
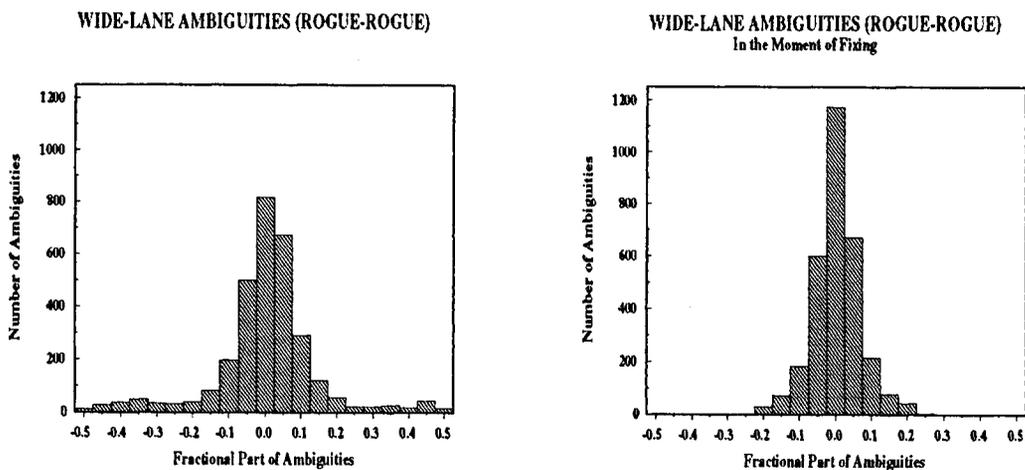
Figure 8.3: Distribution of the fractional parts of wide-lane ambiguities after the initial adjustment and in the moment of fixing (receiver types: Rogue – Rogue)
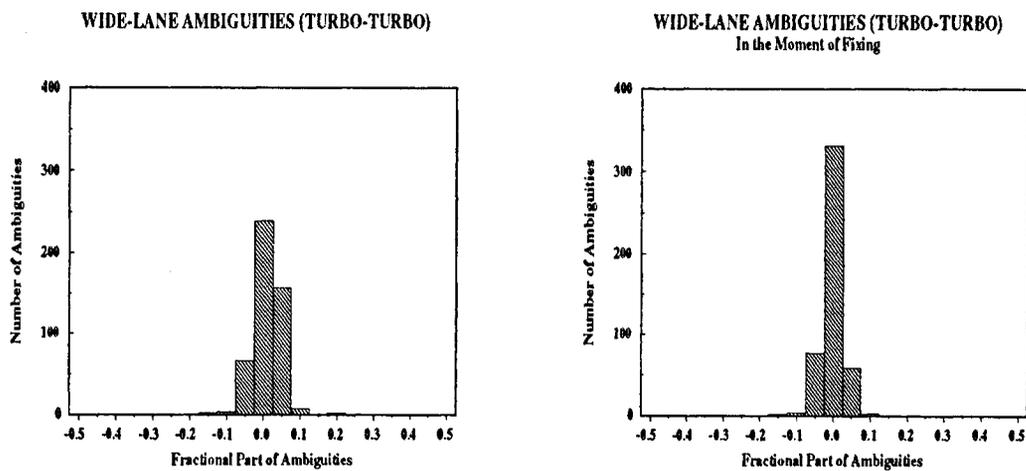
Figure 8.4: Distribution of the fractional parts of wide-lane ambiguities after the initial adjustment and in the moment of fixing (receiver types: Turbo Rogue – Turbo Rogue)

WIDE-LANE AMBIGUITIES (TURBO-ROGUE)

WIDE-LANE AMBIGUITIES (TURBO-ROGUE)
In the Moment of Fixing
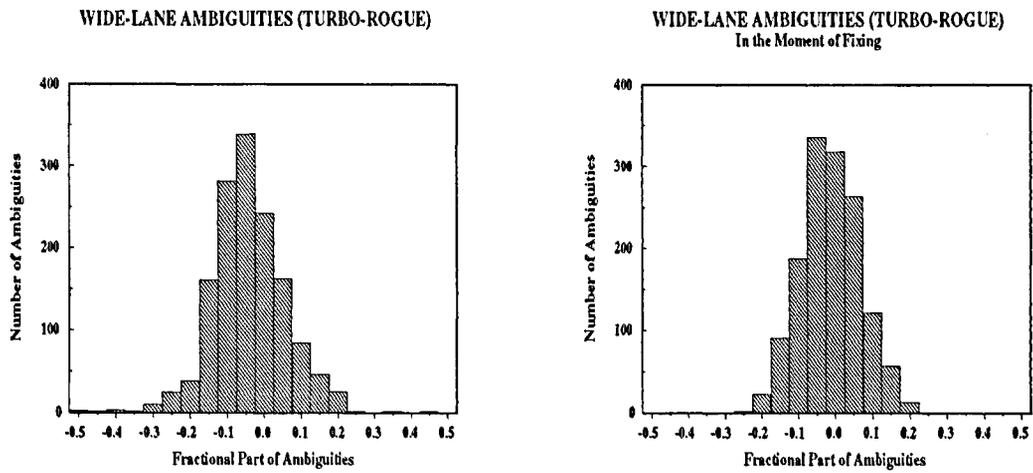
Figure 8.5: Distribution of the fractional parts of wide-lane ambiguities after the initial adjustment and in the moment of fixing (receiver types: Turbo Rogue – Rogue)

WIDE-LANE AMBIGUITIES (TRIMBLE-TRIMBLE)

WIDE-LANE AMBIGUITIES (TRIMBLE-TRIMBLE)
In the Moment of Fixing
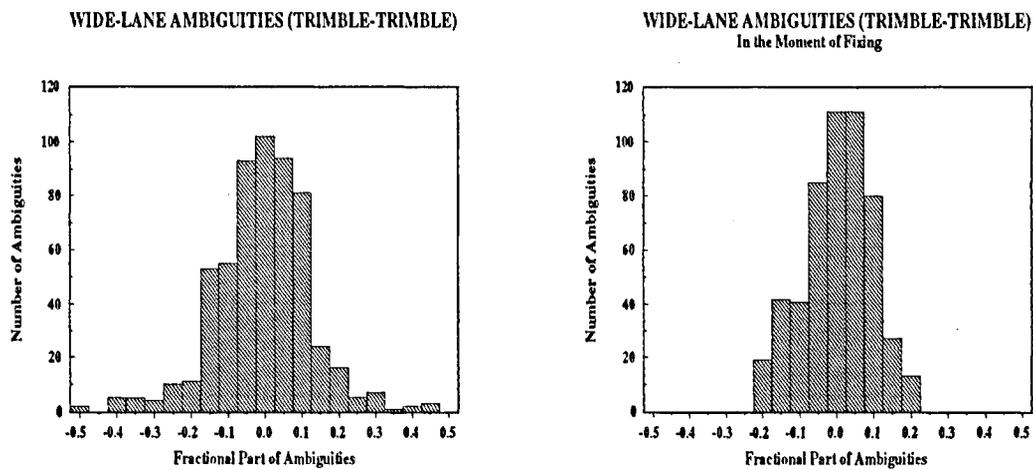
Figure 8.6: Distribution of the fractional parts of wide-lane ambiguities after the initial adjustment and in the moment of fixing (receiver types: Trimble – Trimble)

WIDE-LANE AMBIGUITIES (ROGUE-TRIMBLE)   WIDE-LANE AMBIGUITIES (ROGUE-TRIMBLE)
In the Moment of Fixing
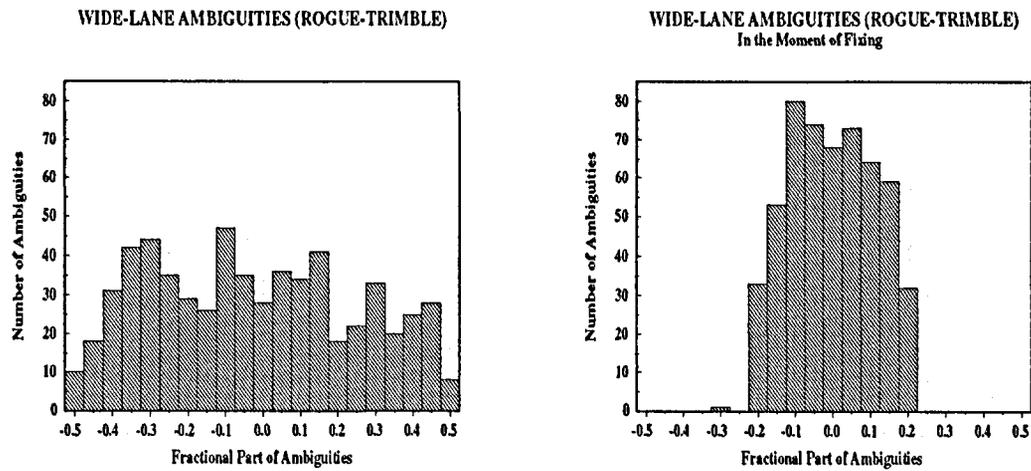
Figure 8.7: Distribution of the fractional parts of wide-lane ambiguities after the initial adjustment and in the moment of fixing (receiver types: Rogue – Trimble)

Figures 8.3 - 8.6 demonstrate the efficiency of the Melbourne-Wübbena method if high quality code measurements are available. The Turbo-Rogue receivers in Onsala and Brussels give very good results in particular.[1] Figure 8.7 shows that on the other hand no good results may be expected if a combination of different receiver types is used. In the entire network we had 7125 wide-lane ambiguities and we were able to resolve 6652 ambiguities (93 %).[2]

Narrow-lane Ambiguity Resolution

From the results of Chapter 7 we conclude that:

- Narrow-lane ambiguity resolution for baselines longer than about 500 km is possible only if orbits of excellent quality are available.

- It is possible to resolve the ambiguities in the baseline mode.

As mentioned above the IGS provides at present two types of orbits, namely orbits computed by the individual processing centers and the combined orbits. We wanted to see whether there is a quality difference between the combined (IGS) orbits and the orbits computed by the Center for Orbit Determination in Europe (COD orbits). The accuracy of the IGS orbits could benefit from the statistics (combining several high quality orbits), the COD orbits might be better for regional analyses in Europe because data from many European stations are used in this case. We used both orbit types and estimated the

---

[1] Code data from Brussels were corrupted on days 006 and 009. Fractional parts of the ambiguities stemming from these two days are not included in Figures 8.1, 8.2, 8.4 and 8.5; we used the data for all further computations, however. There were no problems with phase measurements.

[2] Without data from Brussels on days 006, 009 we would have resolved 6652 of 6865 ambiguities or 97 %.

coordinates of all stations with respect to Wettzell plus the troposphere parameters (one zenith delay per station and per 6 hours interval). We used the repeatability of 14 one-day solutions as the quality criterion. The results are given in Table 8.3.

Table 8.3: Standard deviation of the coordinates (in meters) estimated from 14 1-day solutions

		GRAZ	KOSG	MADR	MATE	TROM	ZIMM	ONSA	METS	NYAL	MASP	JOZE	BRUS	mean
IGS orbits														
	N	0.002	0.002	0.005	0.002	0.006	0.001	0.003	0.004	0.008	0.007	0.003	0.001	0.0034
	E	0.004	0.003	0.011	0.006	0.007	0.003	0.003	0.008	0.008	0.009	0.005	0.003	0.0054
	U	0.004	0.006	0.020	0.009	0.017	0.007	0.009	0.022	0.016	0.034	0.014	0.006	0.0126
COD orbits														
	N	0.002	0.002	0.006	0.002	0.006	0.001	0.003	0.003	0.009	0.006	0.003	0.001	0.0034
	E	0.004	0.003	0.010	0.005	0.007	0.003	0.004	0.008	0.008	0.009	0.006	0.003	0.0054
	U	0.004	0.006	0.021	0.009	0.016	0.007	0.009	0.023	0.011	0.039	0.012	0.005	0.0125

In Chapter 7 we have seen that it was not sufficient to study the coordinate repeatabilities because the resulting network of stations was biased by small rotations if only one station was kept fixed. Therefore we chose the set of a priori coordinates as our reference system. For each 1-day solution we then computed the residuals of the 7-parameter Helmert transformation into this reference system. The repeatability of the residuals is given in Table 8.4.

Table 8.4: Standard deviations of the residuals after the Helmert transformation into the reference system (in meters)

		GRAZ	KOSG	MADR	MATE	TROM	WETT	ZIMM	ONSA	METS	NYAL	MASP	JOZE	BRUS	mean
IGS orbits															
	N	0.0019	0.0019	0.0062	0.0031	0.0046	0.0017	0.0017	0.0017	0.0051	0.0061	0.0150	0.0031	0.0020	0.0042
	E	0.0039	0.0032	0.0116	0.0061	0.0064	0.0023	0.0041	0.0041	0.0083	0.0075	0.0150	0.0047	0.0030	0.0061
	U	0.0064	0.0082	0.0162	0.0084	0.0143	0.0060	0.0071	0.0071	0.0199	0.0142	0.0248	0.0112	0.0080	0.0116
COD orbits															
	N	0.0042	0.0074	0.0099	0.0057	0.0049	0.0039	0.0065	0.0033	0.0107	0.0052	0.0123	0.0068	0.0080	0.0068
	E	0.0031	0.0027	0.0076	0.0038	0.0029	0.0024	0.0033	0.0022	0.0069	0.0069	0.0041	0.0026	0.0031	0.0040
	U	0.0053	0.0069	0.0074	0.0044	0.0085	0.0035	0.0044	0.0044	0.0189	0.0051	0.0054	0.0064	0.0062	0.0067

From the results given in Tables 8.3 and 8.4 we may conclude that there is no significant difference between the quality of IGS and COD orbits looking at the pure repeatability of the coordinates. The standard deviations of the residuals after the Helmert Transformation are slightly better if COD orbits are used. It is important that the repeatability of the coordinates (Table 8.3) is not much worse than the repeatability of the residuals after the Helmert transformation (Table 8.4). This means that there are no significant rotations between any two 1-day orbits and it is possible to use the pure repeatability of

the coordinates as a criterion to check the quality of different solutions. The results are quite different from those of the January 93 campaign (Chapter 7).

FRACTIONAL PARTS OF NARROW-LANE AMBIGUITIES
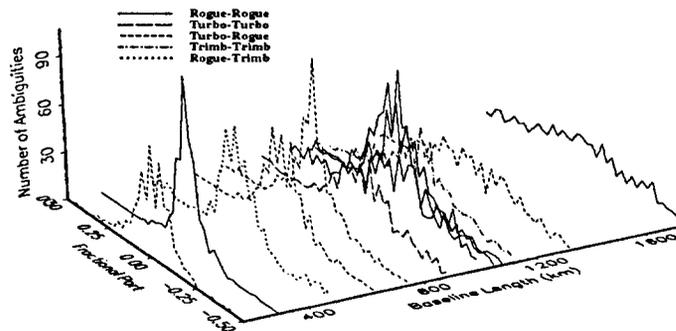
Figure 8.8: Fractional parts of narrow-lane ambiguities for various baselines after the initial adjustment

**FRACTIONAL PARTS OF NARROW-LANE AMBIGUITIES**
In the Moment of Fixing
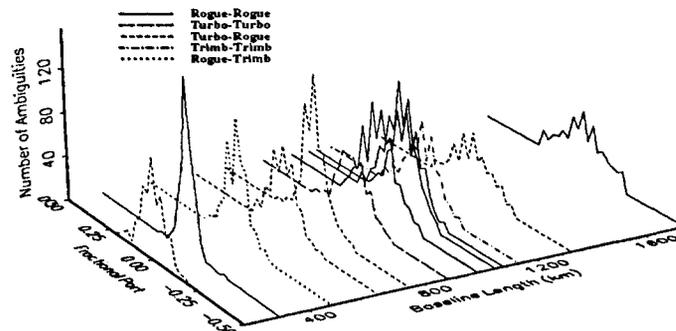
Figure 8.9: Fractional parts of narrow-lane ambiguities for various baselines in the moment of fixing

The narrow-lane ambiguities were resolved in the baseline mode (we processed each baseline separately) where we kept fixed the coordinates of the first station and we estimated the coordinates of the second one (without any constraints); in addition we solved for the troposphere parameters (four per day and station). We used the IGS orbits and

made no attempt to further improve the orbits. We used the iterative approach described in [Mervart et al., 1994] and within one iteration step we did not fix more than three ambiguities. The fractional parts of the narrow-lane ambiguities are given in Figures 8.8 and 8.9:

NARROW-LANE AMBIGUITIES (SHORT BASELINES)

**NARROW-LANE AMBIGUITIES (SHORT BASELINES)**
In the Moment of Fixing
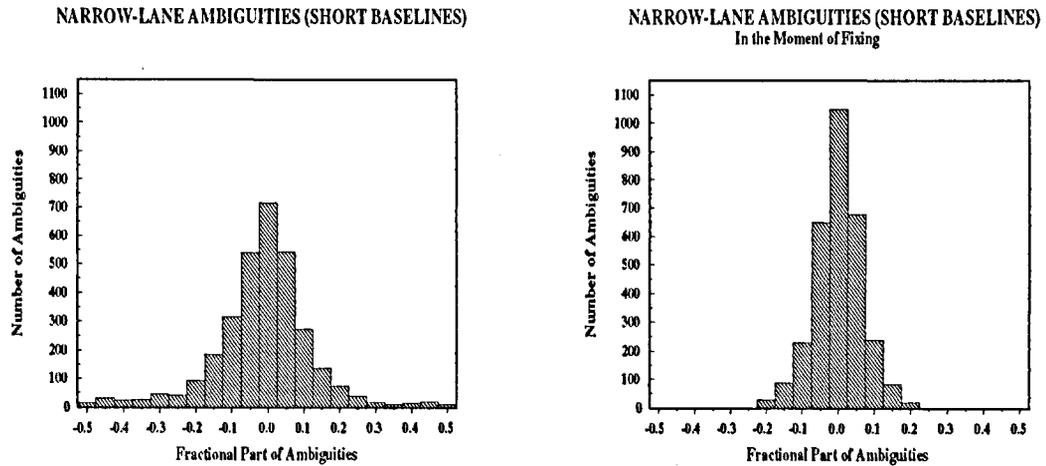
Figure 8.10: Distribution of the fractional part of narrow-lane ambiguities after the initial adjustment and in the moment of fixing (baselines up to 1000 km)

NARROW-LANE AMBIGUITIES (LONG BASELINES)

NARROW-LANE AMBIGUITIES (LONG BASELINES)
In the Moment of Fixing
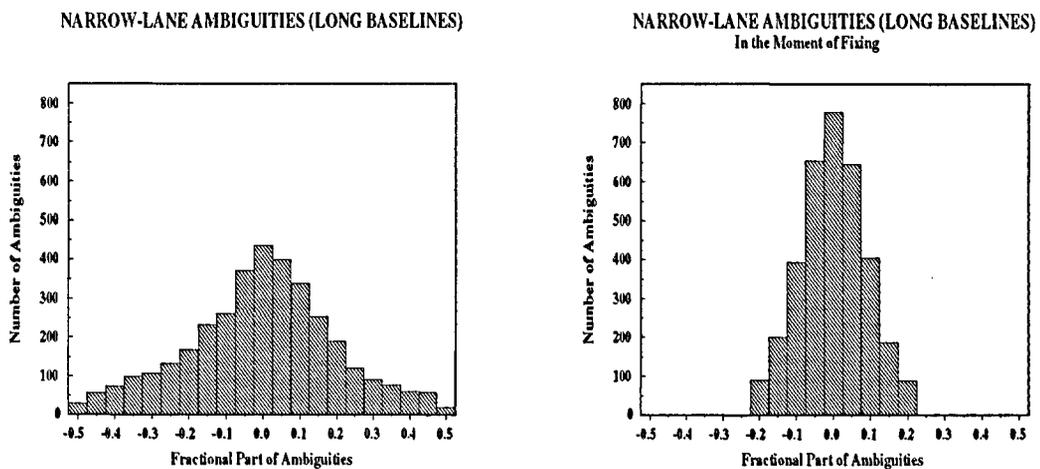
Figure 8.11: Distribution of the fractional part of narrow-lane ambiguities after the initial adjustment and in the moment of fixing (baselines longer than 1000 km)

Figures 8.8 and 8.9 demonstrate that the distribution of the fractional parts of narrow-lane ambiguities depends on the baseline length. This effect is presented once more in Figures 8.10 and 8.11.

These figures show that with high quality orbits narrow-lane ambiguity resolution is possible without major problems up to baseline lengths of about 2000 km. The superiority of the new ambiguity resolution strategy is obvious especially for long baselines. In the entire network we had 7125 narrow-lane ambiguities of which 6652 could be resolved (corresponding wide-lane ambiguities resolved) and we actually resolved 6495 of them. This corresponds to 91 % of all ambiguities and to 98 % of the resolvable (wide-lane resolved) ambiguities. This result is significantly better than that achieved using data from the January 93 campaign (the same confidential level $\xi = 3$ and $\sigma_{max} = 0.07$ in our statistical tests was used in both campaigns) . The reason for the better performance in 1994 is obviously the much improved orbit quality in January 1994.

Influence of Ambiguity Fixing on the Estimated Coordinates

The results presented above indicate that the ambiguities could be resolved in a reliable way. The main questions to be answered are:

- How does ambiguity resolution improve the accuracy of the estimated parameters?

- Which other effects are important?

Let us first inspect the coordinates. We processed the entire network separately for each day and estimated the coordinates of all stations relative to Wettzell. We compared the following processing strategies (ambiguity fixed strategies are bold faced):

Table 8.5: Solution types

Strategy	Amb. Fixed	A Priori Orbits	# Trop. Par.	Min. Elevation
IGS	no	IGS	4	20
IGS A	yes	IGS	4	20
COD	no	COD	4	20
COD A	yes	COD	4	20
COD B	no	COD	12	20
COD C	yes	COD	12	20
COD D	no	COD	4	15
COD E	yes	COD	4	15
COD F	no	COD	12	15
COD G	yes	COD	12	15

The first criterion was the repeatability of the daily coordinate esitmates. Table 8.6 shows the standard deviations of the coordinates in a local system (north, east and up):

Table 8.6: Standard deviations of the coordinates (in meters)

		IGS	IGS A	COD	COD A	COD B	COD C	COD D	COD E	COD F	COD G
GRAZ	N	0.002	0.001	0.002	0.001	0.001	0.001	0.002	0.001	0.002	0.001
	E	0.004	0.001	0.004	0.002	0.003	0.002	0.004	0.001	0.003	0.001
	U	0.004	0.005	0.004	0.005	0.004	0.005	0.004	0.005	0.004	0.004
KOSG	N	0.002	0.002	0.002	0.002	0.002	0.002	0.003	0.003	0.002	0.002
	E	0.003	0.003	0.003	0.002	0.003	0.002	0.004	0.002	0.003	0.002
	U	0.006	0.006	0.006	0.006	0.005	0.004	0.006	0.006	0.005	0.004
MADR	N	0.005	0.004	0.006	0.004	0.005	0.003	0.007	0.004	0.006	0.003
	E	0.011	0.007	0.010	0.006	0.008	0.006	0.012	0.007	0.009	0.006
	U	0.020	0.011	0.021	0.013	0.020	0.011	0.020	0.012	0.018	0.012
MATE	N	0.002	0.001	0.002	0.002	0.002	0.002	0.002	0.002	0.002	0.002
	E	0.006	0.003	0.005	0.003	0.005	0.003	0.005	0.003	0.005	0.003
	U	0.009	0.011	0.009	0.012	0.006	0.010	0.008	0.009	0.006	0.008
TROM	N	0.006	0.006	0.006	0.007	0.005	0.006	0.006	0.007	0.005	0.006
	E	0.007	0.007	0.007	0.005	0.006	0.004	0.009	0.005	0.007	0.004
	U	0.017	0.021	0.016	0.020	0.015	0.019	0.014	0.016	0.013	0.015
WETT	N	0.000	0.000	0.000	0.000	0.000	0.000	0.000	0.000	0.000	0.000
	E	0.000	0.000	0.000	0.000	0.000	0.000	0.000	0.000	0.000	0.000
	U	0.000	0.000	0.000	0.000	0.000	0.000	0.000	0.000	0.000	0.000
ZIMM	N	0.001	0.001	0.001	0.001	0.001	0.001	0.001	0.001	0.001	0.001
	E	0.003	0.001	0.003	0.002	0.003	0.002	0.003	0.002	0.003	0.002
	U	0.007	0.009	0.007	0.010	0.008	0.011	0.006	0.009	0.007	0.009
ONSA	N	0.003	0.003	0.003	0.004	0.002	0.003	0.003	0.004	0.003	0.004
	E	0.003	0.004	0.004	0.003	0.003	0.003	0.005	0.003	0.004	0.002
	U	0.009	0.009	0.009	0.008	0.007	0.007	0.007	0.007	0.007	0.007
METS	N	0.004	0.005	0.003	0.005	0.003	0.004	0.003	0.005	0.003	0.004
	E	0.008	0.005	0.008	0.004	0.007	0.004	0.009	0.004	0.007	0.004
	U	0.022	0.026	0.023	0.029	0.020	0.030	0.019	0.022	0.016	0.021
NYAL	N	0.008	0.009	0.009	0.010	0.007	0.009	0.008	0.010	0.008	0.009
	E	0.008	0.008	0.008	0.006	0.008	0.006	0.010	0.006	0.008	0.005
	U	0.016	0.017	0.011	0.015	0.011	0.016	0.009	0.012	0.009	0.013
MASP	N	0.007	0.007	0.006	0.004	0.006	0.004	0.007	0.004	0.007	0.004
	E	0.009	0.009	0.009	0.009	0.008	0.008	0.010	0.009	0.008	0.008
	U	0.034	0.025	0.039	0.036	0.040	0.036	0.033	0.029	0.035	0.028
JOZE	N	0.003	0.003	0.003	0.002	0.003	0.002	0.003	0.002	0.003	0.002
	E	0.005	0.002	0.006	0.002	0.006	0.002	0.006	0.002	0.006	0.002
	U	0.014	0.012	0.012	0.012	0.010	0.010	0.012	0.011	0.011	0.009
BRUS	N	0.001	0.002	0.001	0.002	0.001	0.001	0.001	0.001	0.001	0.001
	E	0.003	0.001	0.003	0.001	0.002	0.001	0.004	0.002	0.003	0.002
	U	0.006	0.009	0.005	0.009	0.005	0.008	0.005	0.007	0.005	0.007
mean	N	0.0034	0.0034	0.0034	0.0034	0.0029	0.0029	0.0035	0.0034	0.0033	0.0030
	E	0.0054	0.0039	0.0054	0.0035	0.0048	0.0033	0.0062	0.0035	0.0051	0.0032
	U	0.0126	0.0124	0.0125	0.0135	0.0116	0.0128	0.0110	0.0112	0.0105	0.0105

Table 8.7 shows the standard deviations of the residuals after the Helmert transformation into the reference system.

Table 8.7: Standard deviations of the residuals after the Helmert transformation into the reference system (in meters)

		IGS	IGS A	COD	COD A	COD B	COD C	COD D	COD E	COD F	COD G
GRAZ	N	0.0019	0.0029	0.0042	0.0030	0.0047	0.0031	0.0043	0.0036	0.0047	0.0029
	E	0.0039	0.0017	0.0031	0.0022	0.0035	0.0025	0.0030	0.0020	0.0030	0.0016
	U	0.0064	0.0036	0.0053	0.0034	0.0044	0.0031	0.0045	0.0040	0.0038	0.0031
KOSG	N	0.0019	0.0057	0.0074	0.0055	0.0067	0.0048	0.0064	0.0051	0.0065	0.0052
	E	0.0032	0.0022	0.0027	0.0019	0.0023	0.0012	0.0029	0.0019	0.0023	0.0015
	U	0.0082	0.0070	0.0069	0.0069	0.0063	0.0058	0.0057	0.0063	0.0054	0.0056
MADR	N	0.0062	0.0061	0.0099	0.0070	0.0071	0.0063	0.0089	0.0053	0.0061	0.0045
	E	0.0116	0.0042	0.0076	0.0034	0.0060	0.0035	0.0094	0.0039	0.0074	0.0037
	U	0.0162	0.0056	0.0074	0.0069	0.0062	0.0063	0.0052	0.0048	0.0046	0.0047
MATE	N	0.0031	0.0060	0.0057	0.0081	0.0044	0.0076	0.0063	0.0072	0.0050	0.0061
	E	0.0061	0.0023	0.0038	0.0035	0.0027	0.0036	0.0045	0.0030	0.0031	0.0029
	U	0.0084	0.0049	0.0044	0.0055	0.0040	0.0052	0.0047	0.0047	0.0041	0.0048
TROM	N	0.0046	0.0040	0.0049	0.0046	0.0043	0.0043	0.0045	0.0037	0.0040	0.0035
	E	0.0064	0.0023	0.0029	0.0028	0.0033	0.0025	0.0032	0.0026	0.0030	0.0022
	U	0.0143	0.0087	0.0085	0.0096	0.0080	0.0088	0.0071	0.0073	0.0061	0.0064
WETT	N	0.0017	0.0044	0.0039	0.0041	0.0038	0.0035	0.0042	0.0043	0.0044	0.0039
	E	0.0023	0.0017	0.0024	0.0020	0.0026	0.0020	0.0032	0.0021	0.0029	0.0018
	U	0.0060	0.0041	0.0035	0.0036	0.0027	0.0033	0.0031	0.0030	0.0026	0.0027
ZIMM	N	0.0017	0.0071	0.0065	0.0086	0.0073	0.0091	0.0065	0.0073	0.0069	0.0076
	E	0.0041	0.0013	0.0033	0.0014	0.0028	0.0011	0.0033	0.0015	0.0024	0.0010
	U	0.0071	0.0059	0.0044	0.0077	0.0053	0.0084	0.0045	0.0065	0.0048	0.0066
ONSA	N	0.0022	0.0027	0.0033	0.0029	0.0023	0.0023	0.0029	0.0028	0.0021	0.0018
	E	0.0030	0.0027	0.0022	0.0014	0.0019	0.0012	0.0020	0.0016	0.0017	0.0014
	U	0.0067	0.0038	0.0044	0.0040	0.0035	0.0036	0.0035	0.0036	0.0025	0.0026
METS	N	0.0051	0.0101	0.0107	0.0118	0.0095	0.0118	0.0088	0.0087	0.0077	0.0088
	E	0.0083	0.0046	0.0069	0.0047	0.0064	0.0047	0.0056	0.0032	0.0053	0.0032
	U	0.0199	0.0190	0.0189	0.0207	0.0173	0.0205	0.0145	0.0143	0.0129	0.0141
NYAL	N	0.0061	0.0040	0.0052	0.0036	0.0046	0.0032	0.0056	0.0037	0.0048	0.0037
	E	0.0075	0.0038	0.0069	0.0058	0.0073	0.0059	0.0068	0.0049	0.0068	0.0043
	U	0.0142	0.0047	0.0051	0.0078	0.0045	0.0084	0.0036	0.0057	0.0037	0.0056
MASP	N	0.0150	0.0108	0.0123	0.0129	0.0129	0.0123	0.0109	0.0102	0.0115	0.0095
	E	0.0150	0.0041	0.0041	0.0042	0.0046	0.0041	0.0045	0.0034	0.0039	0.0031
	U	0.0248	0.0053	0.0054	0.0064	0.0046	0.0062	0.0045	0.0043	0.0033	0.0039
JOZE	N	0.0031	0.0046	0.0068	0.0048	0.0063	0.0047	0.0073	0.0045	0.0063	0.0036
	E	0.0047	0.0020	0.0026	0.0026	0.0032	0.0019	0.0024	0.0022	0.0030	0.0015
	U	0.0112	0.0054	0.0064	0.0062	0.0060	0.0068	0.0076	0.0061	0.0065	0.0054
BRUS	N	0.0020	0.0073	0.0080	0.0074	0.0069	0.0072	0.0068	0.0061	0.0060	0.0063
	E	0.0030	0.0018	0.0031	0.0019	0.0025	0.0018	0.0034	0.0020	0.0028	0.0017
	U	0.0080	0.0066	0.0062	0.0070	0.0052	0.0070	0.0046	0.0053	0.0037	0.0052
mean	N	0.0042	0.0058	0.0068	0.0065	0.0062	0.0062	0.0064	0.0056	0.0058	0.0052
	E	0.0061	0.0027	0.0040	0.0029	0.0038	0.0028	0.0042	0.0026	0.0037	0.0023
	U	0.0116	0.0065	0.0067	0.0074	0.0060	0.0072	0.0056	0.0058	0.0049	0.0054

In Table 8.8 are the a posteriori rms errors (mean values from 14 least-squares adjustments) based on the values stemming from the parameter estimation program GPSEST.

Table 8.8: Formal rms errors (in meters)

		IGS	IGS A	COD	COD A	COD B	COD C	COD D	COD E	COD F	COD G
GRAZ	N	0.0006	0.0006	0.0006	0.0006	0.0005	0.0006	0.0006	0.0006	0.0005	0.0005
	E	0.0012	0.0004	0.0012	0.0005	0.0011	0.0004	0.0012	0.0005	0.0011	0.0004
	U	0.0040	0.0046	0.0041	0.0050	0.0037	0.0046	0.0033	0.0037	0.0029	0.0033
KOSG	N	0.0007	0.0007	0.0007	0.0008	0.0006	0.0007	0.0007	0.0008	0.0007	0.0007
	E	0.0014	0.0008	0.0014	0.0008	0.0013	0.0008	0.0015	0.0008	0.0014	0.0007
	U	0.0042	0.0049	0.0043	0.0053	0.0039	0.0049	0.0035	0.0041	0.0032	0.0037
MADR	N	0.0009	0.0010	0.0009	0.0011	0.0008	0.0010	0.0009	0.0010	0.0008	0.0009
	E	0.0017	0.0011	0.0017	0.0012	0.0016	0.0011	0.0017	0.0010	0.0016	0.0010
	U	0.0037	0.0042	0.0038	0.0046	0.0035	0.0043	0.0031	0.0035	0.0028	0.0032
MATE	N	0.0007	0.0008	0.0007	0.0009	0.0007	0.0008	0.0007	0.0008	0.0006	0.0007
	E	0.0011	0.0004	0.0012	0.0004	0.0011	0.0004	0.0012	0.0004	0.0011	0.0004
	U	0.0038	0.0043	0.0039	0.0047	0.0036	0.0044	0.0032	0.0036	0.0029	0.0033
TROM	N	0.0017	0.0017	0.0017	0.0019	0.0016	0.0018	0.0016	0.0016	0.0015	0.0015
	E	0.0022	0.0009	0.0022	0.0010	0.0020	0.0009	0.0023	0.0010	0.0021	0.0009
	U	0.0044	0.0049	0.0045	0.0053	0.0042	0.0050	0.0037	0.0042	0.0033	0.0038
WETT	N	0.0000	0.0000	0.0000	0.0000	0.0000	0.0000	0.0000	0.0000	0.0000	0.0000
	E	0.0000	0.0000	0.0000	0.0000	0.0000	0.0000	0.0000	0.0000	0.0000	0.0000
	U	0.0000	0.0000	0.0000	0.0000	0.0000	0.0000	0.0000	0.0000	0.0000	0.0000
ZIMM	N	0.0005	0.0005	0.0005	0.0006	0.0005	0.0005	0.0005	0.0006	0.0005	0.0005
	E	0.0010	0.0004	0.0011	0.0005	0.0010	0.0005	0.0011	0.0005	0.0010	0.0004
	U	0.0030	0.0034	0.0031	0.0037	0.0028	0.0035	0.0025	0.0028	0.0022	0.0026
ONSA	N	0.0009	0.0010	0.0009	0.0010	0.0008	0.0010	0.0009	0.0009	0.0008	0.0009
	E	0.0015	0.0007	0.0015	0.0008	0.0014	0.0007	0.0016	0.0008	0.0014	0.0007
	U	0.0036	0.0042	0.0037	0.0046	0.0034	0.0042	0.0031	0.0035	0.0028	0.0032
METS	N	0.0012	0.0012	0.0012	0.0013	0.0011	0.0012	0.0012	0.0012	0.0011	0.0010
	E	0.0018	0.0010	0.0019	0.0011	0.0017	0.0010	0.0019	0.0010	0.0017	0.0009
	U	0.0040	0.0045	0.0041	0.0048	0.0038	0.0045	0.0034	0.0038	0.0030	0.0034
NYAL	N	0.0022	0.0023	0.0023	0.0025	0.0021	0.0023	0.0021	0.0021	0.0019	0.0019
	E	0.0025	0.0010	0.0025	0.0011	0.0024	0.0010	0.0026	0.0011	0.0024	0.0010
	U	0.0064	0.0075	0.0066	0.0081	0.0061	0.0076	0.0051	0.0060	0.0046	0.0054
MASP	N	0.0015	0.0018	0.0016	0.0019	0.0014	0.0018	0.0014	0.0016	0.0012	0.0014
	E	0.0022	0.0015	0.0023	0.0017	0.0022	0.0016	0.0022	0.0014	0.0021	0.0013
	U	0.0050	0.0056	0.0051	0.0060	0.0048	0.0056	0.0042	0.0046	0.0039	0.0043
JOZE	N	0.0008	0.0007	0.0008	0.0008	0.0007	0.0007	0.0008	0.0008	0.0007	0.0007
	E	0.0015	0.0007	0.0015	0.0007	0.0014	0.0007	0.0016	0.0007	0.0014	0.0006
	U	0.0043	0.0050	0.0044	0.0053	0.0040	0.0050	0.0036	0.0041	0.0033	0.0037
BRUS	N	0.0005	0.0005	0.0005	0.0006	0.0004	0.0005	0.0005	0.0006	0.0005	0.0005
	E	0.0011	0.0006	0.0011	0.0007	0.0010	0.0007	0.0011	0.0006	0.0010	0.0006
	U	0.0028	0.0033	0.0029	0.0035	0.0026	0.0033	0.0024	0.0027	0.0021	0.0025
MEAN	N	0.0009	0.0010	0.0010	0.0011	0.0009	0.0010	0.0009	0.0010	0.0008	0.0009
	E	0.0015	0.0007	0.0015	0.0008	0.0014	0.0008	0.0015	0.0008	0.0014	0.0007
	U	0.0038	0.0043	0.0039	0.0047	0.0036	0.0044	0.0032	0.0036	0.0028	0.0033

The best solution stems from the strategy **COD G** (ambiguity fixed, 12 troposphere parameters per day and minimum elevation = 15°). It is interesting to plot the mean deviations of the coordinates and corresponding formal rms errors as a function of the distance from the fixed station (Wettzell). To show the influence of the resolution of ambiguities the corresponding results obtained by strategy COD F (same options but ambiguity free) are given too.

STANDARD DEVIATIONS AND FORMAL RMS
NORTH COMPONENT

STANDARD DEVIATIONS AND FORMAL RMS
EAST COMPONENT

STANDARD DEVIATIONS AND FORMAL RMS
HEIGHT COMPONENT
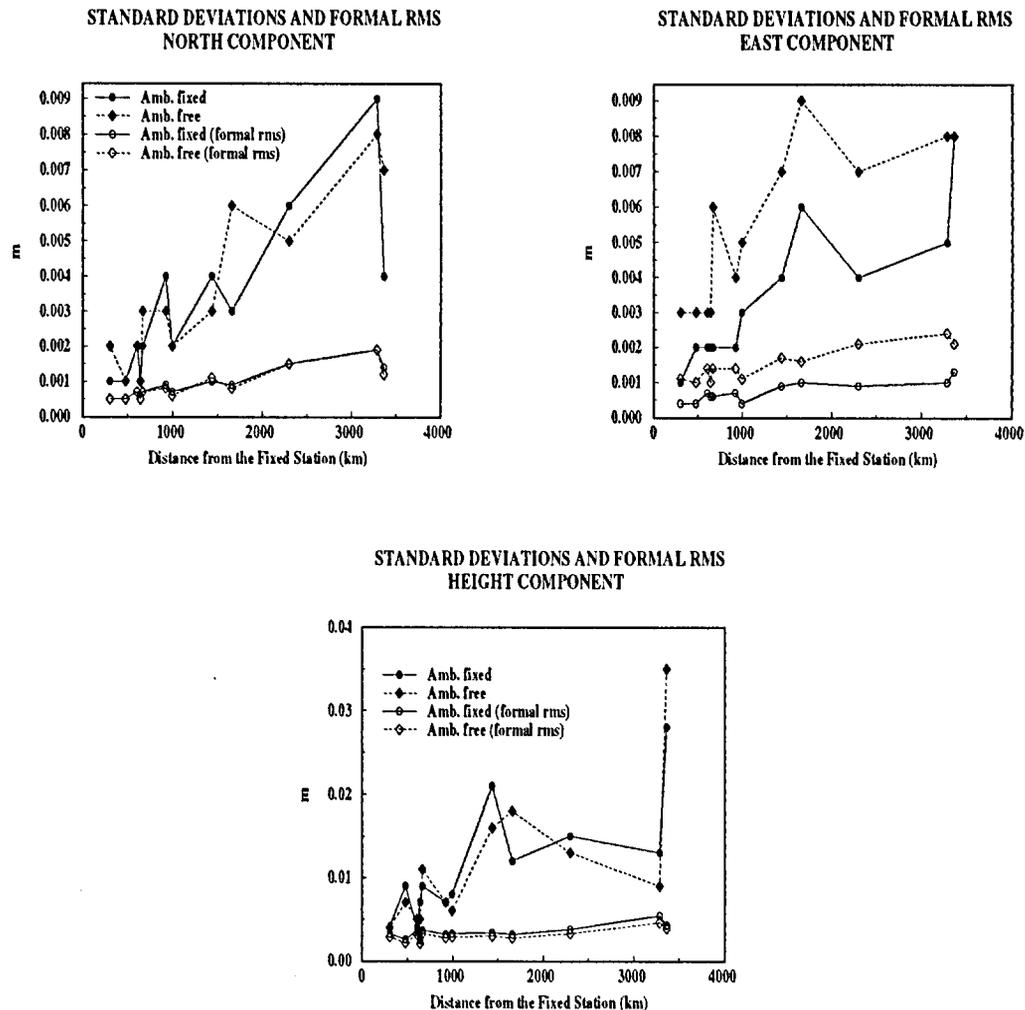
Figure 8.12: Standard deviations of the coordinates and the corresponding formal rms errors

Influence of Ambiguity Fixing on Troposphere Parameters

We estimated the zenith troposphere delays for all stations and for each interval of either 6 or 2 hours. These troposphere parameters seem to be highly correlated with the station heights. Because the ambiguity resolution had almost no influence on the station heights

(Table 8.6) it is interesting to inspect the formal errors of the troposphere parameters. Table 8.9 shows the mean values computed from 14 1-day solutions. Obviously ambiguity resolution does not improve the quality of the estimated troposphere parameters.

Table 8.9: Formal rms errors of the estimated troposphere zenith delays (in meters)

	COD	COD A	COD B	COD C	COD D	COD E	COD F	COD G
BRUS	0.0011	0.0011	0.0012	0.0016	0.0010	0.0010	0.0010	0.0010
KOSG	0.0020	0.0021	0.0022	0.0026	0.0011	0.0013	0.0015	0.0021
MADR	0.0037	0.0051	0.0028	0.0036	0.0041	0.0049	0.0025	0.0029
ONSA	0.0011	0.0018	0.0018	0.0020	0.0010	0.0010	0.0011	0.0011
WETT	0.0011	0.0014	0.0017	0.0022	0.0010	0.0010	0.0012	0.0014
GRAZ	0.0074	0.0096	0.0052	0.0070	0.0076	0.0096	0.0055	0.0067
JOZE	0.0040	0.0051	0.0032	0.0039	0.0034	0.0042	0.0029	0.0034
ZIMM	0.0026	0.0035	0.0027	0.0031	0.0023	0.0027	0.0021	0.0024
MASP	0.0046	0.0056	0.0036	0.0043	0.0044	0.0054	0.0032	0.0038
METS	0.0014	0.0018	0.0020	0.0021	0.0010	0.0010	0.0011	0.0012
TROM	0.0016	0.0020	0.0020	0.0021	0.0010	0.0010	0.0011	0.0012
MATE	0.0021	0.0023	0.0025	0.0030	0.0014	0.0017	0.0022	0.0023
NYAL	0.0021	0.0029	0.0026	0.0034	0.0013	0.0018	0.0020	0.0023
mean	0.0027	0.0034	0.0026	0.0031	0.0024	0.0028	0.0021	0.0024

Influence of Ambiguity Fixing on Orbit Determination

In this section we want to answer two questions:

- What is the quality of *regional* orbits compared to *global* orbits?

- Does ambiguity resolution influence the estimated orbits?

To answer these two questions we used the following approach: for each strategy (Table 8.5) we computed the mean set of coordinates from our 14 one-day solutions. These coordinates we kept fixed in the orbit determination step where we solved for 6 osculating elements, 2 radiation pressure parameters, and in addition for a set of 3 stochastic parameters for the eclipsing satellites (per one revolution) as described in [Beutler et al., 1994a]). In addition we solved for the specified number of troposphere parameters. The ambiguities were kept fixed or free according to the strategy used (Table 8.5). First we computed 14 1-day arcs to find out the best strategy. Table 8.10 shows the mean residuals after fitting one 14-days arc through our 14 1-day arcs (see [Beutler et al., 1994a]).

Table 8.10: Mean residuals after 14 days fit using ORBIMP program [Beutler et al., 1994a] (in cm, non-eclipsing satellites only)

	PRN																
	1	3	7	9	13	14	16	18	19	21	23	25	26	27	28	29	31	mean
COD	998	110	151	515	193	***	188	766	***	374	184	156	104	837	231	248	369	316
COD A	804	48	73	299	60	459	24	232	739	193	148	76	49	586	43	103	143	148
COD B	***	89	122	525	190	***	65	358	***	424	148	134	92	738	228	265	266	260
COD C	***	35	64	259	60	515	58	343	833	74	119	63	60	550	31	223	143	148
COD D	909	78	124	596	192	***	59	367	***	305	155	114	105	529	109	222	412	240
COD E	92	49	70	425	64	424	25	134	419	100	143	63	47	513	45	180	200	147
COD F	511	61	103	687	171	926	49	254	***	278	129	90	86	521	126	269	305	224
COD G	***	33	64	381	51	482	22	78	497	68	111	42	52	436	31	128	178	120

*** : > 10 m

It is interesting to inspect the mean formal rms errors of the orbital parameters in Table 8.11. Obviously ambiguity resolution considerably strengthens the orbital parameters.

Table 8.11: Formal rms errors of the orbital elements

	a	e	i Ω ω u_0	p_0 p_2
	m	10^{-7}	10^{-3} "	10^{-8} m·s^{-2}
COD	0.67	0	1 3 2175 28	0.212 0.198
COD A	0.26	0	0 1 1263 11	0.100 0.072
COD B	0.65	0	1 3 2115 27	0.207 0.193
COD C	0.25	0	0 1 1177 10	0.095 0.068
COD D	0.52	0	1 2 1211 22	0.162 0.156
COD E	0.23	0	0 1 963 10	0.089 0.064
COD F	0.49	0	1 2 1123 21	0.153 0.148
COD G	0.22	0	0 1 869 09	0.082 0.059

We now selected strategies **COD G** (ambiguity fixed, 12 troposphere parameters per day and station, minimal elevation 15°) and COD F (same options but ambiguities free) as our "best" strategies and we computed 12 3-days arcs. From each 3-days solution we extracted the middle day and used the tabular positions of these 12 orbit files as pseudoobservations in an orbit improvement step where one 12-days arc was determined (it is exactly the same approach which we used in routine IGS processing – see Chapter 2). The results are given in Table 8.12. Strategy "Std." in this Table is the standard solution produced by the Center for Orbit Determination in Europe using the data of the global network.

Table 8.12: Mean residuals after 12 days fit (in cm, non-eclipsing satellites only)

	PRN																
	1	3	7	9	13	14	16	18	19	21	23	25	26	27	28	29	31	mean
Std.	15	15	13	16	12	13	14	24	15	16	67	15	11	14	13	20	12	18
COD F	18	28	17	29	16	18	16	28	34	23	68	22	16	28	23	21	29	26
COD G	15	20	16	20	15	15	15	24	23	15	68	15	12	17	15	20	19	20

Table 8.13: Formal rms errors of the orbital elements computed from 12-days fit

	a m	e 10^{-7}	i Ω ω u_0 10^{-3} $''$	p_0 p_2 10^{-10} $m \cdot s^{-2}$
COD F	0.01	0	0 0 70 1	0.326 0.191
COD G	0.00	0	0 0 51 0	0.258 0.058

The results are encouraging. Using only regional (European) data and fixing the ambiguities the resulting orbits are almost of the same quality as the orbits computed using the data from a global network. Figure 8.13 shows the residuals of the best fitting 12 days arc for strategy **COD G** and satellite 26 for the radial (R), the along-track (S) and the out of plane (W) components.

RESIDUALS FOR PRN 26
Strategy COD F
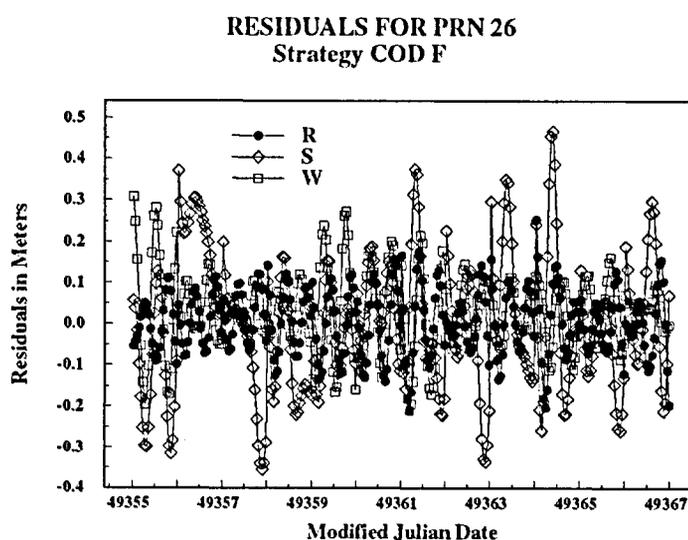
Figure 8.13: Orbit consistency

Short-period Variations of the Coordinates

It is known that ambiguity fixing is of great importance for short sessions ($\leq 1^h$). In this section we want to study short-period variations of the coordinates. The first problem addressed concerns the session length necessary to obtain a coordinate accuracy of about 1 cm. To answer this question we selected day 003 of 1994 and we used strategy COD F to process the entire network. We changed the session lengths from 1 hour up to 24 hours in 1 hour steps. Thus we obtained 24 coordinate sets. Each set of coordinates was transformed into the reference set (mean coordinates from 14 1-day solutions) using a 7-parameter Helmert transformation. The rms of this transformation as a function of the session length is given in Figure 8.14. Apart from strategy **COD G** (ambiguity fixed) the results obtained using strategy COD F (ambiguity free) are given too.

RMS OF THE HELMERT TRANSFORMATION
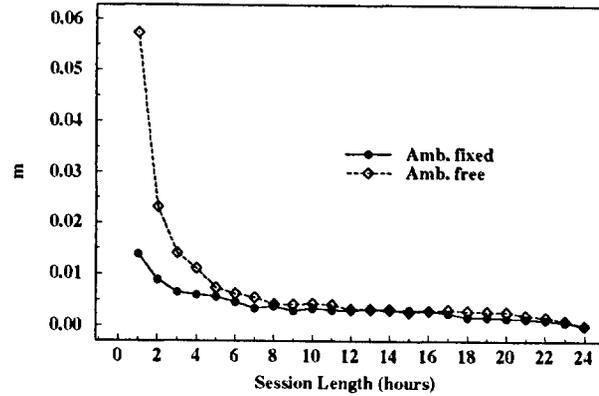
Figure 8.14: Rms of the 7-parameter Helmert transformation with the mean coordinate set

Taking into account the results presented in Figure 8.14 we decided to use 2-hours sessions and strategy **COD G** (ambiguity fixed) to study short-period variations of the coordinates. We processed the entire network and we computed $14 \cdot 12 = 168$ sets of coordinates (14 days, 12 solutions per day: $0^h - 2^h$, $2^h - 4^h$ etc.). The results for stations Brussels and Matera are shown in Figures 8.15, 8.16 and 8.17:
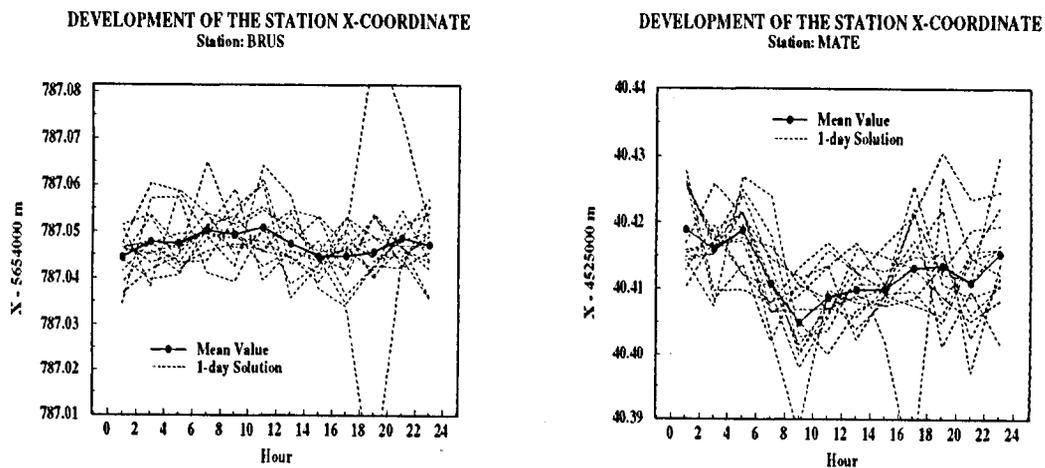
Figure 8.15: Development of the station coordinates stemming from 2 hours sessions

DEVELOPMENT OF THE STATION Y-COORDINATE
Station: BRUS

DEVELOPMENT OF THE STATION Y-COORDINATE
Station: BRUS
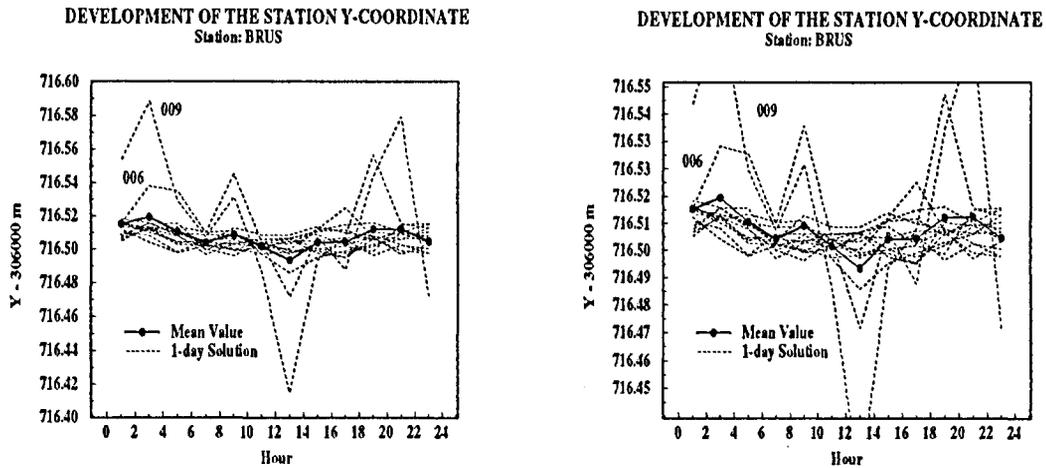
Figure 8.16: Development of the station coordinates stemming from 2 hours sessions

DEVELOPMENT OF THE STATION HEIGHT
Station: BRUS

DEVELOPMENT OF THE STATION HEIGHT
Station: MATE
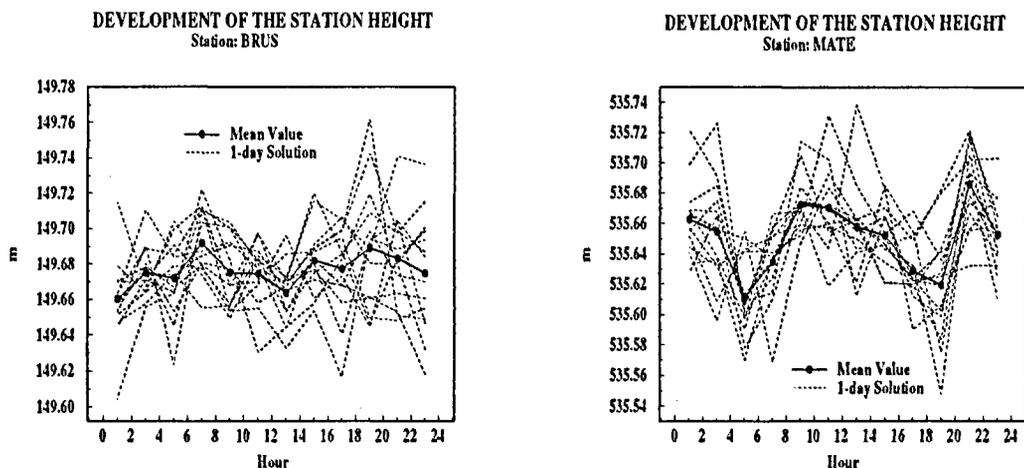
Figure 8.17: Development of the station coordinates stemming from 2 hours sessions

Other stations show very similar variations of the coordinates. In general we may say, that no short-period variations in the position could be detected. Three stations (Kootwijk, Matera and Onsala) show variations of the station height with a period close to 12 hours. In Figure 8.15 we see two outlier days when we inspect the behaviour of the east-west coordinate of the station Brussels. These two outliers are days 006 and 009 where the code data were corrupted and no ambiguities could be resolved for this baseline. This demonstrates that without ambiguity resolution it is almost impossible to study short-period variations of the coordinates.

114

8.2 Ambiguity Resolution under AS after 31 January 1994

In this section we want to study the effect of AS on data processing, in particular on ambiguity resolution after the (hopefully not) permanent turning on of AS. We will proceed as follows:

- in a first step we summarize the key differences of operation of various receiver types in the network without/with AS.

- in a second step we will make an attempt to analyse the data in exactly the same way as in the previous chapter. We will focus on wide-lane ambiguity resolution to check whether or not wide-lane ambiguity resolution is actually possible.

- we will summarize the receiver requirements for the future of the IGS network.

- we will demonstrate that, using the QIF technique outlined in Section 6.4 ambiguity resolution on baselines up to 2000 km is still possible even if no P-code is available.

Data Selection and Ambiguity-Free Solutions

To test the influence of AS on our processing strategies we selected GPS weeks 749 and 750 (15th May – 28th May, 1994). We used the data from the same stations as in the January'94 campaign (see Table 8.1) and we formed exactly the same set of baselines (see Table 8.2). The first important question was whether the ambiguity-free solutions computed from AS data are of the same quality as the results obtained from January'94 campaign. To answer this question we computed 14 one-day solutions using the strategies IGS, COD, COD B, COD D and COD F (see Table 8.5). The results are given in Tables 8.14 and 8.15. These tables correspond to Tables 8.6 and 8.7. They show the repeatabilities of the station coordinates and the mean deviations of the residuals after a Helmert transformation into an arbitrary reference system. Comparing the results from the January'94 campaign (Tables 8.6, 8.7) and from the May'94 campaign (8.14, 8.15) we conclude that AS had little or no influence on the quality of the phase measurements.

Wide-lane Ambiguity Resolution using Melbourne-Wübbena Approach

In the second step we tried to resolve the wide-lane ambiguities in the same way as we did it in the January'94 campaign – using the Melbourne-Wübbena linear combination of phase and code measurements. In previous analyses we demostrated that this strategy is (almost) baseline length independent. The most important criterion seems to be the quality of code measurements. Combining different receiver types might be critical too. The fractional parts of the wide-lane ambiguities are given in Figures 8.18 – 8.20.

WIDE-LANE AMBIGUITIES (ROGUE-ROGUE)

WIDE-LANE AMBIGUITIES (TURBO-ROGUE)
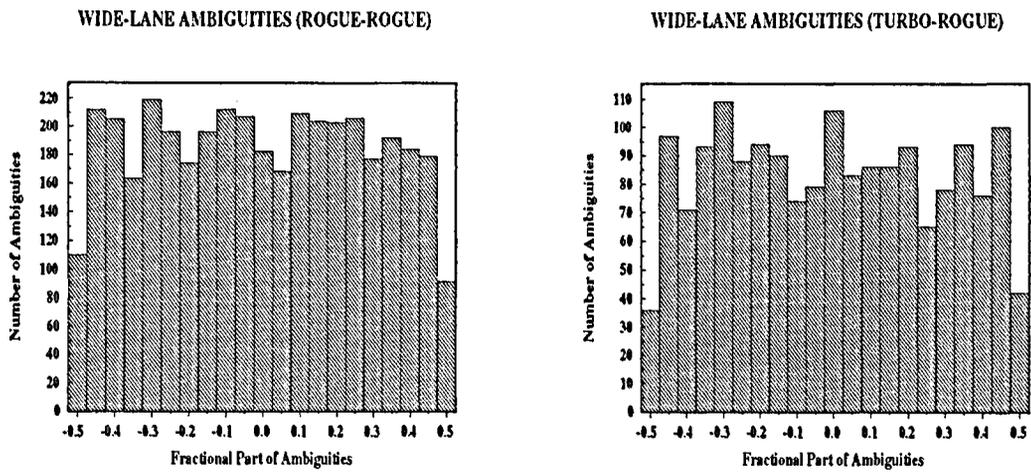
Figure 8.18: Distribution of the fractional parts of wide-lane ambiguities after the initial adjustment (receiver types: Rogue – Rogue and Turbo Rogue – Rogue)

WIDE-LANE AMBIGUITIES (TRIMBLE-TRIMBLE)

WIDE-LANE AMBIGUITIES (ROGUE-TRIMBLE)
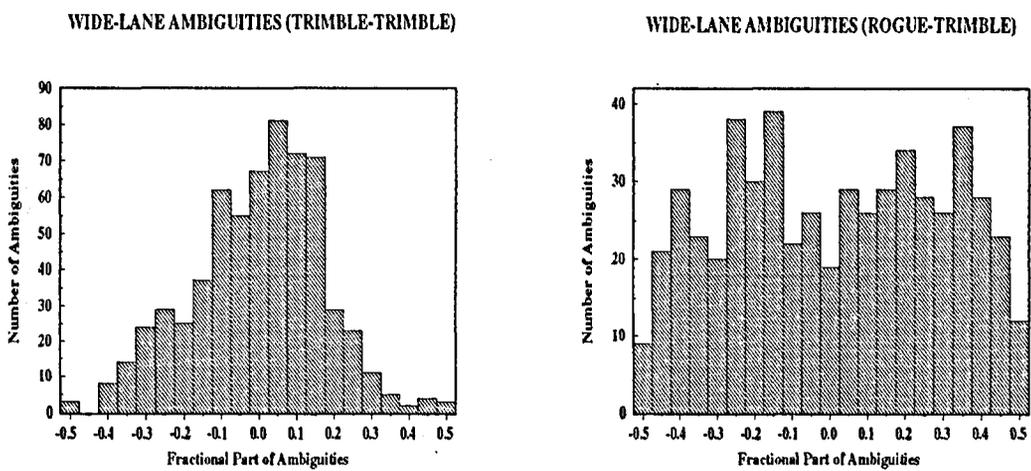
Figure 8.19: Distribution of the fractional parts of wide-lane ambiguities after the initial adjustment (receiver types: Trimble – Trimble and Rogue – Trimble)

116

WIDE-LANE AMBIGUITIES (TURBO-TURBO)

WIDE-LANE AMBIGUITIES (TURBO-TURBO)
In the Moment of Fixing
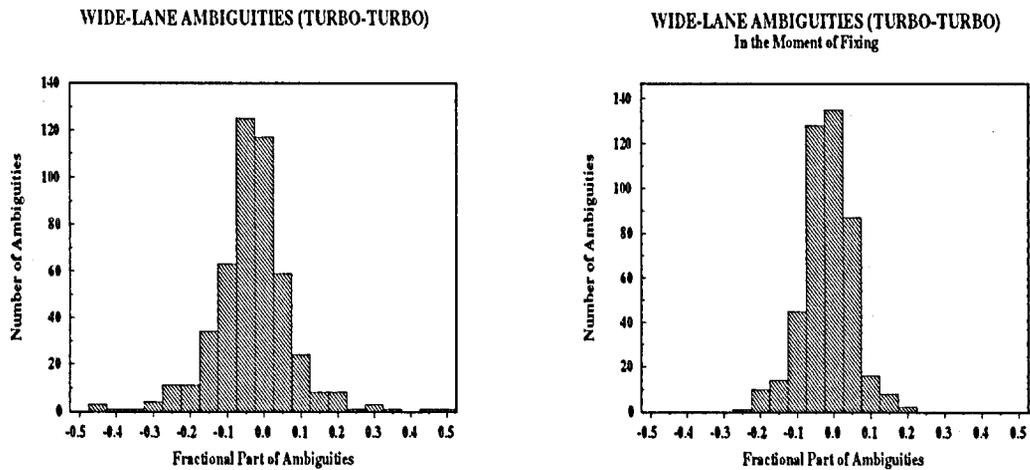
Figure 8.20: Distribution of the fractional parts of wide-lane ambiguities after the initial adjustment and in the moment of fixing (receiver types: Turbo Rogue – Turbo Rogue)

From the results of the wide-lane ambiguity resolution we conclude that the quality of code measurements decreased dramatically after AS was turned on. The code measurements from the Rogue SNR-8, Rogue SNR-8C and Rogue SNR-800 receivers (denoted as "Rogue" above) actually could not be used to resolve the wide-lane ambiguities.

NARROW-LANE AMBIGUITIES (BSON)

NARROW-LANE AMBIGUITIES (BSON)
In the Moment of Fixing
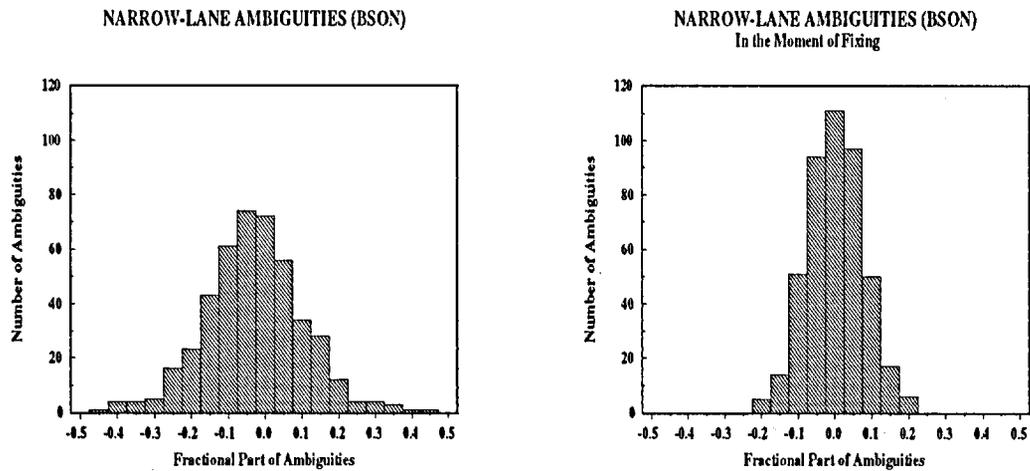
Figure 8.21: Distribution of the fractional parts of narrow-lane ambiguities after the initial adjustment and in the moment of fixing (baseline Brussels – Onsala)

Good results were obtained using the data from Rogue SNR-8000 receivers (denoted as "Turbo Rogue" above) but there were only two receivers of this type available in Europe

117

in May 1994. On this one baseline (Brussels – Onsala) we could resolve the narrow-lane ambiguities in the same way as in the January'94 campaign. The fractional parts of the narrow-lane ambiguities are given in Figure 8.21. With the exception of one baseline (Brussels – Onsala) we had to conclude that it was not possible to use the Melbourne-Wübbena approach for ambiguity resolution.

Code Independent Ambiguity Resolution

The poor quality of the code measurements under AS was one reason to develop an ambiguity resolution strategy not making use of the code measurements at all. The result of this development is the *Quasi Ionosphere-Free (QIF) Ambiguity Resolution Strategy* described in Section 6.4. This strategy uses the L_1 and L_2 phase measurements only. The method is based on a stochastic modeling of the ionospheric delay [Schaer, 1994] and a sophisticated ambiguity resolution algorithm. Using this strategy we were able to resolve 73.5 % of 15534 L_1 and L_2 ambiguities in the entire network (80.8 % on the baselines up to 1000 km and 65.9 % on the baselines between 1000 and 2000 km). We used the value $d_{max} = 0.1$ (equation (6.69)) and we restricted the search range for $\tilde{n}_5$ (equation (6.67)) by the condition $|\tilde{n}_5 - \text{nint}(b_1 - b_2)| \leq 0.5$. The L_5 residuals $\tilde{n}_5$ (equation (6.67)) and the L_3 residuals d_3 (equation (6.69)) are given in Figures 8.22 and 8.23.
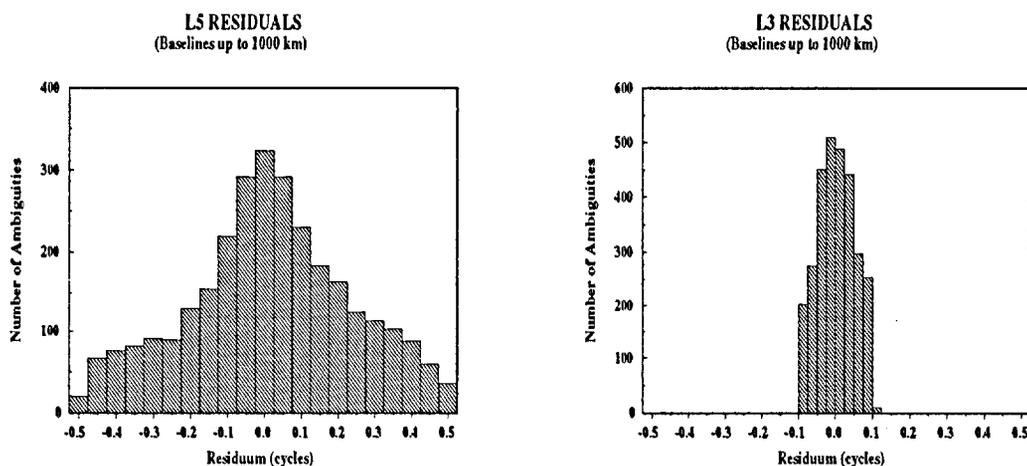
Figure 8.22: L_5 and L_3 residuals (see Section 6.4) – baselines up to 1000 km
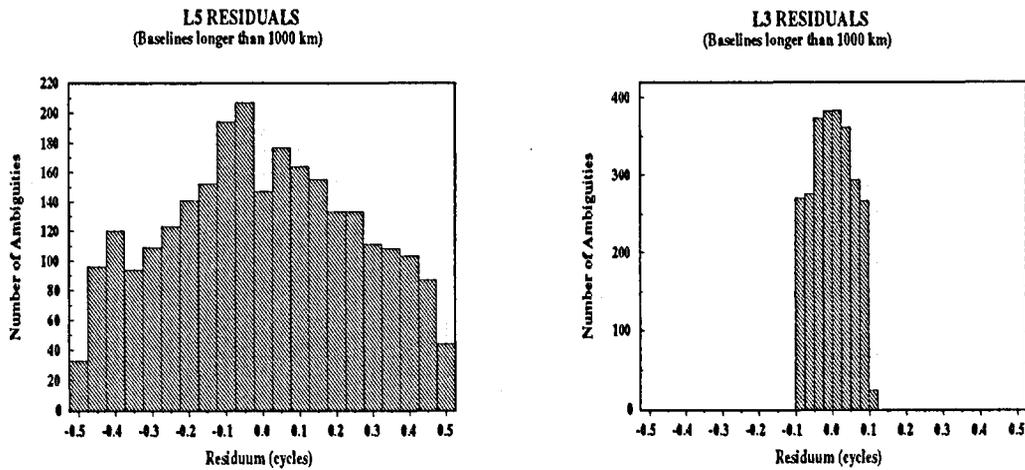
Figure 8.23: L_5 and L_3 residuals (see Section 6.4) – baselines between 1000 km and 2000 km

It is a critical issue to estimate the quality of the ambiguity resolution using the QIF strategy from the distribution of the L_5 and/or L_3 residuals. The L_5 residuals may take on large values due to ionosphere and the L_3 residuals are not allowed to be greater than d_{max} (equation 6.69). Nevertheless Figures 8.22 and 8.23 indicate that this strategy is reliable up to baseline lengths of about 1000 km. It should be mentioned that no deterministic a priori ionosphere model was used (Section 6.4). Developing and using a good a priori ionosphere model should even improve our results. We had a good check of the ambiguity resolution on the baseline Brussels – Onsala (884 km) because we could compare the results of two different strategies, namely QIF and Melbourne-Wübbena. All the ambiguities resolved by both strategies were identical.

Influence of Ambiguity Fixing on the Coordinates and Orbits

In this step we wanted to check whether the ambiguities resolved using the QIF strategy improve the repeatability of the coordinates in the same way as in the January'94 campaign (when we could use P-code measurements and the Melbourne-Wübbena approach). We made the same tests as in Section 8.1; i.e. we computed 14 one-day solutions using the strategies defined in Table 8.5 and we looked at the repeatability of the coordinates and of the coordinate residuals after a Helmert transformation into the reference system (ITRF). The results are given in Tables 8.14 and 8.15.

Table 8.14: Standard deviations of the coordinates (in meters)

		IGS	IGS A	COD	COD A	COD B	COD C	COD D	COD E	COD F	COD G
GRAZ	N	0.003	0.002	0.003	0.002	0.003	0.002	0.003	0.003	0.003	0.002
	E	0.007	0.002	0.007	0.002	0.005	0.002	0.007	0.002	0.006	0.002
	U	0.008	0.010	0.008	0.011	0.008	0.010	0.008	0.008	0.008	0.006
KOSG	N	0.003	0.001	0.003	0.002	0.003	0.002	0.004	0.003	0.003	0.002
	E	0.005	0.004	0.006	0.004	0.005	0.004	0.006	0.004	0.006	0.004
	U	0.014	0.016	0.013	0.015	0.009	0.014	0.009	0.009	0.007	0.009
MADR	N	0.005	0.004	0.006	0.005	0.007	0.005	0.005	0.004	0.006	0.005
	E	0.008	0.006	0.007	0.005	0.009	0.005	0.009	0.005	0.009	0.005
	U	0.017	0.018	0.018	0.020	0.018	0.021	0.015	0.015	0.014	0.017
MATE	N	0.012	0.008	0.011	0.008	0.011	0.008	0.010	0.008	0.008	0.007
	E	0.013	0.004	0.015	0.006	0.012	0.005	0.017	0.006	0.012	0.004
	U	0.020	0.020	0.021	0.024	0.026	0.022	0.020	0.019	0.022	0.020
TROM	N	0.007	0.006	0.009	0.006	0.010	0.008	0.008	0.005	0.008	0.006
	E	0.012	0.007	0.014	0.009	0.014	0.009	0.012	0.008	0.011	0.009
	U	0.013	0.015	0.013	0.010	0.013	0.011	0.014	0.010	0.011	0.009
WETT	N	0.000	0.000	0.000	0.000	0.000	0.000	0.000	0.000	0.000	0.000
	E	0.000	0.000	0.000	0.000	0.000	0.000	0.000	0.000	0.000	0.000
	U	0.000	0.000	0.000	0.000	0.000	0.000	0.000	0.000	0.000	0.000
ZIMM	N	0.002	0.001	0.002	0.001	0.002	0.001	0.002	0.002	0.002	0.001
	E	0.008	0.002	0.008	0.002	0.008	0.002	0.008	0.002	0.007	0.002
	U	0.015	0.008	0.014	0.010	0.015	0.011	0.010	0.007	0.010	0.007
ONSA	N	0.004	0.003	0.004	0.003	0.005	0.003	0.005	0.003	0.005	0.004
	E	0.004	0.004	0.006	0.004	0.004	0.004	0.007	0.004	0.005	0.004
	U	0.013	0.014	0.013	0.012	0.011	0.013	0.011	0.008	0.009	0.009
METS	N	0.005	0.004	0.007	0.005	0.007	0.005	0.007	0.005	0.008	0.006
	E	0.014	0.006	0.015	0.006	0.015	0.006	0.012	0.006	0.010	0.006
	U	0.014	0.014	0.014	0.013	0.013	0.013	0.013	0.010	0.010	0.010
NYAL	N	0.009	0.008	0.011	0.008	0.011	0.010	0.010	0.007	0.009	0.008
	E	0.014	0.007	0.018	0.011	0.018	0.012	0.016	0.011	0.015	0.011
	U	0.011	0.014	0.009	0.012	0.012	0.015	0.015	0.014	0.015	0.015
MASP	N	0.009	0.009	0.009	0.009	0.008	0.009	0.006	0.007	0.007	0.007
	E	0.010	0.007	0.009	0.010	0.010	0.010	0.009	0.010	0.009	0.009
	U	0.027	0.021	0.030	0.024	0.029	0.029	0.026	0.018	0.021	0.018
JOZE	N	0.003	0.003	0.003	0.003	0.003	0.003	0.004	0.003	0.004	0.003
	E	0.007	0.004	0.007	0.004	0.007	0.004	0.008	0.005	0.009	0.004
	U	0.014	0.012	0.014	0.014	0.014	0.013	0.012	0.012	0.012	0.013
BRUS	N	0.002	0.001	0.003	0.002	0.003	0.002	0.004	0.002	0.004	0.003
	E	0.004	0.004	0.005	0.004	0.004	0.004	0.006	0.004	0.006	0.004
	U	0.010	0.011	0.011	0.011	0.009	0.012	0.011	0.007	0.009	0.008
mean	N	0.0049	0.0038	0.0055	0.0042	0.0056	0.0045	0.0052	0.0040	0.0052	0.0042
	E	0.0082	0.0044	0.0090	0.0052	0.0085	0.0052	0.0090	0.0052	0.0081	0.0049
	U	0.0135	0.0133	0.0137	0.0135	0.0136	0.0142	0.0126	0.0105	0.0114	0.0108

Table 8.15: Standard deviations of the residuals after the Helmert transformation into the reference system (in meters)

		IGS	IGS A	COD	COD A	COD B	COD C	COD D	COD E	COD F	COD G
GRAZ	N	0.0043	0.0059	0.0048	0.0064	0.0044	0.0055	0.0032	0.0037	0.0041	0.0042
	E	0.0052	0.0037	0.0047	0.0030	0.0032	0.0024	0.0049	0.0023	0.0032	0.0024
	U	0.0059	0.0089	0.0062	0.0089	0.0073	0.0076	0.0038	0.0056	0.0065	0.0054
KOSG	N	0.0071	0.0058	0.0066	0.0061	0.0058	0.0049	0.0048	0.0048	0.0054	0.0040
	E	0.0041	0.0018	0.0046	0.0017	0.0043	0.0016	0.0038	0.0017	0.0038	0.0016
	U	0.0061	0.0065	0.0059	0.0070	0.0053	0.0063	0.0034	0.0046	0.0046	0.0042
MADR	N	0.0088	0.0083	0.0083	0.0097	0.0075	0.0099	0.0069	0.0075	0.0067	0.0083
	E	0.0064	0.0021	0.0063	0.0026	0.0046	0.0024	0.0083	0.0025	0.0061	0.0025
	U	0.0095	0.0080	0.0094	0.0080	0.0099	0.0079	0.0068	0.0061	0.0066	0.0063
MATE	N	0.0136	0.0143	0.0141	0.0157	0.0162	0.0149	0.0117	0.0124	0.0122	0.0124
	E	0.0135	0.0057	0.0130	0.0067	0.0117	0.0064	0.0143	0.0053	0.0099	0.0050
	U	0.0061	0.0058	0.0070	0.0073	0.0092	0.0096	0.0100	0.0087	0.0079	0.0088
TROM	N	0.0030	0.0032	0.0031	0.0027	0.0031	0.0026	0.0037	0.0025	0.0030	0.0022
	E	0.0052	0.0024	0.0052	0.0020	0.0049	0.0024	0.0045	0.0022	0.0039	0.0018
	U	0.0058	0.0055	0.0060	0.0063	0.0055	0.0058	0.0052	0.0059	0.0051	0.0055
WETT	N	0.0064	0.0060	0.0066	0.0059	0.0055	0.0052	0.0054	0.0039	0.0048	0.0043
	E	0.0048	0.0034	0.0052	0.0032	0.0042	0.0029	0.0056	0.0033	0.0051	0.0031
	U	0.0062	0.0061	0.0060	0.0063	0.0045	0.0055	0.0047	0.0041	0.0042	0.0043
ZIMM	N	0.0091	0.0073	0.0087	0.0073	0.0104	0.0081	0.0071	0.0047	0.0065	0.0045
	E	0.0058	0.0023	0.0056	0.0019	0.0064	0.0016	0.0053	0.0022	0.0060	0.0019
	U	0.0085	0.0072	0.0086	0.0074	0.0109	0.0078	0.0061	0.0057	0.0060	0.0048
ONSA	N	0.0059	0.0061	0.0059	0.0065	0.0057	0.0056	0.0043	0.0050	0.0051	0.0047
	E	0.0034	0.0019	0.0040	0.0018	0.0040	0.0017	0.0041	0.0017	0.0034	0.0017
	U	0.0082	0.0090	0.0081	0.0096	0.0075	0.0089	0.0073	0.0073	0.0072	0.0068
METS	N	0.0092	0.0051	0.0077	0.0044	0.0072	0.0028	0.0057	0.0041	0.0038	0.0027
	E	0.0067	0.0028	0.0063	0.0025	0.0063	0.0023	0.0063	0.0026	0.0060	0.0022
	U	0.0106	0.0084	0.0097	0.0072	0.0086	0.0052	0.0086	0.0060	0.0065	0.0051
NYAL	N	0.0053	0.0034	0.0051	0.0037	0.0058	0.0036	0.0051	0.0034	0.0045	0.0032
	E	0.0060	0.0041	0.0063	0.0037	0.0072	0.0047	0.0069	0.0034	0.0067	0.0032
	U	0.0049	0.0052	0.0050	0.0047	0.0054	0.0050	0.0046	0.0049	0.0048	0.0051
MASP	N	0.0118	0.0101	0.0113	0.0091	0.0102	0.0087	0.0104	0.0071	0.0078	0.0052
	E	0.0084	0.0046	0.0079	0.0050	0.0080	0.0056	0.0082	0.0048	0.0076	0.0049
	U	0.0045	0.0037	0.0041	0.0052	0.0042	0.0058	0.0033	0.0034	0.0040	0.0039
JOZE	N	0.0040	0.0049	0.0042	0.0068	0.0048	0.0060	0.0062	0.0071	0.0050	0.0069
	E	0.0068	0.0038	0.0068	0.0050	0.0080	0.0053	0.0075	0.0052	0.0086	0.0049
	U	0.0055	0.0058	0.0055	0.0079	0.0066	0.0071	0.0073	0.0085	0.0059	0.0082
BRUS	N	0.0055	0.0045	0.0045	0.0042	0.0055	0.0051	0.0059	0.0044	0.0058	0.0041
	E	0.0037	0.0015	0.0037	0.0014	0.0041	0.0012	0.0043	0.0016	0.0040	0.0013
	U	0.0048	0.0043	0.0046	0.0038	0.0061	0.0049	0.0055	0.0040	0.0056	0.0037
mean	N	0.0072	0.0065	0.0070	0.0068	0.0071	0.0064	0.0062	0.0054	0.0057	0.0051
	E	0.0062	0.0031	0.0061	0.0031	0.0059	0.0031	0.0065	0.0030	0.0057	0.0028
	U	0.0067	0.0065	0.0066	0.0069	0.0070	0.0067	0.0059	0.0058	0.0058	0.0055

The results in Tables 8.14 and 8.15 are comparable with those obtained using the Melbourne-Wübbena approach (Tables 8.6 and 8.7). In the next step we computed 3-days solutions using strategies **COD G** (ambiguties fixed) and COD F (ambiguities free) and solved for orbital parameters too. Again we extracted the middle days and define them to be the "final" result. Then we fitted one 12-days arc through these 12 one-day arcs using the program ORBIMP [Beutler et al., 1994a]. The mean residuals after this 12-days fit are given in Table 8.16. In this table there is a fit for the CODE orbits ("Std.") stemming from the global solution (data from the entire Core Network) too.

Table 8.16: Mean residuals after 12-days fit (in cm, non-eclipsing satellites only)

	PRN																		mean
	1	2	4	5	7	14	15	16	17	18	20	21	22	23	24	26	28	29	31	mean
Std.	25	20	22	19	21	16	19	15	24	23	17	18	18	18	22	27	18	24	20	20.3
COD F	27	28	28	29	27	23	32	20	39	73	29	28	35	30	24	31	23	46	26	31.5
COD G	29	34	22	27	26	18	21	18	29	31	23	21	21	20	22	31	24	28	26	24.8

From the results given in Tables 8.14, 8.15 and 8.16 we conclude that *ambiguity resolution using the QIF strategy is comparable to ambiguity resolution using the Melbourne-Wübbena approach* for baselines lengths up to about 2000 km. The main advantage of our strategy consists in the code-independence.

8.3 Code-independent Ambiguity Resolution in Global Networks

The results obtained in Section 8.2 were encouraging enough to set up a routine ambiguity fixing procedure for the global Core Network. This routine processing started on 17th July, 1994 (first day of GPS week 758). Subsequently for each day we resolved the ambiguities using the QIF strategy on all the baselines shorter than 2000 km (about 20 baselines per day). We use the CODE orbits computed without ambiguity resolution as a priori orbits for the ambiguity resolution step. The ambiguities are resolved in the baseline mode (i.e. we process each baseline separately) and we are able to resolve about 75 % of the ambiguities. Then we produce 1-day and 3-days solutions exactly as in our standard IGS processing [Rothacher et al., 1993b] but with ambiguities kept fixed on integer values. The number of unknown parameters decreases significantly from about 7000 to about 5000 for a 3-days solution (apart from the ambiguities we solve for coordinates, troposphere parameters, orbit parameters and earth orientation parameters). In this section we summarize some results obtained from processing the first four weeks (GPS weeks 758 – 761). The estimation of coordinates is corrupted by small errors of the VLBI stations kept fixed on the a priori coordinates. Therefore we do not look at the coordinates at this section. In Section 8.1 we have seen that ambiguity fixing had almost no influence on troposphere parameters estimation. We expect essentially the same result for global analyses. Therefore we do not look at troposphere parameters either. Consequently we focus on

- orbit parameters (osculating elements, radiation pressure parameters and stochastic orbit parameters),

- earth orientation parameters.

We will discuss the influence of ambiguity fixing on the formal errors of these parameters. We will also try to define criteria for the real accuracy of our estimations. It must be admitted that this is a difficult issue because we do not know "true" values for these parameters.

Orbit Parameters

In our standard solution we compute 3-days arcs which are defined by the following parameters:

6 osculating Keplerian elements $a, e, i, \Omega, \omega, u_0$,

2 radiation pressure parameters p_0, p_2,

stochastic orbit parameters (for eclipsing satellites only). For each eclipsing satellite we estimate two stochastic orbit parameters per revolution (12 hours). These stochastic parameters represent velocity changes in radial and out of plane directions [Beutler et al., 1994a].

A first impression of the influence of ambiguity resolution on the orbit parameters is given by Tables 8.17 and 8.18 where the formal rms errors are given for both, the float and ambiguities fixed solutions. No a priori constraints are put on the osculating Keplerian elements and radiation pressure parameters, rather heavy weights are on the stochastic parameters. It should be mentioned that these constraints have an impact on the values in Table 8.18.

Table 8.17: Formal rms errors of the orbital elements from a 3-days solution (days 230–232, mean values over all satellites)

	a	e	i	Ω	ω	u_0	p_0	p_2
	m	10^{-10}			10^{-3} ''			10^{-12} m·s^{-2}
float	0.0038	3.16	0.095	0.16	2.15	0.377	8.95	7.67
fixed	0.0024	2.85	0.068	0.11	1.99	0.241	8.21	5.12
improv.	37 %	10 %	28 %	31 %	7 %	36 %	8 %	33 %

Table 8.18: Formal rms errors of the stochastic orbit parameters from a 3-days solution (days 230–232, mean values over all eclipsing satellites)

	radial along track 10^{-5} m $\cdot$ s^{-1}	
float	0.1150	0.0592
fixed	0.1194	0.0435
improv.	27 %	

Based on Table 8.17 we would expect an improvement of about 30 % in orbit accuracy by fixing the ambiguities. Let us therefore check the orbit consistency using the overlapping orbits. The principle is shown in Figure 8.24.
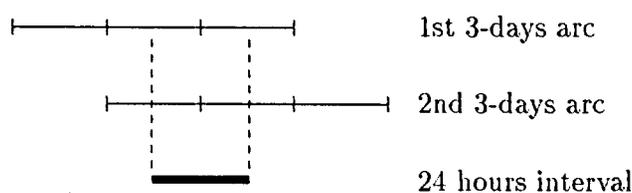
Figure 8.24: Overlapping 24 hours interval used for orbit consistency tests

We used the 24 hours intervals as defined by Figure 8.24 to compute 7-parameter Helmert transformation between the orbit sets of subsequent days. Such Helmert transformations were performed for 31 days (197-198, 198-199, ... 227-228). Because we expected a worse orbit quality for the eclipsing satellites, we used the subset of non-eclipsing satellites only to establish the parameters of the Helmert tranformation. The residuals after the transformation were computed for both, the eclipsing and the non-eclipsing satellites. The rms errors of the transformations are given in Table 8.19.

Table 8.19: Rms errors of a Helmert transformations between the orbit sets of subsequent days

Days	Ambiguities Free				Ambiguities Fixed			
	R	S	W	Total	R	S	W	Total
197-198	0.049	0.299	0.142	0.193	0.085	0.393	0.300	0.290
198-199	0.076	0.347	0.194	0.234	0.074	0.354	0.274	0.262
199-200	0.085	0.418	0.284	0.296	0.089	0.361	0.271	0.265
200-201	0.097	0.465	0.334	0.335	0.088	0.396	0.318	0.298
201-202	0.094	0.465	0.295	0.322	0.094	0.409	0.315	0.303
202-203	0.077	0.383	0.244	0.266	0.078	0.346	0.275	0.259
203-204	0.074	0.364	0.236	0.254	0.065	0.297	0.231	0.221
204-205	0.091	0.420	0.270	0.293	0.082	0.359	0.267	0.262
205-206	0.091	0.411	0.267	0.288	0.089	0.375	0.278	0.274
206-207	0.076	0.360	0.259	0.260	0.075	0.329	0.245	0.241
207-208	0.103	0.599	0.285	0.388	0.104	0.447	0.341	0.330
208-209	0.104	0.468	0.302	0.327	0.086	0.366	0.292	0.275
209-210	0.068	0.298	0.196	0.209	0.059	0.270	0.202	0.198
210-211	0.084	0.398	0.271	0.282	0.086	0.373	0.293	0.278
211-212	0.094	0.493	0.311	0.341	0.086	0.401	0.301	0.294
212-213	0.084	0.379	0.273	0.274	0.084	0.379	0.290	0.280
213-214	0.086	0.387	0.252	0.271	0.075	0.324	0.242	0.238
214-215	0.068	0.346	0.239	0.246	0.076	0.319	0.240	0.234
215-216	0.075	0.380	0.263	0.270	0.078	0.343	0.261	0.253
216-217	0.076	0.353	0.261	0.257	0.077	0.356	0.276	0.264
217-218	0.069	0.333	0.240	0.240	0.076	0.329	0.247	0.242
218-219	0.070	0.369	0.249	0.260	0.069	0.332	0.245	0.241
219-220	0.073	0.315	0.234	0.231	0.074	0.326	0.252	0.242
220-221	0.069	0.295	0.205	0.211	0.067	0.303	0.231	0.224
221-222	0.087	0.436	0.292	0.307	0.092	0.419	0.305	0.304
222-223	0.089	0.432	0.303	0.309	0.099	0.437	0.319	0.318
223-224	0.066	0.298	0.205	0.212	0.067	0.307	0.220	0.222
224-225	0.084	0.379	0.267	0.272	0.076	0.366	0.278	0.269
225-226	0.085	0.428	0.291	0.303	0.072	0.400	0.325	0.300
226-227	0.078	0.383	0.263	0.272	0.063	0.328	0.274	0.250
227-228	0.081	0.383	0.284	0.279	0.070	0.349	0.283	0.262
mean	0.0807	0.3898	0.2584	0.2743	0.0792	0.3578	0.2739	0.2643

No significant difference between ambiguities free and fixed solutions can be seen in Table 8.19. The residuals after the Helmert transformation for individual non-eclipsing satellites are given in Figure 8.25.

MEAN RESIDUALS AFTER A HELMERT TRANSFORMATION
Non-eclipsing Satellites, Amb. Free

MEAN RESIDUALS AFTER A HELMERT TRANSFORMATION
Non-eclipsing Satellites, Amb. Fixed
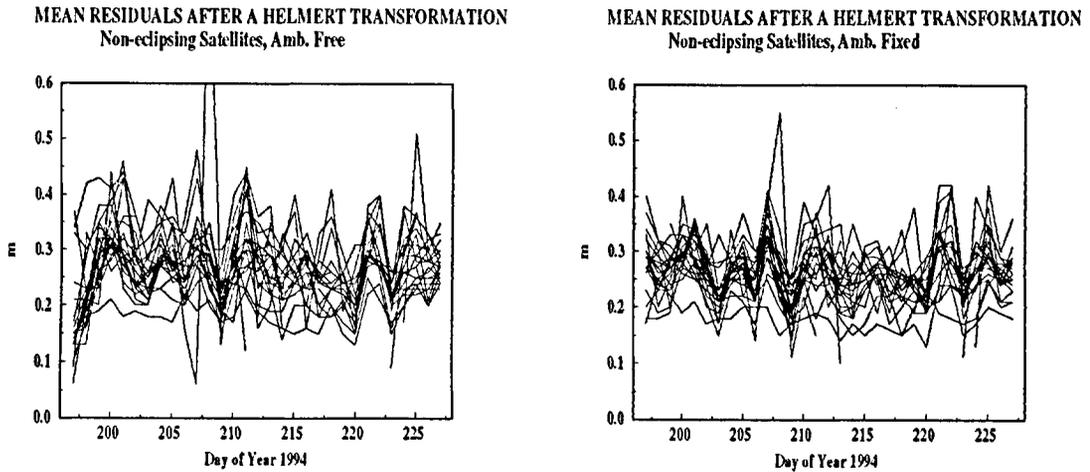
Figure 8.25: Residuals after the Helmert transformations between two sets of orbits (non-eclipsing satellites)

On the other hand there is a significant difference between ambiguities free and fixed solutions in the residuals of the eclipsing satellites which are given in Figure 8.26. In this case the mean residual (mean over all satellites and all days) is 0.293 m in the case of the ambiguities free solution and 0.2143 in the case of the ambiguities fixed solution. This indicates an improvement of about 30 %.

MEAN RESIDUALS AFTER A HELMERT TRANSFORMATION
Eclipsing Satellites, Amb. Free

MEAN RESIDUALS AFTER A HELMERT TRANSFORMATION
Eclipsing Satellites, Amb. Fixed
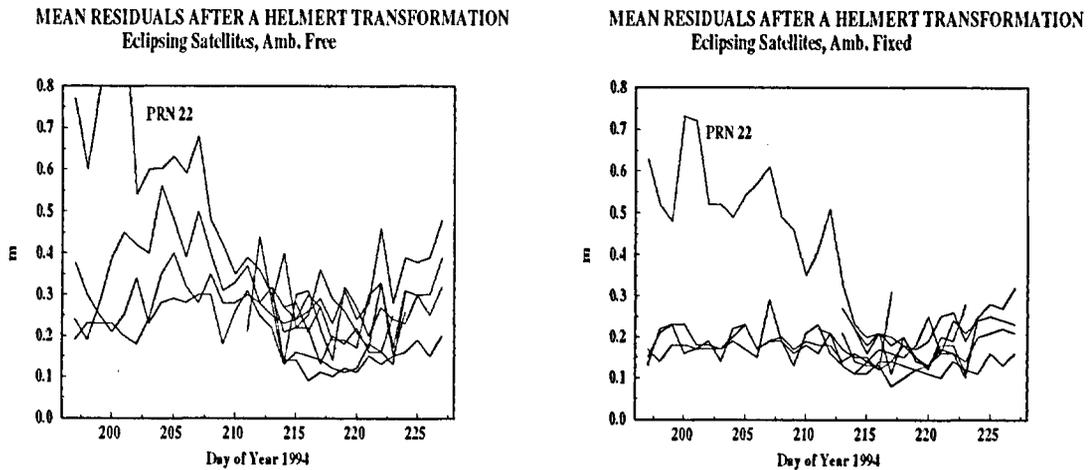
Figure 8.26: Residuals after the Helmert transformations between two sets of orbits (eclipsing satellites)

It is interesting to compare our orbits (stemming from float and fixed solutions) with the combined orbits computed from the results of all IGS Processing Centers. This comparison is given in Table 8.20.

Table 8.20: Results of a Helmert transformation between the CODE orbits (ambiguities fixed and free) and the official IGS orbits

Day	Ambiguities Free								Ambiguities Fixed							
	DX	DY	DZ	RX	RY	RZ	Scale	RMS	DX	DY	DZ	RX	RY	RZ	Scale	RMS
	m			mas			ppb	m	m			mas			ppb	m
198	0.005	0.039	-0.005	-0.17	-0.13	0.31	-0.2	0.12	-0.001	0.014	0.003	-0.35	0.05	0.34	-0.1	0.12
199	0.016	0.021	-0.021	0.01	0.21	0.55	0.1	0.12	0.008	0.024	-0.021	-0.30	0.16	0.64	0.0	0.13
200	0.004	0.015	-0.015	-0.07	-0.03	0.43	0.2	0.11	-0.001	0.012	-0.003	-0.27	-0.01	0.49	-0.2	0.11
201	0.006	0.028	-0.015	-0.81	-0.23	0.26	-0.3	0.14	0.000	0.035	-0.015	-0.61	-0.15	0.49	-0.2	0.13
202	0.000	0.023	-0.015	0.04	-0.15	0.49	-0.1	0.14	-0.010	0.026	-0.016	0.03	-0.29	0.61	-0.2	0.14
203	0.005	0.024	-0.008	0.12	-0.31	0.26	0.1	0.13	-0.005	0.026	0.002	0.15	-0.40	0.28	0.0	0.15
204	0.022	0.035	-0.019	0.18	0.16	0.49	0.1	0.13	0.013	0.034	-0.010	0.02	-0.09	0.41	0.2	0.14
205	0.016	0.011	-0.016	-0.08	-0.38	0.35	-0.2	0.13	0.012	0.013	-0.016	0.02	-0.44	0.87	-0.1	0.13
206	0.007	0.021	-0.018	-0.18	0.05	0.16	-0.1	0.13	0.006	0.022	-0.021	-0.24	0.00	0.28	0.0	0.12
207	0.024	0.024	-0.022	-0.04	0.11	0.04	0.0	0.11	0.014	0.026	-0.020	-0.12	-0.05	0.05	0.0	0.12
208	0.002	0.036	-0.001	-0.23	0.28	0.29	-0.1	0.14	0.002	0.018	-0.004	-0.32	0.27	0.43	-0.2	0.13
209	0.008	0.024	-0.030	0.00	0.19	0.16	0.0	0.12	0.008	0.019	-0.026	-0.11	0.07	0.21	0.0	0.13
210	0.017	0.019	-0.009	0.05	-0.07	0.18	-0.1	0.09	0.012	0.027	-0.017	-0.03	-0.19	0.18	0.2	0.11
211	0.009	0.013	-0.009	-0.40	-0.37	0.15	-0.1	0.11	0.006	0.016	-0.010	-0.38	-0.39	0.26	0.0	0.11
212	0.007	0.029	-0.015	-0.36	-0.22	0.30	0.0	0.11	0.008	0.023	-0.014	-0.17	-0.25	0.45	-0.2	0.11
213	0.009	0.022	-0.019	-0.06	0.04	-0.18	0.1	0.13	0.008	0.024	-0.027	-0.14	-0.06	0.14	-0.1	0.13
214	0.006	0.026	-0.028	0.14	-0.12	0.28	0.1	0.10	0.000	0.034	-0.021	0.08	-0.40	0.54	-0.1	0.11
215	0.007	0.025	-0.013	-0.04	-0.09	0.42	0.0	0.10	0.006	0.033	-0.011	-0.08	-0.35	0.60	-0.1	0.10
216	0.000	0.032	-0.017	-0.40	-0.15	0.62	0.0	0.11	0.000	0.035	-0.016	-0.33	-0.05	0.55	-0.1	0.11
217	0.005	0.022	-0.020	0.12	-0.14	0.72	0.0	0.12	0.000	0.031	-0.018	0.02	-0.04	0.66	0.1	0.12
218	0.006	0.024	-0.022	0.09	0.20	0.64	-0.1	0.12	-0.001	0.027	-0.013	0.20	0.24	0.70	0.0	0.11
219	0.006	0.015	-0.020	0.17	-0.07	-0.08	0.0	0.11	0.003	0.027	-0.017	0.22	-0.12	0.06	0.1	0.11
220	0.005	0.013	-0.013	0.33	-0.08	0.29	0.1	0.09	0.016	0.020	-0.005	0.18	-0.20	0.25	0.1	0.09
221	-0.004	0.022	-0.008	0.09	-0.22	0.20	0.0	0.11	-0.003	0.024	-0.008	0.05	-0.13	0.29	0.1	0.11
222	0.012	0.017	-0.009	0.10	-0.10	0.37	0.2	0.12	0.008	0.026	-0.007	0.08	-0.17	0.63	0.1	0.12
223	0.006	0.021	-0.010	0.01	-0.07	-0.05	0.0	0.11	0.003	0.031	-0.013	-0.07	0.00	0.28	0.2	0.11
224	0.010	0.020	-0.008	-0.16	-0.02	0.15	0.1	0.10	0.011	0.026	-0.012	-0.29	0.00	0.30	0.1	0.10
225	0.008	0.016	-0.004	-0.19	0.11	0.33	0.2	0.11	-0.001	0.015	-0.010	-0.17	-0.05	0.66	0.1	0.12
mean	0.008	0.023	-0.015	-0.06	-0.06	0.29	0.0	0.12	0.004	0.025	-0.013	-0.10	-0.11	0.42	0.0	0.12

Despite of the consistency improvement indicated by Figure 8.26 we cannot conclude from Table 8.20 that the ambiguities fixed solutions are superior to the ambiguities free solutions. Considering that there is a significant difference between eclipsing and non-eclipsing satellites (the eclipsing satellite orbits are modeled by more parameters) and that the eclipsing satellites show better results in ambiguities fixed solution (even better than the non-eclipsing satellites), we might have to conclude, that our standard orbit model is not sufficient for 3-days orbit arcs. To check this assumption we computed 11 one-day arcs (days 230 – 240) and compared these 1-day orbits with our standard IGS orbits through 7-parameter Helmert transformations. The results are given in Table 8.21.

Table 8.21: Results of Helmert transformation between 1-day orbits (fixed and float) and standard IGS orbits

Day	Ambiguities Free								Ambiguities Fixed							
	DX	DY	DZ	RX	RY	RZ	Scale	RMS	DX	DY	DZ	RX	RY	RZ	Scale	RMS
	m			mas			ppb	m	m			mas			ppb	m
230	-0.018	0.027	-0.018	0.13	-0.31	-0.56	0.1	0.16	-0.017	0.012	-0.005	-0.09	-0.12	-0.01	0.1	0.12
231	-0.024	0.002	-0.002	0.21	-0.14	0.00	0.2	0.17	-0.009	-0.008	0.004	-0.01	-0.06	0.10	0.3	0.11
232	0.005	0.017	-0.025	0.49	-0.11	-0.26	-0.3	0.20	0.006	0.002	-0.016	0.49	0.04	0.10	-0.1	0.14
233	-0.009	0.025	-0.010	0.09	-0.36	-0.17	0.1	0.15	0.006	0.001	-0.009	0.22	-0.22	0.03	0.0	0.12
234	-0.014	0.006	-0.022	-0.03	-0.43	0.04	0.2	0.17	-0.030	0.021	-0.012	-0.28	-0.45	-0.08	0.3	0.15
235	-0.019	-0.003	-0.005	-0.35	0.11	-0.26	0.1	0.16	-0.010	-0.003	-0.005	-0.01	0.21	0.11	0.1	0.12
236	-0.020	0.010	0.026	-0.07	-0.71	-0.96	0.4	0.19	0.002	0.018	0.013	-0.05	-0.36	-0.38	0.2	0.11
237	-0.057	0.019	-0.004	-0.12	-0.26	-0.93	0.3	0.21	-0.017	0.001	0.003	0.00	-0.25	-0.24	0.0	0.15
238	-0.019	0.004	-0.019	-0.11	-0.04	0.04	0.1	0.18	-0.009	0.000	-0.017	0.08	0.10	0.12	0.0	0.12
239	-0.007	0.004	0.016	0.28	-0.08	0.31	0.3	0.19	-0.013	-0.005	0.009	0.26	0.08	0.10	0.1	0.11
240	-0.017	0.015	0.002	-0.01	0.01	-0.02	0.0	0.16	-0.009	0.011	-0.010	0.19	0.08	-0.03	-0.1	0.10
mean	-0.018	0.012	-0.006	0.05	-0.21	-0.25	0.1	0.18	-0.009	0.004	-0.004	0.07	-0.09	-0.02	0.1	0.12

In this case the consistency is about 33 % better after ambiguity fixing as we would expect it from Figure 8.26. The result corresponds to an improvement of the formal rms of orbital parameters given in Table 8.17 and 8.18.

Earth Orientation Parameters

In our standard 3-days solutions we model the x- and y-pole coordinates by polynomials of degree one for each day and we ask for continuity of the pole coordinates at the day boundaries. This is equivalent to assuming that each coordinate of the pole is a polygon and to solve for the eop values at 0^h UT on days 1,2,3, and 4. The final orbits are always extracted from the middle day of each 3-days solution. Exactly two values of each pole coordinate (x_0, y_0 at 0^h and x_{24}, y_{24} at 24^h) correspond to this part of the orbit system. Due to format standards the resulting 1-week pole file which we send to IGS Data centers contains only one value of each coordinate per day. These values are computed as $x_{12} = (x_0 + x_{24})/2$ and $y_{12} = (y_0 + y_{24})/2$ respectively.

Table 8.22: Formal rms errors of the earth orientation parameters (mean values from days 197 – 230)

	X-pole	Y-pole	UT1-UTC drift
	10^{-5} "		10^{-6} s/day
float	4.4	4.3	5.7
fixed	4.1	4.1	4.9
improv.	7 %	5 %	14 %

It is not possible to estimate UT1-UTC directly due to close correlation with the right ascensions of the ascending nodes of the satellite orbital planes. Thus one has to solve

for a drift in UT1-UTC only (which is equivalent to solving for the length of day). We model this drift with a polynomial of degree one over three days. In the resulting 1-week pole file we fix the value of UT1-UTC for 0^h of the GPS week on the a priori value. The other values of UT1-UTC are computed from the estimated drifts. The formal rms of the earth orientation parameters are given in Table 8.22. In Figures 8.27, 8.28 and 8.29 the estimated Earth orientation parameters are shown.
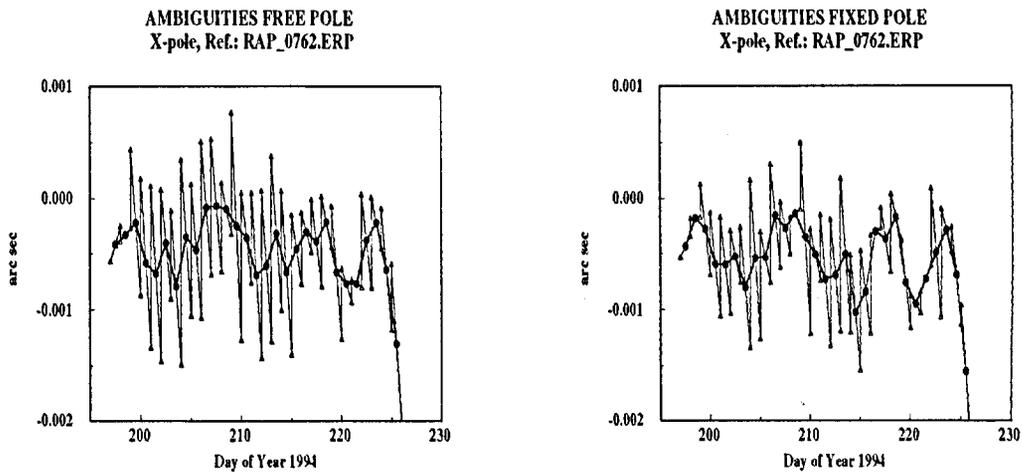

Figure 8.27: CODE earth orientation parameters compared to the IERS Rapid Service pole
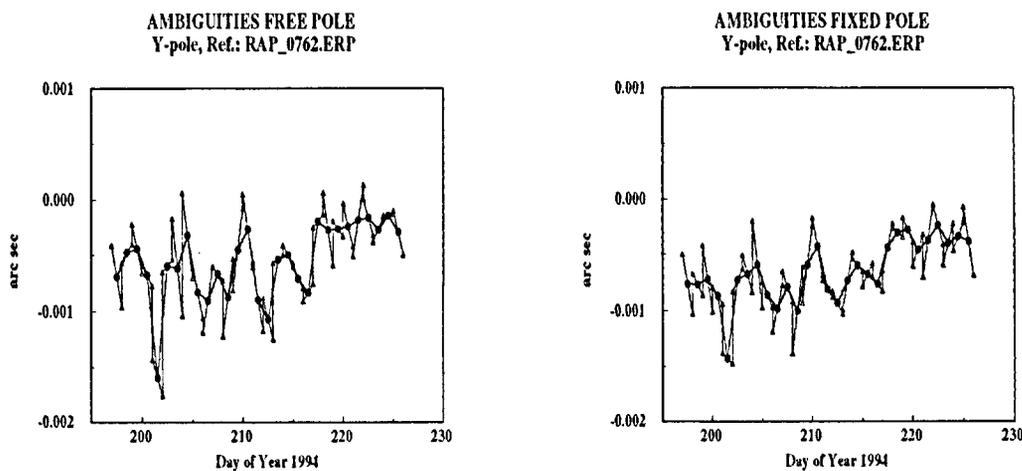
Figure 8.28: CODE earth orientation parameters compared to the IERS Rapid Service pole

UT1-UTC DRIFT
Ref.: RAP_0762.ERP
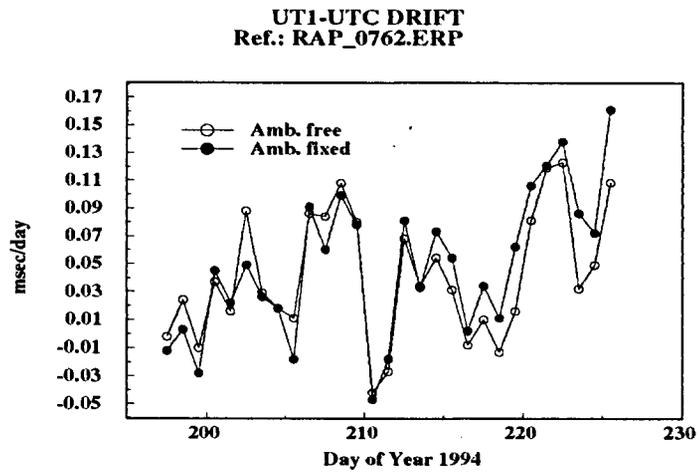
Figure 8.29: CODE Earth orientation parameters compared to the IERS Rapid Service
pole

In Figures 8.27 and 8.28 the thin lines connect the values x_0, x_{24} (or y_0, y_{24}) and the thick lines the mean values x_{12} (or y_{12}). It is rather difficult to judge the quality of the estimations from the mean values x_{12}, y_{12} because no "true" pole is available. It seems, however, that the differences $x_{24} - x_0, y_{24} - y_0$ are somewhat more realistic in the case of the ambiguities fixed solutions. As opposed to the coordinates and the orbit parameters ambiguity resolution does *not* considerably improve the quality of the daily means for x- and y-pole coordinates. This is in agreement with the improvement expected from Table 8.22.

9. Summary and Outlook

The accuracy of GPS analyses in regional and global networks improved dramatically during the last three years. The establishment of the International GPS Service for Geodynamics (IGS) is one of the primary reasons for this development. It is possible now to use the high accuracy orbits computed by the processing centers of the IGS and, since November 1993 the combined IGS orbits. The achievements of the IGS were supported by the development of the processing strategies and software packages and vice versa the resulting IGS products (the high quality orbits in particular) allow to use new processing methods. Here we summarize one result in the field of the resolution of the initial phase ambiguities achieved during the years 1992 – 1994 and the benefit associated with this development for the estimated parameters.

All the results discussed in Chapters 7 and 8 were computed at the Center for Orbit Determination in Europe (CODE), one of the processing centers of the IGS, located at the Astronomical Institute of the University of Berne. The software package used for the analyses was the Bernese GPS Software. This software was subject to a significant and continuous development since 1992. In particular one should mention the automatization of the processing and the improvement of the orbit models. In the framework of this PhD thesis new ambiguity resolution strategies, to be summarized below, were developed and tested.

In 1992, soon after the start of the IGS test campaign (June 21st, 1992), we made some tests concerning the benefit of the ambiguity resolution. The results of the Epoch'92 campaign and the EUREF-CH campaign were described in Chapter 7. The results of these two campaigns allowed to draw the following conclusion:

- If precise code-measurements are available on both frequencies, the Melbourne-Wübbena linear combination may by used for the wide-lane ambiguity resolution. This approach is very reliable and we did not find any limitation concerning the baseline lengths (we processed baselines up to 2000 km).

- Without P-code measurements the wide-lane ambiguity resolution seemed to be critical or even impossible because of ionospheric refraction. Using regional ionosphere models, however, allowed us to resolve the wide-lane ambiguities using the L_5 linear combination up to baseline lengths of about 200 km.

- The success of baseline-wise narrow-lane ambiguity resolution depends on the orbit

131

quality. For baselines longer than about 100 km it is mandatory to use the precise orbits produced by the IGS. The accuracy of the broadcast orbits is not sufficient.

- The optimization of the double-difference ambiguity selection and the iterative ambiguity resolution algorithm proved to be of great importance if longer sessions (several hours) and/or longer baselines should be processed.

- Resolution of the initial phase ambiguities improves the accuracy of the estimated coordinates up to a factor of four if short sessions are used (1 or 2 hours only).

In 1993 we processed a regional network again. During the January'93 campaign we focused on the relation between the accuracy of the orbits and the reliability of ambiguity resolution. We wanted to see whether ambiguity resolution improves the accuracy of results (coordinates in particular). We concluded that

- the orbit accuracy is critical for ambiguity resolution. With the orbit accuracy available in January 1993 we were able to resolve the ambiguities up to baseline lengths of about 2000 km. The ambiguity resolution considerably improved the accuracy of the results for shorter sessions (up to about 8 hours). For 24 hours sessions we saw almost no difference between ambiguities-free and ambiguities-fixed estimations of the coordinates if no further orbit improvement was made.

- Estimating the orbit parameters and introducing new orbit modeling features we observed an improvement of the coordinate repeatabilities of up to 50 % after the fixing of the ambiguities. However, the resulting coordinates were corrupted by small rotations of the entire network (we kept one station fixed only).

In 1994 the situation changed considerably. The IGS went through a remarkable development in 1993 and the accuracy of orbits improved dramatically. We were able to take advantage of this high accuracy and we tried to inspect the influence of the ambiguity fixing on various parameter types. The January'94 campaign showed that:

- The wide-lane ambiguity resolution using Melbourne-Wübbena linear combination is very reliable and does not depend on the baseline length. The combination of different types of receivers proved to be critical. This problem should be studied in detail in future.

- Narrow-lane ambiguity resolution was possible without major problems up to baseline lengths of about 2000 km. The available IGS orbits had an accuracy which allowed to resolve the narrow-lane ambiguities in baseline mode without further orbit improvements.

- An inspection of the results of the 3-days solutions revealed that the formal errors of the east-west coordinates decreased by about 50 % if the ambiguities could be fixed. The ambiguity resolution had no influence on the accuracy of the height component

and on the north-south coordinates (the float estimation of the north-south coordinates was already as accurate as the fixed estimation of the east-west coordinates). The differences in the coordinate repeatabilities between the float and fixed estimations correspond to the relations between formal errors. To achieve these results we did not need to make any further orbit improvement. We used either the combined IGS orbits or the orbits computed at CODE. We detected no difference between the quality of the two orbit types.

- Ambiguity resolution had almost no influence on the estimations of the troposphere zenith delays. These troposphere parameters are obviously strongly correlated with the height components of the station positions.

- Ambiguity fixing allowed to compute regional orbits of almost the same quality as the standard IGS orbits. In this case the ambiguity fixing brought an accuracy improvement of about 30 %. It should be mentioned that no earth orientation parameters were determined in this procedure.

- Ambiguity fixing allowed to study short period variations of the station coordinates. 2-hours sessions were sufficient to detect effects of about 1 cm.

Anti-Spoofing (AS) was turned on (more or less) permanently at the beginning of the GPS week 734. AS severely affected the quality of the code measurements of some receiver types. Unfortunately the Rogue receivers widely used in IGS network show a poor code quality under AS. We were no longer able to use the Melbourne-Wübbena linear combination for wide-lane ambiguity resolution for this receiver type. This was the motivation to develop a code-independent ambiguity resolution strategy. We called it the QIF (Quasi Ionosphere-Free) strategy and we tested it using observations from May 1994 (May'94 campaign) where the same set of stations and baselines was processed as in the January'94 campaign. The following conclusions could be drawn:

- Using no code measurements but using the *Quasi Ionosphere-Free* Strategy it is possible to achieve *the same* quality of results as with precise code measurements and Melbourne-Wübbena method up to baseline lengths of about 1000 km. Up to baseline lengths of about 2000 km it is possible to achieve *almost the same* results depending, however, on the ionospheric conditions.

The results obtained in the regional (European) network encouraged the attempt to resolve the ambiguities in the global IGS Core Network (up to baseline lengths of about 2000 km). For this purpose we set up a routine ambiguity fixing procedure for the IGS network. The first results stem from GPS weeks 758 – 761. Focusing on the orbital parameters and the earth orientation parameters we may conclude:

- Ambiguity resolution in the global network is possible and does improve the accuracy of the orbit solutions. The accuracy improvements actually achieved (about 30 % is expected from an inspection of the formal errors) are as expected for one-day

arcs, whereas no significant improvement could be seen for 3-days arcs. This is an indication that our orbit model is not sufficient for arc lengths $\gg$ 1 day.

- No clear improvement of the earth orientation parameters could be observed when fixing the ambiguities. This again is in agreement with the theoretical expectations. The situation might change if the percentage of successfully resolved ambiguities (at present about 30 % are actually resolved in the entire IGS network) should grow significantly.

The ambiguity resolution procedure is now in a pre-operational phase: the ambiguities are resolved baseline by baseline up to a length of about 2000 km using the QIF strategy and the orbits which at present are our "final orbits". New, and hopefully improved, orbits (1-day and 3-days arc lengths) are produced afterwards. The quality of these new products will be studied in the next few months. Should these tests be satisfactory the ambiguities-fixed solution would become the official solution of the CODE processing center of the IGS.

Let us finally underline that the procedure would be much simpler if high accuracy code information would again become available. We are convinced that ambiguity resolution in the entire (global) IGS network could be performed with success rate of about 60 % if all remaining Rogue receivers would be replaced by Turbo Rogues or by any other receiver type providing good code data (rms < 1 m) under AS, too.

Part III

Appendices

A. Review of the Keplerian motion

Neglecting all the perturbing forces listed in Table 4.1 the equation of motion (4.1) for an artificial satellite reads as

$$\ddot{\underline{r}} + \frac{\mu}{r^3} \cdot \underline{r} = \underline{0} \, , \qquad (A.1)$$

where $\mu = G \cdot M$ is the product of the gravity constant and the mass of the earth. This differential equation may be solved analytically, the result is the so-called *Keplerian motion*. The orbit is a conic section where only the elliptic motion is of interest for our purposes. The elliptic motion may e.g. be described by the six Keplerian orbital parameters listed in Table A.1.

Table A.1: The Keplerian Elements

Parameter	Notation
Ω	Right ascension of the ascending node
i	Inclination of the orbital plane with respect to the equatorial plane
ω	Argument of perigee
a	Semimajor axis of orbital ellipse
e	Numerical eccentricity of ellipse
T_0	Perigee passing time

The interpretation of these parameters follows from Figure A.1. The instantaneous position of the satellite within its orbit is described by angular quantities known as *anomalies*. The *mean* anomaly $M(t)$ is a mathematical abstraction while the *eccentric* anomaly $E(t)$ and the *true* anomaly $v(t)$ have a geometrical meaning (Figure A.1).
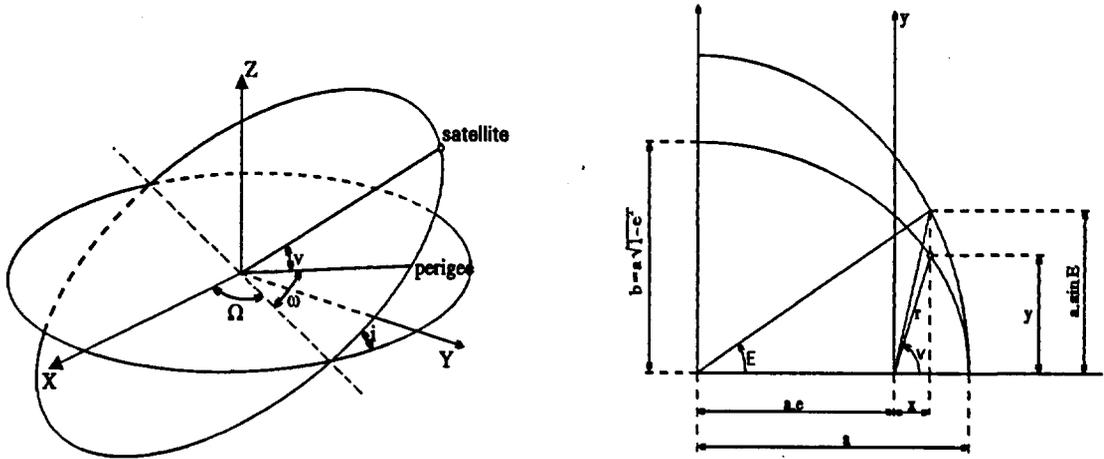
Figure A.1: The Keplerian elements and anomalies

$$M(t) = n(t - T_0) \ , \quad n = \frac{2\,\pi}{U} = \sqrt{\frac{\mu}{a^3}} \ , \tag{A.2}$$

where U is the revolution period and n is the mean motion. The relation between the mean anomaly and the eccentric anomaly is given by *Kepler's equation*

$$E(t) = M(t) + e \cdot \sin E(t) \ , \tag{A.3}$$

and the relation between the eccentric anomaly and the true anomaly by the equation

$$\tan \frac{v(t)}{2} = \sqrt{\frac{1 + e}{1 - e}} \tan \frac{E(t)}{2} \ . \tag{A.4}$$

The length of the geocentric satellite-position vector is given by

$$r(t) = \frac{a \cdot (1 - e^2)}{1 + e \cdot \cos v(t)} = a \cdot (1 - e \cdot \cos E(t)) \ , \tag{A.5}$$

and the components of this vector in the equatorial coordinate system by

$$\underline{r}(t) = \underbrace{R_3(-\Omega) \cdot R_1(-i) \cdot R_3(-\omega)}_{R^T} \cdot r(t) \cdot \begin{pmatrix} \cos v(t) \\ \sin v(t) \\ 0 \end{pmatrix} \ . \tag{A.6}$$

The velocity components in the equatorial system are obtained by taking the derivative of the last equation with respect to time:

$$\underline{\dot{r}}(t) = R^T \cdot \left[\dot{r}(t) \cdot \begin{pmatrix} \cos v(t) \\ \sin v(t) \\ 0 \end{pmatrix} + r(t) \cdot \begin{pmatrix} -\dot{v}(t) \, \sin v(t) \\ \dot{v}(t) \, \cos v(t) \\ 0 \end{pmatrix} \right] \ , \tag{A.7}$$

138

which yields (using (A.5))

$$\underline{\dot{r}}(t) = \boldsymbol{R}^{-1} \cdot \sqrt{\frac{\mu}{a\,(1-e^2)}} \begin{pmatrix} -\sin v(t) \\ \cos v(t) + e \\ 0 \end{pmatrix} . \tag{A.8}$$

On the other hand we may compute the Keplerian elements as a function of the vectors $\underline{r}(t_0) = \underline{r}_0$ and $\underline{\dot{r}}(t_0) = \underline{\dot{r}}_0$. The components of the angular moment $\underline{h}$

$$\underline{h} = \underline{r} \times \underline{\dot{r}} = h \begin{pmatrix} \sin i\ \sin\Omega \\ -\sin i\ \cos\Omega \\ \cos i \end{pmatrix} \tag{A.9}$$

define the angles i and Ω. The vector $\underline{q}$ pointing to the perigee is defined as

$$\underline{q} = -\left(\underline{h} \times \underline{\dot{r}} + \mu\,\frac{\underline{r}}{r}\right) , \tag{A.10}$$

and its length is proportional to the eccentricity e:

$$e = \frac{q}{\mu} , \quad \cos\omega = \frac{\underline{q}}{q} \cdot \begin{pmatrix} \cos\Omega \\ \sin\Omega \\ 0 \end{pmatrix} . \tag{A.11}$$

The semimajor axis follows from the absolute value of vector $\underline{h}$:

$$a = \frac{h^2}{\mu\,(1-e^2)} . \tag{A.12}$$

Using the transformation matrix $\boldsymbol{R}$ – equation (A.6) – it is possible to compute the true anomaly:

$$\boldsymbol{R} \cdot \underline{r} = \begin{pmatrix} x \\ y \\ 0 \end{pmatrix} , \quad v = \arctan\frac{y}{x} . \tag{A.13}$$

The perigee passing time may be computed using equations (A.2) – (A.4). The above equations demonstrate that the six Keplerian elements of Table A.1 are unique functions of the initial conditions (4.2) and vice versa. The six Keplerian elements may be used as the initial conditions for the equation (4.1). In that case they define (together with the parameters p_j, $j = 1, 2, \ldots, n$) a real (non elliptic) orbit. Because the Keplerian orbit defined by the same six Keplerian elements is a good approximation of the perturbed orbit and it is tangential to the real orbit at time $t = t_0$ (the positions and the velocities of both orbits are equal at epoch $t = t_0$) these Keplerian elements are also called *osculating elements*.

B. Approximate Solutions of the Variational Equations

The accuracy requirements for the integration of the variational equations are much less stringent than for the integration of the equations of motion. We may e.g. use the following approximations:

$$A_0 = \left(\frac{\partial(\underline{f}+\underline{a})}{\partial \underline{r}}\right)_{\substack{q=q^a \\ p=p^a}} \doteq \left(\frac{\partial \underline{f}}{\partial \underline{r}}\right)_{\substack{q=q^a \\ p=p^a}} , \quad A_1 = \left(\frac{\partial(\underline{f}+\underline{a})}{\partial \underline{\dot{r}}}\right)_{\substack{q=q^a \\ p=p^a}} \doteq \left(\frac{\partial \underline{f}}{\partial \underline{\dot{r}}}\right)_{\substack{q=q^a \\ p=p^a}} = 0 . \quad (B.1)$$

This leaves us with the equations

$$\underline{\ddot{z}}_{q_i} = A_0 \cdot \underline{z}_{q_i} \tag{B.2}$$

$$\underline{\ddot{z}}_{p_j} = A_0 \cdot \underline{z}_{p_j} + \underline{a}_{p_j} , \tag{B.3}$$

where

$$\underline{a}_{p_j} = \frac{\partial \underline{a}}{\partial p_j} , \tag{B.4}$$

$$A_0 = -\frac{GM}{r^3}\left(I - 3 \cdot \frac{\underline{r} \cdot \underline{r}^T}{r^2}\right) . \tag{B.5}$$

A second idea to solve the variational equations approximately is to transform from the equatorial system (equations (B.2) and (B.3)) into a uniformly rotating system (rotation axis perpendicular to the orbital plane, angular velocity = mean motion of the satellite, the x-axis colinear with the satellite position vector). *For low eccentricity orbits* the transformed variational equations may be simplified considerably. [Colombo, 1989] refers to the resulting equations as *Hill's equations*. The technique was however already established by Leonard Euler (1707–1783) and subsequently used be George William Hill (1838–1914). The same technique was also used by [Beutler et al., 1994a]. The transformation matrix between the two systems may be written as

$$R_3(M(t)) \cdot R , \tag{B.6}$$

where $M(t)$ is the mean anomaly and matrix R is given by equation (A.6). In [Colombo, 1989] it was shown that for *low eccentricity orbits* the variational equations

for a dynamical parameter p_j simply read as (the index j is supressed)

$$\ddot{\underline{\eta}}_p = n^2 \cdot \begin{pmatrix} 3 & 0 & 0 \\ 0 & 0 & 0 \\ 0 & 0 & -1 \end{pmatrix} \cdot \underline{\eta}_p + 2 \cdot n \cdot \begin{pmatrix} 0 & 1 & 0 \\ -1 & 0 & 0 \\ 0 & 0 & 0 \end{pmatrix} \cdot \dot{\underline{\eta}}_p + \tilde{\underline{a}}_p \ , \qquad (B.7)$$

where

$$\underline{\eta}_p = R_3(M(t)) \cdot R \cdot \underline{z}_p \ , \quad \tilde{\underline{a}}_p = R_3(M(t)) \cdot R \cdot \underline{a}_p \qquad (B.8)$$

and n is the mean motion of the satellite. The expression (B.7) is a linear differential equation with constant coefficients for η_p. The variational equation for parameter q_i is given by the homogeneous part of the equation (B.7):

$$\ddot{\underline{\eta}}_q = n^2 \cdot \begin{pmatrix} 3 & 0 & 0 \\ 0 & 0 & 0 \\ 0 & 0 & -1 \end{pmatrix} \cdot \underline{\eta}_q + 2 \cdot n \cdot \begin{pmatrix} 0 & 1 & 0 \\ -1 & 0 & 0 \\ 0 & 0 & 0 \end{pmatrix} \cdot \dot{\underline{\eta}}_q \ . \qquad (B.9)$$

The variational equations (B.7) and (B.9) are linear equations with constant coefficients. The solution of the homogeneous equation (B.9) may be found formally

$$\underline{\eta}_q = \begin{pmatrix} 1 & 0 & \cos M & \sin M & 0 & 0 \\ -3/2\,M & 1 & -2\,\sin M & 2\,\cos M & 0 & 0 \\ 0 & 0 & 0 & 0 & \cos M & \sin M \end{pmatrix} \cdot \begin{pmatrix} c_1 \\ c_2 \\ c_3 \\ c_4 \\ c_5 \\ c_6 \end{pmatrix} = H(t) \cdot \underline{c} \quad (B.10)$$

The initial conditions for epoch t_0 may be written in the general form

$$\underline{\eta}_q(t_0) = R_3(M(t_0)) \cdot R \cdot \frac{\partial \underline{r}_0{}^a}{\partial q_i} = \underline{g}_\eta \ , \qquad (B.11)$$

$$\dot{\underline{\eta}}_q(t_0) = R_3(M(t_0)) \cdot R \cdot \frac{\partial \dot{\underline{r}}_0{}^a}{\partial q_i} + \left[\frac{\mathrm{d}\,R_3(M(t))}{\mathrm{d}\,t} \right]_{t=t_0} \cdot R \cdot \frac{\partial \underline{r}_0{}^a}{\partial q_i} = \dot{\underline{g}}_\eta \ . \qquad (B.12)$$

Introducing the general form for the solutions of the homogenous equations (B.9) into the initial conditions (B.11), (B.12) we get the integration constants c_i, $i = 1, 2, \ldots, 6$.

$$\begin{pmatrix} c_1 \\ c_2 \\ c_3 \\ c_4 \\ c_5 \\ c_6 \end{pmatrix} = \begin{pmatrix} 1 & 0 & \cos M & \sin M & 0 & 0 \\ -3/2\,M & 1 & -2\,\sin M & 2\,\cos M & 0 & 0 \\ 0 & 0 & 0 & 0 & \cos M & \sin M \\ 0 & 0 & -n\,\sin M & n\,\cos M & 0 & 0 \\ -3 & 0 & -2\,n\,\cos M & -2\,n\,\sin M & 0 & 0 \\ 0 & 0 & 0 & 0 & -n\,\sin M & n\,\cos M \end{pmatrix}^{-1} \cdot $$

$$\begin{pmatrix} \underline{g}_\eta \\ \dot{\underline{g}}_\eta \end{pmatrix} = \begin{pmatrix} H(t) \\ \frac{\partial H(t)}{\partial t} \end{pmatrix}^{-1} \cdot \begin{pmatrix} \underline{g}_\eta \\ \dot{\underline{g}}_\eta \end{pmatrix} = G^{-1}(t) \begin{pmatrix} \underline{g}_\eta \\ \dot{\underline{g}}_\eta \end{pmatrix}$$

$$(B.13)$$

Using equations (B.8), (B.10), (B.11), (B.12) and (B.13) it is possible to compute the partial derivative z_{q_i}, $i = 1, \ldots, 6$ of the orbit $\underline{r}(t)$ with respect to the parameters q_i, $i = 1, \ldots, 6$ as a function of the initial conditions (4.13). It is thus possible now to introduce the initial conditions not only for time t_0 but also for other epochs t_i, $i = 1, 2, \ldots$ and to evaluate the variational equations separately for the intervals $< t_{i-1}, t_i >$, $i = 1, 2, \ldots$. The result is a piece-wise continuous orbit with discontinuities at the epochs t_i, $i = 1, 2, \ldots$ In the Bernese GPS software the special case

$$\left(\begin{array}{c} \underline{g}_{\eta,i} \\ \dot{\underline{g}}_{\eta,i} \end{array} \right) = \left(\begin{array}{c} \underline{0} \\ \dot{\underline{g}}_{\eta,i} \end{array} \right) , \quad i = 1, 2, \ldots \tag{B.14}$$

is implemented. We call this approach *pseudo-stochastic orbit model*. The result is a continuous, but not differentiable orbit: obviously the velocity $\dot{\underline{r}}(t)$ will have discontinuities at the epochs t_i, $i = 1, 2, \ldots$

The solution of the *inhomogeneous* equation (B.7) may be obtained by applying the method of variation of constants. Using the notation from equation (B.10) the solution of the inhomogeneous equation may be written in the form

$$\underline{\eta}_p(t) = H(t) \cdot \underline{c}(t) \tag{B.15}$$

Assuming

$$H(t) \cdot \frac{\mathrm{d}\underline{c}}{\mathrm{d}t} = \underline{0} \tag{B.16}$$

and introducing the equation (B.15) into the equation (B.7) we obtain the following differential equation system for the functions $\underline{c}(t)$:

$$\frac{\mathrm{d}\underline{c}}{\mathrm{d}t} = G^{-1}(t) \cdot \left(\begin{array}{c} \underline{0} \\ \underline{a}_p \end{array} \right) . \tag{B.17}$$

Because on the right hand side of the last equation all functions are known, its solution may be found by numerical quadrature. Instead of integrating in steps with a size of a few minutes typically, it is possible to integrate these six equations using a Gaussian quadrature formula (e.g. of order 12) with the revolution period as step size and the perturbing accelerations have to be computed *only 12 times* per revolution. The computational burden (compared to a rigorous numerical integration of the "true" variational equations) is thus considerably reduced.

C. Adjustment Methods

C.1 Least-Squares Adjustment

The adjustment method used in the Bernese GPS software is the standard least-squares adjustment. The following model is used:

$$
\begin{aligned}
\underline{\hat{L}} &= \Psi(\underline{\hat{X}}) \\
\underline{\hat{X}} &= \underline{X}_0 + \underline{x} \\
\underline{\hat{L}} &= \underline{L} + \underline{w} = A\,\underline{x} + \Psi(\underline{X}_0) \\
\underline{w} &= A\,\underline{x} - \underbrace{(\underline{L} - \Psi(\underline{X}_0))}_{\underline{\ell}},
\end{aligned} \tag{C.1}
$$

where

Ψ is the model function,

$\underline{L}$ is the vector of measurements,

$\underline{X}_0$ is the vector of a priori values for unknown parameters,

$\underline{\ell}$ is the vector of reduced measurements (terms "observed – computed"),

$\underline{\hat{L}}$ is the vector of adjusted measurements,

$\underline{\hat{X}}$ is the vector of adjusted parameters,

$\underline{w}$ are the corrections of measurements,

$\underline{x}$ are the corrections to the a priori values of parameters.

The **first design matrix** A is defined by

$$
A = \left(\frac{\partial \Psi(\underline{\hat{X}})}{\partial (\underline{\hat{X}})} \right)_{\underline{\hat{X}} = \underline{X}_0}. \tag{C.2}
$$

We assume that the function Ψ and the a priori values for the parameters $(\underline{X}_0)$ are known. The stochastic model is given by the **covariance matrix**

$$
K_{\ell\ell} = \sigma_0^2\, Q_{\ell\ell} = \sigma_0^2\, P^{-1}. \tag{C.3}
$$

σ_0^2 is the a priori variance and $Q_{\ell\ell}$ is the **cofactor matrix of the observations**. The solution of the system (C.1) follows from the *least-squares principle*

$$
\underline{w}^T P \underline{w} = \text{min.} \,, \tag{C.4}
$$

which leads to the **normal equations**

$$\underbrace{A^T P A}_{N = Q_{xx}^{-1}} \, \underline{x} = \underbrace{A^T P \underline{\ell}}_{\underline{b}} \,, \tag{C.5}$$

where Q_{xx} is the **cofactor matrix of the parameters**. The standard a posteriori root mean square error (a posteriori rms) is given by

$$m_0 = \sqrt{\frac{\underline{w}^T P \underline{w}}{n - u}} = \sqrt{\frac{\underline{\ell}^T P \underline{\ell} - \underline{x}^T \underline{b}}{n - u}} \,, \tag{C.6}$$

where n is the number of measurements and u the number of unknown parameters. The covariance matrix of the parameters is

$$K_{xx} = m_0^2 \, Q_{xx} \,. \tag{C.7}$$

If the measurements $\underline{L}$ are uncorrelated, the weight matrix P is a diagonal matrix ($P = \mathrm{diag}(p_1, p_2, \dots, p_n)$). In this case the elements N_{ik} of the normal matrix N and the elements b_i of the right hand side vector $\underline{b}$ may be computed as (see e.g. [Beutler, 1982])

$$N_{ik} = \sum_{j=1}^{n} p_j A_{ji} A_{jk} \,, \tag{C.8}$$

$$b_i = \sum_{j=1}^{n} p_j A_{ji} \ell_j \,. \tag{C.9}$$

Thus only one row $(A_{j1}, \dots, A_{ju})$ of the matrix A, one element of the vector $\underline{\ell}$ and one element of the diagonal matrix P must be simultaneously available in the storage. It should be mentioned, however, that double differenced data are correlated and therefore they lead to a non-diagonal matrix P.

C.1.1 Parameter Pre-Elimination

Let us (arbitrarily) divide the vector of unknown parameters $\underline{x}$ into two vectors $\underline{x}_1$ and $\underline{x}_2$. The corresponding normal equations may be written as

$$\begin{pmatrix} N_{11} & N_{12} \\ N_{21} & N_{22} \end{pmatrix} \cdot \begin{pmatrix} \underline{x}_1 \\ \underline{x}_2 \end{pmatrix} = \begin{pmatrix} \underline{b}_1 \\ \underline{b}_2 \end{pmatrix} \,. \tag{C.10}$$

From the last system the second part of vector $\underline{x}$ may be computed:

$$\underline{x}_2 = N_{22}^{-1} \, (\underline{b}_2 - N_{21} \underline{x}_1) \,. \tag{C.11}$$

This leads to a new system of equations for the first part of the vector $\underline{x}$:

$$\underbrace{(N_{11} - N_{12} N_{22}^{-1} N_{21})}_{N_{11}^{new}} \, \underline{x}_1 = \underbrace{\underline{b}_1 - N_{12} N_{22}^{-1} \underline{b}_2}_{\underline{b}_1^{new}} \,. \tag{C.12}$$

Let us now assume that $\underline{x}_2$ consists of all ambiguity parameters. If the ambiguities are not going to be resolved they may be *pre-eliminated*. This approach speeds up the parameter estimation process.

C.1.2 Ambiguity Fixing

Let us introduce the following notation:

$\underline{x}_1$ the non-ambiguity parameters,

$\underline{x}_1^0$ their a priori values,

$\underline{x}_2$ the ambiguity parameters,

$\underline{x}_2^0$ their a priori values, and

$\bar{\underline{x}}_2^0$ their known true (integer) values.

In the case of the float solution we have the observation equations

$$(A_1 \ A_2) \cdot \begin{pmatrix} \underline{x}_1 \\ \underline{x}_2 \end{pmatrix} - \underbrace{(\underline{L} - \Psi(\underline{x}_1^0, \underline{x}_2^0))}_{\underline{\ell}} = \underline{w} \tag{C.13}$$

and the system of normal equations

$$\begin{pmatrix} N_{11} & N_{12} \\ N_{21} & N_{22} \end{pmatrix} \cdot \begin{pmatrix} \underline{x}_1 \\ \underline{x}_2 \end{pmatrix} = \begin{pmatrix} A_1^T P \underline{\ell} \\ A_2^T P \underline{\ell} \end{pmatrix} = \begin{pmatrix} \underline{b}_1 \\ \underline{b}_2 \end{pmatrix} , \tag{C.14}$$

which gives the result

$$(N_{11} - N_{12} N_{22}^{-1} N_{21}) \cdot \underline{x}_1 = \underline{b}_1 - N_{12} N_{22}^{-1} \underline{b}_2 . \tag{C.15}$$

Introducing the known integer ambiguities we have

$$A_1 \underline{x}_1 - \underbrace{(\underline{L} - \Psi(\underline{x}_1^0, \bar{\underline{x}}_2))}_{\underline{\ell}'} = \underline{w}' , \tag{C.16}$$

which gives immediately

$$N_{11} \underline{x}_1 = A_1^T P \underline{\ell}' = \underline{b}_1' . \tag{C.17}$$

We may write

$$\underline{\ell} - \underline{\ell}' = \Psi(\underline{x}_1^0, \bar{\underline{x}}_2) - \Psi(\underline{x}_1^0, \underline{x}_2^0) = A_2 \cdot (\bar{\underline{x}}_2 - \underline{x}_2^0) = A_2 \underline{dx}_2 \tag{C.18}$$

and therefore

$$N_{11} \underline{x}_1 = A_1^T P \underline{\ell} - A_1^T P A_2 \underline{dx}_2 . \tag{C.19}$$

To compute the a posteriori rms we may use the following expression:

$$\underline{\ell}'^T P \underline{\ell}' = \underline{\ell}^T P \underline{\ell} - 2 \cdot \underline{dx}_2^T A_2^T P \underline{\ell} + \underline{dx}_2^T A_2^T P A_2 \underline{dx}_2 = \underline{\ell}^T P \underline{\ell} - 2 \cdot \underline{dx}_2^T \underline{b}_2 + \underline{dx}_2^T N_{22} \underline{dx}_2 . \tag{C.20}$$

C.2 Least-Squares Collocation

Adding a signal $\underline{s}$ to the model (C.1) we get an observation equation of the following kind (see e.g. [Gurtner, 1992]):

$$\underline{\ell} = A\,\underline{x} - \underline{s} - \underline{w}\,. \tag{C.21}$$

Using the notation

$$B = (I, I) = \begin{pmatrix} 1 & \dots & 0 & 1 & \dots & 0 \\ \vdots & \ddots & \vdots & \vdots & \ddots & \vdots \\ 0 & \dots & 1 & 0 & \dots & 1 \end{pmatrix}\,, \quad \underline{v} = \begin{pmatrix} \underline{s} \\ \underline{w} \end{pmatrix}\,, \tag{C.22}$$

we may write the least-squares condition as

$$\Omega = \underline{v}^T P \underline{v} + 2\,\underline{k}^T \underbrace{(A\underline{x} - B\underline{v} - \underline{\ell})}_{\underline{0}} = \min.\,, \tag{C.23}$$

where the weight matrix P is

$$P = Q^{-1} = \begin{pmatrix} Q_{ss}^{-1} & 0 \\ 0 & Q_{\ell\ell}^{-1} \end{pmatrix}\,. \tag{C.24}$$

The covariance matrices Q_{ss} and $Q_{\ell\ell}$ are assumed to be known. The conditions

$$\frac{\partial \Omega}{\partial \underline{v}} = 2\,P\underline{v} - 2\,B^T\underline{k} = \underline{0} \Rightarrow \underline{v} = QB^T\underline{k} \tag{C.25}$$

$$\frac{\partial \Omega}{\partial \underline{x}} = 2\,A^T\underline{k} = \underline{0} \tag{C.26}$$

lead to the system

$$\begin{aligned} A^T \cdot \underline{k} &= \underline{0} \\ A \cdot \underline{x} - BQB^T \cdot \underline{k} &= \underline{\ell}\,. \end{aligned} \tag{C.27}$$

The vector of parameters according to (C.12) may be written as

$$\underline{x} = \underbrace{(A^T Q_{zz}^{-1} A)^{-1}}_{Q_{xx}} A^T Q_{zz}^{-1}\underline{\ell}\,, \quad Q_{zz} = BQB^T = Q_{ss} + Q_{\ell\ell}\,. \tag{C.28}$$

C.3 Stochastic Estimation

Estimation based on a Kalman filter estimator is frequently used if a stochastic behaviour for some parameters (e.g. troposphere parameters) is expected. The formulae may be found in many textbooks (see e.g. [Beutler, 1983]). The algorithm consists of two steps: *prediction* and *update* which will be briefly described. During the update step we will use the formulae of the algorithm which are sometimes refered to as *sequential adjustment*.

C.3.1 Sequential Adjustment

This method was already established by Karl Friedrich Gauss (1777-1855) and used for the adjustment of geodetical networks by Friedrich Robert Helmert (1843-1917). Therefore in geodetical textbooks this algorithm is often refered to as Helmert's method. [Brockmann, 1995] applies the sequential adjustment to the estimation of the coordinates and other parameters from long-term GPS observations.

Assuming a partition of the observational model into two parts, and denoting by $\underline{x}_1$ and $\underline{x}_2$ the (same) parameters which are estimated in both parts and by $\underline{y}_1$ and $\underline{y}_2$ the (different) parameters which appear in the first part or in the second part only (and therefore might be pre-eliminated), we may write:

$$A_1\underline{x}_1 + B_1\underline{y}_1 - \underline{\ell}_1 = \underline{w}_1 \tag{C.29}$$

$$A_2\underline{x}_2 + B_2\underline{y}_2 - \underline{\ell}_2 = \underline{w}_2 . \tag{C.30}$$

Let us assume that there are no correlations between the two groups of observations $\underline{\ell}_1$ and $\underline{\ell}_2$. Then the cofactor matrix has a block diagonal structure

$$Q_{\ell\ell} = \begin{pmatrix} P_1^{-1} & 0 \\ 0 & P_2^{-1} \end{pmatrix} , \tag{C.31}$$

where

$$P_1^{-1} = Q_{\ell_1\ell_1} \quad \text{and} \quad P_2^{-1} = Q_{\ell_2\ell_2} . \tag{C.32}$$

The corresponding normal equations are

$$\begin{pmatrix} A_i^T P_i A_i & A_i^T P_i B_i \\ B_i^T P_i A_i & B_i^T P_i B_i \end{pmatrix} \cdot \begin{pmatrix} \underline{x}_i \\ \underline{y}_i \end{pmatrix} = \begin{pmatrix} A_i^T P_i \underline{\ell}_i \\ B_i^T P_i \underline{\ell}_i \end{pmatrix} \quad \text{where} \quad i = 1, 2 . \tag{C.33}$$

Pre-elimination of the parameters $\underline{y}_i$ yields the solution

$$\underline{x}_i = \left(A_i^T P_i A_i - A_i^T P_i B_i (B_i^T P_i B_i)^{-1} B_i^T P_i A_i \right)^{-1} \\ \left(A_i^T P_i \underline{\ell}_i - A_i^T P_i B_i (B_i^T P_i B_i)^{-1} B_i^T P_i \underline{\ell}_i \right) \tag{C.34}$$

and the cofactor matrix

$$Q_{x_ix_i} = \left(A_i^T P_i A_i - A_i^T P_i B_i (B_i^T P_i B_i)^{-1} B_i^T P_i A_i \right)^{-1} , \quad \text{where} \quad i = 1, 2 . \tag{C.35}$$

The resulting vector $\underline{x}$ may be estimated using the two solutions $\underline{x}_1$, $\underline{x}_2$ and the cofactor matrices $Q_{x_1x_1}$, $Q_{x_2x_2}$. The "observation" equations are given by

$$\begin{pmatrix} \underline{x}_1 \\ \underline{x}_2 \end{pmatrix} + \underline{w} = \begin{pmatrix} I \\ I \end{pmatrix} \underline{x} , \tag{C.36}$$

where I is a unit matrix and the weight matrix is given by

$$P = \begin{pmatrix} Q_{x_1x_1}^{-1} & 0 \\ 0 & Q_{x_2x_2}^{-1} \end{pmatrix} . \tag{C.37}$$

This model leads to the normal equations

$$\left(I \ , \ I\right) \left(\begin{array}{cc} Q_{x_1x_1}^{-1} & 0 \\ 0 & Q_{x_2x_2}^{-1} \end{array} \right) \left(\begin{array}{c} I \\ I \end{array} \right) \underline{x} = \left(I \ , \ I\right) \left(\begin{array}{cc} Q_{x_1x_1}^{-1} & 0 \\ 0 & Q_{x_2x_2}^{-1} \end{array} \right) \left(\begin{array}{c} \underline{x}_1 \\ \underline{x}_2 \end{array} \right) \ , \quad (C.38)$$

which may be written as

$$\left(\begin{array}{c} (A_1^T P_1 A_1 + A_2^T P_2 A_2) - A_1^T P_1 B_1 (B_1^T P_1 B_1)^{-1} B_1^T P_1 A_1 - \\ - A_2^T P_2 B_2 (B_2^T P_2 B_2)^{-1} B_2^T P_2 A_2 \end{array} \right) \cdot \underline{x} =$$

$$\left(\begin{array}{c} (A_1^T P_1 \underline{\ell}_1 + A_2^T P_2 \underline{\ell}_2) - A_1^T P_1 B_1 (B_1^T P_1 B_1)^{-1} B_1^T P_1 \underline{\ell}_1 - \\ - A_2^T P_2 B_2 (B_2^T P_2 B_2)^{-1} B_2^T P_2 \underline{\ell}_2 \end{array} \right) \ . \quad (C.39)$$

The sequential adjustment is equal to the adjustment in one block (see e.g. [Brockmann, 1995]) with the result

$$\left(\begin{array}{ccc} (A_1^T P_1 A_1 + A_2^T P_2 A_2) & A_1^T P_1 B_1 & A_2^T P_2 B_2 \\ B_1^T P_1 A_1 & B_1^T P_1 B_1 & 0 \\ B_2^T P_2 A_2 & 0 & B_2^T P_2 B_2 \end{array} \right) \cdot \left(\begin{array}{c} \underline{x} \\ \underline{y}_1 \\ \underline{y}_2 \end{array} \right)$$

$$= \left(\begin{array}{c} (A_1^T P_1 \underline{\ell}_1 + A_2^T P_2 \underline{\ell}_2) \\ B_1^T P_1 \underline{\ell}_1 \\ B_2^T P_2 \underline{\ell}_2 \end{array} \right) \ . \quad (C.40)$$

C.3.2 Kalman Filtering

The first step of the Kalman filter is the so-called *prediction*. The state transition equation describes the dynamics of the parameters:

$$\underline{x}(t_{i+1}) = T(t_{i+1}, t_i) \, \underline{x}(t_i) + \underline{e}(t_{i+1}, t_i) \ , \quad (C.41)$$

where

$\underline{x}(t_i)$ is the vector of parameter values at epoch t_i,

$T(t_{i+1}, t_i)$ is the state transition matrix defining the transition from the state at epoch t_i to the expected state at epoch t_{i+1},

$\underline{x}(t_{i+1})$ is the vector of parameter values at epoch t_{i+1}, and

$\underline{e}(t_{i+1}, t_i)$ is the vector of random perturbations affecting the state during the interval between epochs t_i and t_{i+1}. For non-stochastic parameters $\underline{e}(t_{i+1}, t_i)$ is zero.

Under some assumptions concerning the correlations between the measurement process and the random motion (for details see e.g. [Beutler, 1983]) the cofactor matrix $Q_x(t_{i+1})$ of the state vector $\underline{x}(t_{i+1})$ may be calculated by the law of covariance propagation

$$Q_x(t_{i+1}) = P_x^{-1} = T(t_{i+1}, t_i) \, Q_x(t_i) T^T(t_{i+1}, t_i) + Q_e(t_{i+1}, t_i) \ , \quad (C.42)$$

where the cofactor matrix $Q_e(t_{i+1}, t_i)$ is due to random perturbations. [Rothacher, 1991] uses a random walk stochastic process to model the stochastic behaviour of the troposphere. In this case the state transition matrix $T(t_{i+1}, t_i)$ is equal to the identity matrix and the prediction step is simply

$$\underline{x}(t_{i+1}) = \underline{x}(t_i) , \tag{C.43}$$

$$Q_x(t_{i+1}) = Q_x(t_i) + Q_e(t_{i+1}, t_i) . \tag{C.44}$$

The elements $Q_{e\ ij}$ of the cofactor matrix $Q_e(t_{i+1}, t_i)$ are given by:

$Q_{e\ ij} = 0$ for $i \neq j$

$Q_{e\ ii} = 0$ for non-stochastic parameter i,

$Q_{e\ jj} = \Phi_j \cdot \Delta t$ for stochastic parameter j,

where $\Delta t = t_{i+1} - t_i$ and Φ_j is so-called power spectral density of parameter j, which has to be specified for all stochastic parameters to be estimated with the Kalman filter.

The second step of the Kalman filter is the *update* step. We assume that at epoch t_{i+1} the observations $\underline{\ell}(t_{i+1})$ and the corresponding cofactors $Q_\ell = P_\ell^{-1}$ are available. Using the state transition matrix $T(t_{i+1}, t_i)$ the state vector $\underline{x}(t_{i+1})$ may be predicted without using the observations at time t_{i+1}. We want to correct this prediction using the observations $\underline{\ell}(t_{i+1})$ at time t_{i+1} and compute the corrected state vector $\underline{\hat{x}}(t_{i+1})$. The following model – possibly after a linearization – may be adopted:

$$\begin{aligned} A\underline{\hat{x}}(t_{i+1}) - \underline{\ell}(t_{i+1}) &= \underline{w}_\ell \\ \underline{\hat{x}}(t_{i+1}) - \underline{x}(t_{i+1}) &= \underline{w}_r \end{aligned} \tag{C.45}$$

This is a special case of the sequential adjustment ($B_1 = B_2 = 0$, $A_1 = A$, $A_2 = I$) and the result is given by equation (C.39):

$$\left(A^T P_\ell A + P_x \right) \underline{\hat{x}}(t_{i+1}) = A^T P_\ell \underline{\ell}(t_{i+1}) + P_x \underline{x} . \tag{C.46}$$

Using the notation $\underline{\hat{x}}(t_{i+1}) = \underline{x}(t_{i+1}) + \Delta\underline{x}(t_{i+1})$ the result takes on the form

$$\underline{\hat{x}}(t_{i+1}) = \underline{x}(t_{i+1}) + \Delta\underline{x}(t_{i+1}) = \underline{x}(t_{i+1}) + K\left[\underline{\ell} - A\ \underline{x}(t_{i+1}) \right] , \tag{C.47}$$

where so-called gain matrix K is given by

$$K = \left(A^T P_\ell A + P_x \right)^{-1} A^T P_\ell . \tag{C.48}$$

Using the relation

$$\left(A^T P A + R \right)^{-1} A^T P = R^{-1} A^T \left(P^{-1} + A R^{-1} A^T \right)^{-1} , \tag{C.49}$$

the gain matrix may be written in the form

$$K = Q_x A^T \left(Q_\ell + A Q_x A^T \right)^{-1} . \tag{C.50}$$

References

Ashby, N. (1987): *Relativistic effects in the Global Positioning System.* Relativistic effects in geodesy, Proceedings of the International Association of Geodesy (IAG) Symposia of the XIX General Assembly of IUGG, Vancouver, Canada, August 10–22, Vol. 1, pp. 41–50.

Baueršíma, I. (1982): *NAVSTAR Global Positioning System (GPS) I.* Mitteilungen der Satelliten-Beobachtungsstation Zimmerwald, Bern, Vol. 7.

Baueršíma, I. (1983): *NAVSTAR Global Positioning System (GPS) II, Radiointerferometrische Satellitenbeobachtungen.* Mitteilungen der Satelliten-Beobachtungsstation Zimmerwald, Bern, Vol. 10.

Beutler, G. (1982): *Lösung von Parameterbestimmungsproblemen in Himmelsmechanik und Satellitengeodäsie mit modernen Hilfsmitteln.* Astronomisch-geodätische Arbeiten in der Schweiz, Band 34.

Beutler, G. (1983): *Digitale Filter und Schätzprozesse.* Druckerei der Universität Bern.

Beutler, G., W. Gurtner, I. Baueršíma, R. Langley (1985): *Modelling and Estimation of Orbits of GPS Satellites.* Proceedings of the First International Symposium on Precise Positioning with the Global Positioning System, Rockville, Maryland, April 15–19. Vol. 1, pp. 99–111.

Beutler, G., W. Gurtner, I. Baueršíma, M. Rothacher (1986): *Efficient Computation of the Inverse of the Covariance Matrix of Simultaneous GPS Carrier Phase Difference Observations.* Manuscripta Geodaetica, Vol. 11, pp. 249–255.

Beutler, G. (1990): *Numerische Integration gewöhnlicher Differentialgleichungssysteme: Prinzipien und Algorithmen.* Mitteilung Nr. 23 der Satelliten-Beobachtungsstation Zimmerwald, Druckerei der Universität Bern.

Beutler, G. (1993a): *The 4th IGS Oversight Committee Meeting and the Joint IERS and IGS Meeting in Berne, 24–27 March 1993.* Proceedings of the 1993 IGS Workshop, University of Berne.

Beutler, G. (1993b): *The 1992 IGS Test Campaign, Epoch'92, and the IGS PILOT Service: An Overview.* Proceedings of the 1993 IGS Workshop, Bern, March 25 – 26, pp. 3 – 9.

Beutler, G., E. Brockmann, W. Gurtner, U. Hugentobler, L. Mervart, M. Rothacher, A. Verdun (1994a): *Extended Orbit Modeling Techniques at the CODE Processing Center of the International GPS Service for Geodynamics (IGS): Theory and Initial Results.* Manuscripta Geodaetica, Vol. 19, pp. 367 – 386.

Beutler, G., D. Sauer, S. Schär (1994b): *Resolution of the Initial Carrier Phase Ambiguities: Mathematical Principles.* (in preparation)

Beutler, G., I.I. Mueller, R. Neilan (1994c): *The International GPS Service for Geodynamics (IGS): Development and Start of Official Service on 1 January 1994.* Bulletin Geodesique, Vol. 68, pp. 43 – 51.

Blewitt, G. (1989): *Carrier Phase Ambiguity Resolution for the Global Positioning System Applied to Geodetic Baselines up to 2000 km.* Journal of Geophysical Research, Vol. 94, No. B8.

Bock, Y., S.A. Gourewitch, C.C. Counselmann, R.W. King, R.I. Abbot (1986): *Interferometric analysis of GPS phase observations.* Manuscripta geodaetica, Vol. 11, No. 4, pp. 282–288.

Boucher, C., Z. Altamimi, L. Duhem (1992): *ITRF91 and its associated velocity field.* ITRF Technical Note 12, Central Bureau of IERS, Observatoire de Paris, October.

Brockmann E., G. Beutler, W. Gurtner, M. Rothacher, T. Springer, L. Mervart (1993): *Solutions using European GPS Observations produced at the "Center for Orbit Determination in Europe" (CODE) during the 1992 IGS Campaign.* Proceedings of the 1993 IGS Workshop, Berne, March 25 - 26, pp. 251 - 260.

Brockmann, E. (1995): *PhD Thesis.* Astronomical Institute University of Berne (in preparation)

Brown, R.G., P.Y.C. Hwang (1983): *A Kalman Filter Approach to Precision GPS Geodesy.* Navigation, Vol. 30, No. 4.

Cappellari, J., C. Velez, A. Fuchs (1976): *Mathematical Theory of the Goddard Trajectory Determination System.* Goddard Space Flight Center, X-582-76-77, Greenbelt, MD.

Cocard, M., A. Geiger (1992): *Systematic search for all possible widelanes.* Proceedings of the Sixth International Geodetic Symposium on Satellite Positioning, Columbus, Ohio, March 17–20, pp. 312–318.

Colombo, O.L. (1989): *The Dynamics of Global Positioning Orbits and the Determination of Precise Ephemerides.* Journal of Geophysical Research, Vol. 94, No. B7, pp. 9167–9182.

Counselman, C.C., S.A. Gourevitch (1981): *Miniature interferometer terminals for earth surveying: ambiguity and multipath with the Global Positioning System.* IEEE Transactions on Geoscience and Remote Sensing, GE-19(4): pp. 244–252.

Decker, B.L. (1986): *World Geodetic System 1984.* Proceedings of the Fourth International Geodetic Symposium on Satellite Positioning, Austin, Texas, April 28 - 2 May, Vol. 1, pp. 69–92.

Essen, L., K.D. Froome (1951): *The refractive indices and dielectric constants of air and its pricipal constituents at 24 000 Mc/s.* Proceedings of Physical Society, Vol. 64(B), pp. 862–875.

Fankhauser, S. (1993): *Die Bestimmung von Erdrotationsparametern mit Hilfe von GPS-Beobachtungen.* Mitteilungen der Satelliten-Beobachtungsstation Zimmerwald, Bern, Vol. 29.

Feissel, M. (1993): *IGS'92 Campaign, Comparison of GPS, SLR, and VLBI Earth Orientation Determination, final report.* Proceedings of the 1993 IGS Workshop, Berne, March 25 - 26, pp. 194 - 201.

Fliegel, H.F., T.E. Gallini, E.R. Swift (1992): *Global Positioning System Radiation Force Model for Geodetic Application.* Journal of Geophysical Research, Vol. 97, No. B1, pp. 559–568.

Frei, E., G. Beutler (1990): *Rapid static positioning based on the fast ambiguity resolution approach "FARA": theory and first results.* Manuscripta geodaetica, Vol. 15, No. 6, pp. 325–356.

Frei, E. (1991): *Rapid Differential Positioning with the Global Positioning System (GPS).* Geodätisch-geophysikalische Arbeiten in der Schweiz, Bd. 44, 178 pages.

Gambis, D., N. Essaïfi, E. Eisop, M. Feissel (1993): *Universal Time Derived from VLBI, SLR, and GPS.* Proceedings of the 1993 IGS Workshop, Berne, March 25 - 26, pp. 212 - 217.

Gibson, R. (1983): *A derivation of relativistic effects in satellite tracking.* Naval Surface Weapons Center, Dahlgren, Virginia, Technical Report TR 83-55.

Goad, C.C., L. Goodman (1974): *A Modified Hopfield Tropospheric Refraction Correction Model.* Paper presented at the Fall Annual Meeting of the American Geophysical Union, San Francisco, California, December 12-17.

Goad, C. (1992): *Analysis Standards for the IGS Processing Centers.* The Ohio State University, Columbus, Ohio, June 5.

Goad, C. (1993): *IGS Orbit Comparisons.* Proceedings of the 1993 IGS Workshop, Berne, March 25 - 26, pp. 218 - 225.

Gurtner, W., G. Beutler, I. Baueršíma, T. Schildknecht (1985): *Evaluation of GPS Carrier Difference Observations: The Bernese Second Generation Software Package.* Proceedings of the First International Symposium on Precise Positioning with the Global Positioning System, Rockville, Maryland, April 15-19.

Gurtner, W., G. Beutler, E. Brockmann, S. Fankhauser, M. Rothacher, T. Springer, S. Botton, L. Mervart, A. Wiget, U. Wild (1992): *Automated Data Flow and Processing at the "Center for Orbit Determination in Europe" (CODE) During the 1992 IGS Campaign.* Proceedings of the 7th International Symposium on Geodesy and Physics of the Earth, Potsdam, October 5 - 10.

Gurtner, W., G. Mader (1990): *Receiver Independent Exchange Format Version 2.* CSTG GPS Bulletin Vol.3, No.3, Sept./Oct. 1990, National Geodetic Survey, Rockville.

Gurtner, W. (1992): *Parameterbestimmung und Schätzverfahren.* Astronomisches Institut, Druckerei Universität Bern.

Hofmann-Wellenhof, B., H. Lichtenegger, J. Collins (1992): *Global Positioning System Theory and Practice.* Springer-Verlag Wien, New York.

Hopfield, H.S. (1969): *Two-quadratic tropospheric refractivity profile for correcting satellite data.* Journal of Geophysical Research, Vol. 74(18), pp. 4487–4499.

IAU (1992): *Recommendations I to IX from the Working Group on Reference Systems.* The XXIst General Assembly of the International Astronomical Union.

Janes, H.W., R.B. Langley, S.P. Newby (1989):*A comparison of several models for the prediction of tropospheric propagation delay.* Proceedings of the Fifth International Geodetic Symposium on Satellite Positioning, Las Cruces, New Mexico, March 13-17, Vol 2, pp. 777–788.

Kaplan, G.H. (1981): *The IAU Resolutions of Astronomical Constants, Time Scales, and the Fundamental Reference Frame.* U.S. Naval Observatory Circular No. 163, Washington D.C.

King, R., E. Masters, C. Rizos, A. Stolz, J. Collins (1985): *Surveying with GPS.* The University of New South Wales, School of Surveying, Monograph 9, Kensington, N.S.W.

Landau, H., D. Hagmaier (1986): *Analysis of the Required Force-Modelling for NAVSTAR/GPS Satellites.* GPS Research 1985 at the Institute of Astronomical and Physical Geodesy, Schriftenreihe Universitärer Studiengang Vermessungswesen, Universität der Bundeswehr München, Heft 19, pp. 193–208.

Landau, H. (1988): *Zur Nutzung des Global Positioning Systems in Geodäsie und Geodynamik: Modellbildung, Software-Entwicklung und Analyse.* Heft 36 Schriftenreihe Universität der Bundeswehr München.

Magill, D. (1965): *Optimal Adaptive Estimation of Sampled Stochastic Processes.* IEEE Transaction an Automatic Control, Vol. AC-10, No. 4, pp. 434–439, New York.

McCaskill, T., J. Buisson, S. Stebbins (1985): *Frequency Stability Analysis of GPS NAVSTARs 3 and 4 Rubidium Clocks and the NAVSTARs 5 and 6 Cesium Clocks.* Naval Research Laboratory NRL Report 8778, Washington, DC.

Meehan, T.K., G. Blewitt, K. Larson, R.E. Neilan (1988): *Baseline results of the Rogue GPS receiver from CASA UNO*. Eos Trans. AGU, 69, (44), 1150.

Melbourne, W.G. (1985): *The Case for Ranging in GPS Based Geodetic Systems*. Proceedings of the First International Symposium on Precise Positioning with the Global Positioning System, Rockville, Maryland, April 15-19, pp. 373-386.

Melchior, P. (1983): *The Tides of the Planet Earth*. 2nd edition, Pergamon Press, New York.

Mervart, L., G. Beutler, M. Rothacher, U. Wild (1994): *Ambiguity Resolution Strategies using the Results of the International GPS Geodynamics Service (IGS)*. Bulletin Geodesique, Vol. 68, pp. 29 - 38.

Morgan, P., W. Gurtner (1992): *Guidelines for IGS Data Formats and Communications*. Proceedings of the Sixth International Symposium on Satellite Positioning, Columbus, Ohio, March 17 - 20, pp. 845 - 858.

Mueller, I.I., G. Beutler (1992): *The International GPS Service for Geodynamics - Development and Current Status*. Proceedings of the Sixth International Symposium on Satellite Positioning, Columbus, Ohio, March 17 - 20, pp. 823 - 835.

Mueller, I.I. (1993): *International GPS Service for Geodynamics: Terms of Reference*. Proceedings of the 1993 IGS Workshop, Bern, March 25 - 26, pp. 3 - 9.

Pagiatakis, S.D., R.B. Langley, P. Vaníček (1982): *Ocean Tide Loading: A Global Model for the Analysis of VLBI Observations*. presented at the 3rd International Symposium on the Use of Artificial Satellites for Geodesy and Geodynamics, National Technical University, Athens.

Pešek, I. (1989): *Definion of Time in the System IAU 1976*. No. 8, Edition of the Geodetical Reseach Institute, Zdiby (in Czech).

Remondi, B. (1984): *Using the Global Positioning System (GPS) phase observables for relative geodesy: modeling, processing, and results*. University of Texas at Austin, Center for Space Research.

Remondi, B. (1985a): *Using the Global Positioning System (GPS) Phase Observables for Relative Geodesy: Modeling, Processing and Results*. NOAA Reprint, Rockville, MD.

Remondi, B. (1985b): *Global Positioning System Carrier Phase: Description and use*. NOSS Technical Memorandum NOS NGS-42, Rockwille, MD.

Rothacher, M., G. Beutler, W. Gurtner, A. Geiger, H.G. Kahle, D. Schneider (1986): *The Swiss 1985 GPS Campaign*. Proceedings of the Fourth International Geodetic Symposium on Satellite Positioning, Austin, Texas, April 28 - 2 May, Vol. 2, pp. 979-991.

Rothacher, M. (1991): *Orbits of Satellite Systems in Space Geodesy.* Astronomical Institute, Druckerei Universität Bern.

Rothacher, M., G. Beutler, E. Brockmann, S. Fankhauser, W. Gurtner, T. Springer, S. Botton, L. Mervart, A. Wiget, U. Wild (1992): *Results of the "Center for Orbit Determination in Europe" During the IGS 1992 Campaign*. Proceedings of the 7th International Symposium on Geodesy and Physics of the Earth, Potsdam, October 5 - 10.

Rothacher, M., G. Beutler, W. Gurtner, E. Brockmann, L. Mervart (1993a): *Bernese GPS Software Version 3.4*. Astronomical Institute, Printing office, University of Berne.

Rothacher, M., G. Beutler, W. Gurtner, S. Botton, C. Boucher (1993b): *Results of the IGS Data Processing at the "Center for Orbit Determination in Europe" (CODE)*. Proceedings of the 1993 IGS Workshop, Berne, March 25 - 26, pp. 133 - 144.

Rothacher, M. (1993c): *Advanced Techniques of GPS Data Processing at the AIUB in Berne*. Metodi e procedure di modellizzazione e trattamento dei dati GPS. Udine, Italy.

Saastamoinen, I.I. (1973): *Contribution to the theory of atmospheric refraction.* Bulletin Géodésique, Vol. 107, pp. 13–34.

Schaer, S. (1994): *Stochastische Ionosphaerenmodellierung beim Rapid Static Positioning mit GPS.* Lizentiatsarbeit. Astronomisches Institut, Druckerei Universität Bern.

Schildknecht, T. (1986): *Der Beitrag von GPS Pseudodistanzbeobachtungen für die Auswertung von Phasenmessungen.* Lizentiatsarbeit. Astronomisches Institut, Druckerei Universität Bern.

Schupler, B., T. Clark, B. Williams (1990): *A Consumer's Report on GPS Antennas.* CDP Investigators Meeting, October 25.

Schwarz, K.P. (1983): *Inertial surveying and geodesy.* Reviews of Geophysics and Space Physics, 21(4), pp. 32–36.

Seeber, G. (1989): *Satellitengeodäsie: Grundlagen, Methoden und Anwendungen.* Walter de Gruyter, Berlin, New York.

Seidelmann, P.K. (1982): *1980 IAU Theory of Nutation: The Final Report of the IAU Working Group on Nutation.* Celestial Mechanics, Vol. 27, pp. 79–106.

Seidelmann, P.K. (1992): *Explanatory Supplement to the Astronomical Almanach.* University Science Books, Mill Vallley, California.

Sovers, O.J., J.S. Border (1987): *Observation Model and Parameter Partials for the JPL Geodetic GPS Modeling Software "GPSOMC".* JPL Publication 87–21, Pasadena, CA.

Spilker, J.J. (1980): *GPS signal structure and performance characteristics.* The Institute of Navigation: Global Positioning System, Vol. 1, pp. 29–54.

Springer, T.A., G. Beutler (1993): *Towards an Official IGS Orbit by Combining the Results of all IGS Processing Centers.* Proceedings of the 1993 IGS Workshop, Berne, March 25 – 26, pp. 242 – 249.

Stein, V. (1982): *Modelle der ionosphärischen Elektronendichtverteilung zur Korrektur von Ausbreitungsfehlern elektromagnetischer Wellen.* DFVLR, Mitteilung 82–03, Oberpfaffenhofen.

Wells, D.E., N. Beck, D. Delikaraoglou, A. Kleusberg, E. Krakiwsky, G. Lachapelle, R. Langley, M. Nakiboglu, K.P. Schwarz, J. Transquilla, P. Vaníček (1986): *Guide to GPS Positioning.* Canadian GPS Associates, Fredericton, N.B.

Wild, U., G. Beutler, W. Gurtner, M. Rothacher (1989): *Estimating the ionosphere using one or more dual frequency GPS receivers.* Proceedings of the Fifth International Geodetic Symposium on Satellite Positioning, Las Cruces, New Mexico, March 13–17, Vol 2, pp. 724–736.

Wild, U. (1993): Ionosphere and Ambiguity Resolution. Proceedings of the 1993 IGS Workshop, University of Berne.

Willson, R. (1978): *Accurate Solar 'Constant' Determination by Cavity Pyrheliometers.* Journal of Geophysical Research, Vol. 83, No. C8, pp. 4003–4007.

Wooden, W.H. (1985): *Navstar Global Positioning System: 1985.* Proceedings of the First International Symposium on Precise Positioning with the Global Positioning System, Rockville, Maryland, April 15–19. Vol. 1, pp. 403–412.

Wu, J.T., S.C. Wu, G.A. Hajj, W.I. Bertiger, S.M. Lichten (1992): *Effects of Antenna Orientation on GPS Carrier Phase.* Submitted to Journal of Geophysical Research.

Wübbena, G. (1985): *Software Developments for Geodetic Positioning with GPS Using TI-4100 Code and Carrier Measurements.* Proceedings of the First International Symposium on Precise Positioning with the Global Positioning System, Rockville, Maryland, April 15–19.

Young, L.E., R.E. Neilan, F.R. Bletzacker (1985): *GPS Satellite Multipath: An Experimental Investigation.* Proceedings of the First International Symposium on Precise Positioning with the Global Positioning System, Rockville, Maryland, April 15–19.

Zhu, S., E. Groten, R.S. Pan, H.J. Yan, Z.Y. Cheng, W.Y. Zhu, C. Huang, M. Yao (1987): *Motion of Satellite – the Choice of Reference Frames.* Astrophysical Space Science Series, The Few Body Problem, D. Reidel.

"Geodätisch-geophysikalische Arbeiten in der Schweiz"
(Fortsetzung der Publikationsreihe "Astronomisch-geodätische Arbeiten in der Schweiz")
der Schweizerischen Geodätischen Kommission (ab Bd. 37):

37 1986 Les levés aéromagnetiques de la Suisse. E. Klingelé. 69 Seiten.

38 1986 Lokale Schwerefeldbestimmung und gravimetrische Modellrechnungen im Satelliten (GPS)- Testnetz "Turtmann" (Wallis). I. Bernauer, A. Geiger. 106 Seiten.

39 1989 125 Jahre Schweizerische Geodätische Kommission
    I.   Bedeutung geodätischer Raumverfahren für Landesvermessung und Geodynamik. (R. Sigl)
    II. Beitrag der Geodäsie zur Geodynamik. (H.-G. Kahle)
    III. L'état actuel de la recherche sur les movements de l'écorce terrestre en Suisse. (F. Jeanrichard)
    IV. Die Satellitengeodäsie im Dienste der globalen Geodynamik. (I. Bauersima)
    V. Die Veranstaltungen zum 125 Jahr-Jubiläum der Schweizerischen Geodätischen Kommission. (W. Fischer). 62 Seiten.

40 1989 Integrale Schwerefeldbestimmung in der Ivrea- Zone und deren geophysikalische Interpretation. B. Bürki. 186 Seiten.

41 1990 ALGESTAR satellitengestützte Geoidbestimmung in der Schweiz. U. Marti. 61 Seiten plus Punktprotokolle.

42 1990 Höhensysteme, Schwerepotentiale und Niveauflächen: Systematische Untersuchungen zur zukünftigen terrestrischen und GPS-gestützten Höhenbestimmung in der Schweiz. B. Wirth. 204 Seiten.

43 1990 Gravimetrisches Geoid der Schweiz: Potentialtheoretische Untersuchungen zum Schwerefeld im Alpenraum. A. Geiger. 231 Seiten.

44 1991 Rapid Differential Positioning with the Global Positioning System (GPS). E. Frei. 178 Seiten.

45 1992 Dreidimensionales Testnetz Turtmann 1985-1990 Teil I. F. Jeanrichard (Hrsg.) Autoren: A.Geiger, H.-G. Kahle, R. Köchle, D. Meier, B. Neininger, D. Schneider, B. Wirth. 183 Seiten.

46 1993 Orbits of Satellite Systems in Space Geodesy. M. Rothacher. 243 Seiten.

47 1993 NFP 20. Beitrag der Geodäsie zur geologischen Tiefenstruktur und Alpendynamik. H.-G. Kahle (Hrsg.) Autoren: I. Bauersima, G. Beutler, B. Bürki, M. Cocard, A. Geiger, E. Gubler, W. Gurtner, H.-G. Kahle, U. Marti, B. Mattli, M. Rothacher, Th. Schildknecht, D. Schneider, A. Wiget, B. Wirth. 153 Seiten plus 90 Seiten Anhang.

48 1994 Ionosphere and Geodetic Satellite Systems: Permanent GPS Tracking Data for Modelling and Monitoring: Urs Wild, 155 Seiten.

49 1994 Optical Astrometry of Fast Moving Objects using CCD Detectors: Thomas Schildknecht, 200 Seiten.

50 1995 Geodätische Alpentraverse Gotthard: A. Elmiger, R. Köchle, A. Ryf und F. Chaperon. 214 Seiten.

51 1995 Dreidimensionales Testnetz Turtmann 1985-1993, Teil II (GPS-Netz). F. Jeanrichard (Hrsg.) Autoren: G. Beutler, A. Geiger, M. Rothacher, Stefan Schaer, D.. Schneider, A. Wiget, 173 Seiten.

52 1995 High Precision GPS Processing in Kinematic Mode: M. Cocard. 139 Seiten.

53 1995 Ambiguity Resolution Techniques in Geodetic and Geodynamic Applications of the Global Positioning System. L. Mervart. 155 Seiten.